Verification and Validation of Selected Fire Models for Nuclear Power Plant Applications

Volume 7:
Fire Dynamics Simulator (FDS)

U.S.NRC
UNITED STATES NUCLEAR REGULATORY COMMISSION
Protecting People and the Environment

EPRI | ELECTRIC POWER
RESEARCH INSTITUTE

AVAILABILITY OF REFERENCE MATERIALS
IN NRC PUBLICATIONS

NRC Reference Material

As of November 1999, you may electronically access NUREG-series publications and other NRC records at NRC's Public Electronic Reading Room at http://www.nrc.gov/reading-rm.html.
Publicly released records include, to name a few, NUREG-series publications; *Federal Register* notices; applicant, licensee, and vendor documents and correspondence; NRC correspondence and internal memoranda; bulletins and information notices; inspection and investigative reports; licensee event reports; and Commission papers and their attachments.

NRC publications in the NUREG series, NRC regulations, and *Title 10, Energy,* in the Code of *Federal Regulations* may also be purchased from one of these two sources.
1. The Superintendent of Documents
   U.S. Government Printing Office
   Mail Stop SSOP
   Washington, DC 20402–0001
   Internet: bookstore.gpo.gov
   Telephone: 202-512-1800
   Fax: 202-512-2250
2. The National Technical Information Service
   Springfield, VA 22161–0002
   www.ntis.gov
   1–800–553–6847 or, locally, 703–605–6000

A single copy of each NRC draft report for comment is available free, to the extent of supply, upon written request as follows:
Address: U.S. Nuclear Regulatory Commission
          Office of Administration
          Mail, Distribution and Messenger Team
          Washington, DC 20555-0001
E-mail: DISTRIBUTION@nrc.gov
Facsimile: 301–415–2289

Some publications in the NUREG series that are posted at NRC's Web site address http://www.nrc.gov/reading-rm/doc-collections/nuregs. are updated periodically and may differ from the last printed version. Although references to material found on a Web site bear the date the material was accessed, the material available on the date cited may subsequently be removed from the site.

Non-NRC Reference Material

Documents available from public and special technical libraries include all open literature items, such as books, journal articles, and transactions, *Federal Register* notices, Federal and State legislation, and congressional reports. Such documents as theses, dissertations, foreign reports and translations, and non-NRC conference proceedings may be purchased from their sponsoring organization.

Copies of industry codes and standards used in a substantive manner in the NRC regulatory process are maintained at—
          The NRC Technical Library
          Two White Flint North
          11545 Rockville Pike
          Rockville, MD 20852–2738

These standards are available in the library for reference use by the public. Codes and standards are usually copyrighted and may be purchased from the originating organization or, if they are American National Standards, from—
          American National Standards Institute
          11 West 42nd Street
          New York, NY 10036–8002
          www.ansi.org
          212–642–4900

Legally binding regulatory requirements are stated only in laws; NRC regulations; licenses, including technical specifications; or orders, not in NUREG-series publications. The views expressed in contractor-prepared publications in this series are not necessarily those of the NRC.

The NUREG series comprises (1) technical and administrative reports and books prepared by the staff (NUREG–XXXX) or agency contractors (NUREG/CR–XXXX), (2) proceedings of conferences (NUREG/CP–XXXX), (3) reports resulting from international agreements (NUREG/IA–XXXX), (4) brochures (NUREG/BR–XXXX), and (5) compilations of legal decisions and orders of the Commission and Atomic and Safety Licensing Boards and of Directors' decisions under Section 2.206 of NRC's regulations (NUREG–0750).

Verification & Validation of Selected Fire Models for Nuclear Power Plant Applications

Volume 7: Fire Dynamics Simulator

NUREG-1824   **EPRI 1011999**

Final Report

May 2007

DISCLAIMER OF WARRANTIES AND LIMITATION OF LIABILITIES

THIS DOCUMENT WAS PREPARED BY THE ORGANIZATION(S) NAMED BELOW AS AN ACCOUNT OF WORK SPONSORED OR COSPONSORED BY THE ELECTRIC POWER RESEARCH INSTITUTE, INC. (EPRI). NEITHER EPRI NOR ANY MEMBER OF EPRI, ANY COSPONSOR, THE ORGANIZATION(S) BELOW, OR ANY PERSON ACTING ON BEHALF OF ANY OF THEM:

(A) MAKES ANY WARRANTY OR REPRESENTATION WHATSOEVER, EXPRESS OR IMPLIED, (I) WITH RESPECT TO THE USE OF ANY INFORMATION, APPARATUS, METHOD, PROCESS, OR SIMILAR ITEM DISCLOSED IN THIS DOCUMENT, INCLUDING MERCHANTABILITY AND FITNESS FOR A PARTICULAR PURPOSE, OR (II) THAT SUCH USE DOES NOT INFRINGE ON OR INTERFERE WITH PRIVATELY OWNED RIGHTS, INCLUDING ANY PARTY'S INTELLECTUAL PROPERTY, OR (III) THAT THIS DOCUMENT IS SUITABLE TO ANY PARTICULAR USER'S CIRCUMSTANCE; OR

(B) ASSUMES RESPONSIBILITY FOR ANY DAMAGES OR OTHER LIABILITY WHATSOEVER (INCLUDING ANY CONSEQUENTIAL DAMAGES, EVEN IF EPRI OR ANY EPRI REPRESENTATIVE HAS BEEN ADVISED OF THE POSSIBILITY OF SUCH DAMAGES) RESULTING FROM YOUR SELECTION OR USE OF THIS DOCUMENT OR ANY INFORMATION, APPARATUS, METHOD, PROCESS, OR SIMILAR ITEM DISCLOSED IN THIS DOCUMENT.

ORGANIZATION(S) THAT PREPARED THIS DOCUMENT:

U.S. Nuclear Regulatory Commission, Office of Nuclear Regulatory Research

Science Applications International Corporation

National Institute of Standards and Technology

NOTE

For further information about EPRI, call the EPRI Customer Assistance Center at 800.313.3774 or
e-mail askepri@epri.com.

Electric Power Research Institute, EPRI, and TOGETHER...SHAPING THE FUTURE OF ELECTRICITY are registered service marks of the Electric Power Research Institute, Inc.

CITATIONS

This report was prepared by

U.S. Nuclear Regulatory Commission
Office of Nuclear Regulatory Research (RES)
Two White Flint North, 11545 Rockville Pike
Rockville, MD 20852-2738

Principal Investigators:
K. Hill
J. Dreisbach

National Institute of Standards and Technology
Building Fire Research Laboratory (BFRL)
100 Bureau Drive, Stop 8600
Gaithersburg, MD 20899-8600

Principal Investigators:
K McGrattan
R. Peacock
A. Hamins

Electric Power Research Institute (EPRI)
3420 Hillview Avenue
Palo Alto, CA 94303

Science Applications International Corp (SAIC)
4920 El Camino Real
Los Altos, CA 94022

Principal Investigators:
F. Joglar
B. Najafi

Volume 1, Main Report: B. Najafi, F. Joglar, J. Dreisbach
Volume 2, Experimental Uncertainty: A. Hamins, K. McGrattan
Volume 3, FDT^S: J. Dreisbach, K. Hill
Volume 4, FIVE-Rev1: F. Joglar
Volume 5, CFAST: R. Peacock, P. Reneke (NIST)
Volume 6, MAGIC: F. Joglar, B. Guatier (EdF), L. Gay (EdF), J. Texeraud (EdF)
Volume 7, FDS: K. McGrattan

This report describes research sponsored jointly by U.S. Nuclear Regulatory Commission, Office of Nuclear Regulatory Research (RES) and Electric Power Research Institute (EPRI).

The report is a corporate document that should be cited in the literature in the following manner:

Verification and Validation of Selected Fire Models for Nuclear Power Plant Applications, Volume 7: Fire Dynamics Simulator (FDS), U.S. Nuclear Regulatory Commission, Office of Nuclear Regulatory Research (RES), Rockville, MD, 2007, and Electric Power Research Institute (EPRI), Palo Alto, CA, NUREG-1824 and EPRI 1011999.

ABSTRACT

There is a movement to introduce risk-informed and performance-based analyses into fire protection engineering practice, both domestically and worldwide. This movement exists in the general fire protection community, as well as the nuclear power plant (NPP) fire protection community. The U.S. Nuclear Regulatory Commission (NRC) has used risk-informed insights as part of its regulatory decision making since the 1990's.

In 2002, the National Fire Protection Association (NFPA) developed NFPA 805, *Performance-Based Standard for Fire Protection for Light-Water Reactor Electric Generating Plants, 2001 Edition*. In July 2004, the NRC amended its fire protection requirements in Title 10, Section 50.48, of the *Code of Federal Regulations* (10 CFR 50.48) to permit existing reactor licensees to voluntarily adopt fire protection requirements contained in NFPA 805 as an alternative to the existing deterministic fire protection requirements. In addition, the NPP fire protection community has been using risk-informed, performance-based (RI/PB) approaches and insights to support fire protection decision-making in general.

One key tool needed to further the use of RI/PB fire protection is the availability of verified and validated fire models that can reliably predict the consequences of fires. Section 2.4.1.2 of NFPA 805 requires that only fire models acceptable to the Authority Having Jurisdiction (AHJ) shall be used in fire modeling calculations. Furthermore, Sections 2.4.1.2.2 and 2.4.1.2.3 of NFPA 805 state that fire models shall only be applied within the limitations of the given model, and shall be verified and validated.

This report is the first effort to document the verification and validation (V&V) of five fire models that are commonly used in NPP applications. The project was performed in accordance with the guidelines that the American Society for Testing and Materials (ASTM) set forth in ASTM E 1355, *Standard Guide for Evaluating the Predictive Capability of Deterministic Fire Models*. The results of this V&V are reported in the form of ranges of accuracies for the fire model predictions.

FOREWORD

Fire modeling and fire dynamics calculations are used in a number of fire hazards analysis (FHA) studies and documents, including fire risk analysis (FRA) calculations; compliance with and exemptions to the regulatory requirements for fire protection in 10 CFR Part 50; the Significance Determination Process (SDP) used in the inspection program conducted by the U.S. Nuclear Regulatory Commission (NRC); and, most recently, the risk-informed performance-based (RI/PB) voluntary fire protection licensing basis established under 10 CFR 50.48(c). The RI/PB method is based on the National Fire Protection Association (NFPA) Standard 805, *Performance-Based Standard for Fire Protection for Light-Water Reactor Generating Plants*.

The seven volumes of this NUREG-series report provide technical documentation concerning the predictive capabilities of a specific set of fire dynamics calculation tools and fire models for the analysis of fire hazards in postulated nuclear power plant (NPP) scenarios. Under a joint memorandum of understanding (MOU), the NRC Office of Nuclear Regulatory Research (RES) and the Electric Power Research Institute (EPRI) agreed to develop this technical document for NPP application of these fire modeling tools. The objectives of this agreement include creating a library of typical NPP fire scenarios and providing information on the ability of specific fire models to predict the consequences of those typical NPP fire scenarios. To meet these objectives, RES and EPRI initiated this collaborative project to provide an evaluation, in the form of verification and validation (V&V), for a set of five commonly available fire modeling tools.

The road map for this project was derived from NFPA 805 and the American Society for Testing and Materials (ASTM) Standard E 1355, *Standard Guide for Evaluating the Predictive Capability of Deterministic Fire Models*. These industry standards form the methodology and process used to perform this study. Technical review of fire models is also necessary to ensure that those using the models can accurately assess the adequacy of the scientific and technical bases for the models, select models that are appropriate for a desired use, and understand the levels of confidence that can be attributed to the results predicted by the models. This work was performed using state-of-the-art fire dynamics calculation methods/models and the most applicable fire test data. Future improvements in the fire dynamics calculation methods/models and additional fire test data may impact the results presented in the seven volumes of this report.

This document does not constitute regulatory requirements, and NRC participation in this study neither constitutes nor implies regulatory approval of applications based on the analysis contained in this text.
The analyses documented in this report represent the combined efforts of individuals from RES and EPRI. Both organizations provided specialists in the use of fire models and other FHA tools to support this work. The results from this combined effort do not constitute either a regulatory position or regulatory guidance. Rather, these results are intended to provide technical analysis of the predictive capabilities of five fire dynamic calculation tools, and they may also help to identify areas where further research and analysis are needed.

Brian W. Sheron, Director
Office of Nuclear Regulatory Research
U.S. Nuclear Regulatory Commission

CONTENTS

FIGURES

TABLES

REPORT SUMMARY

This report documents the verification and validation (V&V) of five selected fire models commonly used in support of risk-informed and performance-based (RI/PB) fire protection at nuclear power plants (NPPs).

Background
Since the 1990s, when it became the policy of the NRC to use risk-informed methods to make regulatory decisions where possible, the nuclear power industry has been moving from prescriptive rules and practices toward the use of risk information to supplement decision-making. Several initiatives have furthered this transition in the area of fire protection. In 2001, the National Fire Protection Association (NFPA) completed the development of NFPA Standard 805, *Performance-Based Standard for Fire Protection for Light-Water Reactor Electric Generating Plants*, 2001 Edition. Effective July 16, 2004, the NRC amended its fire protection requirements in Title 10, Section 50.48(c), of the *Code of Federal Regulations* [10 CFR 50.48(c)] to permit existing reactor licensees to voluntarily adopt fire protection requirements contained in NFPA 805 as an alternative to the existing deterministic fire protection requirements. RI/PB fire protection often relies on fire modeling for determining the consequence of fires. NFPA 805 requires that the "fire models shall be verified and validated," and "only fire models that are acceptable to the Authority Having Jurisdiction (AHJ) shall be used in fire modeling calculations."

Objectives
- To perform V&V studies of selected fire models using a consistent methodology (ASTM I 1335)

- To investigate the specific fire modeling issue of interest to NPP fire protection applications

- To quantify fire model predictive capabilities to the extent that can be supported by comparison with selected and available experimental data.

Approach
This project team performed V&V studies on five selected models: (1) NRC's NUREG-1805 Fire Dynamics Tools (FDTS), (2) EPRI's Fire-Induced Vulnerability Evaluation Revision 1 (FIVE-Rev1), (3) National Institute of Standards and Technology's (NIST) Consolidated Model of Fire Growth and Smoke Transport (CFAST), (4) Electricité de France's (EdF) MAGIC, and (5) NIST's Fire Dynamics Simulator (FDS). The team based these studies on the guidelines of the ASTM E 1355, *Standard Guide for Evaluating the Predictive Capability of Deterministic Fire Models*. The scope of these V&V studies was limited to the capabilities of the selected fire

models and did not cover certain potential fire scenarios that fall outside the capabilities of these fire models.

Results

The results of this study are presented in the form of relative differences between fire model predictions and experimental data for fire modeling attributes such as plume temperature that are important to NPP fire modeling applications. While the relative differences sometimes show agreement, they also show both under-prediction and over-prediction in some circumstances. These relative differences are affected by the capabilities of the models, the availability of accurate applicable experimental data, and the experimental uncertainty of these data. The project team used the relative differences, in combination with some engineering judgment as to the appropriateness of the model and the agreement between model and experiment, to produce a graded characterization of each fire model's capability to predict attributes important to NPP fire modeling applications.

This report does not provide relative differences for all known fire scenarios in NPP applications. This incompleteness is attributable to a combination of model capability and lack of relevant experimental data. The first problem can be addressed by improving the fire models, while the second problem calls for more applicable fire experiments.

EPRI Perspective

The use of fire models to support fire protection decision-making requires a good understanding of their limitations and predictive capabilities. While this report makes considerable progress toward this goal, it also points to ranges of accuracies in the predictive capability of these fire models that could limit their use in fire modeling applications. Use of these fire models presents challenges that should be addressed if the fire protection community is to realize the full benefit of fire modeling and performance-based fire protection. Persisting problems require both short-term and long-term solutions. In the short-term, users need to be educated on how the results of this work may affect known applications of fire modeling, perhaps through pilot application of the findings of this report and documentation of the resulting lessons learned. In the long-term, additional work on improving the models and performing additional experiments should be considered.

Keywords

PREFACE

This report is presented in seven volumes. Volume 1, the Main Report, provides general background information, programmatic and technical overviews, and project insights and conclusions. Volume 2 quantifies the uncertainty of the experiments used in the V&V study of these five fire models. Volumes 3 through 7 provide detailed discussions of the verification and validation (V&V) of the following five fire models:

Volume 3   Fire Dynamics Tools (FDT^s)

Volume 4   Fire-Induced Vulnerability Evaluation, Revision 1 (FIVE-Rev1)

Volume 5   Consolidated Model of Fire Growth and Smoke Transport (CFAST)

Volume 6   MAGIC

Volume 7   Fire Dynamics Simulator (FDS)

ACKNOWLEDGMENTS

LIST OF ACRONYMS

AGA	American Gas Association
AHJ	Authority Having Jurisdiction
ASME	American Society of Mechanical Engineers
ASTM	American Society for Testing and Materials
BE	Benchmark Exercise
BFRL	Building and Fire Research Laboratory
BRE	Building Research Establishment
BWR	Boiling-Water Reactor
CDF	Core Damage Frequency
CFAST	Consolidated Fire Growth and Smoke Transport Model
CFD	Computational Fluid Dynamics
CFR	*Code of Federal Regulations*
CSR	Cable Spreading Room
EdF	Electricité de France
EPRI	Electric Power Research Institute
FDS	Fire Dynamics Simulator
FDT^s	Fire Dynamics Tools (NUREG-1805)
FHA	Fire Hazard Analysis
FIVE-Rev1	Fire-Induced Vulnerability Evaluation, Revision 1

FM/SNL	Factory Mutual & Sandia National Laboratories
FPA	Foote, Pagni, and Alvares
FRA	Fire Risk Analysis
GRS	Gesellschaft für Anlagen-und Reaktorsicherheit (Germany)
HGL	Hot Gas Layer
HRR	Heat Release Rate
IAFSS	International Association of Fire Safety Science
iBMB	Institut für Baustoffe, Massivbau und Brandschutz
ICFMP	International Collaborative Fire Model Project
IEEE	Institute of Electrical and Electronics Engineers
IPEEE	Individual Plant Examination of External Events
MCC	Motor Control Center
MCR	Main Control Room
MQH	McCaffrey, Quintiere, and Harkleroad
MOU	Memorandum of Understanding
NBS	National Bureau of Standards (now NIST)
NFPA	National Fire Protection Association
NIST	National Institute of Standards and Technology
NPP	Nuclear Power Plant
NRC	U.S. Nuclear Regulatory Commission
NRR	Office of Nuclear Reactor Regulation (NRC)
PMMA	Polymethyl-methacrylate
PWR	Pressurized Water Reactor

RCP	Reactor Coolant Pump
RES	Office of Nuclear Regulatory Research (NRC)
RI/PB	Risk-Informed, Performance-Based
SBDG	Stand-By Diesel Generator
SDP	Significance Determination Process
SFPE	Society of Fire Protection Engineers
SWGR	Switchgear Room
V&V	Verification & Validation

1
INTRODUCTION

As the use of fire modeling increases in support of day-to-day nuclear power plant (NPP) applications and fire risk analyses, the importance of verification and validation (V&V) also increases. V&V studies build confidence in a model by evaluating its underlying assumptions, capabilities, and limitations, and quantifying its performance in predicting the fire conditions that have been measured in controlled experiments.

This volume documents a V&V study for the Fire Dynamics Simulator (FDS), a computational fluid dynamics (CFD) model, for applications relevant to NPPs. Guidance has been provided by ASTM E 1355, *Standard Guide for Evaluating the Predictive Capability of Deterministic Fire Models* [Ref. 1], including the basic structure of this report.

FDS was developed, and is maintained, by the National Institute of Standards and Technology (NIST). Version 4 was officially released in July 2004, and several minor updates had been released as of the time of publication of this report. All of the simulations performed for the current V&V study were done with Version 4.06. With support from the U.S. Nuclear Regulatory Commission (NRC), the FDS Technical Reference Guide for Version 4 [Ref. 2] was rewritten to follow the basic outline suggested by ASTM E 1355. However, the Guide does not specifically address NPPs. The primary purpose of this report is to document the accuracy of FDS in predicting the results of six sets of large-scale fire experiments that are relevant to NPPs. These results are found in Appendix A and discussed in Chapter 6 of this report. Chapters 2 through 5 provide brief summaries of corresponding chapters within the FDS Technical Reference Guide, which discuss the underlying theory and the numerical methods:

Chapter 2 provides background information about FDS and the V&V process.

Chapter 3 presents a brief technical description of FDS, including a review of the underlying physics and chemistry.

Chapter 4 discusses the mathematical and numerical robustness of FDS.

Chapter 5 addresses the sensitivity of FDS results to various numerical and physical input parameters, the most important of which are the size of the numerical grid and the heat release rate.

Chapter 6 presents an assessment of the accuracy of FDS predictions of experimental measurements made during fire tests that are relevant for nuclear facilities.
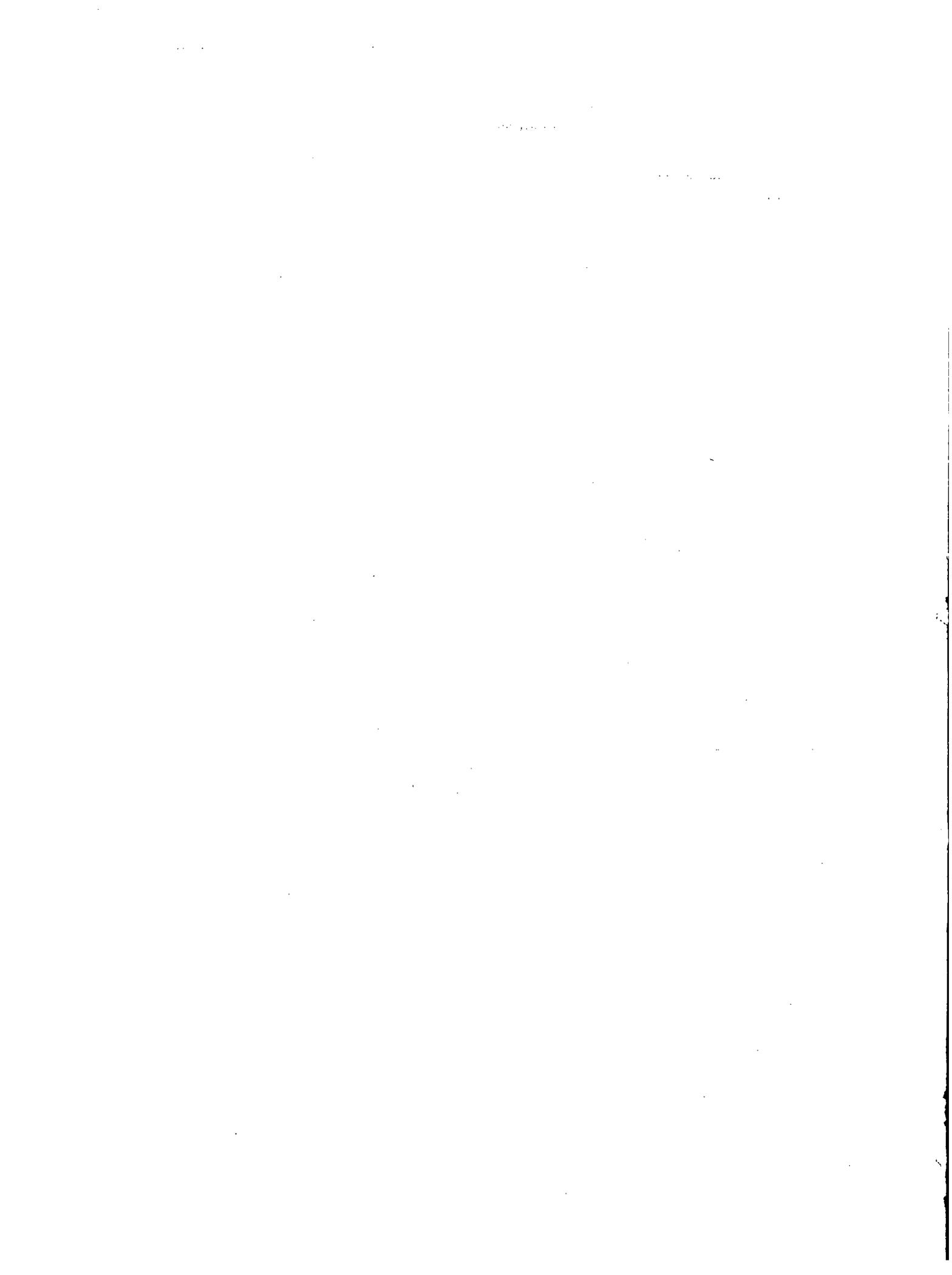
2
MODEL DEFINITION

This chapter contains information about the Fire Dynamics Simulator (FDS), its development, and its use in fire protection engineering. Most of the information has been extracted from the FDS Technical Reference Guide [Ref. 2], which contains a comprehensive description of the governing equations and numerical algorithms used to solve them. The format of this chapter follows that of ASTM E 1355, *Standard Guide for Evaluating the Predictive Capability of Deterministic Fire Models*.

2.1 Name and Version of the Model

Fire Dynamics Simulator (FDS) is a computer program that solves the governing equations of fluid dynamics with a particular emphasis on fire and smoke transport. Smokeview is a companion program that produces images and animations of the FDS calculations. Version 1 of FDS/Smokeview was publicly released in February 2000, Version 2 in December 2001, and Version 3 in November 2002. The present version of FDS/Smokeview is Version 4, which was released in July 2004. Changes in the version number correspond to major changes in the physical model or input parameters. For minor changes and bug fixes, incremental versions are released, referenced according to fractions of the integer version number. Version 4.06 was used for the current study.

2.2 Type of Model

FDS is a computational fluid dynamics (CFD) model of fire-driven fluid flow. The model numerically solves a form of the Navier-Stokes equations appropriate for low-speed, thermally driven flow with an emphasis on smoke and heat transport from fires. The partial derivatives of the conservation equations of mass, momentum, and energy are approximated as finite differences, and the solution is updated in time on a three-dimensional, rectilinear grid. Thermal radiation is computed using a finite volume technique on the same grid as the flow solver. Lagrangian particles are used to simulate smoke movement and sprinkler sprays.

2.3 Model Developers

FDS was developed, and is currently maintained, by the Fire Research Division in the Building and Fire Research Laboratory (BFRL) at the National Institute of Standards and Technology (NIST). A substantial contribution to the development of the model was made by VTT Building and Transport in Finland.

2.4 Relevant Publications

FDS is documented by two publications, the Technical Reference Guide [Ref. 2] and the FDS User's Guide [Ref. 3]. Smokeview is documented in the Smokeview User's Guide [Ref. 4]. The FDS User's Guide describes how to use the model, and the Technical Reference Guide describes the underlying physical principles, provides a comparison with some experimental data, and discusses the limitations of the model.

NIST has developed a public Web site to distribute FDS and Smokeview and support users of the programs. The Web site (http://fire.nist.gov/fds/) also includes documents that describe various parts of the model in detail.

2.5 Governing Equations and Assumptions

Hydrodynamic Model: FDS numerically solves a form of the Navier-Stokes equations appropriate for low-speed, thermally driven flow with an emphasis on smoke and heat transport from fires. The core algorithm is an explicit predictor-corrector scheme, second-order accurate in space and time. Turbulence is treated by means of the Smagorinsky (1963) form of large eddy simulation (LES). It is possible to perform a direct numerical simulation (DNS) if the underlying numerical grid is fine enough.

Combustion Model: For most applications, FDS uses a mixture fraction combustion model. The mixture fraction is a conserved scalar quantity that is defined as the fraction of gas at a given point in the flow field that originated as fuel. The model assumes that combustion is mixing-controlled, and the reaction of fuel and oxygen is infinitely fast. The mass fractions of all of the major reactants and products can be derived from the mixture fraction by means of "state relations," empirical expressions arrived at by a combination of simplified analysis and measurement.

Radiation Transport: Radiative heat transfer is included in the model via the solution of the radiation transport equation for a non-scattering gray gas. In a limited number of cases, a wide band model can be used in place of the gray gas model. The radiation equation is solved using a technique similar to a finite volume method for convective transport, thus the name given to it is the finite volume method.

Geometry: FDS approximates the governing equations on one or more rectilinear grids. The user prescribes rectangular obstructions that are forced to conform to the underlying grid.

Boundary Conditions: All solid surfaces are assigned thermal boundary conditions, plus information about the burning behavior of the material. Usually, material properties are stored in a database and invoked by name. Heat and mass transfer to and from solid surfaces is usually handled with empirical correlations.

<u>Sprinklers and Detectors</u>: The activation of sprinklers and heat and smoke detectors are modeled using fairly simple correlations based on thermal inertia in the case of sprinklers and heat detectors, and the lag in smoke transport through smoke detectors. Sprinkler sprays are modeled by Lagrangian particles that represent a sampling of the water droplets ejected from the sprinkler.

2.6 Input Data Required To Run the Model

All of the input parameters required by FDS to describe a particular scenario are conveyed via one or two text files created by the user. These files contain information about the numerical grid, ambient environment, building geometry, material properties, combustion kinetics, and desired output quantities. The numerical grid is one or more rectilinear meshes with (usually) uniform cells. All geometric features of the scenario have to conform to this numerical grid. An obstruction that is smaller than a single grid cell is either approximated as a single cell or rejected. The building geometry is input as a series of rectangular obstructions. Materials are defined by their thermal conductivity, specific heat, density, thickness, and burning behavior. There are various ways that this information is conveyed, depending on the desired level of detail. A significant part of the FDS input file directs the code to output various quantities in various ways. Much like in an actual experiment, the user must decide before the calculation begins what information to save. There is no way to recover information after the calculation is over if it was not requested at the start. A complete description of the input parameters required by FDS can be found in the FDS User's Guide [Ref. 3].

2.7 Property Data

A number of material properties are needed as inputs for FDS, most related either to solid objects or the fuel. In many fire scenarios, the solid objects are the fuel. For solid surfaces, FDS needs the density, thermal conductivity, specific heat, and emissivity. Note that FDS does not distinguish between walls and various other solid objects, sometimes regarded as "targets" in simpler models.

For the fuel, FDS needs to know whether it is a solid, liquid, or gas; its heat of combustion; its heat of vaporization (liquids and solids); the stoichiometric coefficients of the ideal reaction; the soot and carbon monoxide (CO) yields; and the fraction of energy released in the form of thermal radiation. The radiative fraction is not an inherent property of the fuel, but rather a measured quantity that varies with the size and geometric configuration of the fire. It can be computed directly by FDS, but it is often input directly because it cannot be predicted reliably with the present form of the combustion model.

Some of the property data needed by FDS are commonly available in fire protection engineering and materials handbooks. Depending on the application, properties for specific materials may not be readily available (especially burning behavior at different heat fluxes). A small file distributed with the FDS software contains a database with thermal properties of common materials. This data are given as examples, and users should verify the accuracy and appropriateness of the data.

2.8 Model Results

FDS computes the temperature, density, pressure, velocity and chemical composition within each numerical grid cell at each discrete time step. There are typically hundreds of thousands to several million grid cells and thousands to hundreds of thousands of time steps. In addition, FDS computes at solid surfaces the temperature, heat flux, mass loss rate, and various other quantities. The user must carefully select what data to save, much like one would do in designing an actual experiment. Even though only a small fraction of the computed information can be saved, the output typically consists of fairly large data files. Typical output for the gas phase includes the following quantities:

- gas temperature
- gas velocity
- gas species concentration [water vapor, carbon dioxide (CO_2), CO, and nitrogen (N_2)]
- smoke concentration and visibility estimates
- pressure
- heat release rate per unit volume
- mixture fraction (or air/fuel ratio)
- gas density
- water droplet mass per unit volume

On solid surfaces, FDS predicts additional quantities associated with the energy balance between gas and solid phases, including the following examples:

- surface and interior temperature
- heat flux, both radiative and convective
- burning rate
- water droplet mass per unit area

In addition, the program records the following global quantities:

- total heat release rate (HRR)
- sprinkler and detector activation times
- mass and energy fluxes through openings or solids

Time histories of various quantities at a single point in space or global quantities like the fire's heat release rate (HRR) are saved in simple, comma-delimited text files that can be plotted using a spreadsheet program. However, most field or surface data are visualized with a program called Smokeview, a tool specifically designed to analyze data generated by FDS. FDS and Smokeview are used in concert to model and visualize fire phenomena. Smokeview performs this visualization by presenting animated tracer particle flow, animated contour slices of computed gas variables and animated surface data. Smokeview also presents contours and vector plots of static data anywhere within a scene at a fixed time.

The FDS User's Guide [Ref. 3] provides a complete list of FDS output quantities and formats. The Smokeview User's Guide [Ref. 4] explains how to visualize the results of an FDS simulation.

2.9 Model Limitations

Although FDS can address most fire scenarios, there are limitations in all of its various algorithms. Some of the more prominent limitations of the model are listed here. More specific limitations are discussed as part of the description of the governing equations in the FDS Technical Reference Guide [Ref. 2].

Low-Speed Flow Assumption: The use of FDS is limited to low-speed[1] flow with an emphasis on smoke and heat transport from fires. This assumption rules out using the model for any scenario involving flow speeds approaching the speed of sound, such as explosions, choke flow at nozzles, and detonations.

Rectilinear Geometry: The efficiency of FDS is attributable to the simplicity of its rectilinear numerical grid and the use of fast, direct solvers for the pressure field. This can be a limitation in some situations where certain geometric features do not conform to the rectangular grid, although most building components do. There are techniques in FDS to lessen the effect of "sawtooth" obstructions used to represent nonrectangular objects, but these cannot be expected to produce good results if, for example, the intent of the calculation is to study boundary layer effects. For most practical large-scale simulations, the increased grid resolution afforded by the fast pressure solver offsets the approximation of a curved boundary by small rectangular grid cells.

Fire Growth and Spread: FDS was originally intended for design scenarios where the heat release rate of the fire is specified and the transport of heat and exhaust products is the principal aim of the simulation. However, for fire scenarios where the heat release rate is *predicted* rather than *prescribed*, the uncertainty of the model is higher. There are several reasons for this:
(1) properties of real materials and real fuels are often unknown or difficult to obtain,
(2) the physical processes of combustion, radiation, and solid phase heat transfer are more complicated than their mathematical representations in FDS, and (3) the results of calculations are sensitive to both the numerical and physical parameters.

Combustion: For most applications, FDS uses a mixture fraction combustion model. The mixture fraction is a conserved scalar quantity that is defined as the fraction of gas at a given point in the flow field that originated as fuel. The model assumes that combustion is mixing-controlled, and that the reaction of fuel and oxygen is infinitely fast, regardless of the temperature. For large-scale, well-ventilated fires, this is a good assumption. However, if a fire is in an under-ventilated compartment, or if a suppression agent like water mist or CO_2 is introduced, fuel and oxygen may mix but may not burn. Also, a shear layer with high strain rate separating the fuel stream from an oxygen supply can prevent combustion from taking place. The physical mechanisms underlying these phenomena are complex, and even simplified models still rely on an accurate prediction of the flame temperature and local strain rate. Sub-grid scale modeling of gas phase suppression and extinction is still an area of active research in the combustion community. Until reliable models can be developed for building-scale fire simulations, simple empirical rules can be used that prevent burning from taking place when the atmosphere immediately surrounding the fire cannot sustain the combustion.

---

[1]   Mach numbers less than about 0.3

Radiation: Radiative heat transfer is included in the model via the solution of the radiation transport equation for a non-scattering gray gas, and in some limited cases using a wide band model. The equation is solved using a technique similar to finite volume methods for convective transport, thus the name given to it is the finite volume method. There are several limitations of the model. First, the absorption coefficient for the smoke-laden gas is a complex function of its composition and temperature. Because of the simplified combustion model, the chemical composition of the smoky gases, especially the soot content, can affect both the absorption and emission of thermal radiation. Second, the radiation transport is discretized via approximately 100 solid angles. For targets far away from a localized source of radiation, like a growing fire, the discretization can lead to a non-uniform distribution of the radiant energy. This can be seen in the visualization of surface temperatures, where "hot spots" show the effect of the finite number of solid angles. The problem can be lessened by the inclusion of more solid angles, but at a price of longer computing times. In most cases, the radiative flux to far-field targets is not as important as those in the near-field, where coverage by the default number of angles is much better.

3
THEORETICAL BASIS FOR FDS

This chapter provides a brief overview of the major routines within FDS. A comprehensive description is given in the FDS Technical Reference Guide [Ref. 2], including the assumptions and approximations behind the governing equations, a review of the relevant literature, and the availability of required input data. However, not all of FDS capabilities have been verified and validated in this study.

Table 3-1: FDS Capabilities Included in the V&V Study

Fire Phenomena	Algorithm/Methodology	V&V
Predicting Hot Gas Layer Temperature and Smoke Layer Height in a Room Fire With Natural Ventilation Compartment	Large Eddy Simulation transport for a specified fire	Yes
Predicting Hot Gas Layer Temperature in a Room Fire With Forced Ventilation Compartment	LES transport with forced flow boundary condition	Yes
Predicting Hot Gas Layer Temperature in a Fire Room With Door Closed	LES transport, Mixture Fraction combustion model	Yes
Estimating Burning Characteristics of Liquid Pool Fire, Heat Release Rate, Burning Duration and Flame Height	Mixture Fraction combustion model	Yes
Estimating Wall Fire Flame Height, Line Fire Flame Height Against the Wall, and Corner Fire Flame Height	Mixture Fraction combustion model	No
Estimating Radiant Heat Flux From Fire to a Target	Finite Volume Radiation Model	Yes
Estimating the Ignition Time of a Target Fuel	One dimensional heat conduction in solid with global one-step pyrolysis	No
Estimating Burning Duration of Solid Combustibles	Same	No
Estimating Centerline Temperature of a Buoyant Fire Plume	Large Eddy Simulation of a specified fire	Yes

Fire Phenomena	Algorithm/Methodology	V&V
Estimating Sprinkler Activation	RTI/C-Factor Algorithm	No
Suppression by water spray	Surface cooling or empirical correlation	No
Estimating Smoke Detector Response Time	Heskestad smoke detector model	No
Predicting Compartment Flashover	Mixture Fraction combustion with local extinction	No
Estimating Pressure Rise Attributable to a Fire in a Closed Compartment	Global conservation of mass and energy, plus leakage algorithm	Yes
Calculating the Fire Resistance of Structural Members	One-Dimensional conduction and radiative/convective heat flux	No
Estimating Visibility Through Smoke	Fixed smoke yield from fire and basic LES transport	Yes

3.1   Hydrodynamic Model

FDS solves conservation equations of mass, momentum, and energy for an expandable mixture of ideal gases in the low Mach number limit [Ref. 5]. This means that the equations do not permit acoustic waves, the result of which is that the time step for the numerical solution is bounded by the flow speed, rather than the sound speed. The assumption also reduces the number of unknowns by one, as density and temperature can be related to a known background pressure. Flow turbulence is treated by large eddy simulation, specifically, Smagorinsky's method [Ref. 6].

3.2   Combustion Model

For most simulations, FDS uses a mixture fraction combustion model. The mixture fraction is a conserved scalar that represents the mass fraction of gases at a given point that originate in the fuel stream. In short, the combustion is assumed to be controlled by the rate at which fuel and oxygen mix, and the reaction is instantaneous, regardless of temperature. The reaction occurs at an infinitely thin "flame sheet," for which the location in the flow is dictated by the basic stoichiometry of the reaction.

Because the mixture fraction model assumes that fuel and oxygen react readily on contact, it is necessary to supplement the model with an empirical description of flame extinction in oxygen-limited compartments. A simple model, based on the work of Quintiere [Ref. 7]

and Beyler [Ref. 8], uses the local temperature and oxygen concentration near the flame sheet to determine if combustion can be sustained.

3.3 Thermal Radiation Model

Soot is the combustion product that contributes the most to thermal radiation in large-scale fire scenarios. FDS treats the combustion product mixture as a gray medium because the radiation spectrum of soot is continuous. Using the gray gas approximation, FDS solves the radiation transport equation (RTE) using a finite volume numerical algorithm supplemented by a "look-up" table of absorption coefficients from a narrow-band model called RadCal [Ref. 9]. The spatial discretization of the RTE is achieved by dividing the unit sphere into roughly 100 solid angles by default. This is a user-controlled parameter.

3.4 Thermal Boundary Conditions

FDS applies different boundary conditions depending on the type of surface. Sometimes the user specifies that a fuel surface heats up and burns according to the heat feedback from the fire and the surrounding gases. At other times, fuel surfaces are simply assumed to burn at a prescribed rate. Some surfaces, like inert walls, do not burn at all. For an LES calculation, FDS uses a combination of natural and forced convection correlations to determine the convective heat flux to a surface. If a solid material is assumed to be thermally thick, a one-dimensional heat conduction equation determines its temperature and burning rate. If a material is assumed to be thermally thin, its temperature is assumed to be uniform throughout its thickness. The burning rate of liquid fuels is dictated by the Clausius-Clapeyron relationship of partial pressures [Ref. 10]. Heat transfer and burning of charring materials are modeled using a one-dimensional model from Atreya [Ref. 11] and modified by Ritchie et al. [Ref. 12].

3.5 Numerical Methods

Spatial derivatives in the Navier-Stokes equations are written as second-order finite differences on the rectilinear grid. Scalar quantities are assigned in the center of a cell, whereas vector quantities are assigned on the face of a cell. The flow variables are updated in time with an explicit, second-order predictor-corrector scheme. The convective terms of the mass transport equations are written as upwind-biased differences in the predictor step and downwind-biased differences in the corrector step. Thermal and material diffusion terms are pure central differences. The temperature is extracted from the density via the equation of state, and the heat release rate is extracted from the gradient of the mixture fraction across the flame sheet (essentially the mass flux of either fuel or oxygen times the heat of combustion). The temperatures of a solid are updated in time with an implicit Crank-Nicholson scheme. Wall temperatures are coupled to the fluid calculation via a "ghost" cell inside the wall, where temperatures and densities are specified based on empirical correlations. The time step is constrained by one condition, which ensures that the solution of the equations cannot be updated with a time step larger than the amount of time a parcel of fluid can cross a grid cell (Courant condition), and by another condition for very small grid cells typical of explicit, second-order schemes for solving parabolic partial differential equations. The Poisson equation for pressure is derived by taking the divergence of the momentum equation.

This equation is an elliptic partial differential equation solved with a direct Fast Fourier Transform (FFT) method.

3.6 Theoretical Development of the Model

ASTM E 1355 includes guidance on assessing the theoretical basis of the model including a review of the model "by one or more recognized experts fully conversant with the chemistry and physics of fire phenomenon, but not involved with the production of the model." FDS has been subjected to independent review both internally (at NIST), and externally. NIST documents and products receive extensive reviews by NIST staff who are not directly associated with their development. Internal reviews have been conducted on all previous versions of the FDS Technical Reference Guide over the last decade. Externally, the theoretical basis for the model has been published in peer-reviewed journals and conference proceedings. In addition, FDS is used worldwide by fire protection engineering firms, which validate the model for their particular applications. Some of these firms also publish in the open literature reports documenting internal efforts to validate the model for a particular use. Finally, FDS is referenced in the NFPA 805 standard.

3.6.1 Assessment of the Completeness of Documentation

The two primary documents on FDS are the FDS Technical Reference Guide [Ref. 2] and the FDS User's Guide [Ref. 3]. The Technical Reference Guide documents the governing equations, assumptions, and approximations of the various sub-models. At the request of the NRC, the Technical Reference Guide was formatted according to the outline suggested in ASTM E 1355. It describes the fundamental governing equations of the model and how they are solved numerically, but refers to papers and books for the full derivations of equations or numerical techniques used. The FDS User's Guide provides details on the actual execution of the program, the input parameters, output, and so forth.

Most FDS users are able to read the manuals and perform simulations without the benefit of a formal training course. The users frequently contact the developers at NIST to request further explanation of the documentation or to suggest clarifications.

3.6.2 Assessment of Justification of Approaches and Assumptions

The technical approach and assumptions of FDS have been presented in the peer-reviewed scientific literature and at technical conferences. All documents released by NIST go through an internal editorial review and approval process. FDS is subjected to continuous scrutiny because it is available to the general public and is used internationally by specialists in fire safety design and post-fire reconstruction. The source code for FDS is released publicly, and has been used at various universities worldwide, both in research and the classroom as a teaching tool. As a result, flaws in the theoretical development and the computer program itself have been identified and fixed.

3.6.3 Assessment of Constants and Default Values

No single document provides a comprehensive assessment of the numerical and physical parameters used in FDS. Specific parameters have been tested in various V&V studies performed at NIST and elsewhere. Numerical parameters are taken from the literature and do not undergo formal review. The model user is expected to assess the appropriateness of the FDS default values and change them if necessary.
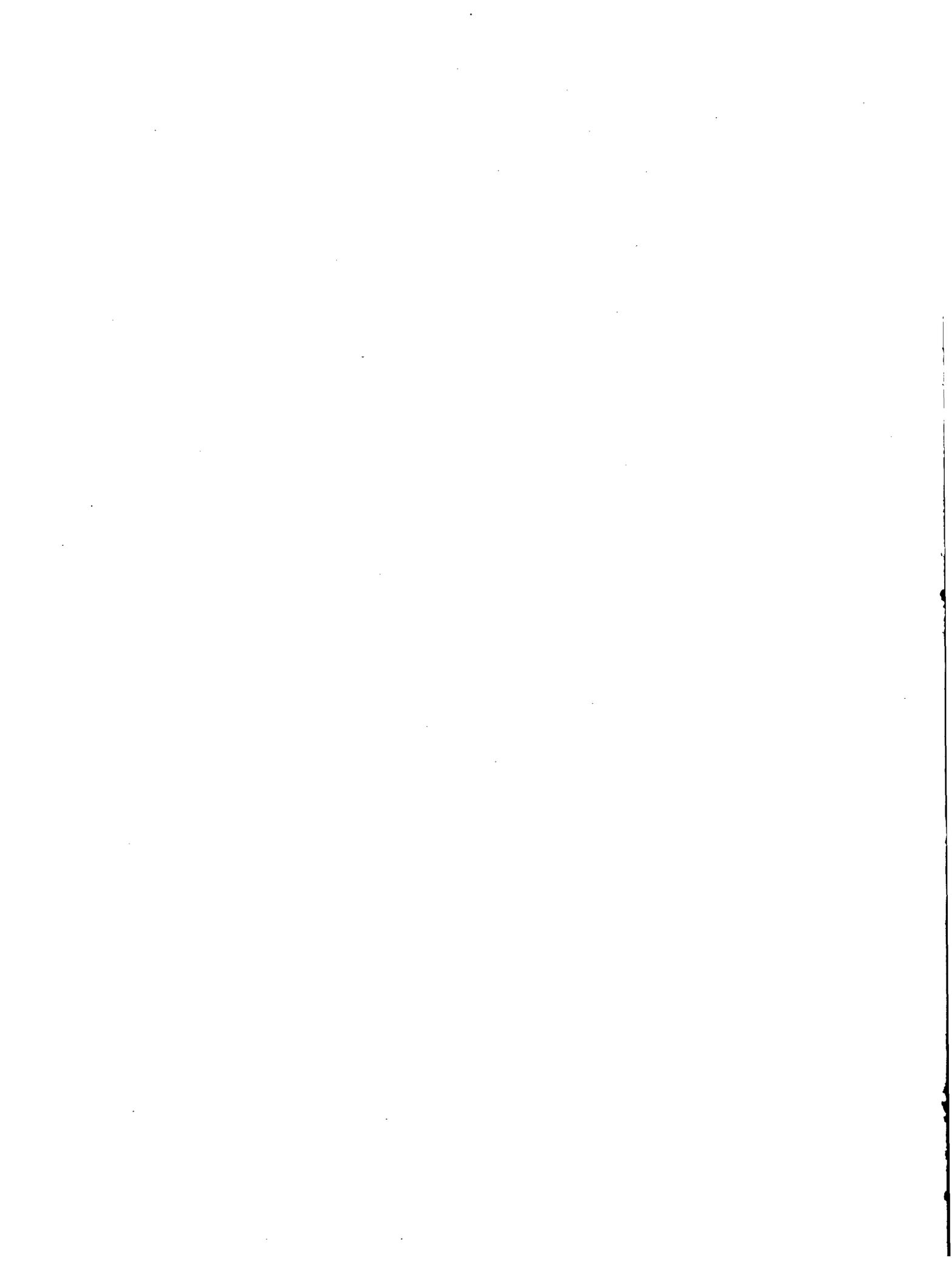
4
MATHEMATICAL AND NUMERICAL ROBUSTNESS

4.1 Introduction

This chapter briefly describes how the mathematical and numerical robustness of FDS has been verified in accordance with the general criteria listed in ASTM E 1355:

Analytical Tests: Comparison of the computed solutions with closed-form solutions of the governing equations.

Code Checking: Verification of the basic structure of the computer code, either manually or automatically with a code-checking program, to detect irregularities and inconsistencies.

Numerical Tests: Assessment of the magnitude of the residuals from the solution of a numerically solved system of equations (as an indicator of numerical accuracy) and the reduction in residuals (as an indicator of numerical convergence).

4.2 Analytical Tests

There are no closed-form mathematical solutions for the fully turbulent, time-dependant Navier-Stokes equations. CFD provides an approximate solution for the non-linear partial differential equations by replacing them with discretized algebraic equations that can be solved using a powerful computer. Certain sub-models address phenomena that have analytical solutions (e.g., one-dimensional heat conduction through a solid). The developers of FDS routinely use analytical solutions to test sub-models to verify the correctness of the coding of the model [Refs. 13 and 14]. Such routine verification efforts are relatively simple and the results may not always be published or included in the documentation. With each new release of FDS, a standard set of verification calculations is run to ensure that no new errors have been introduced into the source code. Some of these include the following examples:

- heat conduction into a semi-infinite solid
- evaporation of water droplets in uniform temperature environment
- radiation heat transfer from a uniform temperature hot object
- pressure increase in a sealed or slightly leaky compartment attributable to fire or fan
- idealized reaction of fuel and oxygen in an adiabatic chamber

The common thread in all of these exercises is the well-defined initial and final states, which test the basic conservation laws. Less straightforward is the simulation of fluid motion. Rehm, Baum, and coworkers checked the hydrodynamic solver that evolved to form the core of FDS against analytical solutions of simplified fluid flow phenomena [Refs. 16, 17, and 18]. This early work tested the stability and consistency of the basic hydrodynamic solver, especially the velocity-pressure coupling that is vitally important in low Mach number applications. Many numerical algorithms developed up to that time were intended for high-speed flow applications (e.g., aerospace applications). The developers of FDS adopted many techniques originally developed for meteorological models, and the techniques had to be tested to determine whether they were appropriate for describing relatively low-speed flow within enclosures. In more recent years, simulations of plumes, ceiling jets, and other commonly studied fire-driven flows have replaced the analytical solutions of simplified flows because of the need to consider turbulence.

4.3 Code Checking

FDS has been compiled and run on computers manufactured by several companies and run under various operating systems, including UNIX®, Linux®, Microsoft Windows®, and Macintosh OSX®. Various FORTRAN compilers have been used as well. Each combination of hardware, operating system, and compiler involves a slightly different set of compiler and run-time options. Compliance with the FORTRAN 90 ISO/ANSI standard improves the *portability* of the program. By adhering to the standard, the code is streamlined and outdated or potentially harmful code is removed.

NIST also publicly releases the FDS source code. Individual users have modified the source code for their specific applications and compiled and run it successfully, have provided useful feedback to NIST on the organization of the code, and increased the code's portability.

This V&V project began using Version 4.05 of FDS. As part of the V&V process, several improvements were made and a minor bug was corrected in this version. The improvements were mostly to expand the output options, as illustrated by the following examples:

- FDS can automatically compute hot gas layer (HGL) temperature and height. These are not part of a CFD calculation.

- FDS can now predict thermocouple temperatures, rather than gas temperatures. Because temperatures are usually measured by thermocouples, this capability is useful when comparing FDS temperature outputs to experimental data.

- FDS now has the capability to mimic radiometers, net heat flux gauges, and total heat flux gauges. These are the most common measurement tools for heat flux. This capability is useful when comparing FDS heat flux outputs to experimental data.

A minor bug was identified and fixed as a result of using FDS in this V&V process. The bug involved a flaw in the smoke species boundary condition, which allowed the smoke concentration to increase even after the fire was suppressed. This bug only occurred in simulations of sealed compartments, something not commonly done with FDS to date.

The final version of FDS used in this study is Version 4.06 and includes the changes described above.

4.4   Numerical Tests

The use of finite differences to approximate spatial and temporal partial derivatives introduces error into the FDS calculation. This numerical error is dependent on the grid size. As the numerical grid is refined, the numerical error decreases. If the grid is refined to about 1 mm (0.04 inch) or less, the simulation becomes a *direct numerical simulation* (DNS), where no assumptions about the underlying turbulence need to be made. While DNS simulations are too costly for practical fire calculations, they can be useful in checking the numerics because there exist in the literature a variety of small-scale fluid flow and combustion experiments that can be simulated in great detail. Numerous comparisons between experiments and DNS solutions using FDS [Refs. 19, 20, 21, and 22] have shown that the hydrodynamic solver is robust and without serious flaws.
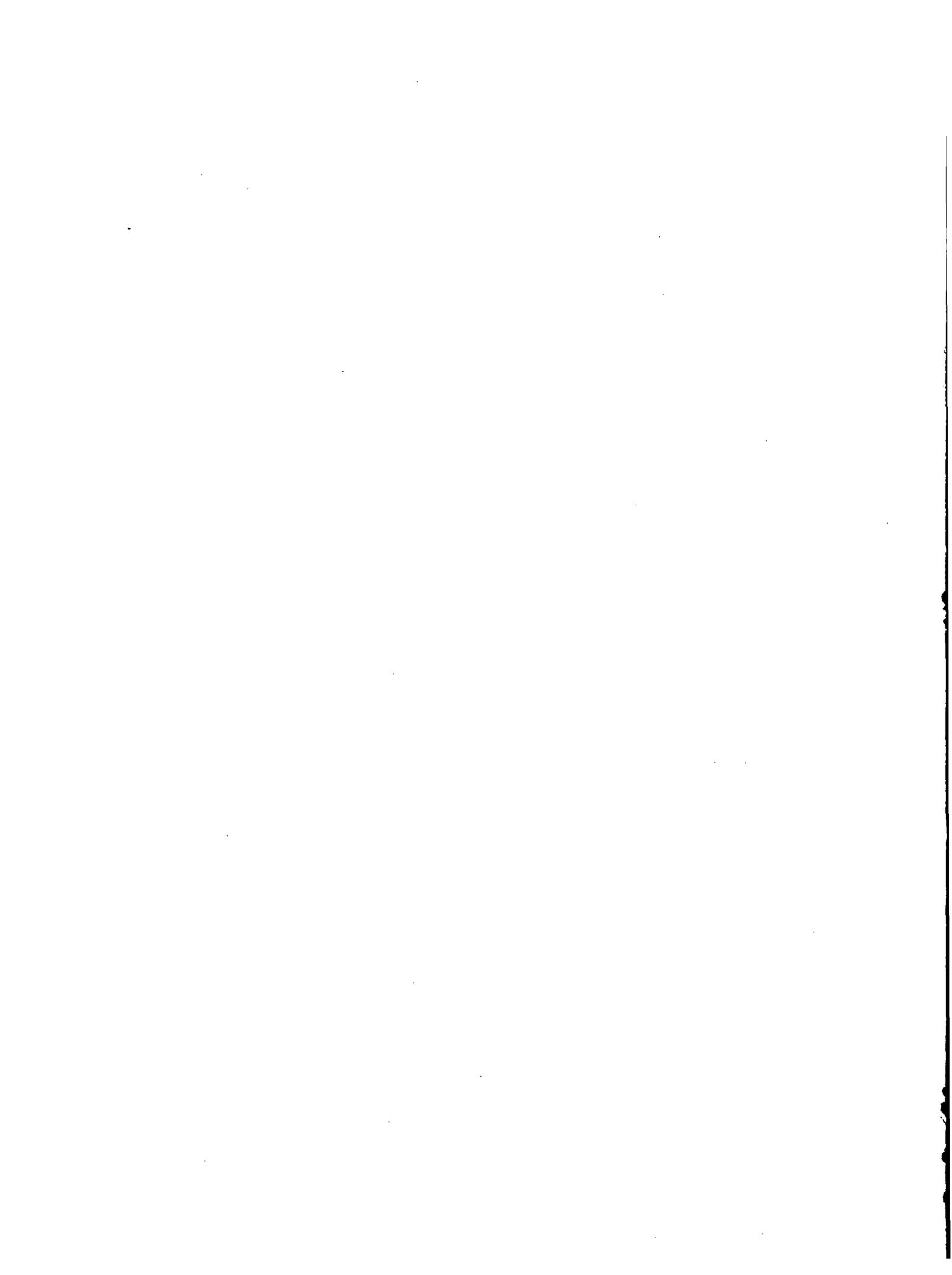
5
MODEL SENSITIVITY

This chapter discusses the issue of model sensitivity, or how changes in the FDS input parameters affect the model'ss results. Input parameters can be divided into two groups, namely numerical and physical. For a CFD model, an important numerical parameter is the size of the underlying numerical grid. Physical parameters range from the size of the fire, wall material properties, and product yields. Chapter 5 of the FDS Technical Reference Guide [Ref. 2] reviews sensitivity studies of the various *numerical* parameters in FDS. Chapter 6 of the Reference Guide discusses the influence of the dozens of *physical* parameters that are input to the model. The present chapter considers both numerical and physical parameters, in light of the validation experiments that are discussed in the next chapter.

5.1   Sensitivity to Grid Size

The most important numerical parameter in FDS is the grid cell size. CFD models solve an approximate form of the conservation equations of mass, momentum, and energy on a numerical grid. The error associated with the discretization of the partial derivatives is a function of the size of the grid cells and the type of differencing used. FDS uses second-order accurate approximations of both the temporal and spatial derivatives of the Navier-Stokes equations, meaning that the discretization error is proportional to the square of the time step or cell size. In theory, reducing the grid cell size by a factor of 2 reduces the discretization error by a factor of 4. However, it also increases the computing time by a factor of 16 (a factor of 2 for the temporal and each spatial dimension). Clearly, there is a point of diminishing returns as one refines the numerical mesh. Determining what size grid cell to use in any given calculation is known as a *grid sensitivity study*.

A grid sensitivity study was performed for all of the experimental test series that are discussed in Chapter 6. For example, Figure 5-1 displays predictions of the plume temperature for Test 5 of the FM/SNL series, computed on 10-cm, 7.5-cm, and 5-cm (4-inch, 3-inch, and 2-inch) grids. The 10-cm simulation required a few hours to complete on a single 2.4-GHz Pentium processor, whereas the 5-cm (2-inch) simulation required a few days. The prediction is noticeably better on the 5-cm (2-inch) grid because the entrainment of air into the hot plume is described with much greater fidelity in the 5-cm (2-inch) case. Refining the mesh further does not make a noticeable difference in the results, even though the fidelity of the simulation continues to improve. With any grid resolution study, a point of diminishing returns is reached when the improvement in the quality of the results is outweighed by the "cost" of the computation. When this point is reached depends on the application. It also depends on the quantities that are of interest. Some quantities, like HGL temperature or height, do not typically require as fine a numerical grid as quantities such as the heat flux to targets near the fire.
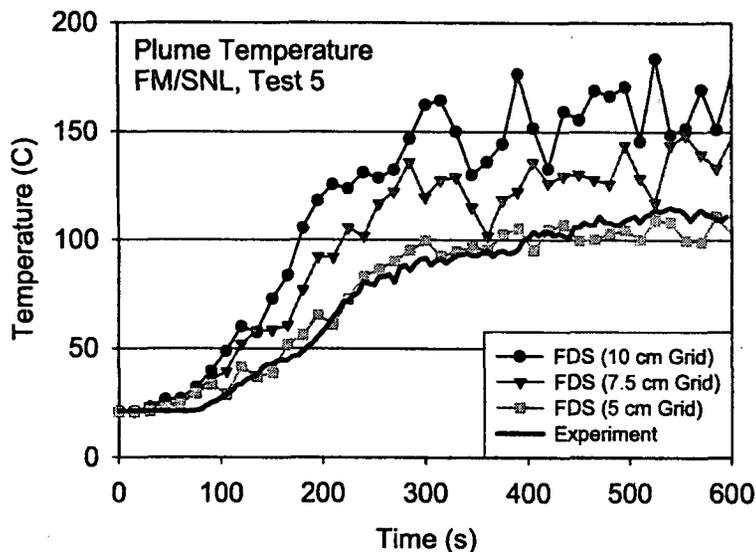
Figure 5-1: Grid Sensitivity Study for FM/SNL Test 5

A case in point is Test 3 of the International Collaborative Fire Model Project (ICFMP) Benchmark Exercise (BE) #3. This simulation has been performed with a variety of different input parameters, most notably a 10-cm grid versus a 20-cm grid (4-inch vs. 8-inch). Sample results of the 10-cm and 20-cm grids are shown in Figure 5-2. Even on the coarse grid, the basic conservation equations still ensure a reasonably good prediction of the average HGL temperature, and there are no steep gradients in the selected quantities that would have been more sensitive to the grid size. So why is the 10-cm grid chosen for the final validation study? Consider what is not shown in Figure 5-2. The cable trays and other targets, which are difficult to resolve even on the fine grid, are simply too small to include on the coarse grid. The door and vent are less accurately prescribed on the coarse grid, leading to greater error in the computation of the compartment pressure. Still worse, had the fire scenario required a prediction of the heat release rate or flame spread along the cable trays, even the fine grid is not necessarily fine enough to predict these parameters accurately.

Coarse grid CFD can provide reasonable predictions of certain quantities, especially those that can be traced directly to conservation equations of mass and energy, like average temperatures and pressures. However, the user has to be aware that the results are generally less reliable than those obtained from a finer grid, and certain results cannot be obtained at all.
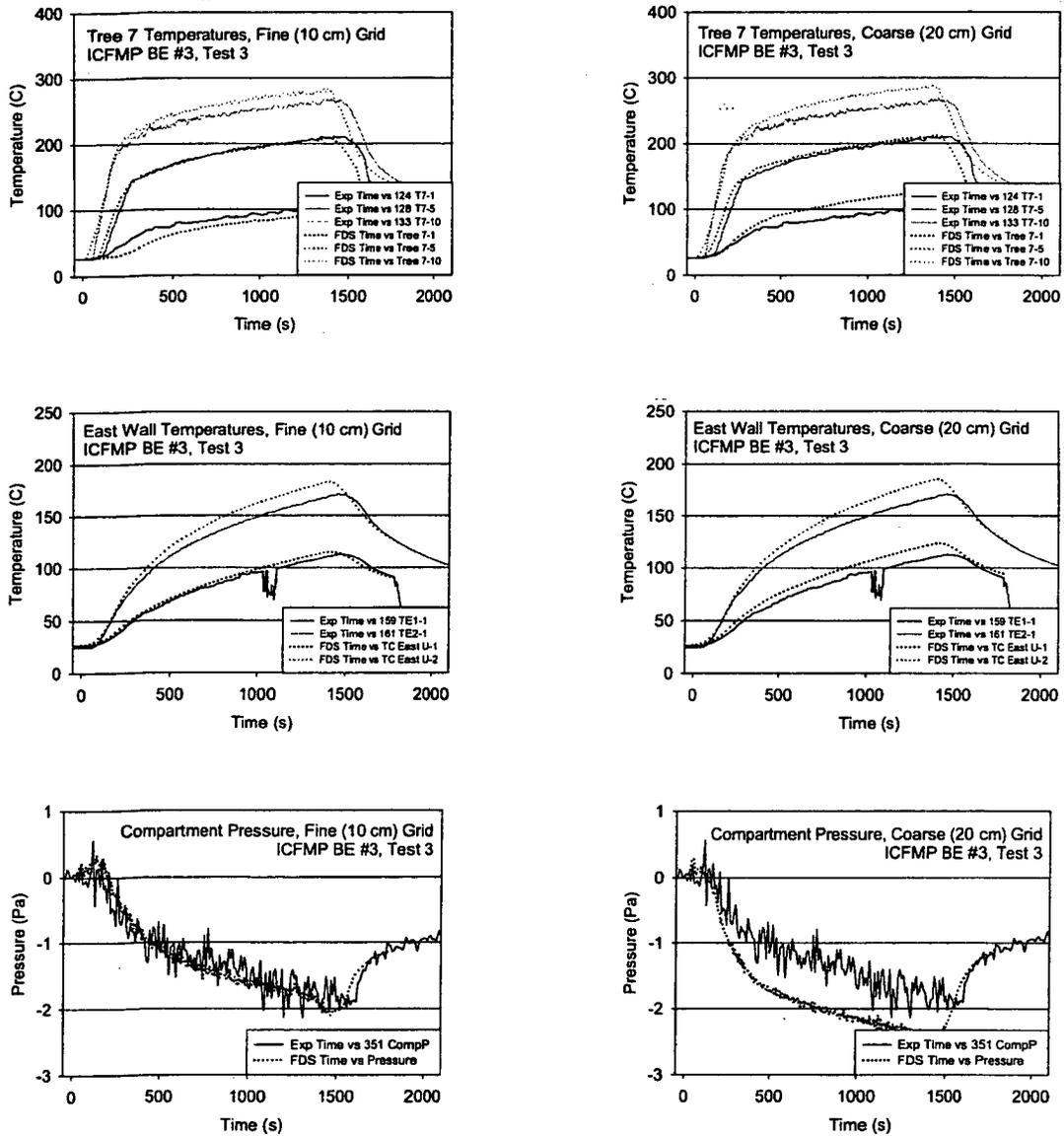
Figure 5-2: Fine (Left) and Coarse (Right) Simulations of ICFMP BE #3, Test 3

5.2 Sensitivity to Radiation Parameters

The grid size determines the fidelity of the finite-difference approximation of the governing hydrodynamic equations. The spatial resolution of the discretized radiation transport equation is another important consideration for applications in which heat flux to targets is important. FDS uses about 100 solid angles with which to distribute radiant energy from the fire and hot gases throughout the compartment and beyond. The decision to use 100 angles as a default is based on a desire for both accuracy and practicality. It has been observed that the use of 100 angles is consistent with the degree of spatial resolution afforded by the grid for the hydrodynamics solver. As an example, for ICFMP BE #3, Test 3, a simulation using 200 radiation angles can be compared with one using the default 100 angles (see Figure 5-3). The absence of any noticeable change in the results confirms, *in this case*, that the default number of angles is adequate. However, this does not mean that the default settings are always appropriate. Sensitivity studies like the one performed here ought to be used to determine if and when to change the default settings.
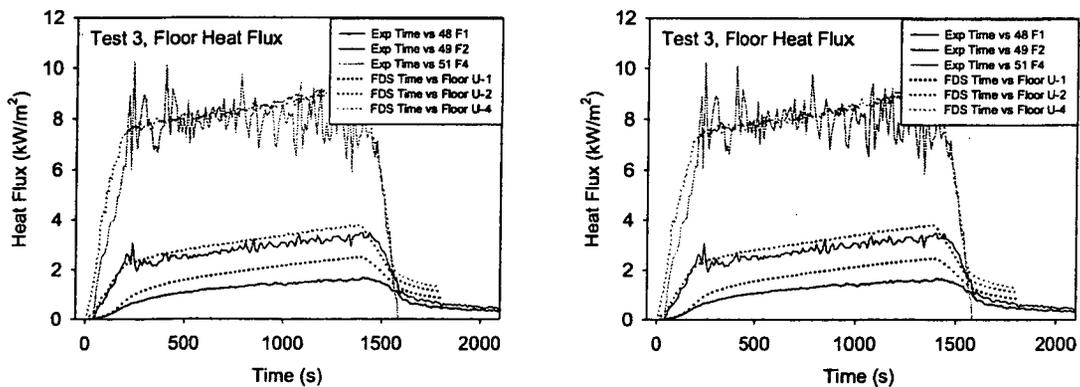
Figure 5-3: ICFMP BE #3 Test 3 Results Using 200 Radiation Angles (Left) and 100 (Right)

5.3 Sensitivity to Turbulence Parameters

FDS uses the Smagorinsky form of the LES technique, in which the viscosity of the gas mixture is modeled with a mathematical expression involving the grid cell size, the local strain rate, and an empirical constant. The thermal conductivity and material diffusivity are related to the modeled viscosity by way of "turbulent" Prandtl and Schmidt numbers. In all, three empirical parameters are needed in the model, all of which are assumed to be constant even though there is considerable debate as to what their values ought to be. The default values in FDS Version 4 are based on simulations of smoke movement in various compartments [Ref. 23].

A typical user of FDS does not modify the turbulence parameters. Nonetheless, it is important to consider their effect on the results of different types of calculations, especially those in which the mixing of different gas species or gases of different temperatures play a key role in the outcome. For example, the simulations of ICFMP BE #2 are time-consuming because of the need for a fairly fine numerical grid to well-resolve the 19-m (62.3-ft) high smoke plume. For one of these cases, the Smagorinsky coefficient (the empirical constant in the expression

for the viscosity) can be reduced from 0.20 to 0.15 to determine its effect on the results.
This reduces the magnitude of the "artificial" viscosity added to the numerical solution, allowing
for a greater level of eddy formation and, thus, greater mixing. In this case, the reduction
in the coefficient leads to about a 15% reduction in the plume temperature, moving the simulation
closer to the experiment. While the rationale for reducing the coefficient is grounded in physics,
it has been found over the years that the lower value makes FDS more prone to numerical instabilities.
Because FDS is used for a wide variety of applications, the Smagorinsky coefficient has been
chosen to balance accuracy and numerical stability.

5.4 Sensitivity to Heat Release Rate

Of all the physical input parameters, the simulation results are most sensitive to the heat release
rate. In this section, one of the validation experiments (ICFMP BE #3, Test 3) is used to demonstrate
the result of increasing and decreasing the specified heat release rate by 15%. Shown in Figure 5-4
are plots of various output quantities demonstrating their sensitivity to the change in heat release rate.
Gas and surface temperatures, oxygen concentration, and compartment pressure show roughly
10% diversions from baseline, whereas the heat fluxes show roughly 20% diversions. The height
of the hot gas layer is relatively insensitive to changes in the heat release rate. These results
are not unexpected, and are consistent with the analysis described in Volume 2 to assess the sensitivity
of the quantities of interest to the uncertainty in the measured heat release rate.
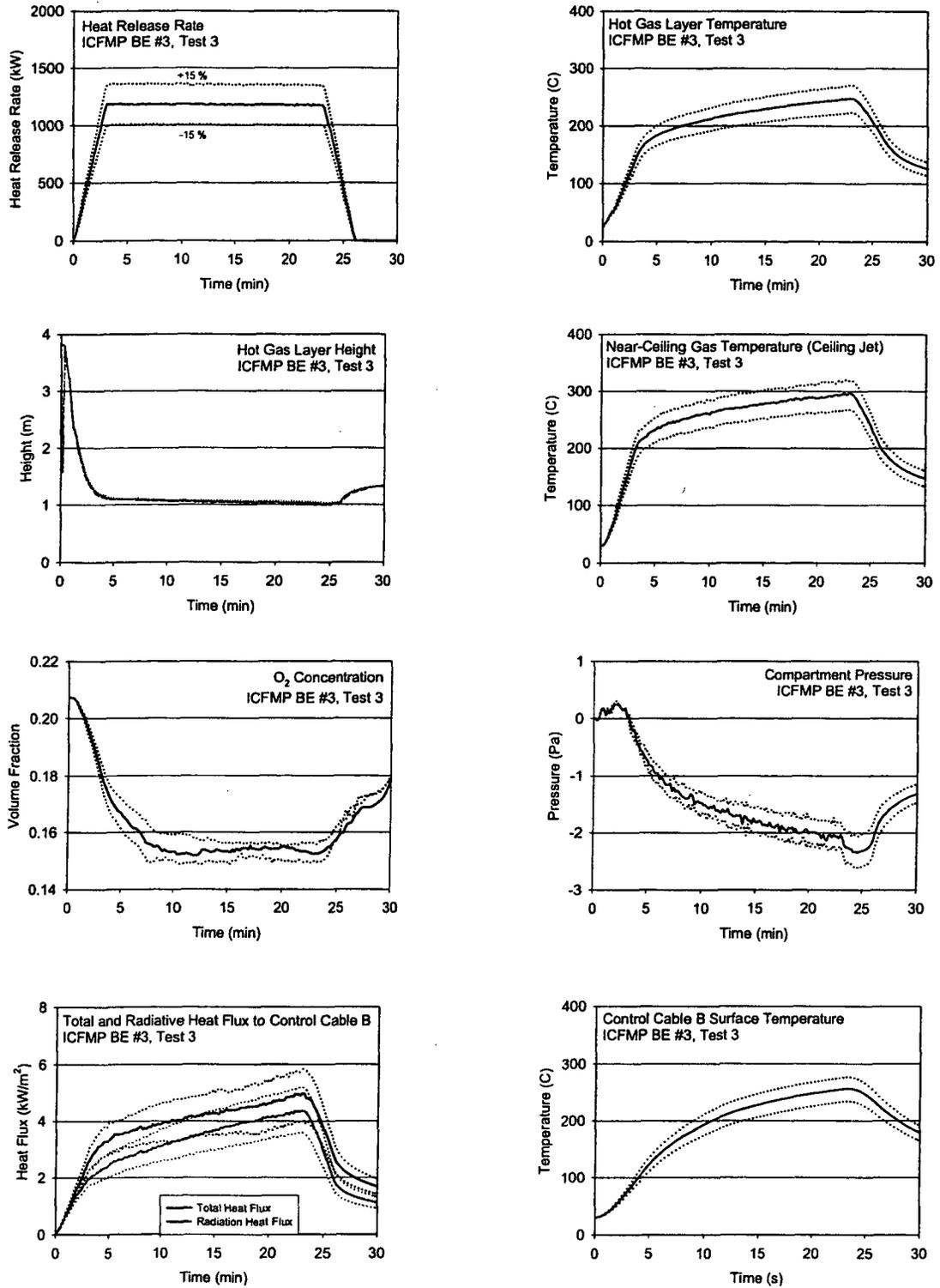
Figure 5-4: Sensitivity of Various Output Quantities to Changes in HRR

5.5 Sensitivity to Other Physical Input Parameters

This chapter describes the sensitivity of FDS results to changes in the major numerical and physical input parameters. Throughout Chapter 6 (Model Validation) and Appendix A are additional examples that demonstrate how changes in various input parameters affect the FDS predictions, as illustrated by the following examples:

- Figure A-13 shows how the temperature of the hot gas layer changes as a result of increased ventilation in the FM/SNL test series.

- Figure A-15 through Figure A-17 show how the temperature of the hot gas layer changes as a result of the opening of a door in the NBS Multi-Room test series.

- Figure A-26 and Figure A-27 show how the upper-layer oxygen and carbon dioxide concentrations change as a result of increased ventilation in the ICFMP BE #3 test series.

- Figure A-31 and Figure A-32 show how the compartment pressure is very sensitive to the leakage rate in the closed-door tests of the ICFMP BE #3 test series.

- Section A.8 shows how the cable surface temperature is sensitive to the surrounding gas temperature and the diameter of the cable.
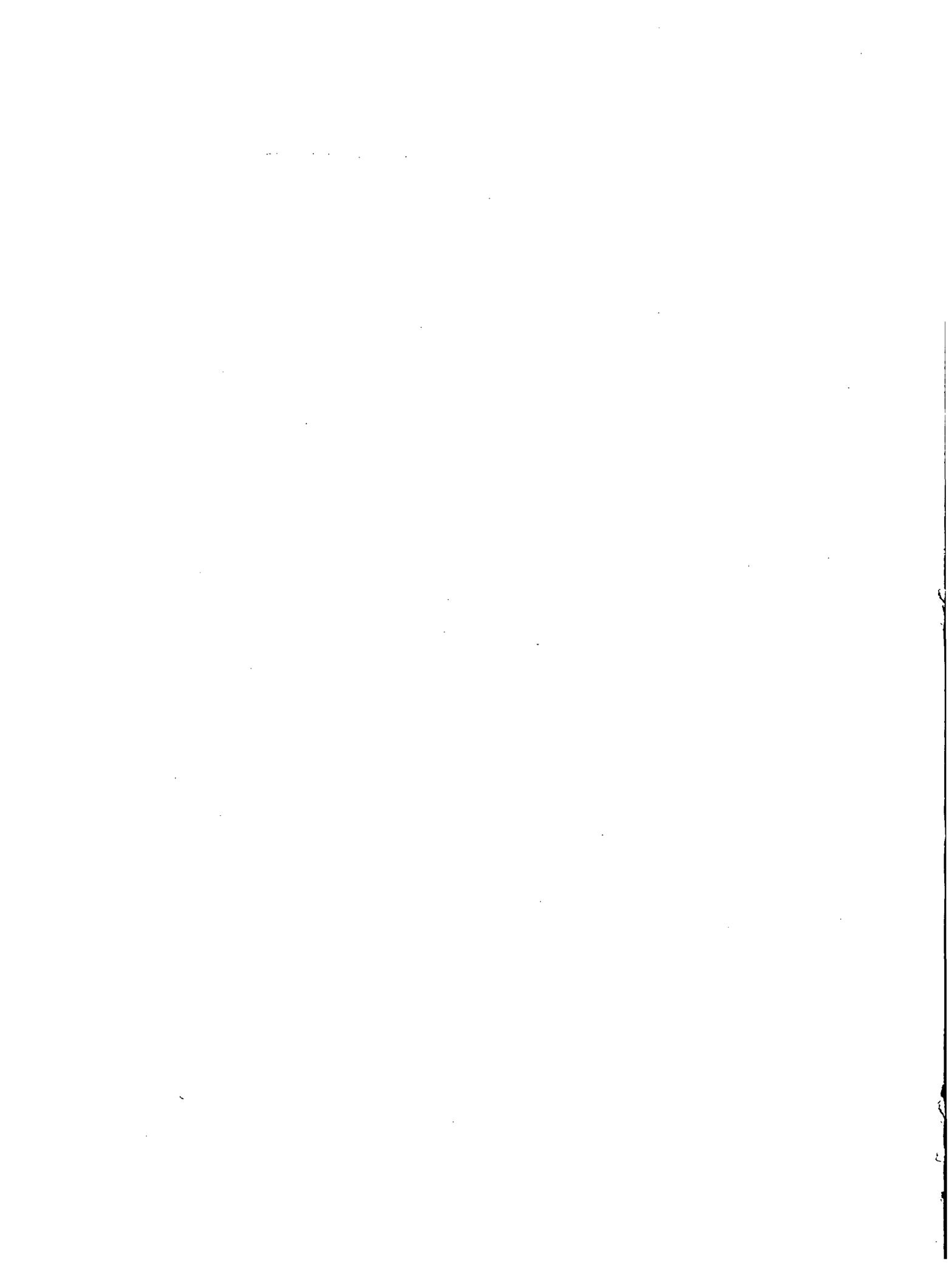
6
MODEL VALIDATION

This chapter summarizes the results of a validation study conducted for FDS, in which its predictions are compared with measurements collected from six sets of large-scale fire experiments. A brief description of each set of experiments is given here. Further details can be found in Volume 2 and in the individual test reports.

ICFMP BE #2: Benchmark Exercise #2 consists of eight experiments, representing three sets of conditions, to study the movement of smoke in a large hall with a sloped ceiling. The results of the experiments were contributed to the International Collaborative Fire Model Project (ICFMP) for use in evaluating model predictions of fires in larger volumes representative of turbine halls in NPPs. The tests were conducted inside the VTT Fire Test Hall, which has dimensions of 19 m high x 27 m long x 14 m wide (62 ft x 88.5 ft x 46 ft). Each case involved a single heptane pool fire, ranging from 2 MW to 4 MW.

ICFMP BE #3: Benchmark Exercise #3, conducted as part of the ICFMP and sponsored by the NRC, consists of 15 large-scale tests performed at NIST in June 2003. The fire sizes range from 350 kW to 2.2 MW in a compartment with dimensions of 21.7 m high x 7.1 m long x 3.8 m wide (71.2 ft x 23.3 ft x 12.5 ft), designed to represent a variety of spaces in a NPP containing power and control cables. The walls and ceiling are covered with two layers of marinate boards, while the floor is covered with one layer of gypsum board on top of plywood. The room has one door with dimensions of 2 m x 2 m (6.6 ft x 6.6 ft), and a mechanical air injection and extraction system. Ventilation conditions and fire size and location are varied, and the numerous experimental measurements include gas and surface temperatures, heat fluxes, and gas velocities.

ICFMP BE #4: Benchmark Exercise #4 consists of kerosene pool fire experiments conducted at the Institut für Baustoffe, Massivbau und Brandschutz (iBMB) of the Braunschweig University of Technology in Germany. The results of two experiments were contributed to the ICFMP. These fire experiments involve relatively large fires in a relatively small [3.6 m x 3.6 m x 5.7 m (12 ft x 12 ft x 19 ft)] concrete enclosure. Only one of the two experiments (Test 1) was selected for the present V&V study.

ICFMP BE #5: Benchmark Exercise #5 consists of fire experiments conducted with realistically routed cable trays in the same test compartment as BE #4. The compartment was configured slightly differently, and the height was 5.6 m (18.4 ft) in BE #5. Only Test 4 was selected for the present evaluation, and only the first 20 minutes, during which an ethanol pool fire pre-heated the compartment.

FM/SNL Series: The Factory Mutual & Sandia National Laboratories (FM/SNL) Test Series is a series of 25 fire tests conducted for the US NRC by Factory Mutual Research Corporation

(FMRC), under the direction of Sandia National Laboratories (SNL). The primary purpose of these tests was to provide data with which to validate computer models for various types of NPP compartments. The experiments were conducted in an enclosure measuring 18 m long x 12 m wide x 6 m high (60 ft x 40 ft x 20 ft), constructed at the FMRC fire test facility in Rhode Island. All of the tests involved forced ventilation to simulate typical NPP installation practices. The fires consist of a simple gas burner, a heptane pool, a methanol pool, or a polymethyl-methacrylate (PMMA) solid fire. Four of these tests were conducted with a full-scale control room mockup in place. Parameters varied during testing are the heat release rate, enclosure ventilation rate, and fire location. Tests 4, 5 and 21 were used in the present evaluation. Test 21 involved the full-scale mockup. All were gas burner fires.

NBS Multi-Room Series: The National Bureau of Standards (NBS, now the National Institute of Standards and Technology, NIST) Multi-Compartment Test Series consists of 45 fire tests representing 9 different sets of conditions, with multiple replicates of each set, which were conducted in a three-room suite. The suite consists of two relatively small rooms, connected via a relatively long corridor. The fire source, a gas burner, is located against the rear wall of one of the small compartments. Fire tests of 100, 300, and 500 kW were conducted, but only three 100-kW fire experiments (Tests 100A, 100O, and 100Z) were used for the current V&V study.

This chapter documents the comparison of FDS predictions with the experimental measurements for the six test series. Technical details of the calculations, including output of the model and comparison with experimental data are provided in Appendix A. The results are organized by quantity as follows:

- hot gas layer (HGL) temperature and height
- ceiling jet temperature
- plume temperature
- flame height
- oxygen and carbon dioxide concentration
- smoke concentration
- compartment pressure
- radiation heat flux, total heat flux, and target temperature
- wall heat flux and surface temperature

The model predictions are compared to the experimental measurements in terms of the relative difference between the maximum (or where appropriate, minimum) values of each time history:

$$\varepsilon = \frac{\Delta M - \Delta E}{\Delta E} = \frac{(M_p - M_o) - (E_p - E_o)}{(E_p - E_o)}$$

ΔM is the difference between the peak value of the model prediction, M_p, and its original value, M_o. ΔE is the difference between the experimental measurement, E_p, and its original value, E_o. A positive value of the relative difference indicates that the model over-predicted the severity of the fire (e.g., a higher temperature, lower oxygen concentration, higher smoke concentration, etc.).

The measure of model "accuracy" used throughout this study is related to experimental uncertainty. Volume 2 discusses this issue in detail. In brief, the accuracy of a *measurement*, for example,

a gas temperature, is related to the measurement device, a thermocouple. In addition, the accuracy of the *model prediction* of the gas temperature is related to the simplified physical description of the fire and the accuracy of the input parameters, especially the *specified* heat release rate. Ideally, the purpose of a validation study is to determine the accuracy of the model in the absence of any errors related to the measurement of both its inputs and outputs. Because it is impossible to eliminate experimental uncertainty, at the very least a combination of the uncertainty in the measurement of model inputs and output can be used as a yardstick. If the numerical prediction falls within the range of uncertainty attributable to both the measurement of the input parameters and the output quantities, it is not possible to further quantify its accuracy. At this stage, it is said that the prediction is *within experimental uncertainty*.

Each section in this chapter contains scatter plots that summarize the relative difference results for all of the predictions and measurements of the quantity under consideration. Details of the calculations, the input assumptions, and the time histories of the predicted and measured output are included in Appendix A. Only a brief discussion of the results is included in this chapter. At the end of each section, a color rating is assigned to each of the output categories, indicating, in a very broad sense, how well the model treats these quantities. A detailed discussion of this rating system is included in Volume 1. For FDS, only the Green and Yellow ratings have been assigned to the 13 quantities of interest. The color Green indicates that the research team has concluded that the model physics accurately represent the experimental conditions, and the differences between model prediction and experimental measurement are less than the combined experimental uncertainty. The color Yellow suggests that one should exercise caution when using the model to evaluate this quantity; consider carefully the assumptions made by the model, how the model has been applied, and the accuracy of its results. There is specific discussion of model limitations for the quantities assigned a Yellow rating.

In assessing the accuracy of FDS in predicting the 13 quantities, it is important to keep in mind that a CFD model, unlike a zone model or empirical correlation, has the potential to produce ever-more accurate results as the numerical grid is refined. However, FDS calculations require hours or days to complete, depending on the size of the numerical grid and the desired level of accuracy. Engineers using FDS need results in a reasonable amount of time; thus, they need guidance on what size grid to use for a given application that will produce good results in a timely manner. A few simple rules have been developed over the past few years that provide this information, and these rules have been applied in the calculations for which results are included in Appendix A and summarized below.

Table 6-1 lists some common metrics used to assess the size of the fire relative to the size of the compartment. The following is a brief description of the various quantities included in Table 6-1:

Heat Release Rate (HRR or $\dot{Q}$): The most important parameter of any fire experiment is the overall heat release rate. In some cases, the fire model is used to predict the heat release rate. In the present study, however, the heat release rate is specified, and the model is used to predict how the fire's energy is transported throughout the compartment. A non-dimensional quantity relating the HRR to the diameter of the fire, D, is commonly known as $Q*$:

$$Q^* = \frac{\dot{Q}}{\rho_\infty c_p T_\infty \sqrt{gD} D^2}$$

where $\dot{Q}$ is the heat release rate, ρ_∞ is the ambient density, T_∞ is the ambient temperature, c_p is the specific heat, and g is the acceleration of gravity. A large value of Q^* describes a fire for which the energy output is relatively large compared to its physical diameter, like an oil well blowout fire. A low value describes a fire for which the energy output is relatively small compared to its diameter, like a brush fire. Most common accidental fire scenarios have Q^* values on the order of 1. Its relevance to the current validation study is mainly in the assessment of flame height.

Table 6-1: Summary of the Fire Experiments in Terms of Commonly Used Metrics

Test Series	$\dot{Q}$ (kW)	Q^*	D (m)	D^* (m)	δx (m)	$\frac{D^*}{\delta x}$	H (m)	$\frac{H}{D^*}$
ICFMP BE #2	1800--3600	1.0	1.2-1.6	1.2-1.6	0.13	9-12	19	12-16
ICFMP BE #3	400--2300	0.4-1.9	1.0	0.7-1.3	0.10	7-13	3.8	3-5
ICFMP BE #4	3500	2.6	1.1	1.6	0.10	16	5.7	3.6
ICFMP BE #5	400	0.6	0.8	0.7	0.10	7	5.6	8
FM/SNL	500	0.5	0.9	0.7	0.05	14	6.1	9
NBS Multi-Room	100	1.3	0.34	0.4	0.10	4	2.4	6

<u>Fire Diameter</u>: The physical diameter of the fire is not always a well-defined property. A compartment fire does not have a well-defined diameter, whereas a circular pan filled with a burning liquid fuel has an obvious diameter. Regardless, it is not the physical diameter of the fire that matters when assessing the "size" of the fire, but rather its characteristic diameter, D^*:

$$D^* = \left(\frac{\dot{Q}}{\rho_\infty c_p T_\infty \sqrt{g}} \right)^{2/5}$$

In many instances, D^* is comparable to the physical diameter of the fire (in which case, Q^* is on the order of 1). FDS employs a numerical technique known as large eddy simulation (LES) to model the unresolvable or "sub-grid" motion of the hot gases. The effectiveness of the technique is largely a function of the ratio of the fire's characteristic diameter, D^*, to the size of a grid cell, δx. In short, the greater the ratio $D^*/\delta x$, the more the fire dynamics are resolved directly, and the more accurate the simulation. Past experience has shown that a ratio of 5 to 10 usually produces favorable results at a moderate computational cost [Ref. 24].

<u>Compartment Size</u>: The quantities Q^* and D^* relate the fire's HRR to its physical dimensions. Equally important in determining the right numerical grid for a CFD simulation is the relationship between the fire "size" and the size of the overall compartment, particularly its height, H. The height of the compartment relative to D^* indicates the relative importance of the fire plume to the overall transport of the hot gases. Much of the mixing of fresh air and combustion products takes place within the plume, and this dilution of the smoke and the decrease in the gas temperature ultimately determine the hot gas layer temperature. Thus, the parameter H/D^* can be used to assess the importance of the plume relative to other features of the fire-driven value of flow, like the ceiling jet or doorway flow.

The rule of thumb about the parameter $D^*/\delta x$ is not a substitute for a *grid resolution study*. For all of the simulations described in this report, the numerical grid was gradually refined until the results were not observed to change from run to run. Of the six test series, the most challenging were BE #2 and the FM/SNL series because each involved a fairly large space and a relatively small fire. To achieve the desired level of resolution in the plume, a fine grid was used to capture the very important entrainment of fresh air, while coarse grids were used elsewhere. Ironically, the least challenging simulations in terms of computational effort were the NBS Multi-Room experiments, even though they required the lowest value of $D^*/\delta x$ to obtain suitably converged results. For these tests, the ceiling height was relatively low, and the plume dynamics were not as important in dictating the average compartment quantities. Thus, even though the burner was spanned by only four grid cells, the predicted temperatures in all three compartments were within experimental uncertainty.

6.1   Hot Gas Layer (HGL) Temperature and Height

All six sets of fire experiments include several floor-to-ceiling arrays of thermocouples
for measuring the compartment temperature. From these measurements, it is possible to calculate
an average upper-layer temperature, as well as an estimate of the height of the hot gas layer
above the floor. The FDS simulations predict the time history of each thermocouple,
and the predicted temperatures are then used to derive an average HGL temperature and height
in the exact same manner as the measured temperatures. Figure 6-1 summarizes the relative
differences between the predicted and measured HGL properties for the six test series. Note that
a positive value of the relative difference means that the numerical prediction is greater than
the corresponding measurement. Note also that the layer *depth* is the ceiling height minus
the layer height. Figure 6-2 presents the same results in a different format, emphasizing
the actual values of the HGL temperature and depth.
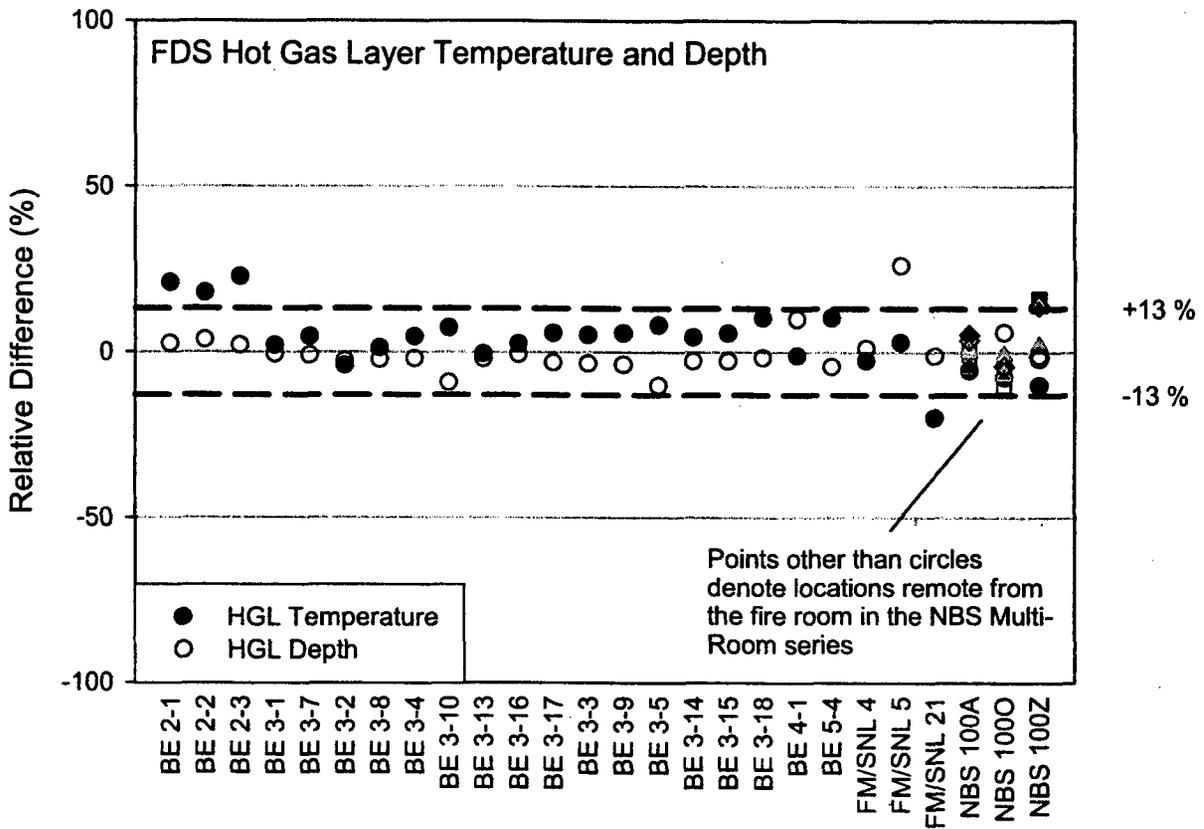
Figure 6-1: Summary of FDS Predictions of HGL Temperature and Depth
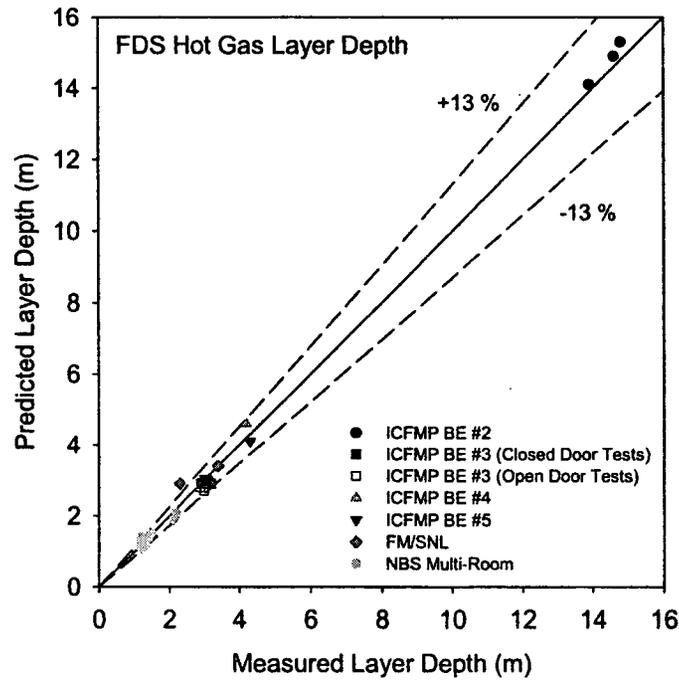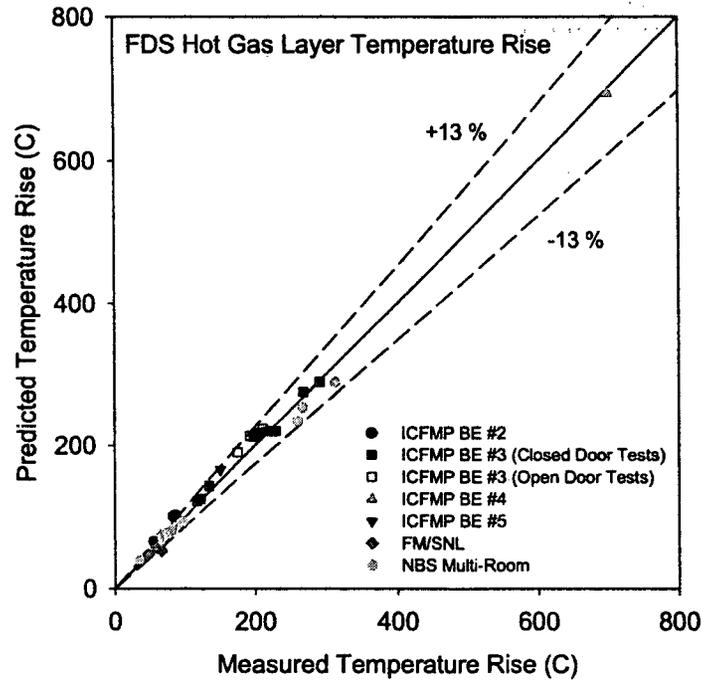
Figure 6-2: Summary of HGL Temperature and Depth Predictions

<u>ICFMP BE #2</u>: FDS over-predicts the HGL temperature by about 20% for all three cases. This falls outside of the experimental uncertainty range and can be traced to an over-prediction in the flame height and plume temperature. These errors are discussed below in the appropriate sections. FDS predicts the HGL height for all three cases in BE #2 to within experimental uncertainty.

<u>ICFMP BE #3</u>: FDS predicts the HGL temperature and height to within experimental uncertainty for all 15 tests.

<u>ICFMP BE #4</u>: FDS predicts the HGL temperature and height to within experimental uncertainty for the single test (BE 4-1), but there is some discrepancy in the shapes of the curves. It is not clear whether this is related to the measurement or the model. See further discussion in Appendix A.

<u>ICFMP BE #5</u>: FDS predicts the HGL temperature and height to within experimental uncertainty for the single test (BE 5-4), although again there is a noticeable difference in the overall shape of the temperature curves.

<u>FM/SNL</u>: FDS predicts the HGL temperature to within experimental uncertainty for Tests 4 and 5. For Test 21, there is an apparent 20% under-prediction, but this appears to be attributable to an error in the HRR measurement for this test. FDS predicts the HGL height to within experimental uncertainty for Tests 4 and 21. Both of these tests have a low ventilation rate. For Test 5, with a high ventilation rate, FDS over-predicts the HGL depth by 26%. However, the uncertainty in the HGL depth measurement is about 25% for the FM/SNL series because only five thermocouples in the vertical direction are used to assess the height of the smoke layer, and these five TCs are relatively close to the ceiling. See Volume 2 and the FM/SNL test report for details.

<u>NBS Multi-Room</u>: FDS predicts the HGL temperature and height to within experimental uncertainty for all three tests considered. Note that individual calculations of the temperature and depth have been made at four locations [one in the burn room, two in the corridor, and one in the target room (or exit if the target room is closed)].

Summary: FDS is suitable for predicting HGL temperature and height, with no specific caveats, in both the room of origin and adjacent rooms. In terms of the ranking system adopted in this report, FDS merits a Green for this category, based on the following:

- The FDS low Mach number hydrodynamic model is appropriate for predicting compartment temperatures and smoke filling. Note that FDS does not require the ceiling to be flat, and it can directly incorporate ceiling obstructions like ducts, beam pockets, and cable trays so long as they can be approximated as rectangular objects that conform to the overall numerical grid.

- The FDS predictions of the HGL temperature and height are, with a few exceptions, within experimental uncertainty.

- For some of the test series, like the NBS Multi-Room experiments, the simulations require only about half a day to complete, whereas others require several days. This is not atypical of CFD models. Whenever FDS is used, the numerical grid should be determined by performing a grid resolution study. A description can be found in Chapter 5.

6.2 Ceiling Jet Temperature

FDS does not have a ceiling jet algorithm per se. Rather, it predicts the temperature and velocity of the gases anywhere in the compartment, including near the ceiling. Two of the six test series (ICFMP BE #3 and FM/SNL) involve a ceiling jet that forms over a relatively wide, flat ceiling. The results of these simulations are summarized in Figure 6-3.

ICFMP BE #3: FDS predicts the ceiling jet temperature to within experimental uncertainty for the closed-door tests, except Tests 5 and 17. Test 5 is ventilated with a fan that is not well-characterized in terms of its flow rate and direction. A number of spurious results can be linked to the difficulty in modeling the fan. Test 17 is a short test with no replicates. It is difficult to draw any firm conclusions from it. FDS over-predicts the ceiling jet for the open-door tests by about 15%. Although this is within the experimental uncertainty bounds, the trend is consistent in all the open-door tests. The trend cannot be explained solely in terms of measurement or model input uncertainty. Rather, it is most likely caused by a lack of resolution in the numerical grid. Near the fire, the grid cells are about 10 cm (4 in) in all dimensions. However, the grid cells stretch in the horizontal dimensions away from the plume to save on computational cost (see Figure 6-4). In addition, the 10-cm grid spans the relatively shallow ceiling jet with just a few grid cells. As a result, the mixing of hot and cooler gases within the jet is slightly under-predicted and the temperature, thus, slightly over-predicted. While the slight over-prediction of ceiling jet temperature could be considered conservative for some applications, for scenarios involving sprinkler or heat detector activation, the increased temperature in the ceiling jet would lead to a quicker response of the simulated sprinkler or heat detector.

FM/SNL: FDS predicts the ceiling jet temperature at two locations in Test 4 and 5 to within experimental uncertainty. FDS under-predicts Test 21 by about 20%, but this discrepancy is likely attributable to a flaw in the HRR measurement for this particular test.
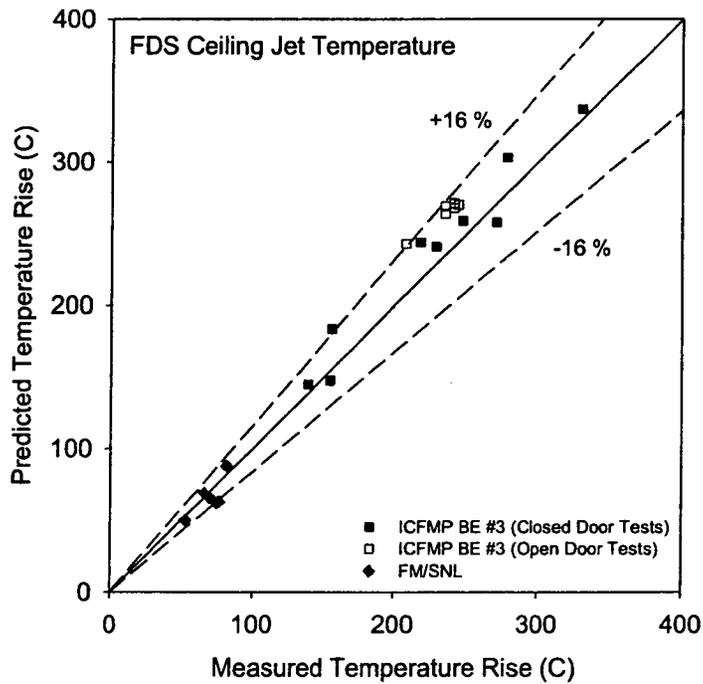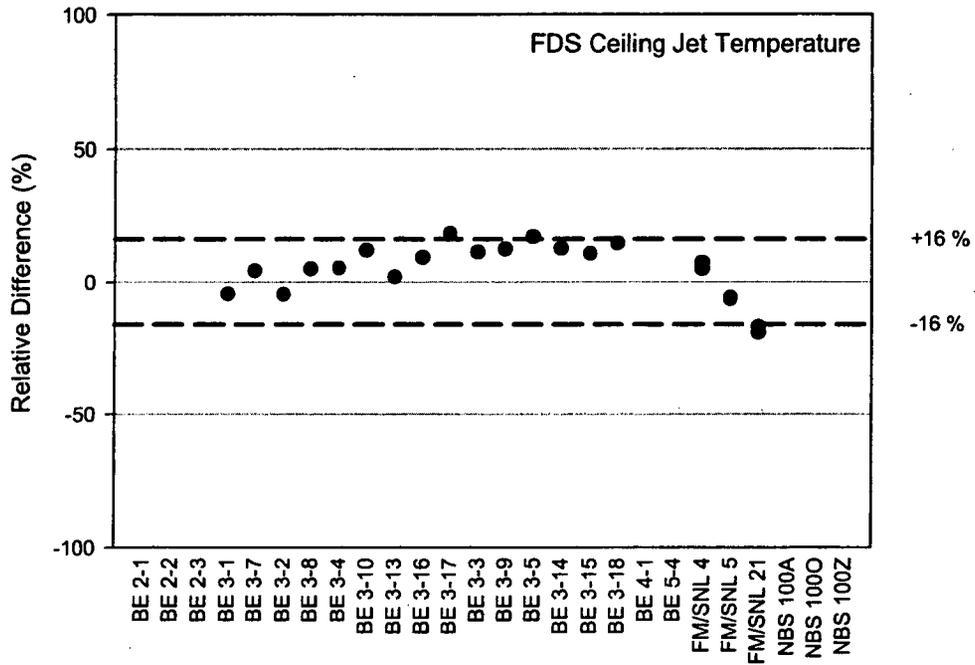
Figure 6-3: Summary of FDS Predictions of Ceiling Jet Temperature

Summary: FDS merits a Green ranking for ceiling jet temperature prediction, for the following reasons:

- The FDS hydrodynamic solver is suited for this application, assuming that the user performs a grid sensitivity study to determine a suitable grid cell size.

- Overall, FDS is slightly less accurate in its prediction of the near-ceiling temperature than of the overall HGL temperature. This makes sense because the ceiling jet, as with the fire plume, is a region of the flow field exhibiting relatively high levels of buoyancy and/or shear-induced turbulence. Inaccuracies in its prediction tend to be averaged out when examining the bulk HGL temperature, but it is important to consider this higher degree of inaccuracy if the objective of the calculation is to assess the damage to or activation of some object or device near the ceiling.
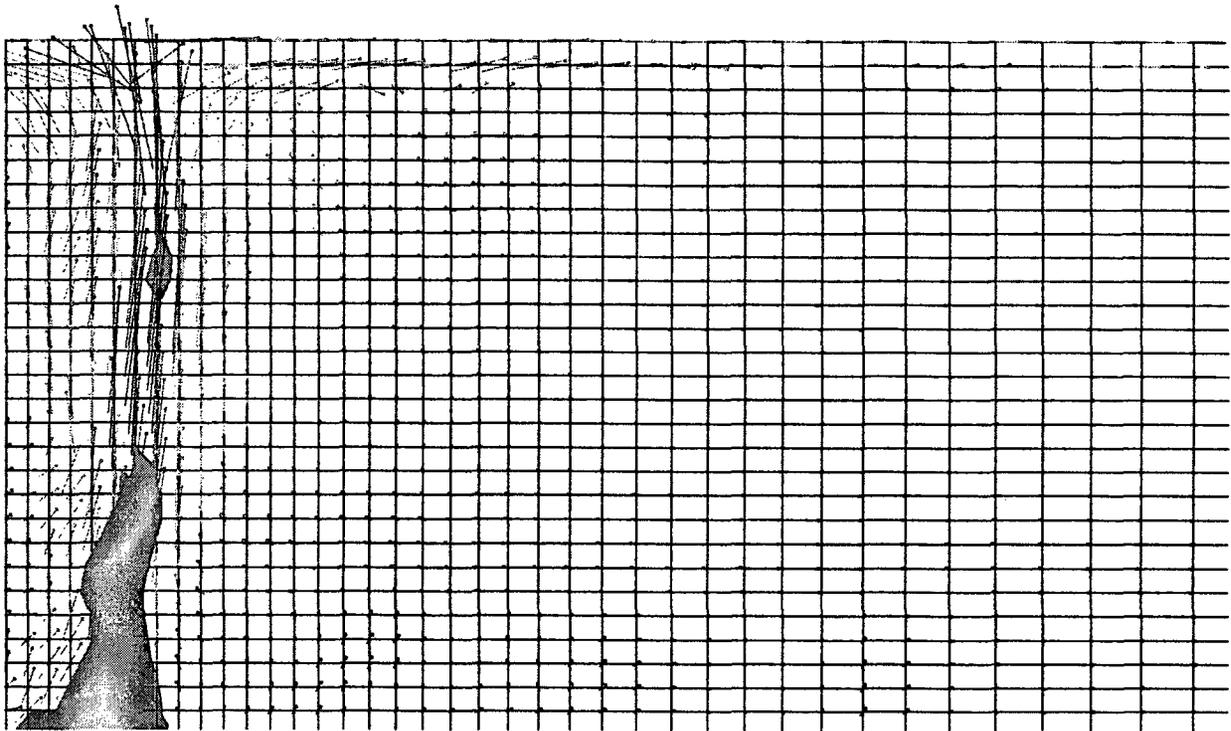
Figure 6-4: Snapshot of FDS Simulation of ICFMP BE #3, Test 3

6.3 Plume Temperature

As with the ceiling jet, FDS has no specific plume algorithm. It simply computes the temperature and velocity everywhere. However, predicting temperatures within the fire plume is particularly important because this is where much of the mixing of the hot combustion products and surrounding air takes place. Data from ICFMP BE #2 and the FM/SNL test series have been used to assess the accuracy of plume temperature predictions. Figure 6-5 summarizes the results.

ICFMP BE #2: As previously discussed, FDS over-predicts the HGL temperature in this test series. Not surprisingly, FDS also over-predicts the plume temperature, especially at the lower thermocouple, 6 m (19.7 ft) above the fire pan. The flame height of the fires has been estimated to vary from 4 m to 5 m (13.1 ft to 16.4 ft), whereas FDS predicts the height to vary from 5 m to 6 m (16.4 ft to 19.7 ft). Consequently, FDS predicts higher temperatures in the region just beyond the flame tip where the temperatures decrease rapidly with height. At the higher thermocouple location, the relative difference between the predicted and measured temperatures is about 15%, just at the upper edge of the experimental uncertainty range.

FM/SNL: FDS predicts the plume temperatures in Test 4 and 5 to within experimental uncertainty, with the same under-prediction in Test 21 as for the HGL and ceiling jet temperatures, about 20%. FDS uses 5-cm (2-in) grid cells in the vicinity of the plume to achieve these results. As discussed above, $D^*/\delta x=14$, a fairly high value requiring several days of computing time.

Summary: FDS merits a Yellow (Caution) ranking in this category for the following reasons:

- The FDS hydrodynamic solver is well-suited for this application.

- FDS over-predicts the lower plume temperature in BE #2 because it over-predicts the flame height. FDS predicts the FM/SNL plume temperature to within experimental uncertainty.

- The simulations of BE #2 and the FM/SNL series are the most time-consuming of all six test series, mainly because of the need for a fairly fine numerical grid near the plume. It is important that a user understand that considerable computation time may be necessary to well-resolve temperatures within the fire plume. Even with a relatively fine grid, it is still challenging to accurately predict plume temperatures, especially in the fire itself or just above the flame tip.

- There are only nine plume temperature measurements in the data set. A more definitive conclusion about the accuracy of FDS in predicting plume temperature would require more experimental data.
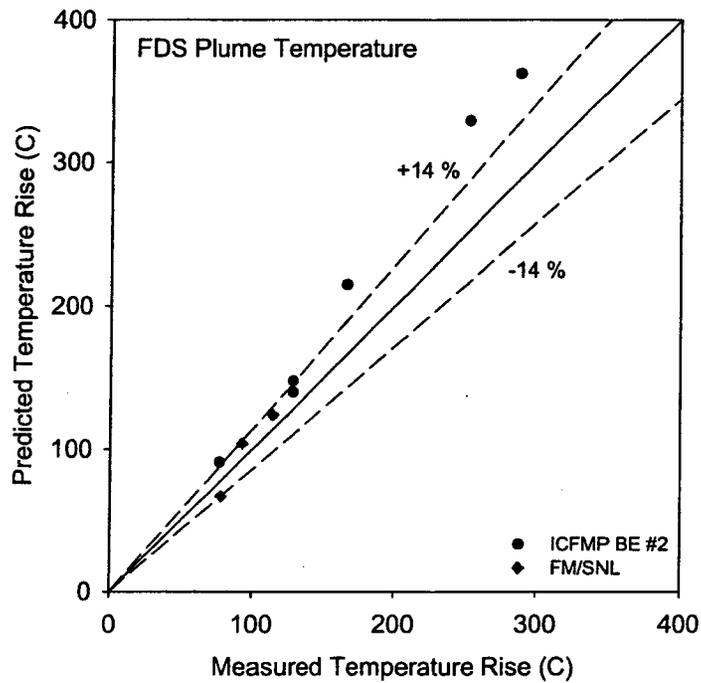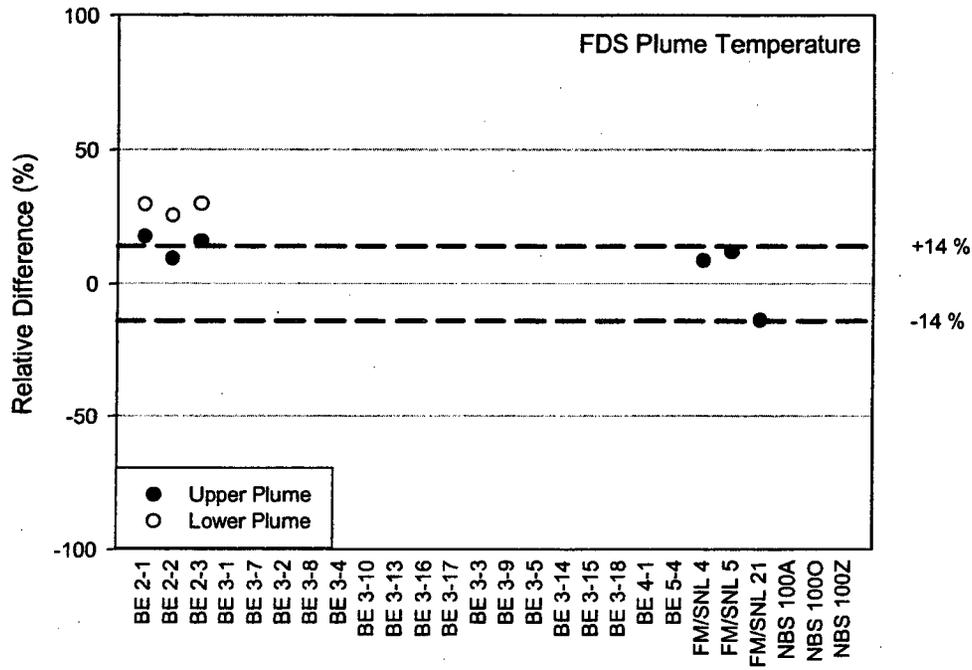
Figure 6-5: Summary of FDS Predictions of Plume Temperature

6.4   Flame Height

Flame height is recorded by visual observations, photographs, or video footage. Videos and photographs from the ICFMP BE #3 test series and photographs from BE #2 are available. Several photographs from both test series are included in Section A.4 of Appendix A. It is difficult to precisely measure the flame height, but the photos and videos allow one to make estimates accurate to within roughly a pan diameter.

ICFMP BE #2: The height of the visible flame in the photographs of BE #2 has been estimated to be between 2.4 and 3 pan diameters [3.8 m to 4.8 m (12.5 ft to 15.7 ft)]. The height of the simulated fire fluctuates from 5 m to 6 m (16 ft to 19 ft) during the peak heat release rate phase. This over-prediction is attributable to the simplified combustion model in FDS along with the limited grid resolution spanning the fire itself. In this type of simulation (small fire in a large compartment), it is challenging to design a numerical grid that spans the entire volume, but at the same time provides adequate resolution over the fire. In this case, the volume of the test hall is about 6,000 m^3 (200,000 ft^3) while the fire occupies roughly 6 m^3 (200 ft^3). The over-prediction of flame height, *in this test series*, contributes to the over-prediction of plume and HGL temperature discussed above.

ICFMP BE #3: FDS correctly predicts the flame height in this test series, at least to the accuracy of visual observations and a few photographs taken before the HGL obscures the upper part of the flame. The experiments were not designed to measure the flame height other than through visual observation.

Summary: FDS merits a Yellow (Caution) for Flame Height prediction, for the following reasons:

- The FDS mixture fraction combustion model assumes that fuel and oxygen mix along a thin "flame sheet." Although a simple description of the combustion, the model is capable of predicting the flame height of a well-ventilated fire.

- FDS over-predicts the flame height of the only BE #2 fire for which photographs are available. FDS predicts the flame height for the BE #3 tests to an accuracy commensurate with visible observations. The uncertainty in interpreting the photographs, videos, and eye-witness accounts is considerable, as is the very definition of "flame height."

- There is not enough information about flame heights in the data sets to reach any definite conclusions about FDS predictions of flame height.

6.5 Oxygen and Carbon Dioxide Concentration

FDS uses a mixture fraction combustion model, meaning that the concentrations of all of the major gas species are related to a single scalar variable for which a single transport equation is solved. Assuming that the basic stoichiometry of the combustion process is known, predicting oxygen and carbon dioxide concentrations is similar, mathematically, to predicting temperatures. Gas sampling data is available from ICFMP BE #3 and BE #5. A summary of the FDS predictions is presented in Figure 6-6.

ICFMP BE #3: FDS predicts the upper-layer concentrations of oxygen and carbon dioxide close to experimental uncertainty, with the notable exception of Test 5 (BE 3-5), for which the relative difference between FDS and measurement is about 60% for both species. This over-prediction of the gases in the upper layer is most likely the result of the specification of boundary conditions at the ventilation duct. The fan, mounted halfway up the long wall of the compartment, blew air upward at roughly a 45° angle from the horizontal. The velocity profile was measured before the test began, but this profile (and the flow rate) changed during the test as a result of changing compartment conditions. As a result, both the volume flow rate and the flow direction are subject to considerable uncertainty, and this is reflected in the results of Test 5, the only open-door test involving the ventilation system. The large FDS over-prediction does not occur for the closed-door tests with ventilation (Tests 4, 10, and 16).

FDS predictions of the lower gas layer (LGL) oxygen concentration are close to experimental uncertainty except for Tests 1, 7, and 5. Tests 1 and 7 are replicate tests. They are relatively small fires (400 kW), the doors are closed, there is no ventilation, and the lower-layer oxygen concentration gradually decreases to about 15% in about 25 minutes. There is nothing in particular that might explain the over-prediction. Test 5 has the fan blowing into the upper layer, and the lower-layer concentration is over-predicted by about the same percentage as the upper-layer oxygen and carbon dioxide concentrations.

ICFMP BE #5: FDS predicts the upper-layer oxygen concentration in Test 4 of this test series (BE 5-4) to within experimental uncertainty. The carbon dioxide is slightly over-predicted by about 20%, but the concentrations are relatively low (0.013 measured, 0.016 predicted).

Summary: FDS merits a Green ranking for prediction of major gas species, for the following reasons:

- The FDS mixture fraction model is capable of making predictions of major gas species concentrations, assuming that the basic stoichiometry of the combustion reaction is known and that the fire is well-ventilated.

- With a few exceptions, the FDS predictions of major gas species concentrations are within experimental uncertainty.

- FDS has only been evaluated for oxygen and carbon dioxide. The conclusions should not be extended to carbon monoxide, smoke, or other exhaust products whose yields and/or transport properties are not as well-characterized as oxygen and carbon dioxide.
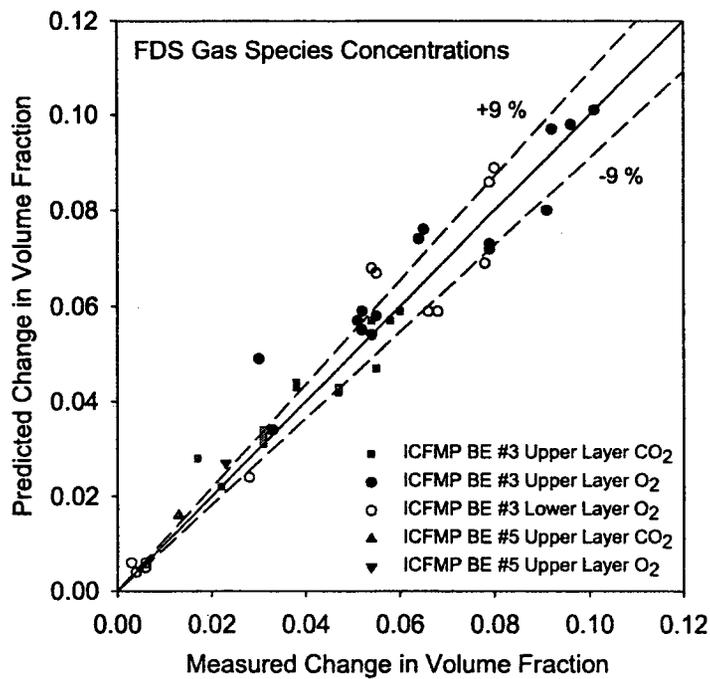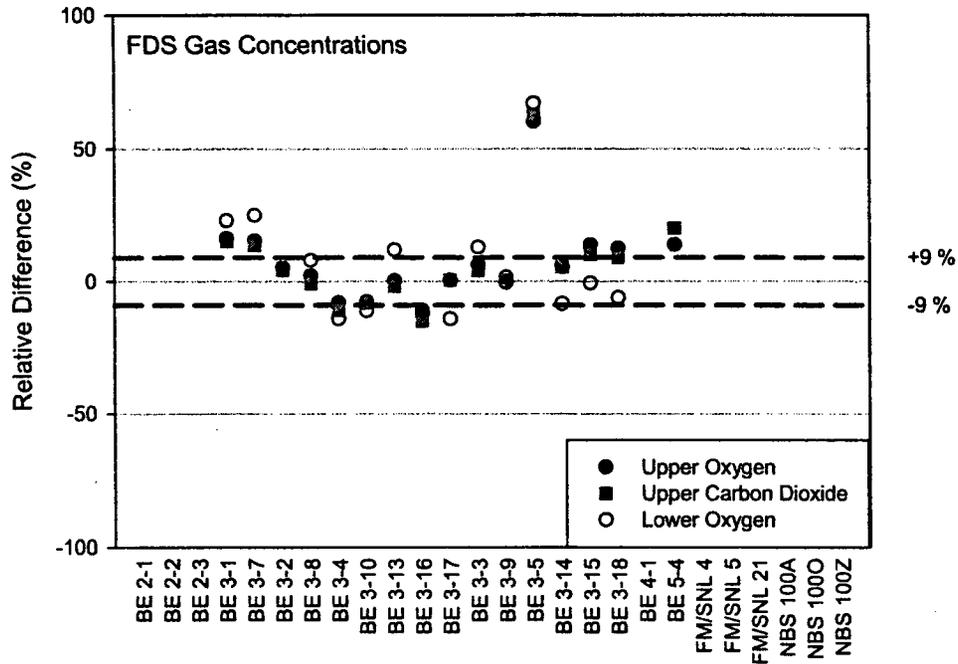
Figure 6-6: Summary of FDS Predictions of Major Gas Concentrations

6.6   Smoke Concentration

FDS treats smoke like all other combustion products, basically a tracer gas for which the local mass concentration is a function of the local mixture fraction. To model smoke movement, the user need only prescribe the smoke yield (that is, the fraction of the fuel mass that is converted to smoke particulate).

Only ICFMP BE #3 was used to assess predictions of smoke concentration. For these tests, the smoke yield was specified as one of the input parameters. A summary of the results is shown in Figure 6-7. There are two obvious trends in the results: first, the predicted concentrations are about 50% higher than the measured in the open-door tests. Second, the predicted concentrations are as much as six times the measured concentrations in the closed-door tests. The experimental uncertainty for these measurements has been estimated to be 33% (see Volume 2). It may be possible to explain the open-door results in terms of uncertainty in the measurement and the specified smoke yield, but the closed-door tests cannot be explained in these terms.

Assuming that the mixture fraction model is valid, at least for the open-door tests, it can be assumed that virtually all of the carbon atoms in the fuel are transported either by the CO_2 or the soot (with relatively small amounts in the CO, unburned hydrocarbons, etc.). It can also be assumed that the soot (smoke) and CO_2 are transported together with no significant separation or reaction. If these assumptions are true, there is no reason to expect the predicted smoke concentration to be roughly 50% higher than the measured value unless the soot yield uncertainty and the measurement uncertainty combine to cause it. Indeed, in Figure A-30 the predicted CO concentrations, also based on a fixed yield, do not exhibit the same behavior as the smoke predictions in either the open or closed-door tests.

The difference between model and experimental predictions of smoke concentration is far more pronounced in the closed-door tests. Given that the oxygen, carbon dioxide, and carbon monoxide predictions are no worse in the closed-door tests, there is evidence that the smoke does not behave like the other exhaust gases, or that there are flaws in the data reduction for closed-door (i.e., under-ventilated) fires. Consider, for example, Figure 6-8, which shows the smoke and oxygen concentrations for a closed-door test with no ventilation (Test 8). The HRR is ramped up to 1,190 kW in 176 seconds, followed by 434 seconds of steady burning and then a rapid shutdown of the fuel supply. Assuming a 1.5% smoke yield, no smoke loss, and a uniform distribution of smoke throughout the compartment, the maximum smoke concentration ought to be about 360 mg/m^3. FDS does allow for smoke to escape through leakage paths; thus, it predicts a lower peak concentration at the measurement location, about 300 mg/m^3, at about 10 minutes after ignition when the fuel is shut off. The measured smoke concentration peaks at 100 mg/m^3 at about 8 minutes and then decreases. At about this same time, the oxygen concentration near the fire drops to about 15%, at which point the fire becomes under-ventilated, and the combustion chemistry presumably changes. Curiously, the smoke production rate appears to decrease as the fire becomes more oxygen-starved, or possibly the optical properties of the smoke change, leading to a misleading measurement of the smoke mass per unit volume.

Figure 6-7: Summary of FDS Predictions of Smoke Concentration
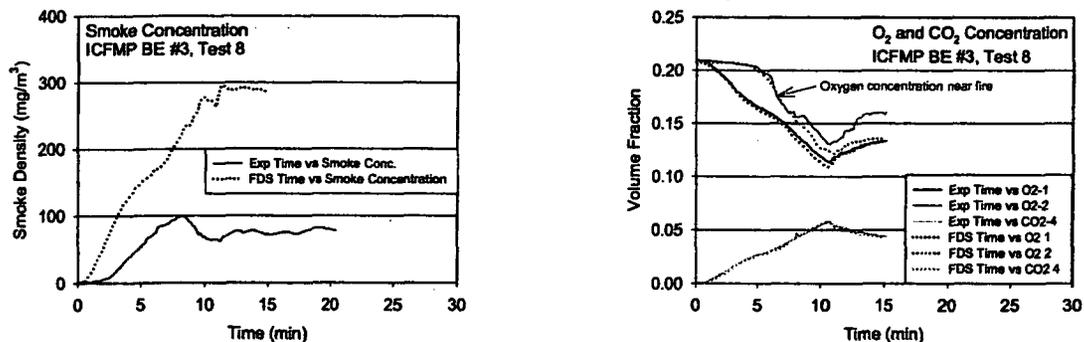
Figure 6-8: Smoke and Oxygen Concentration, ICFMP BE #3 Test 8

Summary: FDS merits a Yellow (Caution) for predicting smoke concentration, for the following reasons:

- FDS is capable of transporting smoke throughout a compartment, assuming that the production rate is known and that its transport properties are comparable to gaseous exhaust products. This assumption may break down in closed-door fires, or if an appreciable part of the flame extends into the upper layer.

- FDS over-predicts the smoke concentration in all of the BE #3 tests. For the open-door tests, it is possible to explain the discrepancy in terms of the uncertainty of both the specified smoke yield and the optical measurement of the smoke concentration. There is no clear explanation for the discrepancy in the closed-door tests. FDS does not over-predict the CO concentration, another fixed yield product of incomplete combustion, in either the open- or closed-door tests.

- No firm conclusions can be drawn from this one data set. The measurements in the closed-door experiments are inconsistent with basic conservation of mass arguments, or there is a fundamental change in the combustion process as the fire becomes oxygen-starved. FDS does not have a sub-model to adjust the production rate or the optical properties of smoke, regardless of whether or not this would explain the discrepancy between the measurements and the model predictions.

6.7 Compartment Pressure

Comparisons between measurement and prediction of compartment pressure for BE #3 are shown in Section A.7 of Appendix A, and the results are summarized in Figure 6-9. For those tests in which the door to the compartment is open, the over-pressures are only a few Pascals, whereas when the door is closed, the over-pressures are several hundred Pascals.

In general, the predicted pressures are within 50% of the measured pressures, consistent with the reported uncertainties in the leakage area and the ventilation rate (see Volume 2). The one notable exception is Test 16. This experiment was performed with the door closed and the ventilation on, and there is considerable uncertainty in the magnitude of both the supply and exhaust flow rates. Test 16 is a 2.3-MW fire, whereas Test 10 is a 1.2-MW fire. The measured supply velocity is greater and the measured exhaust velocity is less in Test 10, compared to Test 16. This is probably the result of the higher pressure caused by the larger fire in Test 16. FDS does not adjust the ventilation rate based on the compartment pressure, which is why the specified fan velocities are comparable in Tests 10 and Test 16. This also is the most likely explanation for the over-prediction of compartment pressure in Test 16. Figure 6-10 presents the measured (solid lines) and specified (dashed lines) air velocities 15 cm (5.9 inches) from the lower edge of the supply duct, and 35 cm (13.8 inches) from the lower edge of the exhaust duct, for Tests 10 and 16. Also shown are the measured (solid lines) and predicted (dashed lines) compartment over-pressures for these tests.
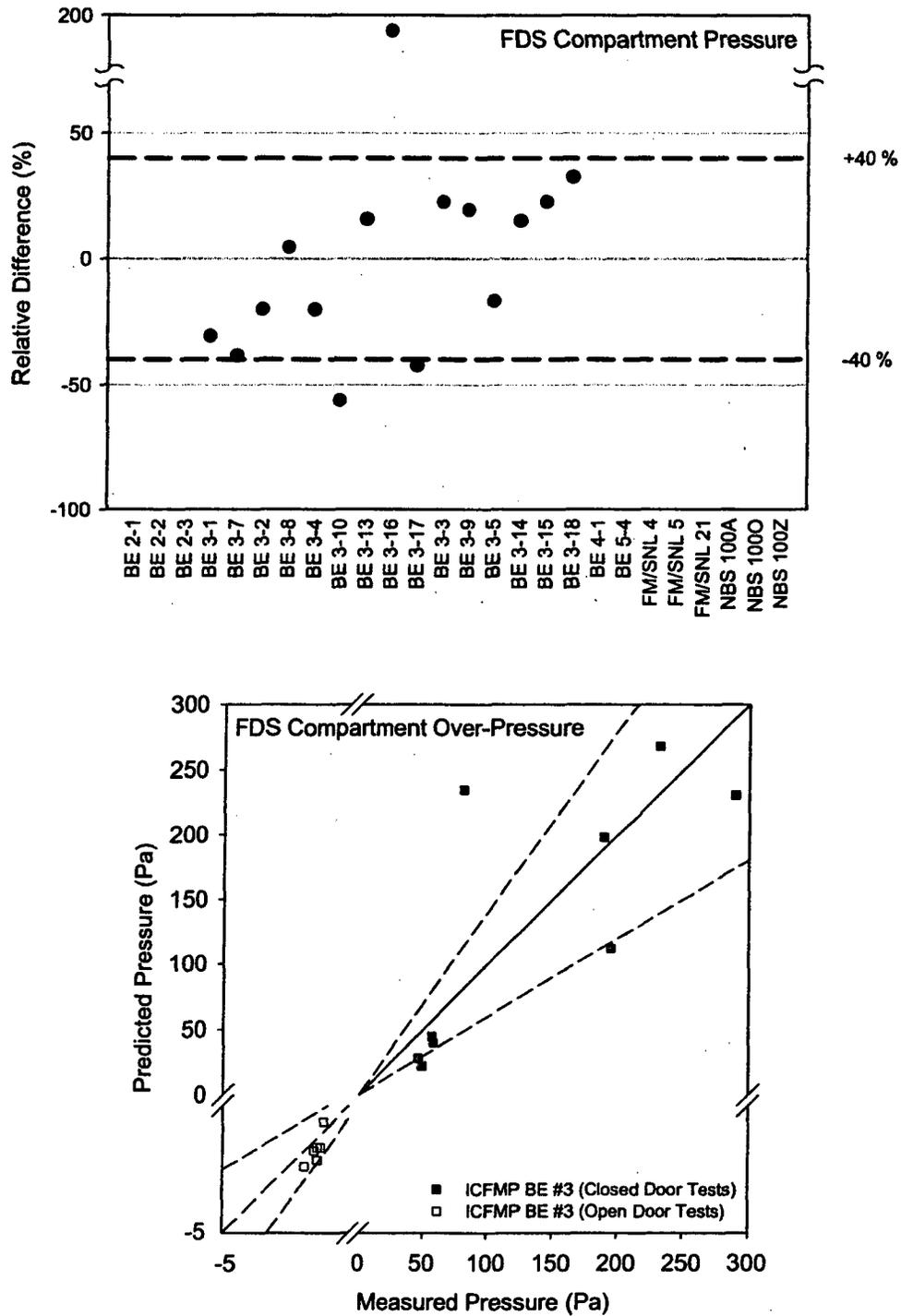
Figure 6-9: Summary of FDS Predictions of Compartment Pressure
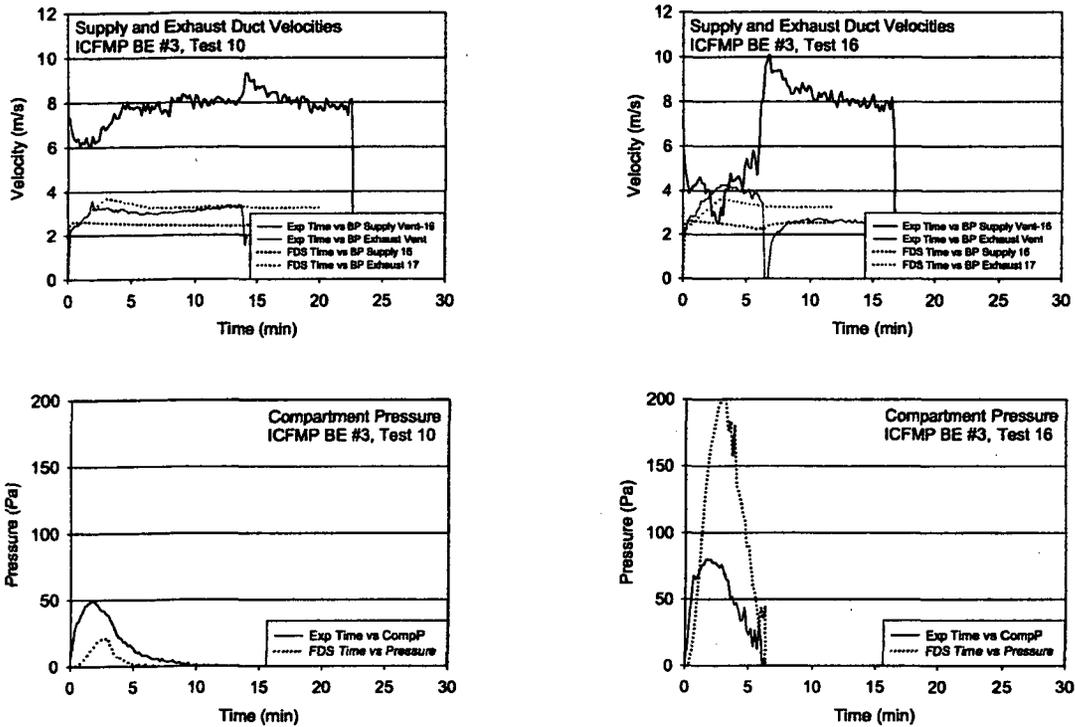
Figure 6-10: Ventilation Rates and Pressures for BE #3, Tests 10 and 16

Summary: FDS merits a Green rating in predicting compartment pressure, for the following reasons:

- The basic mass and energy conservation equations solved by FDS ensure reliable predictions of compartment pressure.

- The FDS pressure predictions for BE #3 are within experimental uncertainty, with an exception related to the behavior of a ventilation fan.

- Compartment pressure predictions are extremely sensitive to the leakage area and forced ventilation. The fractional uncertainty in predicted pressure is roughly double that of the leakage area or ventilation rate.

6.8 Radiation and Total Heat Flux and Target Temperature

Target temperature and heat flux data are available from ICFMP BE #3, #4, and #5. In BE #3, the targets are various types of cables in various configurations — horizontal, vertical, in trays, or free-hanging. In BE #4, the targets are three rectangular slabs of different materials instrumented with heat flux gauges and thermocouples. In BE #5, the targets are again cables, in this case, bundled power and control cables in a vertical ladder.

Figure 6-11 summarizes the relative differences between predicted and measured radiative and total heat flux and surface temperature.

<u>ICFMP BE #3</u>: There are nearly 200 comparisons of heat flux and surface temperature on four different cables that are graphed in Appendix A and summarized above. It is difficult to make sweeping generalizations about the accuracy of FDS. At best, one can scan the graphs, tables, and summary charts to get a sense of the overall performance. The experimental uncertainty is about 20% for both heat flux and surface temperature. Discounting those comparisons for which the relative difference is less than 20%, the rest need to be examined on a case-by-case basis. Note the following trends:

- There is an overall trend toward over-prediction of radiative heat flux and under-prediction of total heat flux. From this observation, it is assumed that the convective heat flux, the difference between the total and the radiative heat flux, is generally under-predicted. It is difficult to more accurately quantify this observation because the heat flux gauges in the experiment are mounted on steel, L-shaped brackets while the convective heat flux prediction by FDS is based on a flat plate empirical correlation. Thus, the model does not predict, nor does the experiment measure, the true convective heat flux to the cables themselves.

- The predicted and measured cable surface temperatures are often virtually identical to the local gas temperature (see graphs in Appendix A). Good predictions of the gas temperature often lead to good predictions of the cable temperature, regardless of the accuracy of the heat flux. Indeed, the scatter in the temperature predictions is less than that in the heat flux predictions.

- Most of the over-predictions of cable surface temperatures occur in Tests 4, 5, 10, and 16, which include the ventilation fan. Cables B, D, and F are located near the supply vent, and the air blows over the measurement locations. The fan's flow rate and direction are not well-characterized in the test specification; thus, there is more uncertainty in these tests than in the others. It is difficult to quantify this uncertainty, however, other than to look at similar tests that do not have the fan turned on. Tests 2 and 8 are the same as 4 and 10, but without the fan. Test 3 is Test 5 without the fan. Test 13 is Test 16 without the fan. The cable surface temperatures are not over-predicted in these unventilated tests.
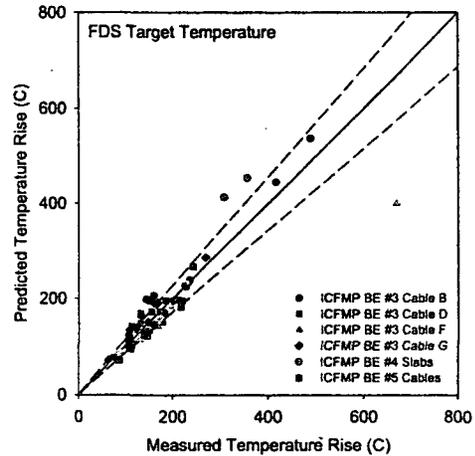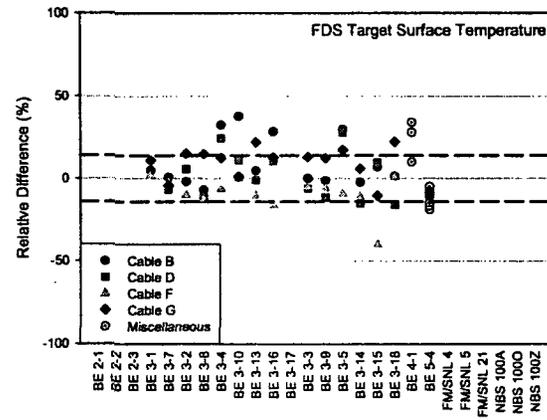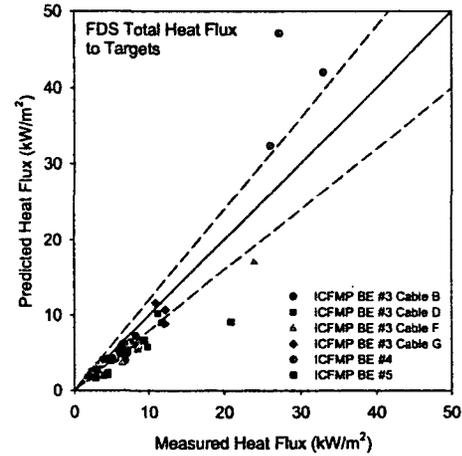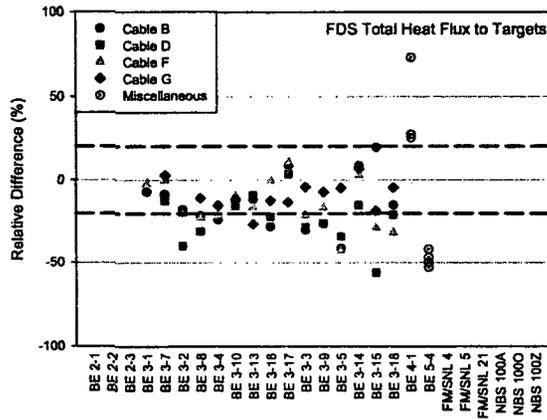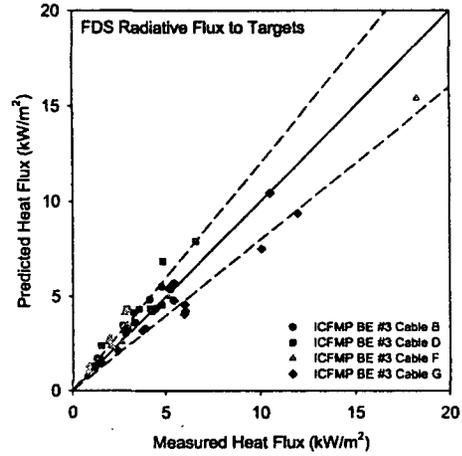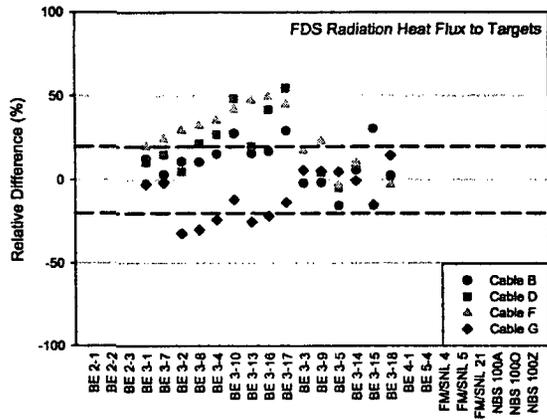
Figure 6-11: Summary of FDS Predictions of Target Temperature

<u>ICFMP BE #4</u>: FDS over-predicts both the heat flux and surface temperature of three "slab" targets located about 1 m (3.3 ft) from the fire. The trend is consistent, but it cannot be explained solely in terms of experimental uncertainty. Part of the discrepancy appears to be attributable to the plume lean in FDS, which leads to the significant over-prediction of heat flux to the steel target in the back of the compartment.

<u>ICFMP BE #5</u>: Predictions and measurements of gas temperature, total heat flux and cable surface temperature are available at four vertical locations along a cable tray. FDS over-predicts the gas temperatures by about 10% at these locations, under-predicts heat flux by about 50%, and under-predicts the cable surface temperature by 10% to 20%. Although the surface temperature predictions are within experimental uncertainty, the heat flux predictions are not. It is possible that in this case, two wrongs (gas temperature and heat flux) make a right (surface temperature). However, only one test from this series has been used in the evaluation, thus, it is hard to draw any firm conclusions. Also, given that BE #5 uses the same compartment as BE #4, it is curious that FDS over-predicts the heat fluxes in BE #4, but under-predicts in BE #5.

Summary: FDS merits a Yellow (Caution) in this category, for the following reasons:

- FDS has the appropriate radiation and solid phase models for predicting the radiative and convective heat flux to targets, assuming the targets are relatively simple in shape. FDS is capable of predicting the surface temperature of a target, assuming that its shape is relatively simple and its composition fairly uniform.

- FDS predictions of heat flux and surface temperature are generally within experimental uncertainty, but there are numerous exceptions attributable to a variety of reasons. The accuracy of the predictions generally decreases as the targets move closer to, or go inside of, the fire. There is not enough near-field data to challenge the model in this regard.

6.9 Wall Heat Flux and Surface Temperature

Heat flux and wall surface temperature measurements are available from ICFMP BE #3, and wall surface temperature measurements are also available from BE #4 and BE #5. As with target heat flux and surface temperature (discussed above), there is a considerable amount of data to consider. Figure 6-12 summarizes the relative differences for the wall (total) heat flux and wall surface temperature predictions.

ICFMP BE #3: FDS generally predicts the heat flux and surface temperature of the compartment walls and ceiling to within experimental uncertainty (20%). However, the predicted floor temperatures are as much as 90% higher than the measurements. In fact, the over-predicted surface temperatures are almost all for the floor, both near and far-field. The predicted heat fluxes to the floor do not indicate this level of error, which means that the material properties of the floor need to be considered. The compartment walls and ceiling are constructed of Marinite I, an industrial-strength insulating material for which the properties have been measured by the manufacturer (BNZ Materials, Inc.) for the range of temperatures experienced in the tests. The floor is constructed of one layer of ordinary gypsum board atop common construction-grade plywood. (It is assumed in the simulations that the gypsum board is twice as thick because FDS cannot accept two layers of materials.) The thermal properties of the gypsum board and the plywood were not measured, and the exact composition of each batch changes depending on the supply of raw materials. Therefore, it cannot be concluded that FDS is less accurate in predicting floor temperatures than it is predicting wall or ceiling temperatures.

ICFMP BE #4: FDS predicted two wall surface temperatures to within 4% of the measured values. The two points are presumably very close to the fire because the temperatures are 600 °C to 700 °C (1,100 °F to 1,300 °F) above ambient. This is a curious result because FDS does not predict the temperatures of the nearby slab targets this accurately.

ICFMP BE #5: FDS under-predicts wall temperatures at two locations in the compartment by about 30%. However, FDS slightly over-predicts the gas temperatures at these same vertical locations. These results are similar to those discussed above for the cable targets in BE #5.

Summary: FDS merits a Yellow (Caution) rating in this category, for reasons similar to those for target flux and temperature (discussed above):

- FDS has the necessary radiation and solid phase sub-models for predicting the radiative and convective heat flux to walls, and the subsequent temperature rise within the walls. It is assumed that the composition of the wall liner is fairly uniform, and its thermal properties are well-characterized.

- FDS predictions of heat flux and surface temperature are generally within experimental uncertainty, but there are several exceptions attributable to a variety of reasons. As with targets, the accuracy of the predictions typically decreases closer to the fire or plume impingement region. Although there is no clear difference in near and far field predictions in the current study, past experience urges caution when making near-field predictions.
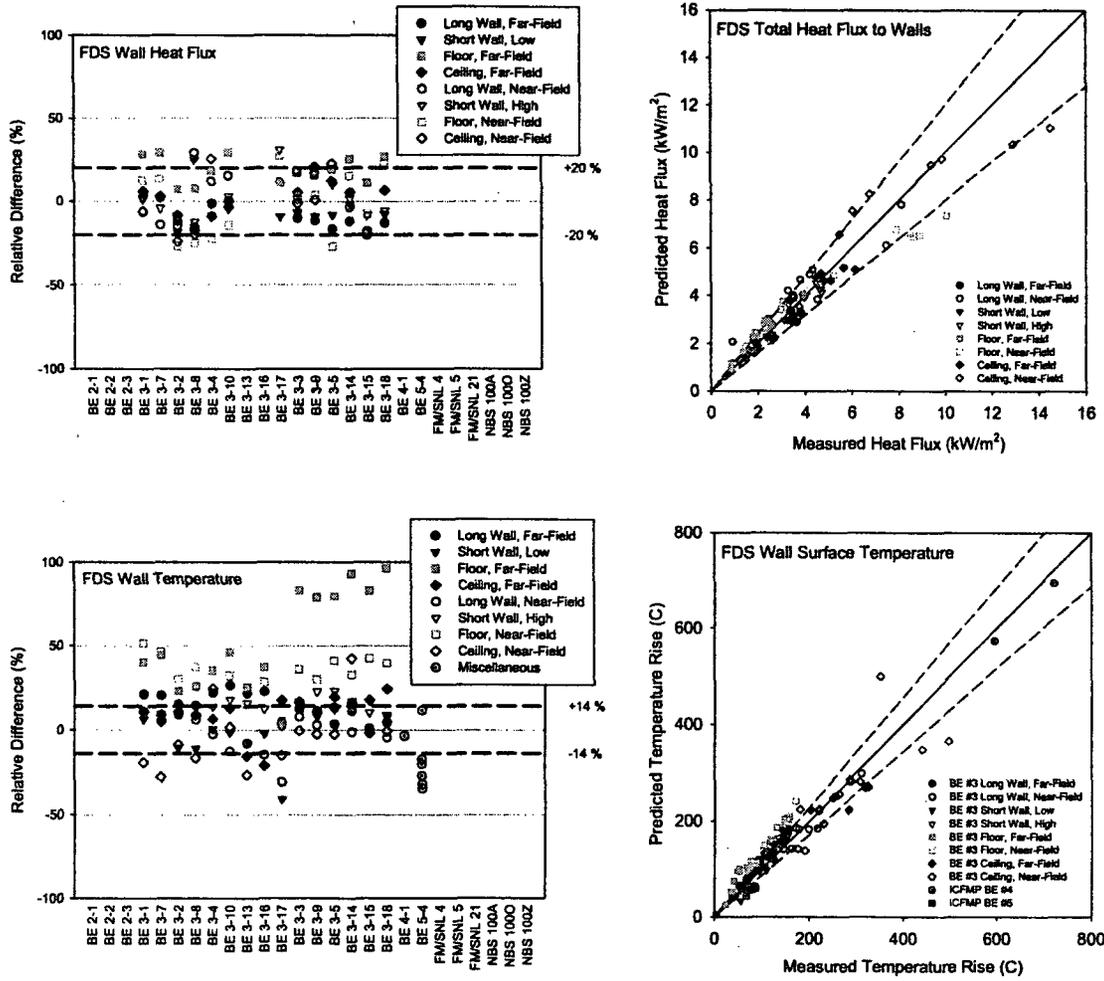
Figure 6-12: Summary of FDS Predictions of Wall Heat Flux and Temperature

6.10 Summary

The results presented in this chapter validate the basic hydrodynamic and radiative heat transport algorithms within FDS. For a fire for which the heat release rate is known, FDS can reliably predict gas temperatures, major gas species concentrations, and compartment pressures to within about 15%, and heat fluxes and surface temperatures to within about 25%.

For the experiments considered, the FDS predictions are not significantly better than those of the two-zone models (CFAST and MAGIC) that are also evaluated in this study. Only in the predictions of heat flux and surface temperature is FDS noticeably better. The reason is that the experiments used in the evaluation conform to the simple two-layer assumption that is the basis of CFAST and MAGIC. In addition, two-zone models use well-established empirical correlations to predict the plume, ceiling jet, and flame height; whereas FDS simply solves the basic transport equations. In this sense, FDS truly is a *predictive* model. However, the cost of solving the basic equations is substantial. The two-zone models produce answers in seconds to minutes, whereas FDS produces comparable answers in hours to days. An obvious question to ask is why use FDS or any CFD model? The answer is that these experiments were designed to evaluate all types of fire models, from simple hand calculations to CFD. Rarely do real fire scenarios conform as neatly to the simplifying assumptions inherent in the models. Fire plumes are rarely free and clear of obstacles because fires often occur in cabinets or near walls. Ceilings are rarely flat and unobstructed because duct work and cable trays often block the clear paths. Although two-zone models can be applied in some of these instances, their accuracy cannot be ensured. Indeed, in the present study the heat flux and surface predictions by FDS are more accurate than those of the two-zone models because FDS computes the local temperature within the hot gas layer, and the radiative heat flux is a function of this local temperature raised to the fourth power. Obstructions near the ceiling create pockets of hotter gases, which can have a substantial effect on the local heat flux to targets and walls.

Most practicing fire protection engineers use a combination of models to assess the hazards of fire. For the fire scenarios considered in the current validation study, and for the output quantities of interest, the two-layer models are most suitable. The hand calculations are limited in applicability, and FDS is overly time-consuming. However, the experiments do provide a means to validate all of the models in a consistent way. Once validated for the simple compartment geometries, FDS can then be used to look at more complicated geometries where non-uniformities of temperature, and non-idealized gas flows cannot be addressed by simple two-zone models.
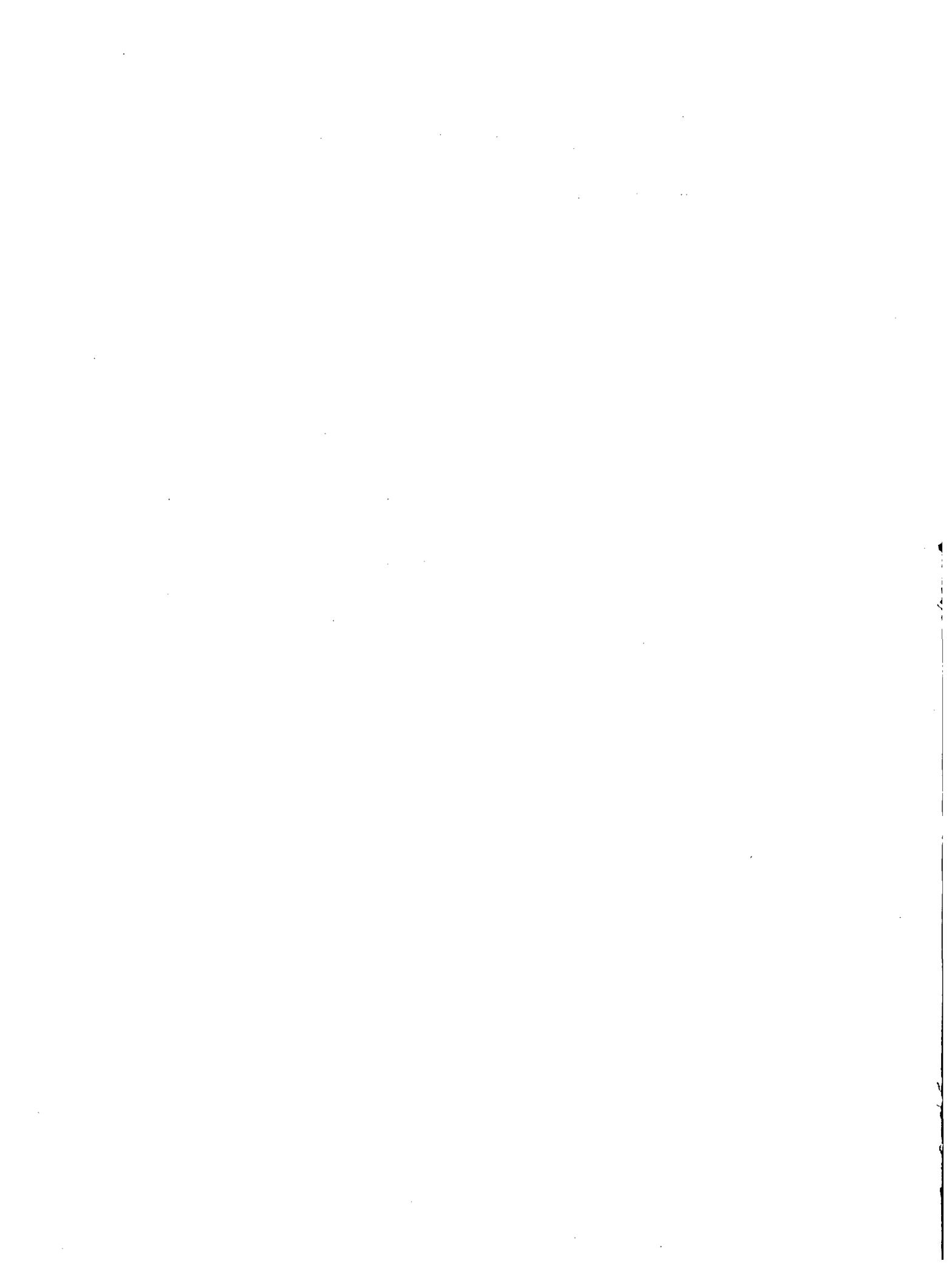
7
REFERENCES

1. *Standard Guide for Evaluating the Predictive Capability of Deterministic Fire Models,* ASTM E 1355-05a, American Society for Testing and Materials, West Conshohocken, PA, 2005.

2. "Fire Dynamics Simulator (Version 4) Technical Reference Guide" (K. McGrattan, Editor), NIST Special Publication 1018, National Institute of Standards and Technology, Gaithersburg, MD, 2004.

3. McGrattan, K., and G.P. Forney, "Fire Dynamics Simulator (Version 4) User's Guide," NIST Special Publication 1019, National Institute of Standards and Technology, Gaithersburg, MD, 2005.

4. Forney, G.P., and K. McGrattan, "User's Guide for Smokeview Version 4 — A Tool for Visualizing Fire Dynamics Simulation Data," NIST Special Publication 1017, National Institute of Standards and Technology, Gaithersburg, MD, 2004.

5. Rehm, R.G., and H.R. Baum, "The Equations of Motion for Thermally Driven, Buoyant Flows," *Journal of Research of the NBS,* 83:297–308, National Bureau of Standards, Washington, DC, 1978.

6. Smagorinsky, J., "General Circulation Experiments with the Primitive Equations. I. The Basic Experiment," *Monthly Weather Review,* 91(3):99–164, Weather Bureau, Department of Commerce, Washington, DC, 1963.

7. Quintiere, J., "A Perspective on Compartment Fire Growth," *Combustion Science and Technology,* 39:11–54, Gordon and Breach Science Publishers, New York, NY, 1984.

8. Beyler, C., "Flammability Limits of Premixed and Diffusion Flames," *SFPE Handbook of Fire Protection Engineering,* 3rd Edition, National Fire Protection Association, Quincy, Massachusetts, 2002.

9. Grosshandler, W., "RadCal: A Narrow Band Model for Radiation Calculations in a Combustion Environment," NIST Technical Note TN 1402, National Institute of Standards and Technology, Gaithersburg, MD, 1993.

10. Prasad, K., C. Li, K. Kailasanath, C. Ndubizu, R. Ananth, and P.A. Tatem, "Numerical Modeling of Methanol Liquid Pool Fires," *Combustion Theory and Modeling,* 3:743–768, Taylor & Francis, Abingdon, UK, 1999.

11. Atreya, A., "Pyrolysis, Ignition and Fire Spread on Horizontal Surfaces of Wood," NBS GCR 83-449, National Bureau of Standards (now NIST), Gaithersburg, MD, 1983.

12. Ritchie, S.J., K.D. Steckler, A. Hamins, T.G. Cleary, J.C. Yang, and T. Kashiwagi, "The Effect of Sample Size on the Heat Release Rate of Charring Materials," *Proceedings of the 5th International Symposium on Fire Safety Science,* pp. 177–188, International Association for Fire Safety Science, Melbourne, Australia, 1997.

13. Mell, W., K. McGrattan, and H. Baum, "Numerical Simulation of Combustion in Fire Plumes," *Twenty-Sixth Symposium (International) on Combustion*, Combustion Institute, Pittsburgh, PA, 1996.

14. McGrattan, K., H.R. Baum, and R.G. Rehm, "Large Eddy Simulations of Smoke Movement," *Fire Safety Journal*, 30:161–178, Elsevier, Oxford, UK, 1998.

15. Xin, Y., J.P. Gore, K. McGrattan, R.G. Rehm, and H.R. Baum, "Large Eddy Simulation of Buoyant Turbulent Pool Fires," *Proceedings of the 2002 Spring Technical Meeting, Central States Section*, Combustion Institute, Pittsburgh, PA, April 2002.

16. Baum, H.R., R.G. Rehm, P.D. Barnett, and D.M. Corley, "Finite Difference Calculations of Buoyant Convection in an Enclosure, Part I: The Basic Algorithm," *SIAM Journal of Scientific and Statistical Computing*, 4(1):117–135, Society of Industrial and Applied Mathematics, New York, NY, 1983.

17. Baum, H.R., and R.G. Rehm, "Finite Difference Solutions for Internal Waves in Enclosures," *SIAM Journal of Scientific and Statistical Computing*, 5(4):958–977, Society of Industrial and Applied Mathematics, New York, NY, 1984.

18. Rehm, R.G., H.R. Baum, P.D. Barnett, and D.M. Corley, "Finite Difference Calculations of Buoyant Convection in an Enclosure, Part II: Verification of the Nonlinear Algorithm," *Applied Numerical Mathematics*, 1:515–529, Elsevier, Oxford, UK, 1985.

19. McGrattan, K., R.G. Rehm, and H.R. Baum, "Fire-Driven Flows in Enclosures," *Journal of Computational Physics*, 110(2):285–292, Elsevier, Oxford, UK, 1994.

20. Mell, W., and T. Kashiwagi, "Dimensional Effects on Microgravity Flame Transition," *Twenty-Seventh Symposium (International) on Combustion*, Combustion Institute, Pittsburgh, PA, 1998.

21. Jhalani A., "A Numerical Study of Stretch in Partially Premixed Flames," Master's Thesis, University of Illinois at Chicago, Chicago, IL, 2001.

22. Hamins, A., M. Bundy, I. Puri, K.B. McGrattan, and W.C. Park, "Suppression of Low Strain Rate Non-Premixed Flames by an Agent," *Proceedings of the 6th International Microgravity Combustion Workshop*, NASA/CP-2001-210826, pp. 101–104, National Aeronautics and Space Administration, Lewis Research Center, Cleveland, OH, May 2001.

23. Zhang, W., A. Hamer, M. Klassen, D. Carpenter, and R. Roby, "Turbulence Statistics in a Fire Room Model by Large Eddy Simulation," *Fire Safety Journal*, Elsevier, Oxford, UK, 2002.

24. McGrattan, K., J. Floyd, G. Forney, H. Baum, and S. Hostikka, "Improved Radiation and Combustion Routines for a Large Eddy Simulation Fire Model," *Fire Safety Science — Proceedings of the Seventh International Symposium*, International Association for Fire Safety Science, Boston, MA, 2003.

A
TECHNICAL DETAILS OF THE FDS VALIDATION STUDY

Appendix A provides comparisons of FDS predictions and experimental measurements for the six series of fire experiments under consideration. The sections to follow contain assessments of the model predictions for the following quantities:

A.1   Hot Gas Layer Temperature and Height
A.2   Ceiling Jet Temperature
A.3   Plume Temperature
A.4   Flame Height
A.5   Oxygen and Carbon Dioxide Concentration
A.6   Smoke Concentration
A.7   Compartment Pressure
A.8   Target Heat Flux and Surface Temperature
A.9   Wall Heat Flux and Surface Temperature

The model predictions are compared to the experimental measurements in terms of the relative difference between the maximum (or where appropriate, minimum) values of each time history:

$$\varepsilon = \frac{\Delta M - \Delta E}{\Delta E} = \frac{(M_p - M_o) - (E_p - E_o)}{(E_p - E_o)}$$

ΔM is the difference between the peak value of the model prediction, M_p, and its original value, M_o. ΔE is the difference between the experimental measurement, E_p, and its original value, E_o. A positive value of the relative difference indicates that the model has over-predicted the severity of the fire (e.g., a higher temperature, lower oxygen concentration, higher smoke concentration, etc.).

A.1 Hot Gas Layer Temperature and Height

Like any CFD model, FDS does not perform direct calculations of the HGL temperature or height. These are constructs unique to two-zone models, like CFAST and MAGIC. Nonetheless, FDS does make predictions of gas temperature at the same locations as the thermocouples in the experiments, and these values can be reduced in the same manner as the experimental measurements to produce an "average" HGL temperature and height. Regardless of the validity of the reduction method, the FDS predictions of the HGL temperature and height ought to be representative of the accuracy of its predictions of the individual thermocouple measurements that are used in the HGL reduction.

The temperature measurements from all six test series are used to compute an HGL temperature and height with which to compare to FDS. The same layer reduction method is used for five of the six test series. Only the NBS Multi-Room series uses another method.

A brief description of each test series is included below, followed by graphs comparing the predicted and measured HGL temperature and layer height. A summary table is provided at the end of the section that displays the relative differences between predictions and measurements for all six test series. Note that the calculation of relative difference is based on the temperature *rise* above ambient, and the layer *depth*, that is, the distance from the ceiling to where the hot gas layer descends. Where the model over-predicts the HGL temperature or the *depth* of the HGL, the relative difference is a positive number. This convention is used throughout this appendix — where the model over-predicts the severity of the fire, the relative difference is positive; where it under-predicts, the relative difference is negative.

ICFMP BE #2

The HGL temperature and depth are calculated from the averaged gas temperatures from three vertical thermocouple arrays using the standard reduction method. There are 10 thermocouples in each vertical array, spaced 2 m (6.6 ft) apart in the lower two-thirds of the hall, and 1 m (3.3 ft) apart near the ceiling. Figure A-1 presents a snapshot from one of the simulations. Note in the figure that all of the obstructions, including the slanted roof and exhaust duct, are approximated in the model as rectangular to conform with the rectilinear grid.
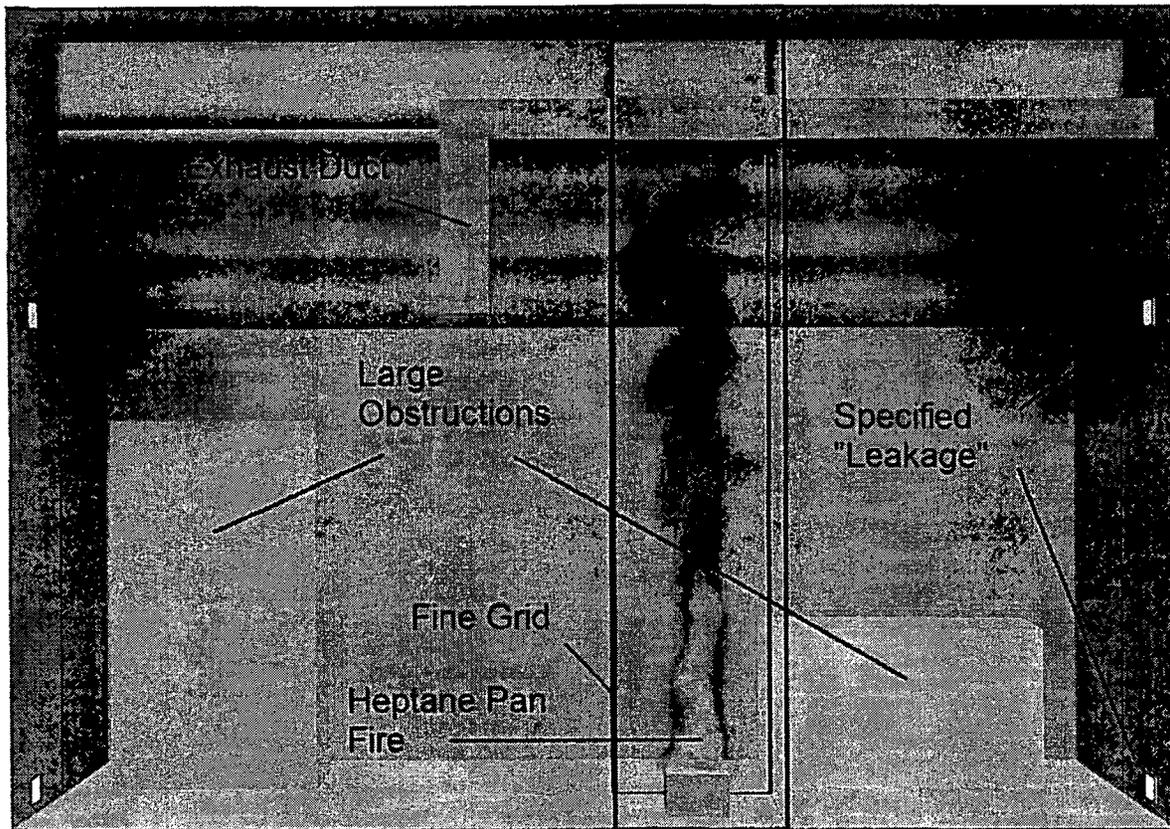
Figure A-1: Cut-Away View of the Simulation of ICFMP BE #2, Case 2
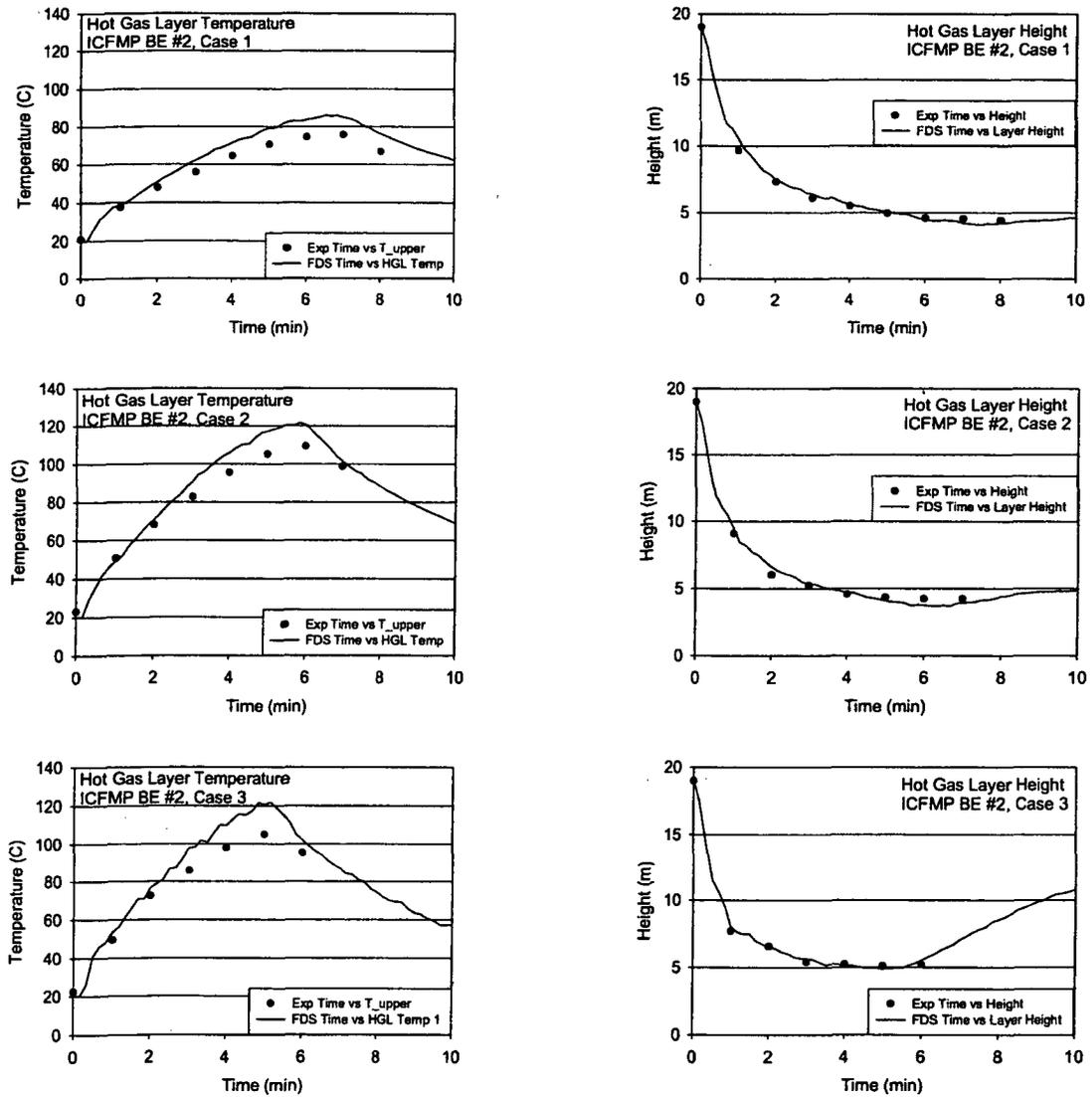
Figure A-2: Hot Gas Layer (HGL) Temperature and Height, ICFMP BE #2

ICFMP BE #3

BE #3 consists of 15 liquid spray fire tests with different heat release rates, pan locations, and ventilation conditions. The basic geometry, including the numerical grid, is shown in Figure A-3. Gas temperatures were measured using seven floor-to-ceiling thermocouple arrays (or "trees") distributed throughout the compartment. The average hot gas layer temperature and height are calculated using thermocouple Trees 1, 2, 3, 5, 6 and 7. Tree 4 is not used because one of its thermocouples (4-9) malfunctioned during most of the experiments.

Door on West Side   Control Cable B   Cable Tray D   Power Cable F
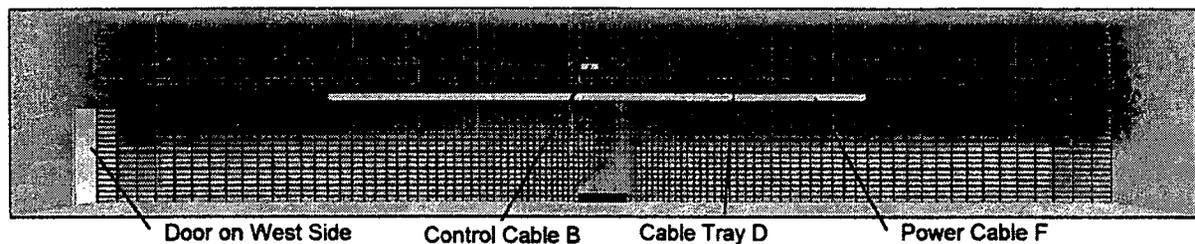
Figure A-3: Snapshot of the Simulation of ICFMP BE #3, Test 3

A few observations about the simulations are worthy of note:

- During Tests 4, 5, 10, and 16, a fan blew air into the compartment through a vent in the south wall. The measured velocity profile of the fan is not uniform, with the bulk of the air blowing from the lower third of the duct toward the ceiling at a roughly 45° angle. The exact flow pattern is difficult to replicate in the model, thus, the results for Tests 4, 5, 10, and 16 should be evaluated with this in mind. The effect of the fan on the hot gas layer is small, but it does have some effect on target temperatures near the vent.

- For all of the tests involving a fan, the predicted HGL height rises after the fire is extinguished, while the measured HGL drops. This appears to be a curious artifact of the layer reduction algorithm. It is not included in the calculation of the relative difference.

- In the closed-door tests, the hot gas layer descends all the way to the floor. However, the reduction method, used on both the measured and predicted temperatures, does not account for the formation of a single layer and, therefore, does not indicate that the layer drops all the way to the floor. This is neither a flaw in the measurements nor in FDS, but rather in the layer reduction method.

- The HGL reduction method produces spurious results in the first few minutes of each test because no clear layer has yet formed. These early times are not included in the relative difference calculation.
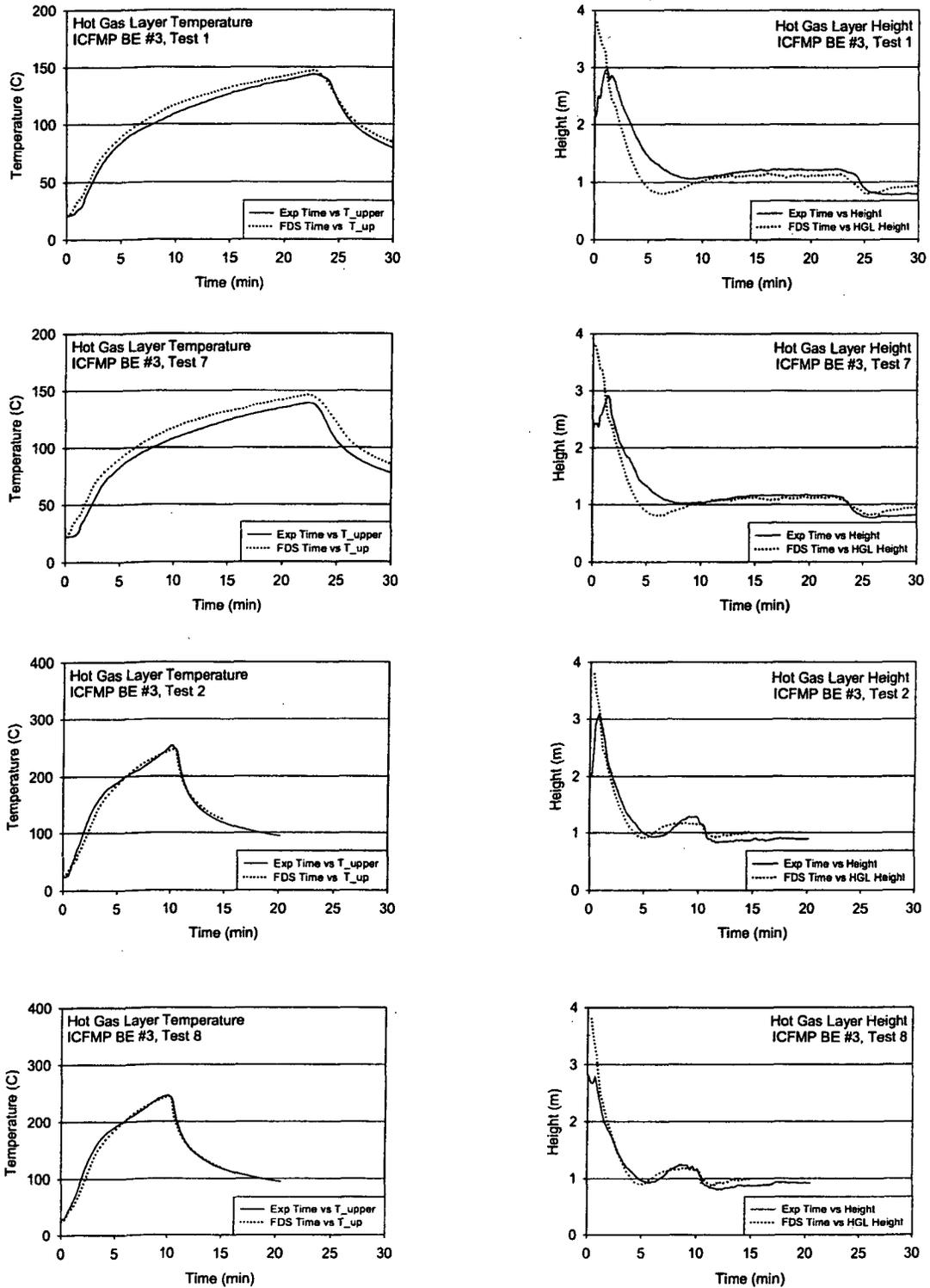
Figure A-4: Hot Gas Layer (HGL) Temperature and Height, ICFMP BE #3, Closed-Door Tests
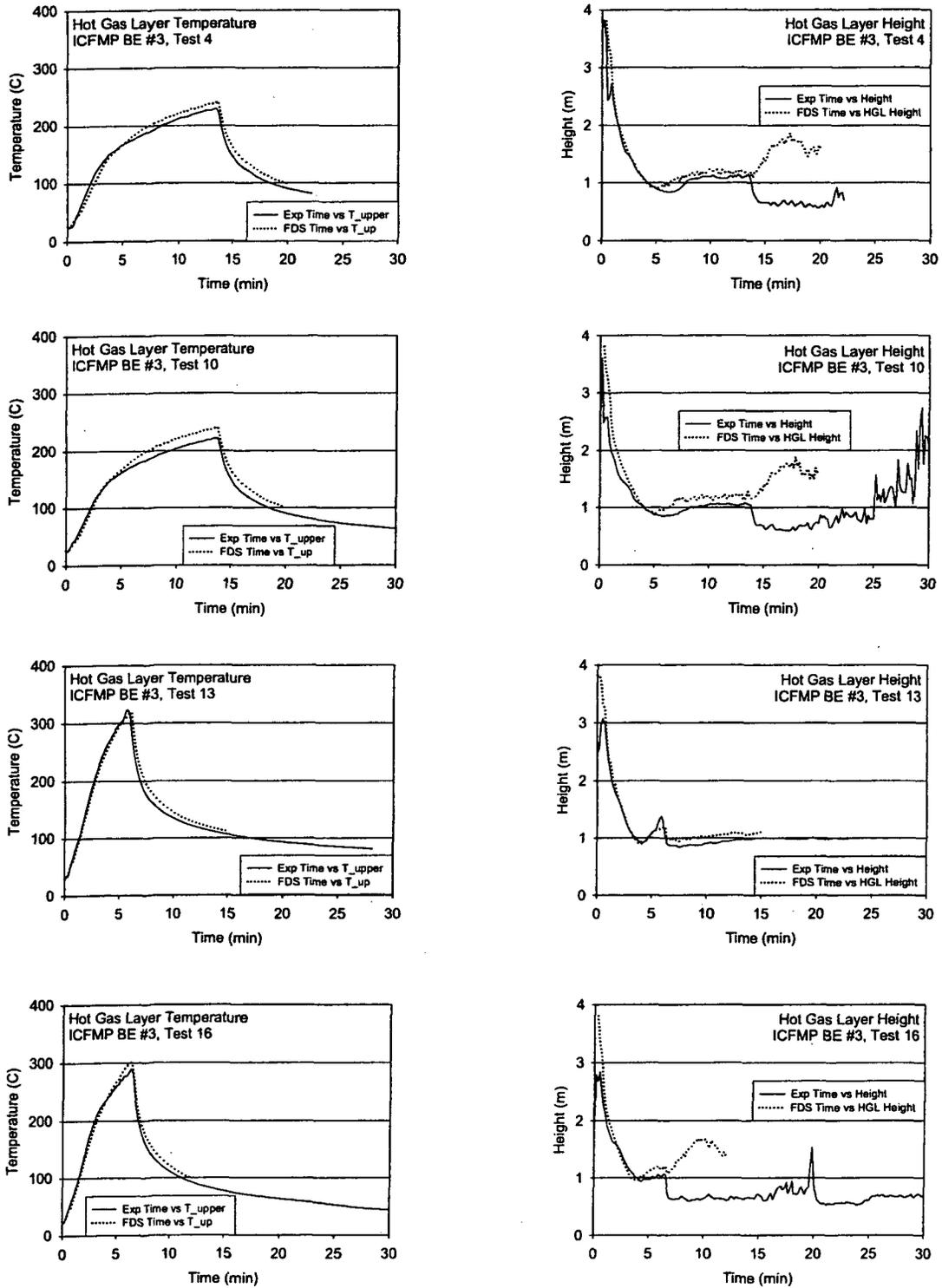
Figure A-5: Hot Gas Layer (HGL) Temperature and Height, ICFMP BE #3, Closed-Door Tests
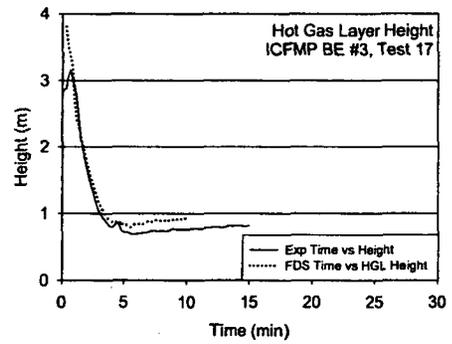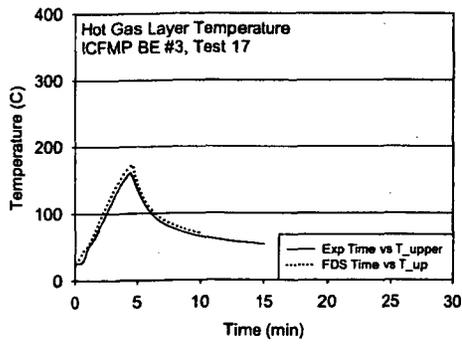
Open Door Tests to Follow
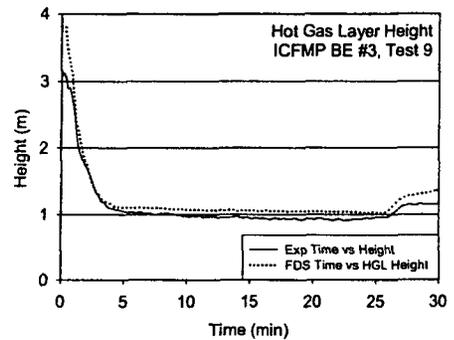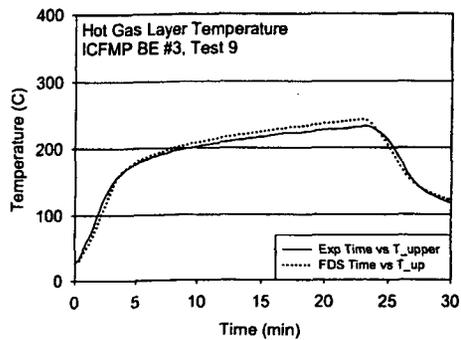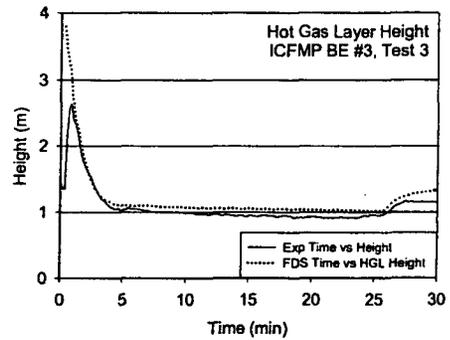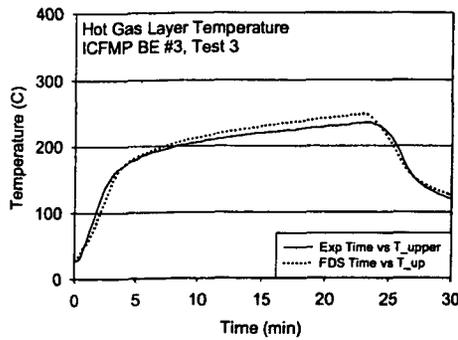
Figure A-6: Hot Gas Layer (HGL) Temperature and Height, ICFMP BE #3, Open-Door Tests
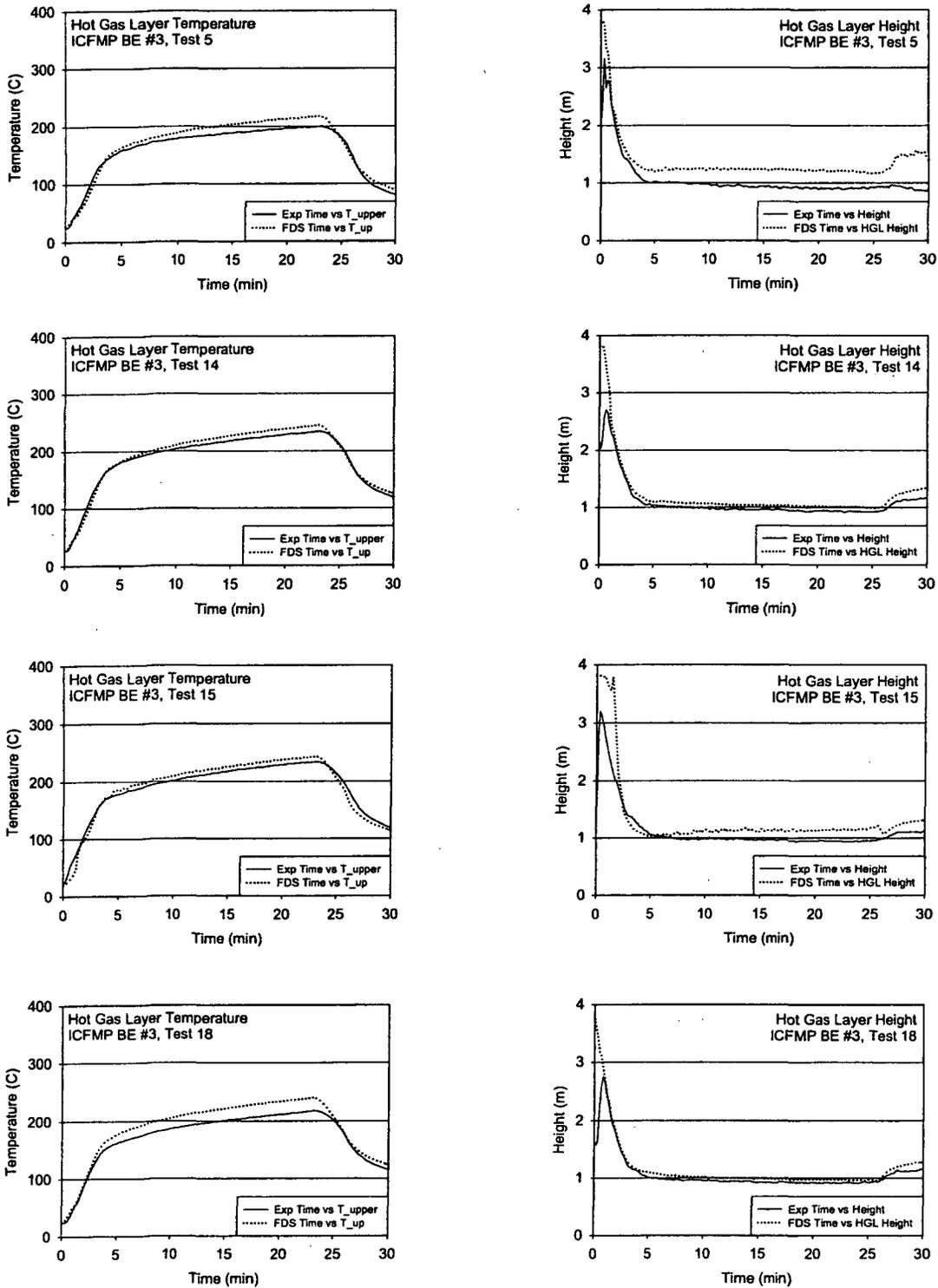
Figure A-7: Hot Gas Layer (HGL) Temperature and Height, ICFMP BE #3, Open-Door Tests

ICFMP BE #4

ICFMP BE #4 consists of two experiments, of which one (Test 1) was chosen for validation. Compared to the other experiments, this fire was relatively large in a relatively small compartment. Thus, its HGL temperature is considerably higher than the other fire tests under study. As shown in Figure A-8, the compartment geometry is fairly simple, with most of the objects contained within it being rectangular and easily conforming to the simple 10 cm uniform grid used by FDS. The only exception is a cylindrically-shaped waste container located just behind the fire pan, which according to the simulation, is engulfed by the fire. In the model, the cylindrical barrel is approximated as a rectangular solid.
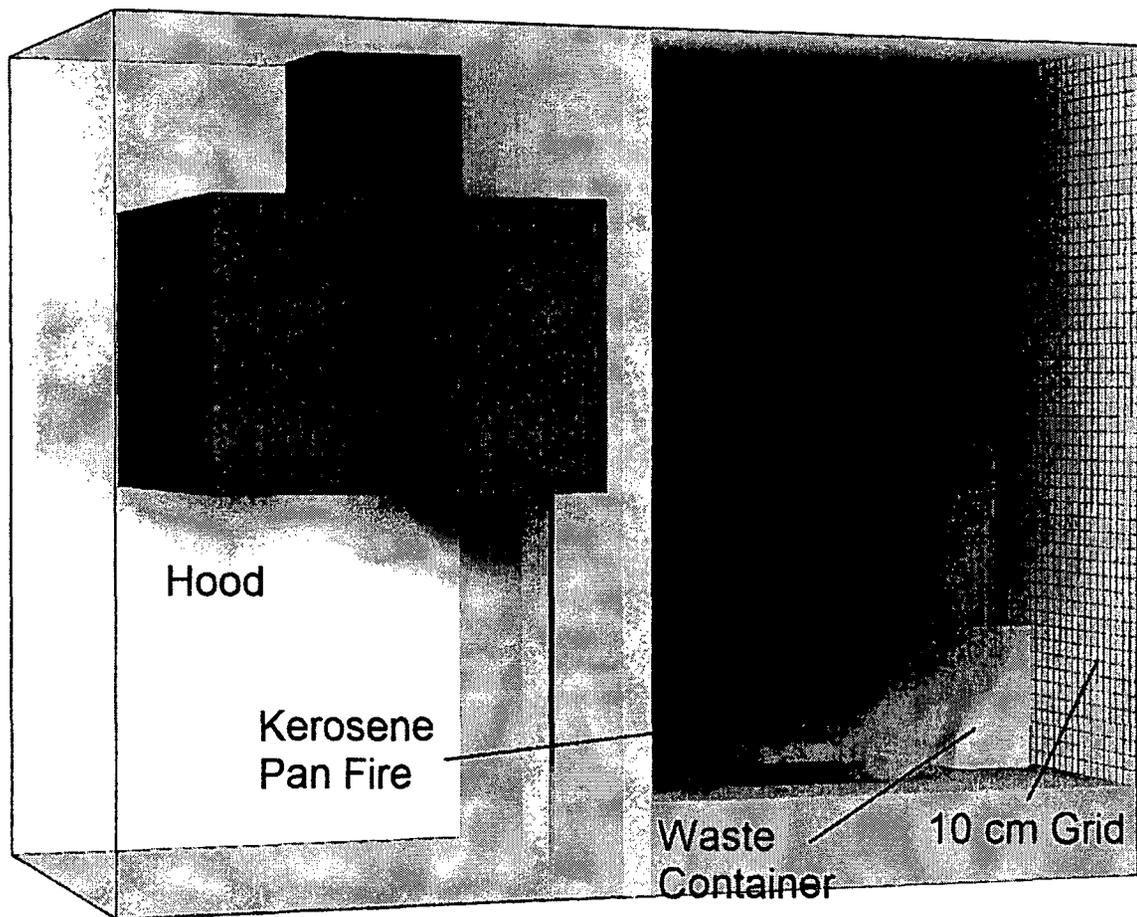
Figure A-8: Snapshot of the Simulation of ICFMP BE #4, Test 1

The HGL temperature prediction, while matching the experiment in maximum value, has a noticeably different shape than the measured profile, both in the first 5 minutes and following extinction. The HGL height prediction is distinctly different in the first 10 minutes and differs by about 30% after that time. There appears to be an error in the reduction of the experimental data.
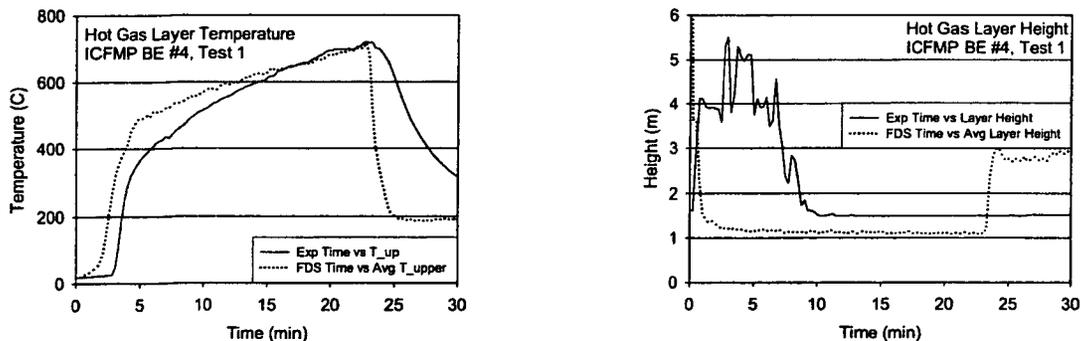
Figure A-9: Hot Gas Layer (HGL) Temperature and Height, ICFMP BE #4, Test 1

ICFMP BE #5

BE #5 was performed in the same fire test facility as BE #4. Figure A-10 displays the overall geometry of the compartment, as idealized by FDS. Test 4 is the only experiment from this test series that was used in the evaluation, and only the first 20 minutes of the test, during the "pre-heating" stage when only the ethanol pool fire is active. The burner was lit after that point, and the cables began to burn.
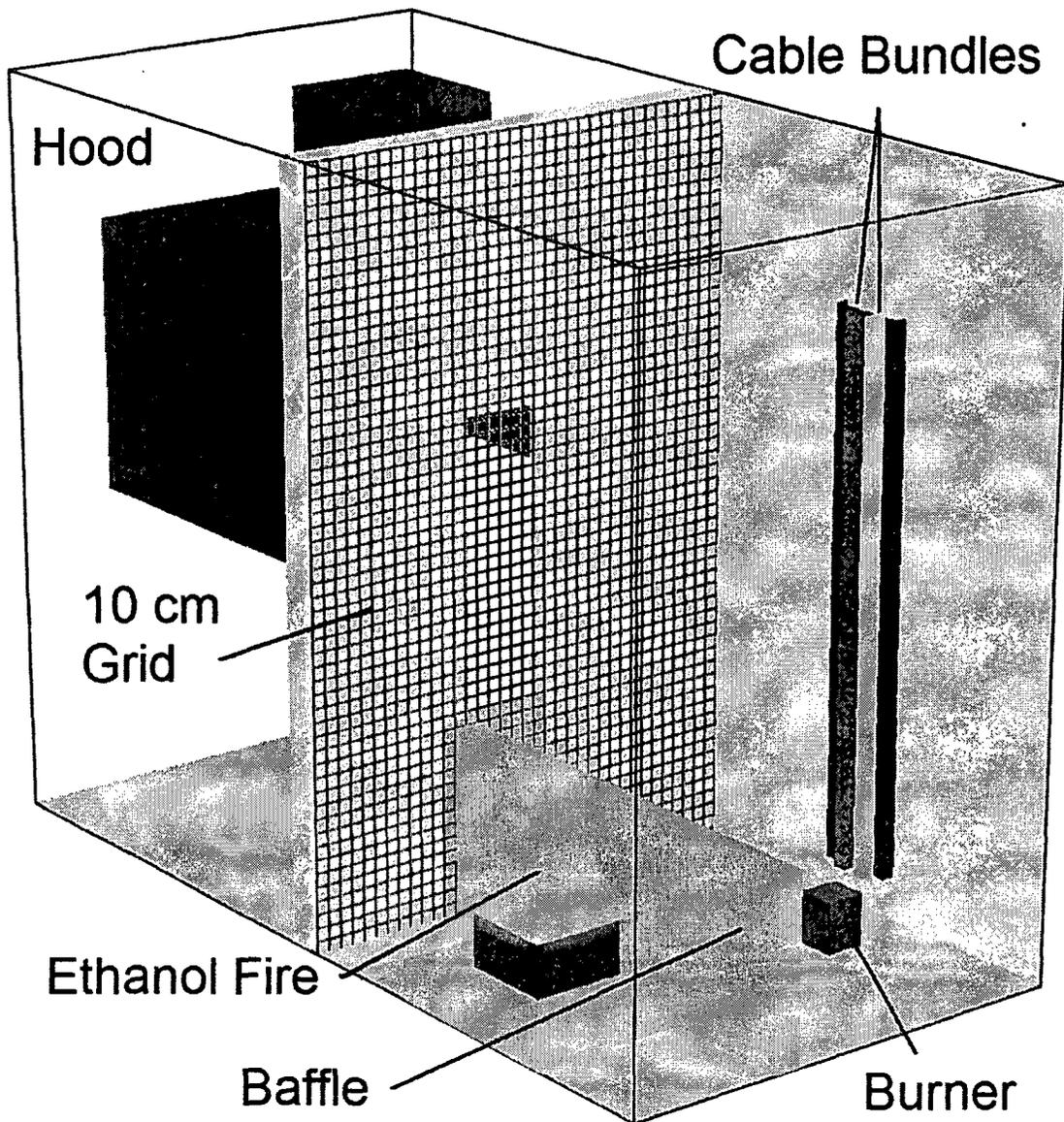
Figure A-10: Snapshot of the Simulation of ICFMP BE #5, Test 4
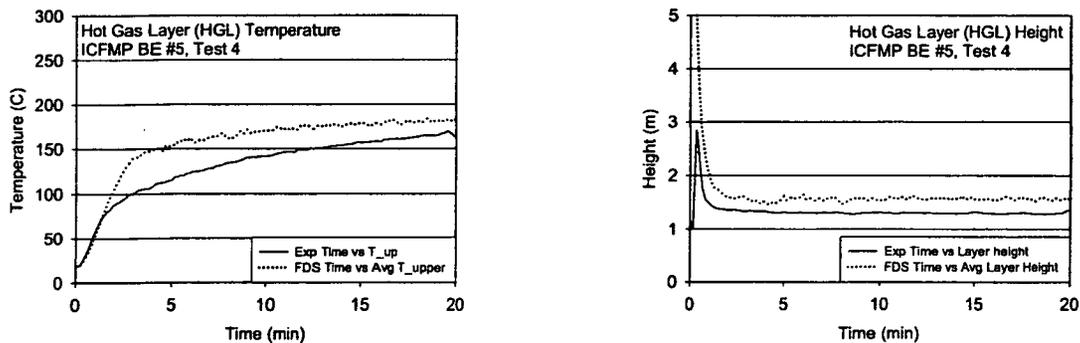
Figure A-11: Hot Gas Layer (HGL) Temperature and Height, ICFMP BE #5, Test 4

FM/SNL Test Series

Tests 4, 5, and 21 from the FM/SNL test series were selected for comparison. The hot gas layer temperature and height were calculated using the standard method. The thermocouple arrays referred to as Sectors 1, 2, and 3 were averaged (with an equal weighting for each) for Tests 4 and 5. For Test 21, only Sectors 1 and 3 were used, as Sector 2 falls within the smoke plume.
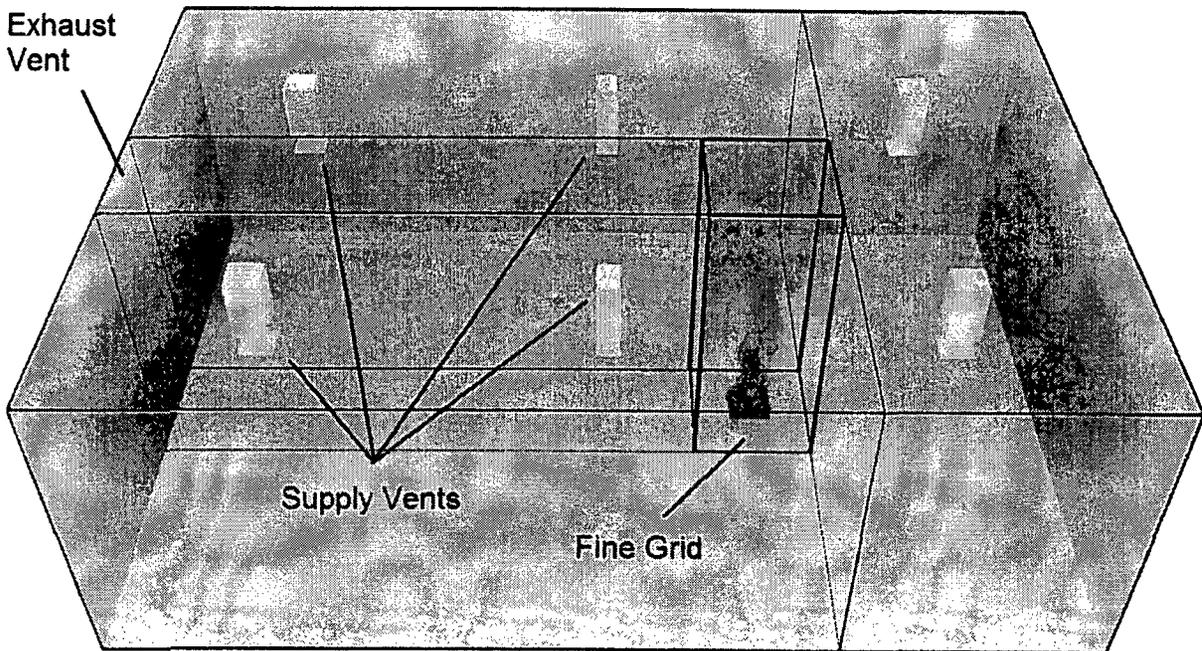
Figure A-12: Snapshot of the Simulation of FM/SNL Test 5

Note the following:

- The HGL heights, both measured and predicted, are somewhat noisy because of the effect of ventilation ducts in the upper layer.

- The ventilation was turned off after 9 minutes in Test 5, the effect of which was a slight increase in both the measured and predicted HGL temperatures.

- The measured HGL temperature was noticeably greater than the prediction in Test 21. This is possibly attributable to an increase in the HRR toward the end of the test. The simulations all used fixed HRRs after the 4-minute ramp-up.
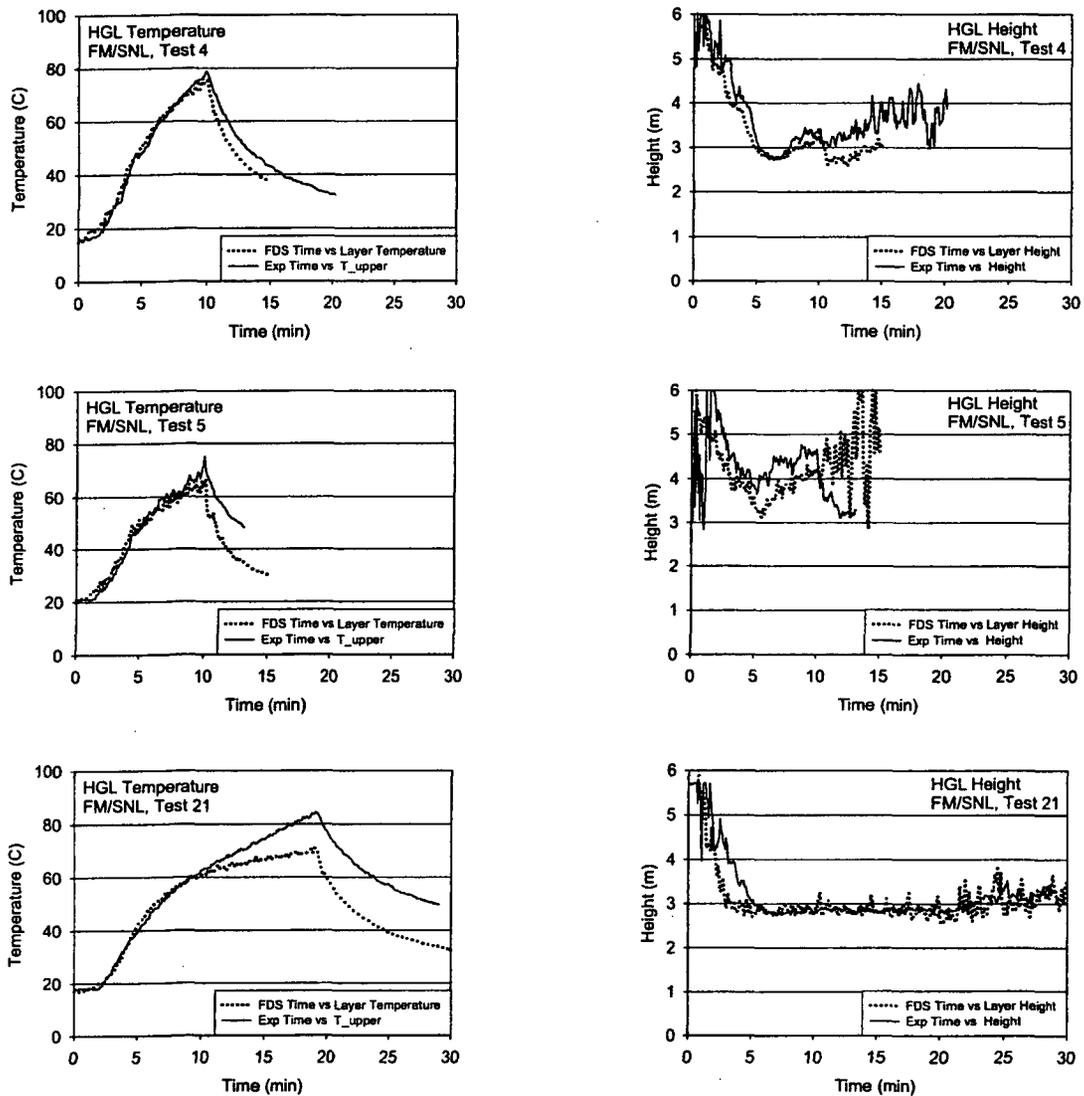
Figure A-13: Hot Gas Layer (HGL) Temperature and Height, FM/SNL Series

NBS Multi-Room Test Series

This series of experiments consists of two relatively small rooms connected by a long corridor. The fire was located in one of the rooms. Eight vertical arrays of thermocouples were positioned throughout the test space (one in the burn room, one near the door of the burn room, three in the corridor, one in the exit to the outside at the far end of the corridor, one near the door of the other or "target" room, and one inside the target room). Four of the eight arrays were selected for comparison with model predictions [the array in the burn room (BR), the array in the middle of the corridor (5.5 m (18 ft) from the BR), the array at the far end of the corridor (11.6 m (38 ft) from the BR), and the array in the target room (TR)]. In Tests 100A and 100O, the target room was closed, in which case, the array in the exit (EXI) doorway was used.

The test director reduced the layer information individually for the eight thermocouple arrays using an alternative method[2]. These results are included in the original data sets. However, for the current validation study, the selected TC trees were reduced using the conventional method common to all the experiments considered. The results are presented below.

110 kW Fire

Burn Room (BR)
TC Tree

Target Room (TR)
TC Tree

TC Tree "18"

TC Tree "EXI"

TC Tree "38"
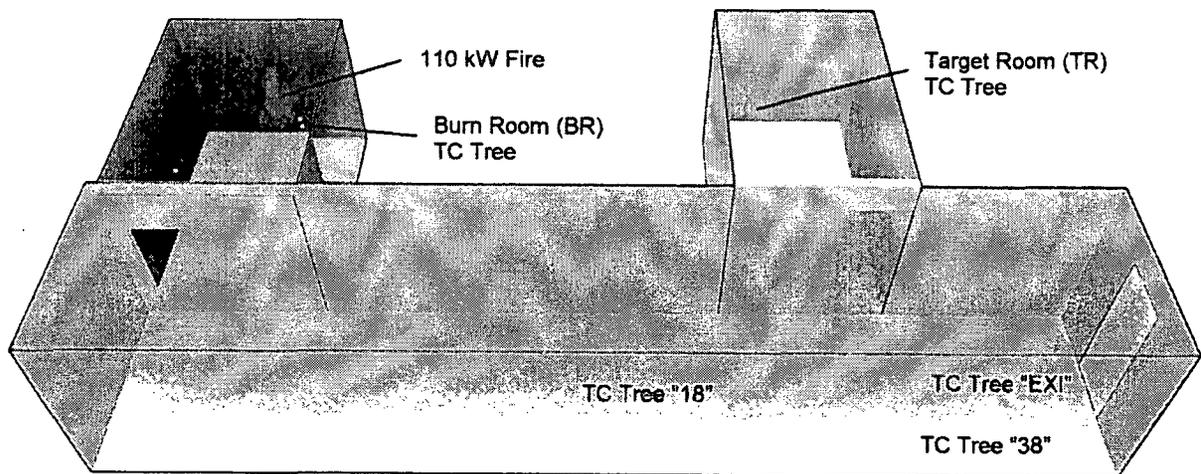
Figure A-14: Snapshot of the Simulation of NBS Multi-Room Test 100Z

---

[2]   Peacock, R.D., and V. Babrauskas, "Analysis of Large-Scale Fire Test Data," *Fire Safety Journal*, Vol. 17, pp. 387–414, 1991.
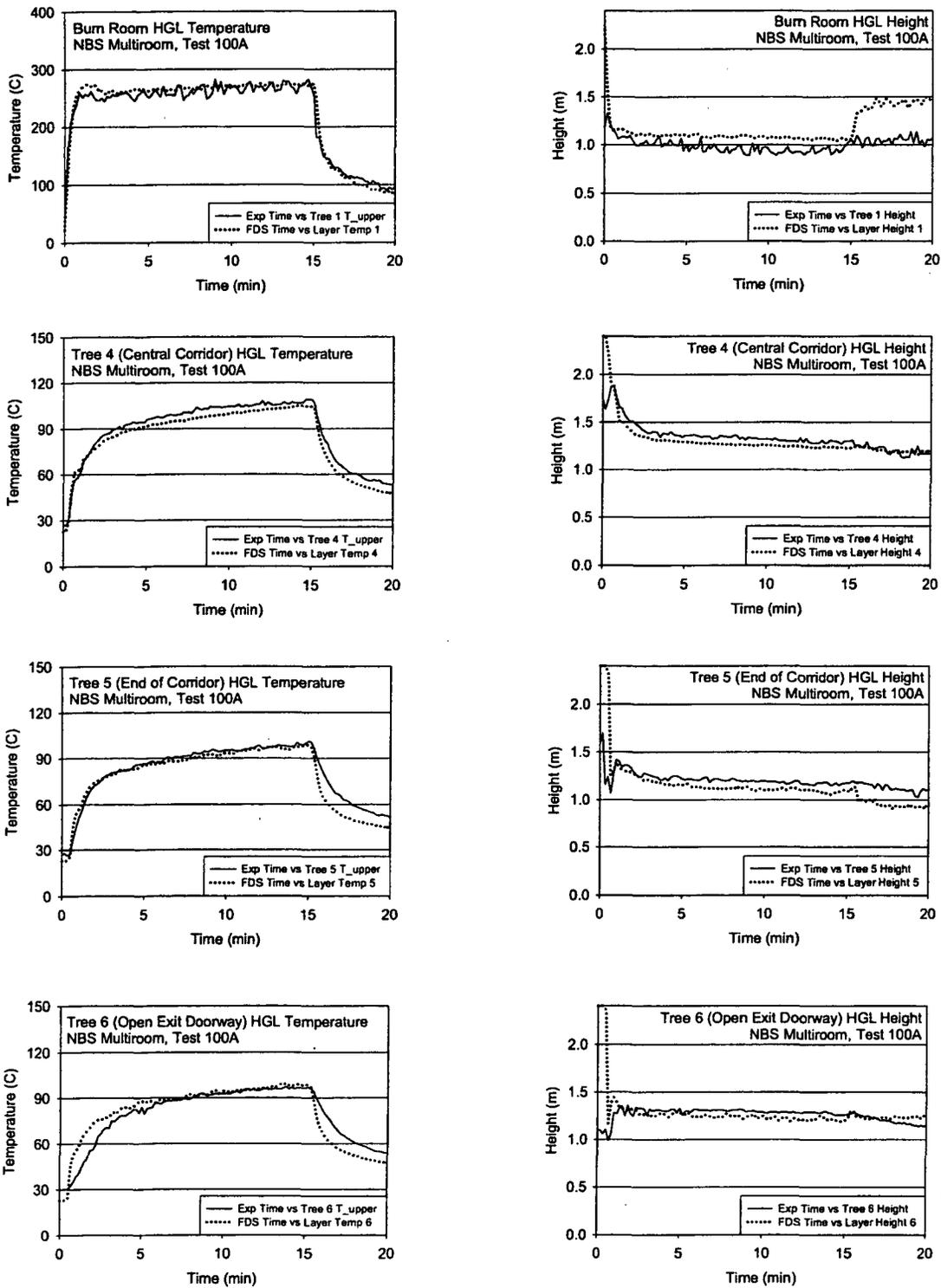
Figure A-15: Hot Gas Layer (HGL) Temperature and Height, NBS Multi-Room Test 100A
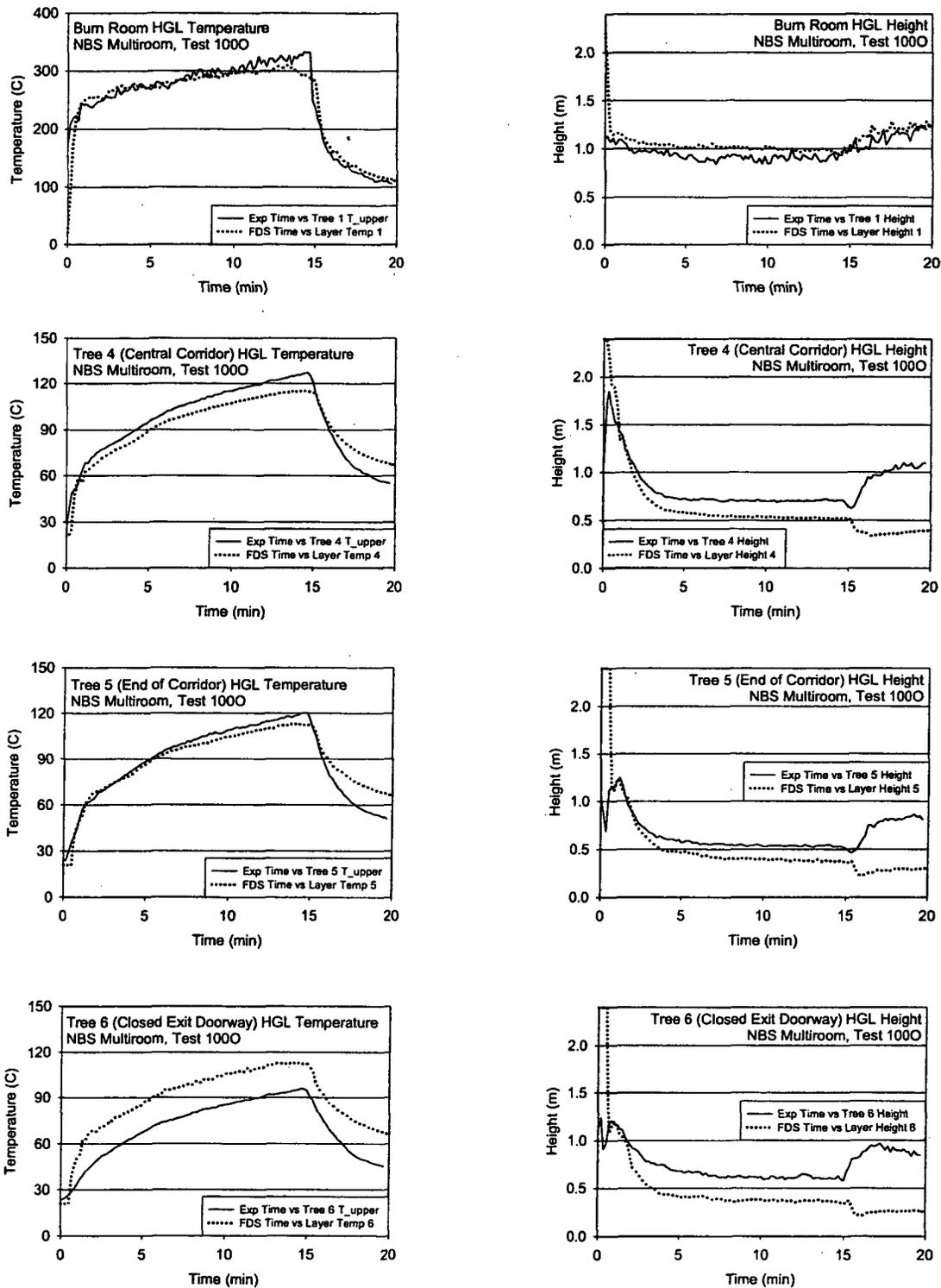
Figure A-16: Hot Gas Layer (HGL) Temperature and Height, NBS Multi-Room Test 100O
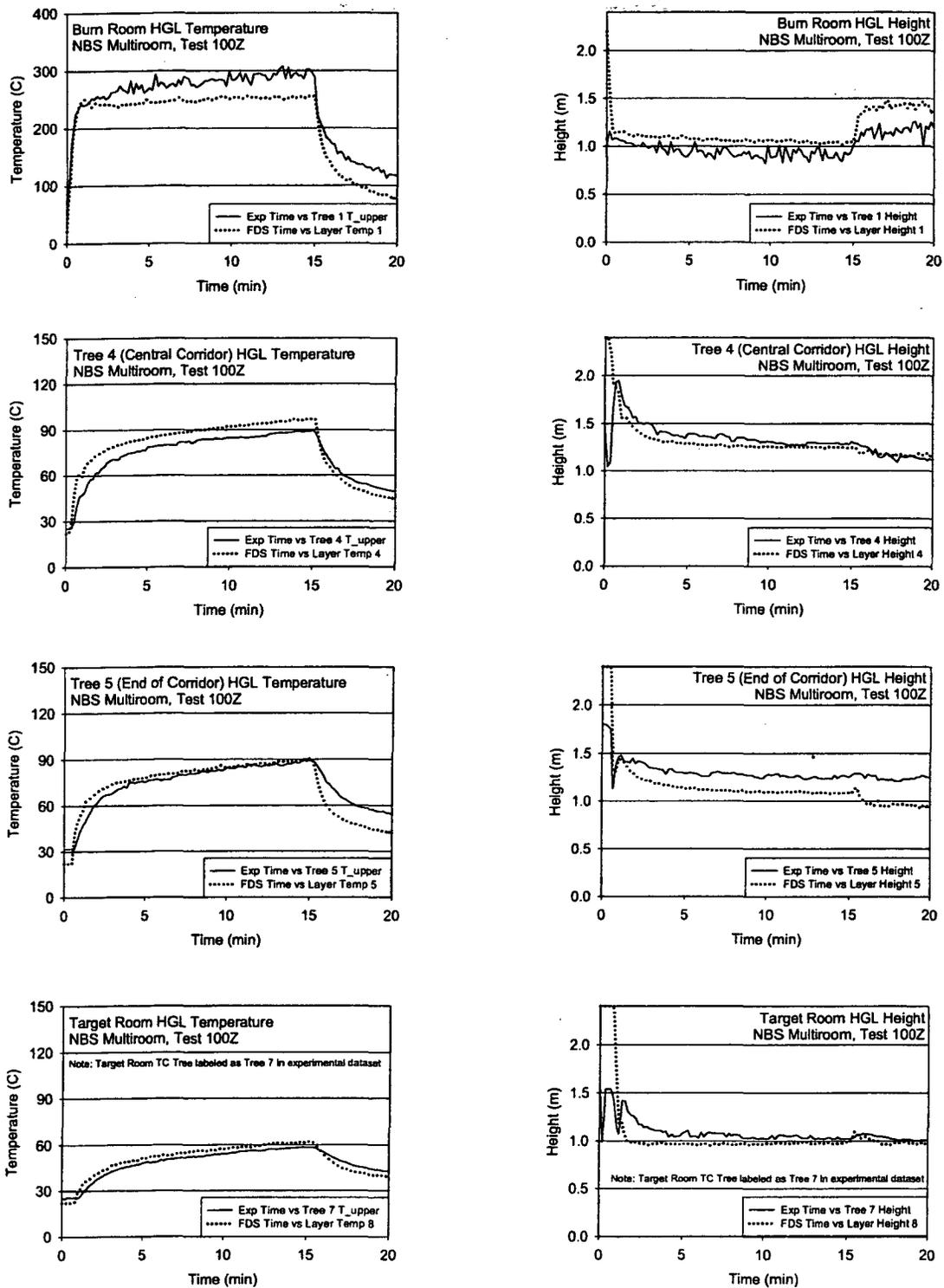
Figure A-17: Hot Gas Layer (HGL) Temperature and Height, NBS Multi-Room Test 100Z

Table A-1: Summary of HGL Temperature and Depth Comparisons

			HGL Temperature Rise			HGL Depth		
			ΔE (°C)	ΔM (°C)	Diff. (%)	ΔE (m)	ΔM (m)	Diff. (%)
BE #2	Case1		55	66	21	14.6	14.9	3
	Case2		86	102	18	14.8	15.3	4
	Case3		83	101	23	13.9	14.1	2
BE #3	Test 1		123	125	2	3.0	3.0	-1
	Test 7		117	122	5	3.1	3.0	-1
	Test 2		229	220	-4	3.0	2.9	-3
	Test 8		218	220	1	3.0	2.9	-2
	Test 4		204	214	5	3.0	2.9	-2
	Test 10		198	212	7	3.2	2.9	-9
	Test 13		291	289	-1	3.0	2.9	-2
	Test 16		268	275	2	2.9	2.9	-1
	Test 17		135	143	6	3.1	3.0	-3
	Test 3		207	218	5	2.9	2.8	-3
	Test 9		204	216	6	2.9	2.8	-4
	Test 5		176	190	8	3.0	2.7	-10
	Test 14		208	218	4	2.9	2.8	-3
	Test 15		211	223	6	2.9	2.8	-3
	Test 18		193	213	10	2.9	2.9	-2
BE #4 Test 1			700	693	-1	4.2	4.6	10
BE #5 Test 4			151	166	10	4.3	4.1	-4
FM/ SNL	Test 4		59	58	-3	3.4	3.4	1
	Test 5		47	48	3	2.3	2.9	26
	Test 21		66	53	-20	3.4	3.4	-1
NBS Multi-Room	100A	BR	267	253	-5	1.2	1.1	-5
		18	81	82	1	1.3	1.2	-8
		38	75	75	0	1.4	1.4	0
		EXI	73	77	5	1.2	1.3	4
	100O	BR	313	289	-8	1.2	1.2	6
		18	98	94	-4	2.1	1.9	-10
		38	93	92	-1	2.2	2.1	-7
		EXI	–	92	--	2.2	2.1	-4
	100Z	BR	260	234	-10	1.2	1.1	-2
		18	65	75	16	1.2	1.2	-1
		38	67	68	2	1.2	1.4	13
		TR	35	40	14	1.5	1.5	-1

A.2 Ceiling Jet Temperature

FDS is a computational fluid dynamics (CFD) model and has no explicit ceiling jet model. Rather, temperatures throughout the fire compartment are computed directly from the governing conservation equations. Nonetheless, temperature measurements near the ceiling can be used to evaluate the model's ability to predict the flow of hot gases across a relatively flat ceiling. Measurements for this category are available from ICFMP BE #3 and the FM/SNL series.

ICFMP BE #3

The thermocouple nearest the ceiling in Tree 7, located toward the back of the compartment, was chosen as a surrogate for the ceiling jet temperature. Curiously, the difference between measured and predicted temperatures is noticeably greater for the open-door tests. Certainly, the open door changes the flow pattern of the exhaust gases. However, the predicted HGL heights for the open-door tests, shown in the previous section, do not show a noticeable difference from their closed-door counterparts. The predicted HGL temperatures are only slightly less than those measured in the open-door tests, largely because of the contribution of Tree 7 in the layer reduction calculation.
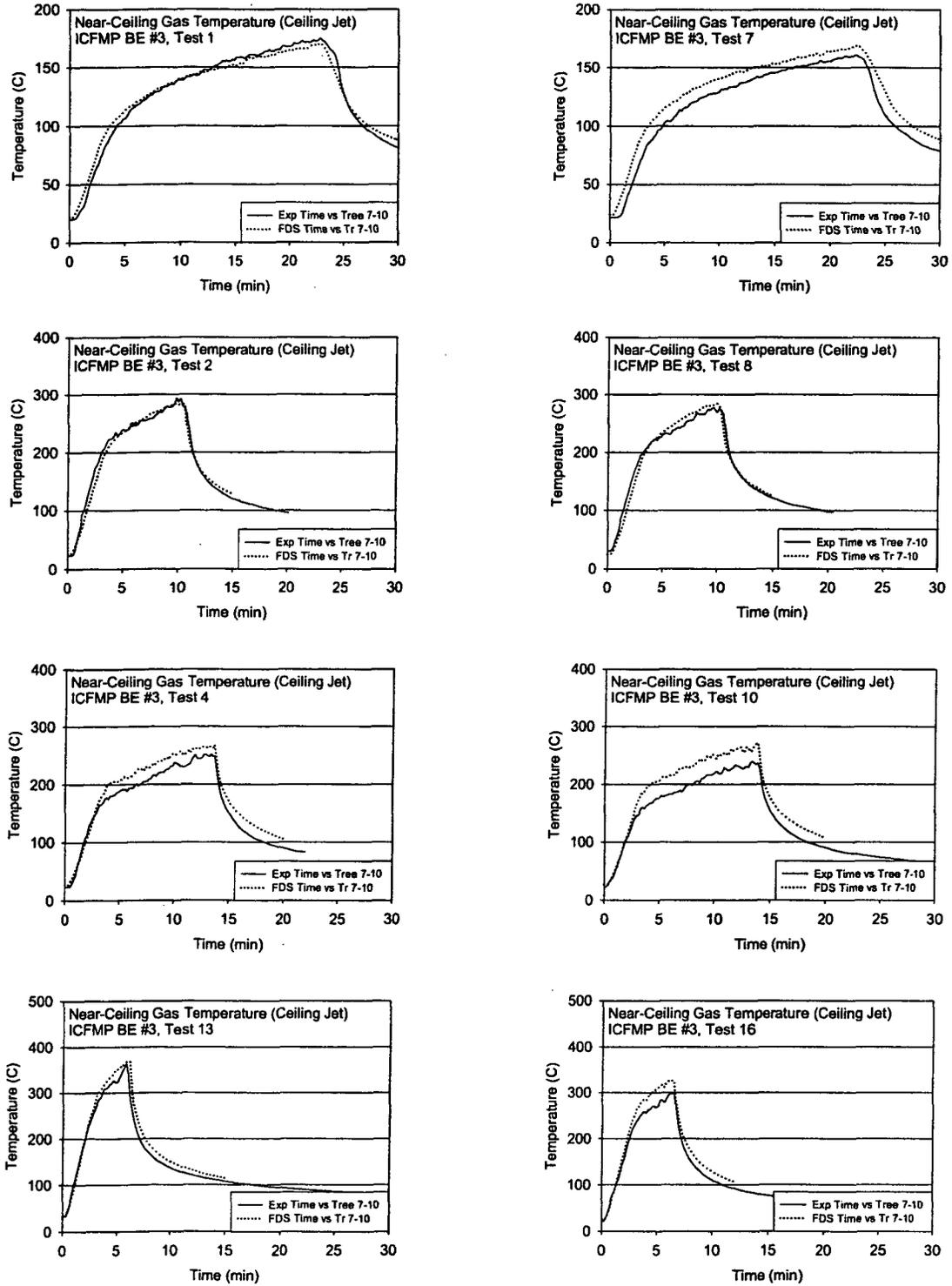
Figure A-18: Near-Ceiling Gas Temperatures, ICFMP BE #3, Closed-Door Tests

Open Door Tests to Follow
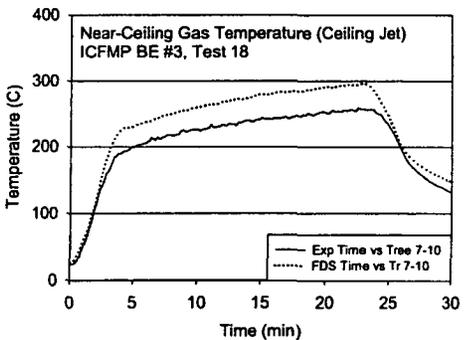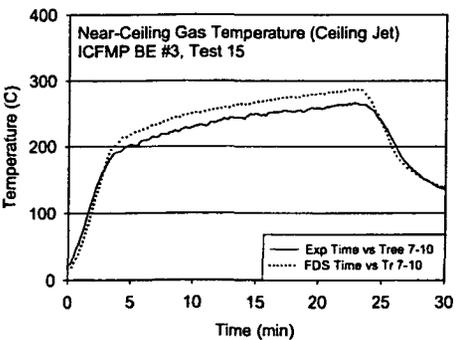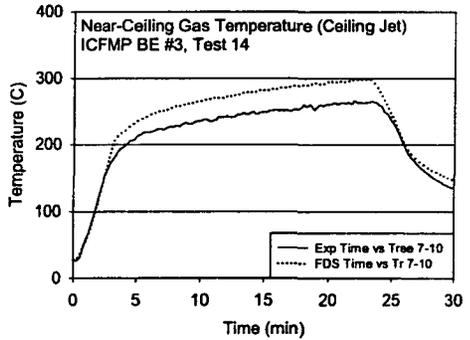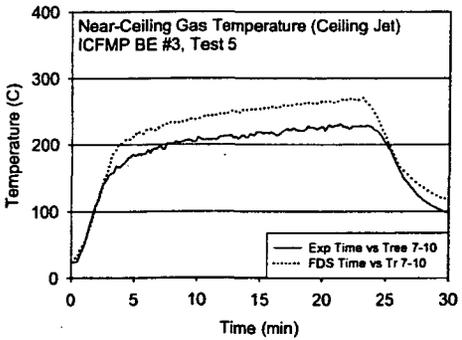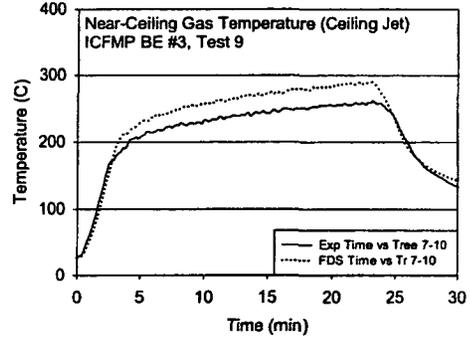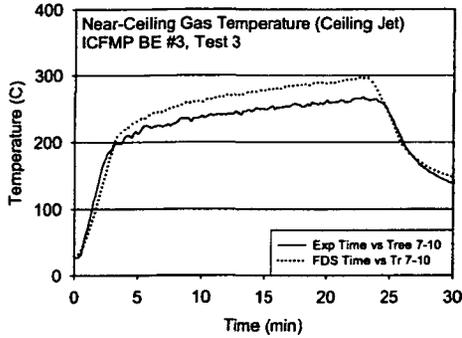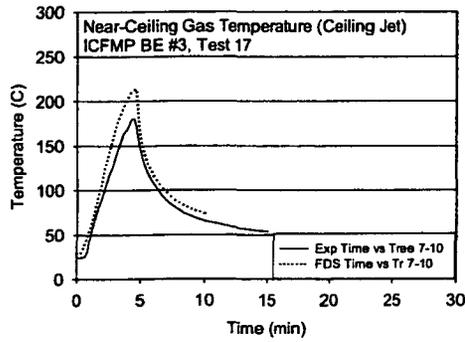
Figure A-19: Near-Ceiling Gas Temperatures, ICFMP BE #3, Closed-Door Tests

A-23

FM/SNL Test Series

The near-ceiling thermocouples in Sectors 1 and 3 were chosen as surrogates for the ceiling jet temperature. The results are shown below. The only noticeable discrepancy is in Test 21, and it is the same pattern that was observed in the HGL temperature comparison for this test.
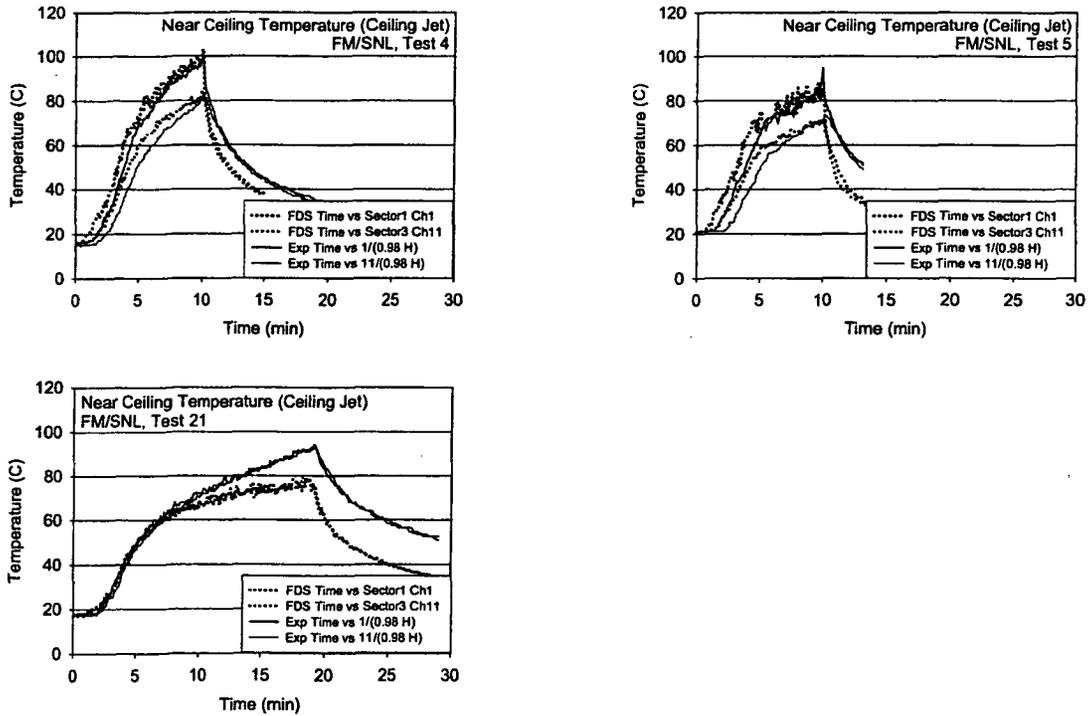
Figure A-20: Near-Ceiling Gas Temperatures, FM/SNL Series, Sectors 1 and 3

Table A-2: Summary of Ceiling Jet Temperature Comparisons

			Ceiling Jet Temperature Rise		
			ΔE (°C)	ΔM (°C)	Diff. (%)
ICFMP BE #3		Test 1	155	148	-4
		Test 7	139	145	4
		Test 2	271	258	-5
		Test 8	247	259	5
		Test 4	229	241	5
		Test 10	218	244	12
		Test 13	330	337	2
		Test 16	278	303	9
		Test 17	156	184	18
		Test 3	241	268	11
		Test 9	235	264	12
		Test 5	208	243	17
		Test 14	241	271	13
		Test 15	244	270	11
		Test 18	235	269	15
FM/SNL	Test 4	Sec 1	82	88	7
		Sec 3	66	69	5
	Test 5	Sec 1	70	66	-6
		Sec 3	53	50	-6
	Test 21	Sec 1	75	62	-17
		Sec 3	77	63	-19

A.3 Plume Temperature

Plume temperature measurements are available from ICFMP BE #2 and the FM/SNL series. For all other series of experiments, the temperature above the fire was not reported, or the fire plume leaned because of the flow pattern within the compartment, or the fire was positioned against a wall. Only for BE #2 and the FM/SNL series are the plumes relatively free from perturbations.

ICFMP BE #2

BE #2 consisted of liquid fuel pan fires conducted in the middle of a large fire test hall. Plume temperatures were measured at two heights above the fire, 6 m and 12 m (19.7 ft and 39.4 ft). The flames extended to about 4 m (13.1 ft) above the fire pan. FDS over-predicts the 6-m measurement by 20% to 30%. This is a challenging prediction because the temperature decreases rapidly just above the flame tip (Figure A-21). The 12-m measurement is less challenging because the temperatures are not decreasing as rapidly at this height.
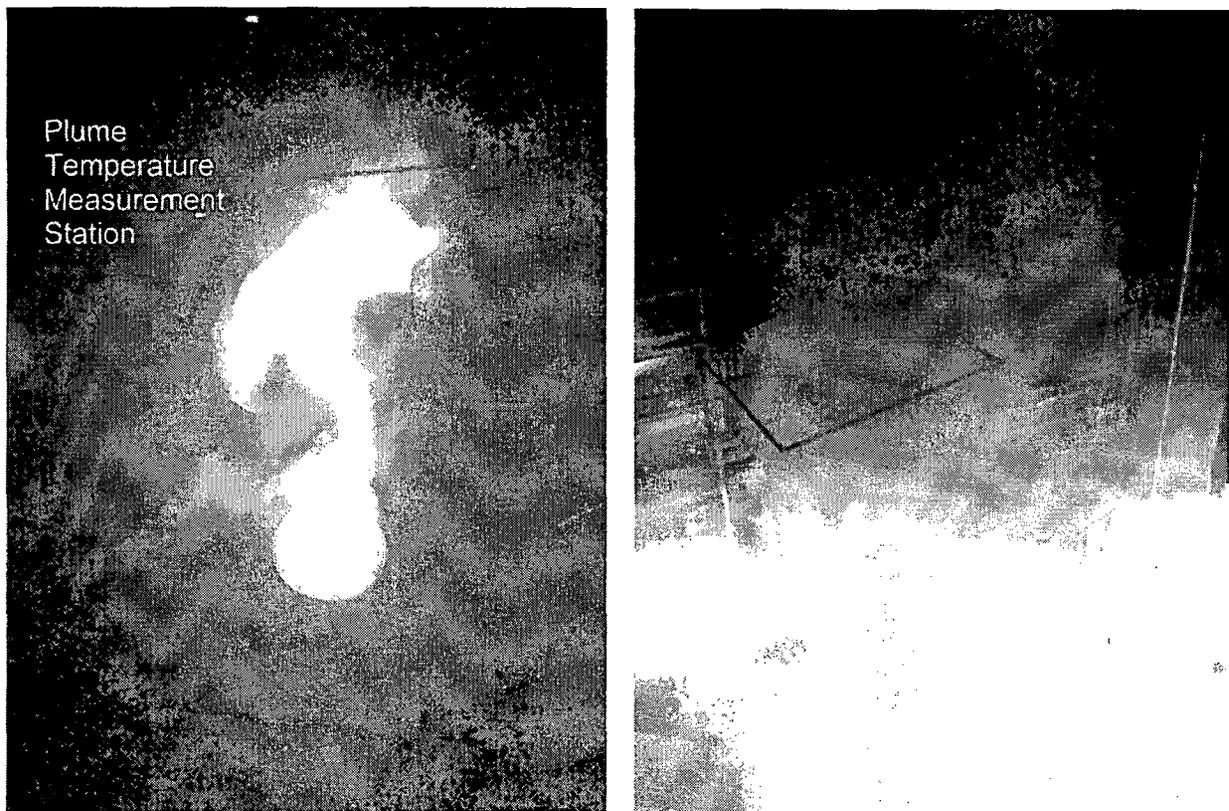
**Figure A-21: Photographs of Fire Plumes in ICFMP BE #2
(Courtesy of Simo Hostikka, VTT Building and Transport, Espoo, Finland.)**

The FM-SNL Test Series

In Tests 4 and 5, thermocouples were positioned near the ceiling directly over the fire pan. In Test 21, the fire was located within an empty electrical cabinet, and the closest near ceiling thermocouple was used to assess the "plume" temperature. Note that in Test 5, the FDS plume temperature curve was smoothed to better assess the relative difference between the peak values of the model and the measurement.
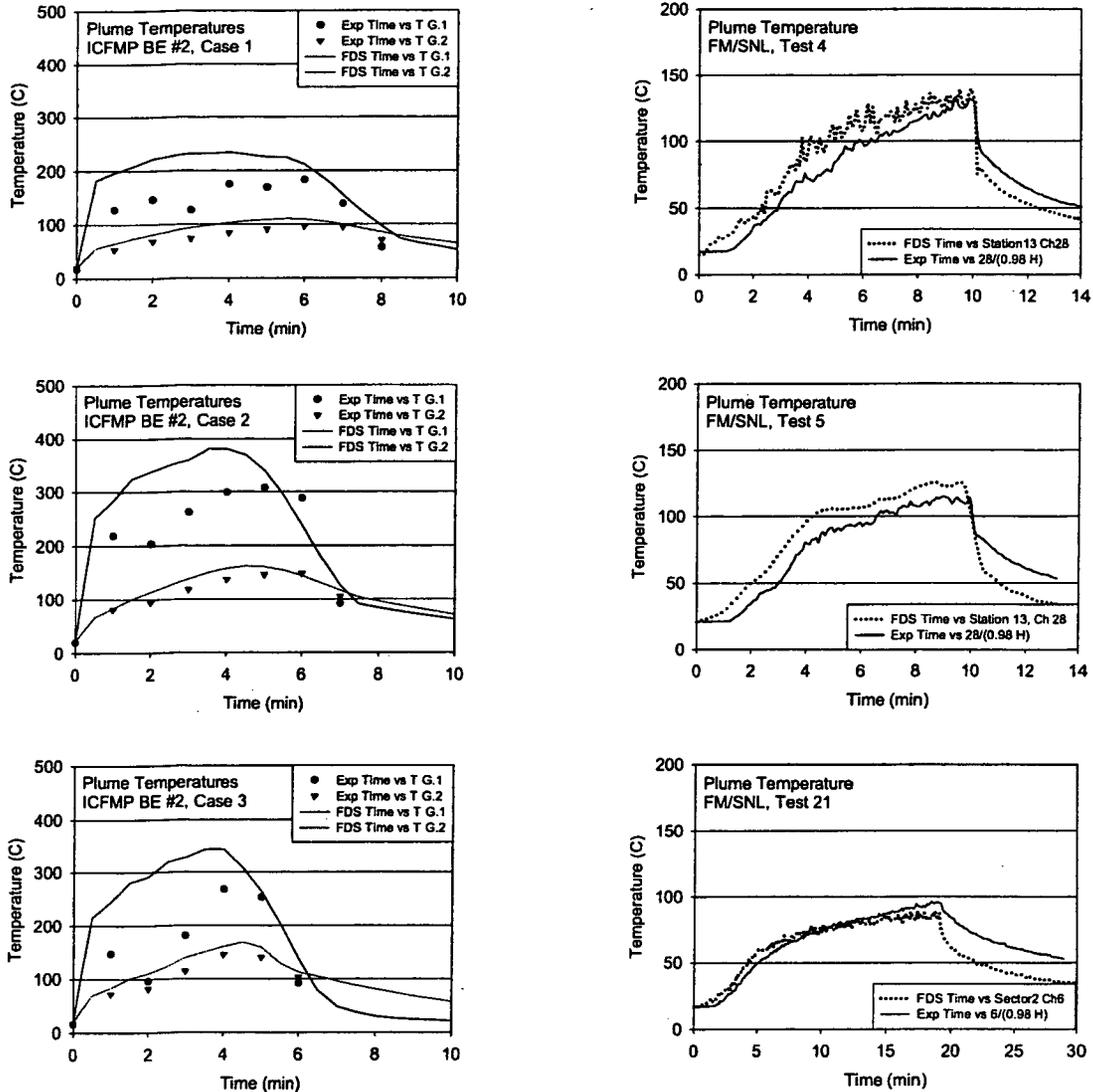
Figure A-22: Plume Temperature, ICFMP BE #2 (Left) and the FM/SNL Series (Right)

Table A-3: Summary of Plume Temperature Comparisons

			Plume Temperature Rise		
			ΔE (°C)	ΔM (°C)	Diff. (%)
BE #2	Case 1	T G.1	166	215	30
		T G.2	77	91	18
	Case 2	T G.1	288	362	26
		T G.2	128	140	9
	Case 3	T G.1	252	329	31
		T G.2	128	148	16
FM/ SNL	Test 4	Ch 28	114	124	9
	Test 5	Ch 28	93	104	12
	Test 21	Ch 6	78	67	-14

A.4 Flame Height

Flame height is recorded by visual observations, photographs, or video footage. Videos are available from the ICFMP BE #3 test series and photographs from BE #2. It is difficult to precisely measure the flame height, but the photos and videos allow one to make estimates accurate to within a pan diameter.

Similarly, flame height in FDS is assessed using the visualization program Smokeview. There are various ways to render the fire in Smokeview. The most direct method is to show, via three-dimensional surface plots, the volume within which the energy from the fire is being released. The other method is to show the stoichiometric iso-surface of the mixture fraction. FDS tracks the fuel and oxygen via a single scalar variable called the mixture fraction. The stoichiometric iso-surface is essentially a sheet on which combustion occurs. The average vertical extent of either the volume in which energy is being released or the stoichiometric mixture fraction iso-surface is the FDS predicted flame height.

ICFMP BE #2

Shown in Figure A-23 are snapshots from the simulation of the 1.6-m (5.2-ft) diameter heptane pan fire. The pan has been approximated as a square because of the requirement by FDS of rectangular geometry. Figure A-24 contains photographs of the actual fire. The height of the visible flame in the photographs has been estimated to be between 2.4 and 3 pan diameters [3.8 m to 4.8 m (12.5 ft to 15.8 ft)]. The height of the simulated fire fluctuates from 5 m to 6 m (15.4 ft to 19.7 ft) during the peak heat release rate phase.
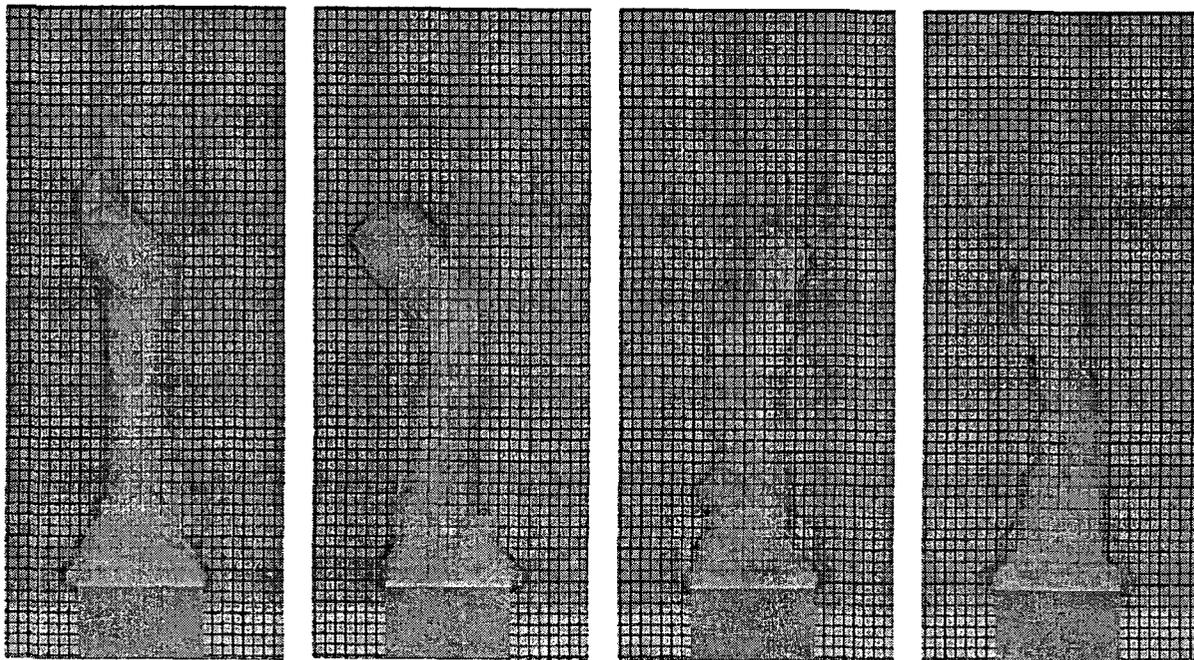
Figure A-23: Snapshots of Fire from ICFMP BE #2, Case 2 Simulation
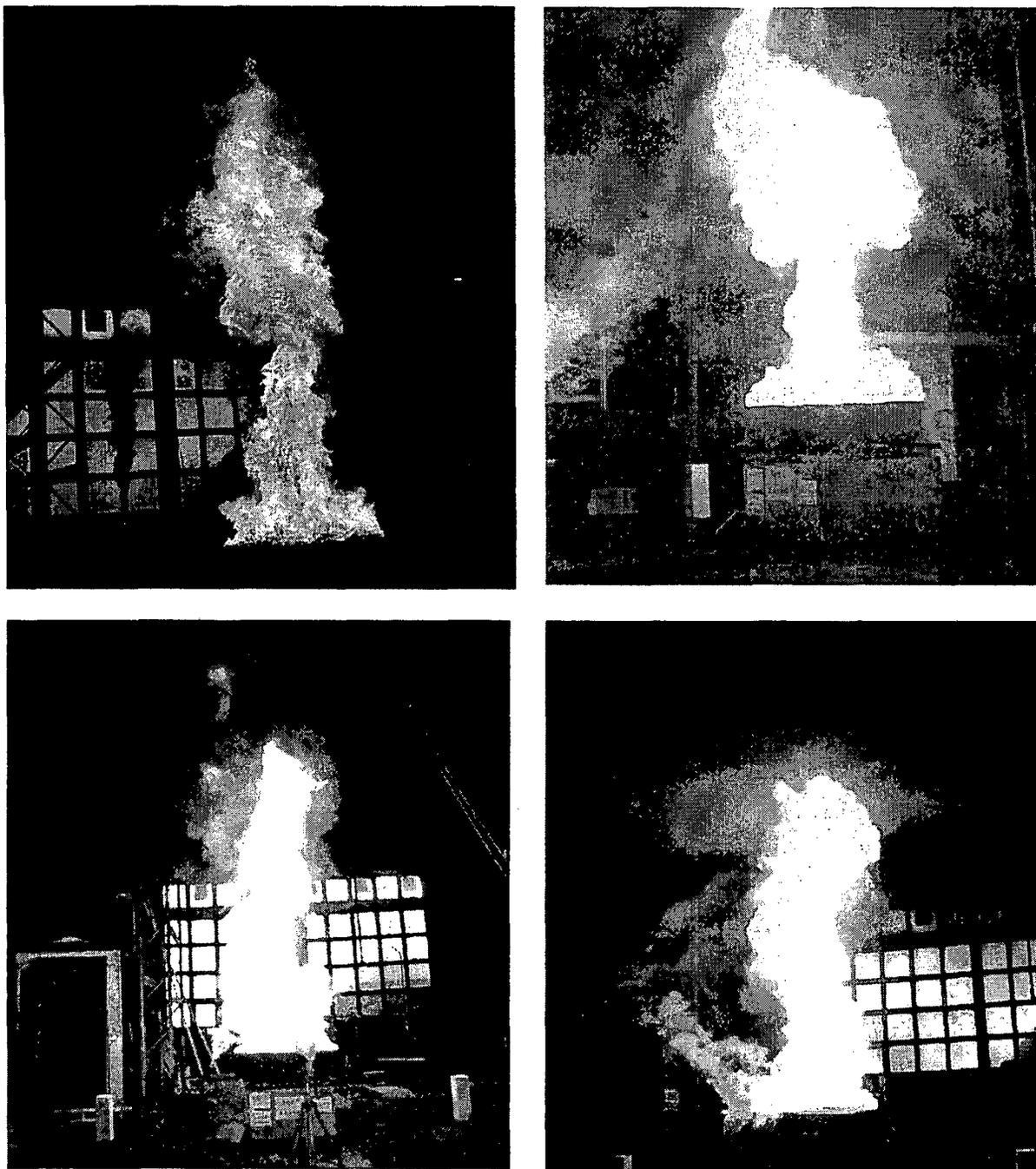
**Figure A-24: Photographs of Heptane Pan Fires, ICFMP BE #2, Case 2
(Courtesy of Simo Hostikka, VTT Building and Transport, Espoo, Finland.)**

ICFMP BE #3

No measurements of flame height are reported for BE #3, but numerous photographs are available. These photographs provide at least a qualitative assessment of the FDS flame height prediction.
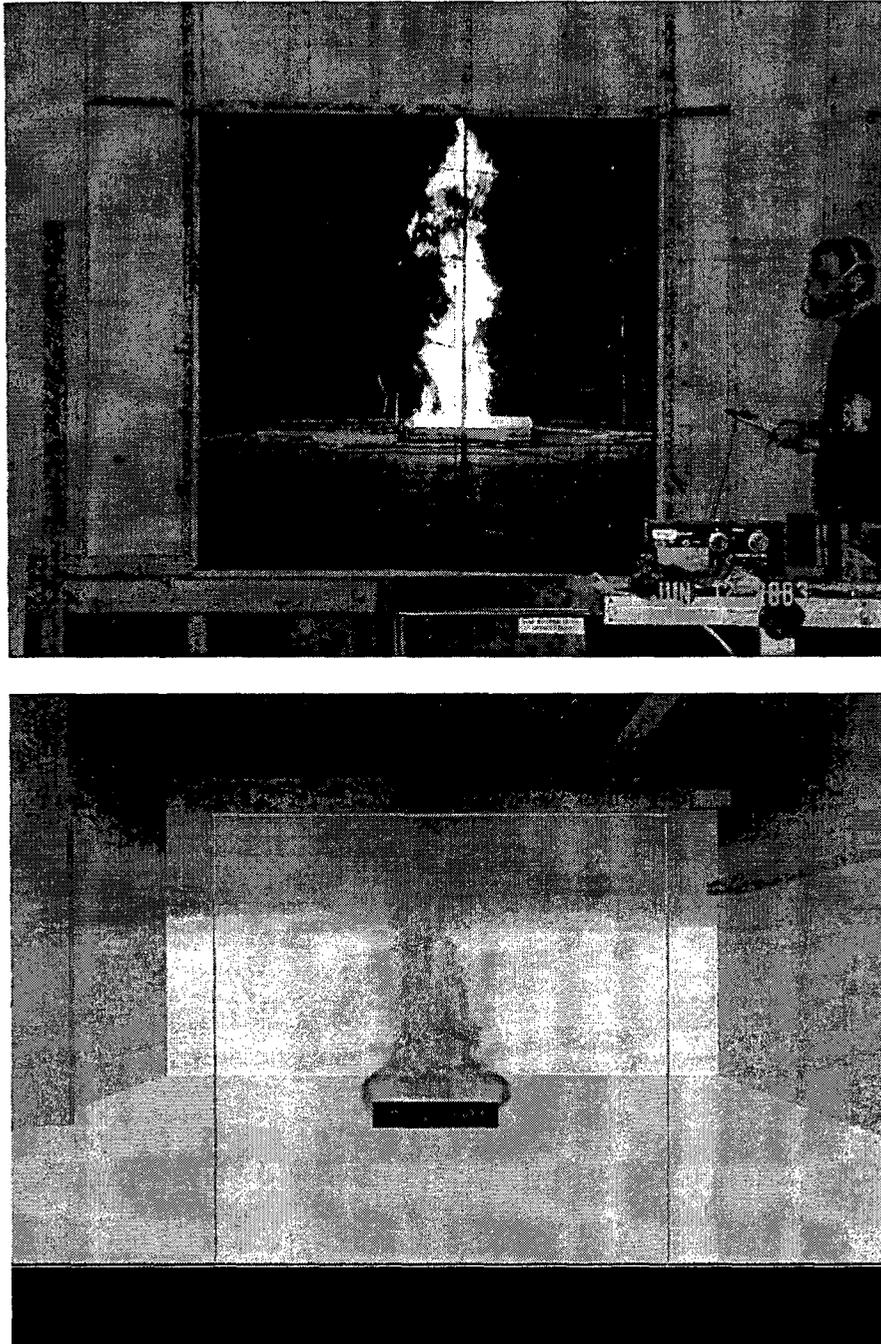
Figure A-25: Photograph and Simulation of ICFMP BE #3, Test 3, as seen through the 2 m x 2 m doorway (Photo courtesy of Francisco Joglar, SAIC.)

A.5 Oxygen and Carbon Dioxide Concentration

FDS uses a mixture fraction combustion model, meaning that all gas species within the compartment are assumed to be functions of a single scalar variable. FDS solves only one transport equation for this variable, and reports gas concentrations at any given point at any given time by extracting its value from a pre-computed "lookup" table. For the major species, like carbon dioxide and oxygen, the predictions are essentially an indicator of how well FDS is predicting the bulk transport of combustion products throughout the space. For minor species, like carbon monoxide and soot, FDS Version 4 does not account for changes in combustion efficiency, relying only on fixed yields of carbon monoxide and soot from the combustion process. In reality, the generation rate of carbon monoxide and soot change depending on the ventilation conditions in the compartment.

The following pages present comparisons of oxygen and carbon dioxide concentration predictions with measurement for BE #3 and BE #5. In BE #3, there are two oxygen measurements, one in the upper layer and one in the lower layer. There is only one carbon dioxide measurement in the upper layer. For BE #5, Test 4, a plot of upper-layer oxygen and carbon dioxide is included along with the results for BE #3.

All of the comparisons are for single-point measurements. Unlike the HGL temperature, there were only single-point measurements made in either the upper or lower layers of the compartment.
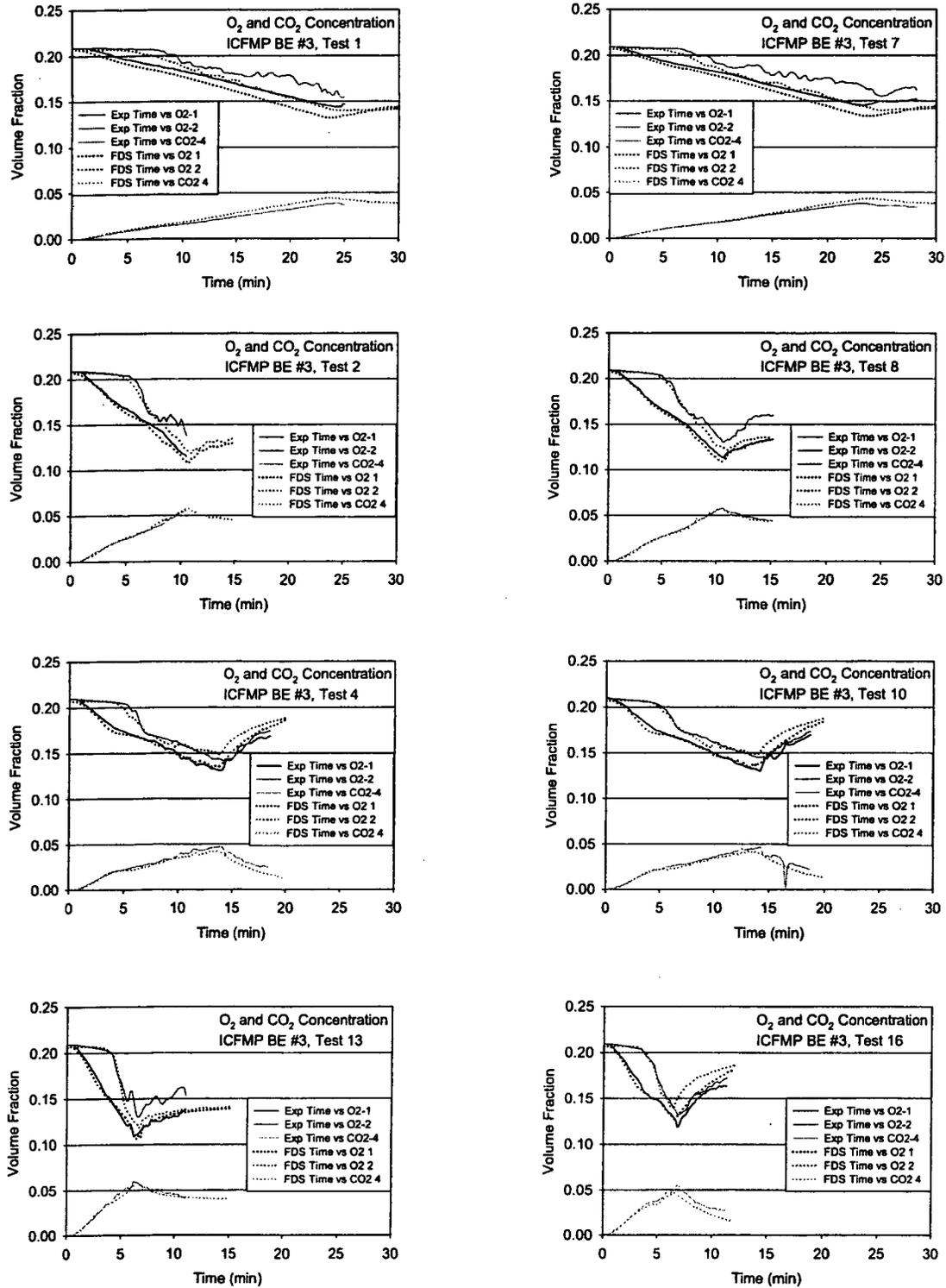
Figure A-26: O₂ and CO₂ Concentrations, ICFMP BE #3, Closed-Door Tests
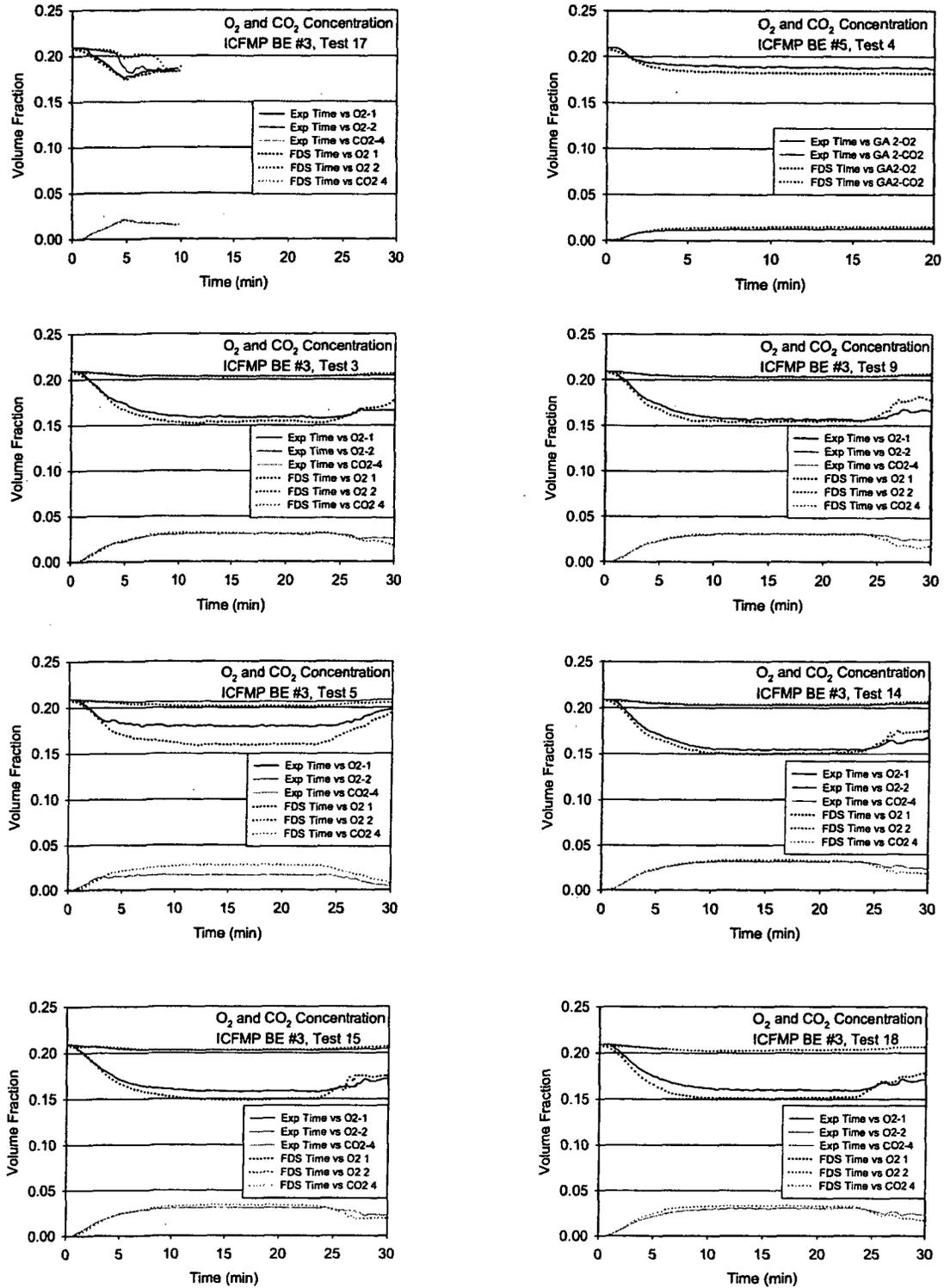
Figure A-27: O_2 and CO_2 Concentrations, ICFMP BE #3, Open-Door Tests (Note that the single test from ICFMP BE #5 is included at the upper right.)

Table A-4: Summary of Oxygen and Carbon Dioxide Comparisons

		HGL CO₂ Concentration			HGL O₂ Concentration Decrease			LGL O₂ Concentration Decrease		
		ΔE (mol/ mol)	ΔM (mol/ mol)	Diff. (%)	ΔE (mol/ mol)	ΔM (mol/ mol)	Diff. (%)	ΔE (mol/ mol)	ΔM (mol/ mol)	Diff. (%)
ICFMP BE #3	Test 1	0.038	0.044	15	0.065	0.076	16	0.055	0.067	23
	Test 7	0.038	0.043	13	0.064	0.074	15	0.054	0.068	25
	Test 2	0.054	0.057	4	0.092	0.097	5	—	0.084	—
	Test 8	0.058	0.057	-1	0.096	0.098	2	0.079	0.086	8
	Test 4	0.047	0.042	-11	0.079	0.072	-8	0.068	0.059	-14
	Test 10	0.047	0.043	-8	0.079	0.073	-8	0.066	0.059	-11
	Test 13	0.060	0.059	-2	0.101	0.101	0	0.080	0.089	12
	Test 16	0.055	0.047	-15	0.091	0.080	-12	0.078	0.069	-11
	Test 17	0.022	0.022	0	0.033	0.034	1	0.028	0.024	-14
	Test 3	0.031	0.032	4	0.052	0.055	6	0.006	0.006	13
	Test 9	0.031	0.031	0	0.054	0.054	-1	0.006	0.006	1
	Test 5	0.017	0.028	63	0.030	0.049	60	0.003	0.006	67
	Test 14	0.032	0.034	5	0.055	0.058	5	0.006	0.005	-8
	Test 15	0.031	0.034	10	0.052	0.059	14	0.006	0.006	-1
	Test 18	0.031	0.033	9	0.051	0.057	13	0.004	0.004	-6
BE #5, Test 4		0.013	0.016	20	0.023	0.027	14			

A.6   Smoke Concentration

FDS treats smoke like all other combustion products, basically a tracer gas for which the mass fraction is a function of the mixture fraction. To model smoke movement, the user need only prescribe the smoke yield (that is, the fraction of the fuel mass that is converted to smoke particulate). For the simulations of BE #3, the smoke yield is specified as one of the test parameters.

Figure A-28 and Figure A-29 contain comparisons of measured and predicted smoke concentration at one measuring station in the upper layer. There are two obvious trends in the figures. First, the predicted concentrations are about 50% higher than the measured in the open-door tests. Second, the predicted concentrations are roughly three times the measured concentrations in the closed-door tests.

As a contrast, Figure A-30 displays the time history of carbon monoxide concentration for six of the BE #3 tests. Like smoke, the carbon monoxide concentration is specified in FDS via a fixed yield, measured along with smoke and reported in the test document. The large differences between model and measurement seen in the smoke data do not appear in the carbon monoxide data.
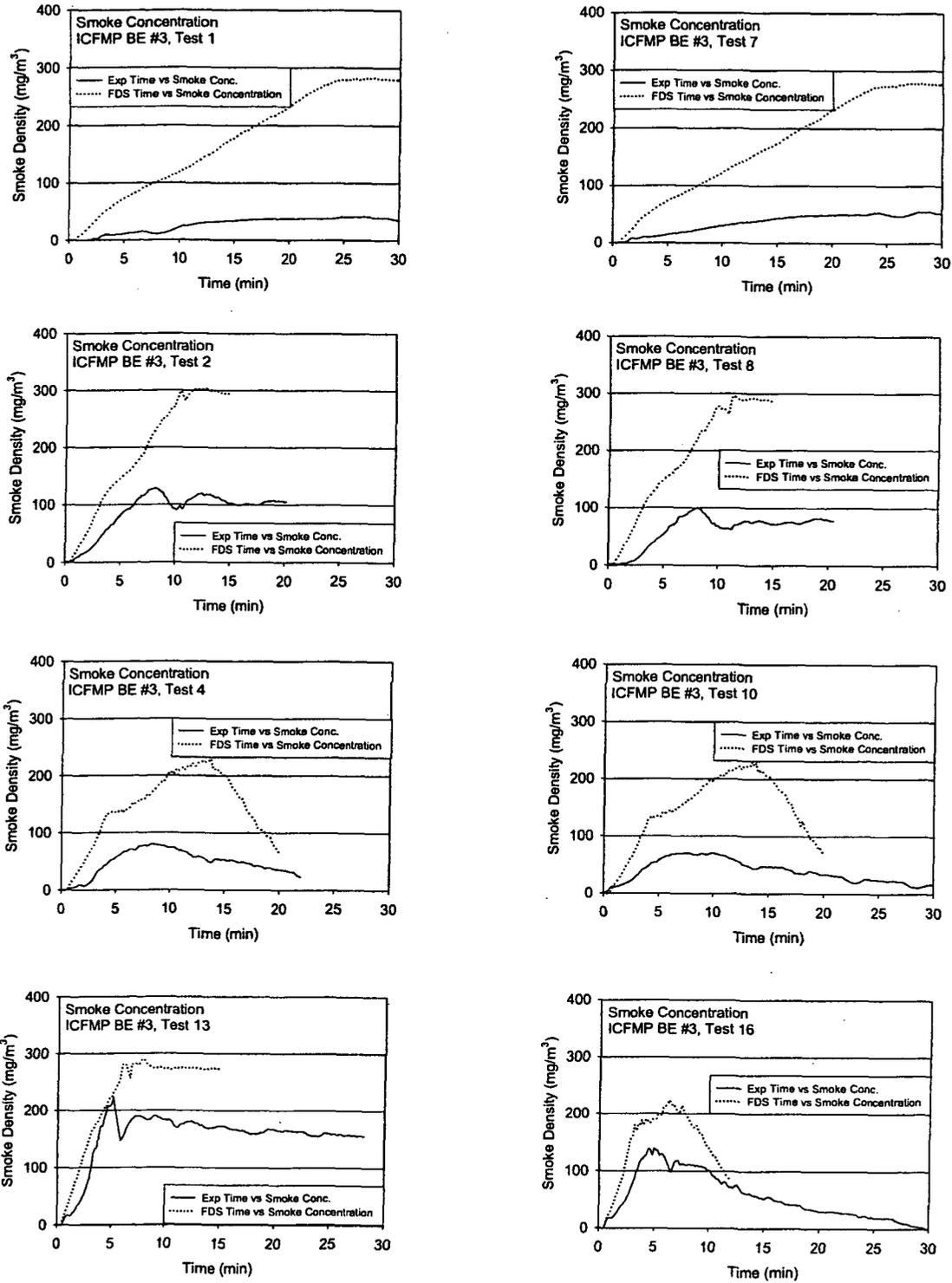
Figure A-28: Smoke Concentration, ICFMP BE #3, Closed-Door Tests
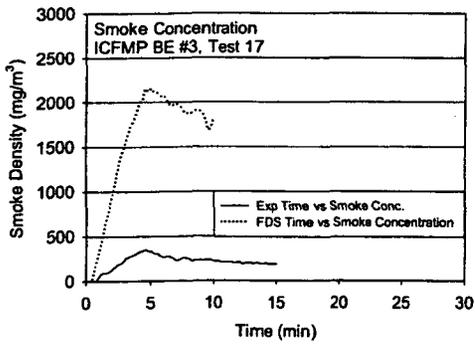
Open Door Tests to Follow
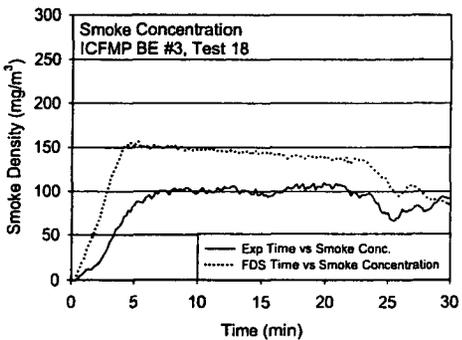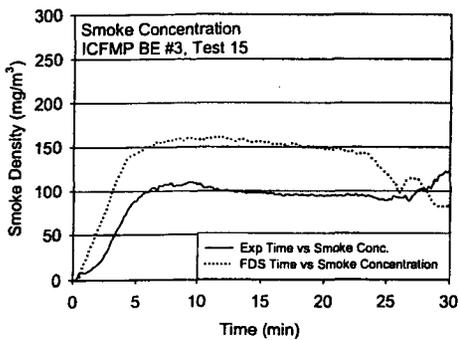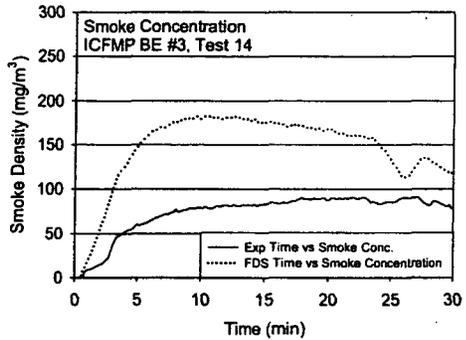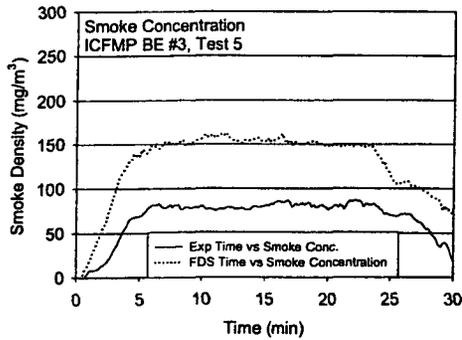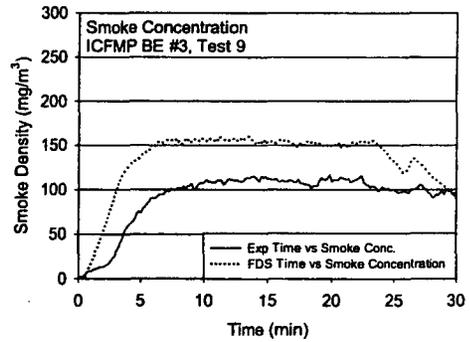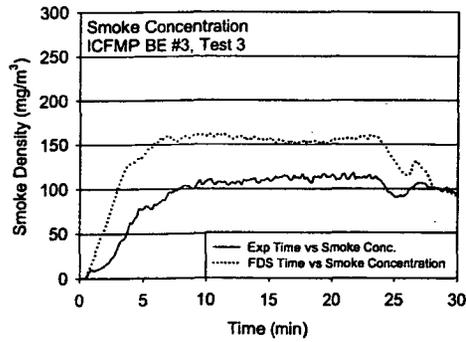
Figure A-29: Smoke Concentration, ICFMP BE #3, Open-Door Tests

Table A-5: Summary of Smoke Concentration Comparisons

		Smoke Concentration		
		ΔE (mg/m³)	ΔM (mg/m³)	Diff. (%)
ICFMP BE #3	Test 1	42	283	582
	Test 7	55	279	406
	Test 2	128	303	137
	Test 8	100	296	197
	Test 4	80	230	188
	Test 10	71	231	227
	Test 13	224	291	30
	Test 16	139	224	61
	Test 17	353	2164	513
	Test 3	118	163	38
	Test 9	117	160	37
	Test 5	87	162	86
	Test 14	91	183	101
	Test 15	123	163	32
	Test 18	110	156	42
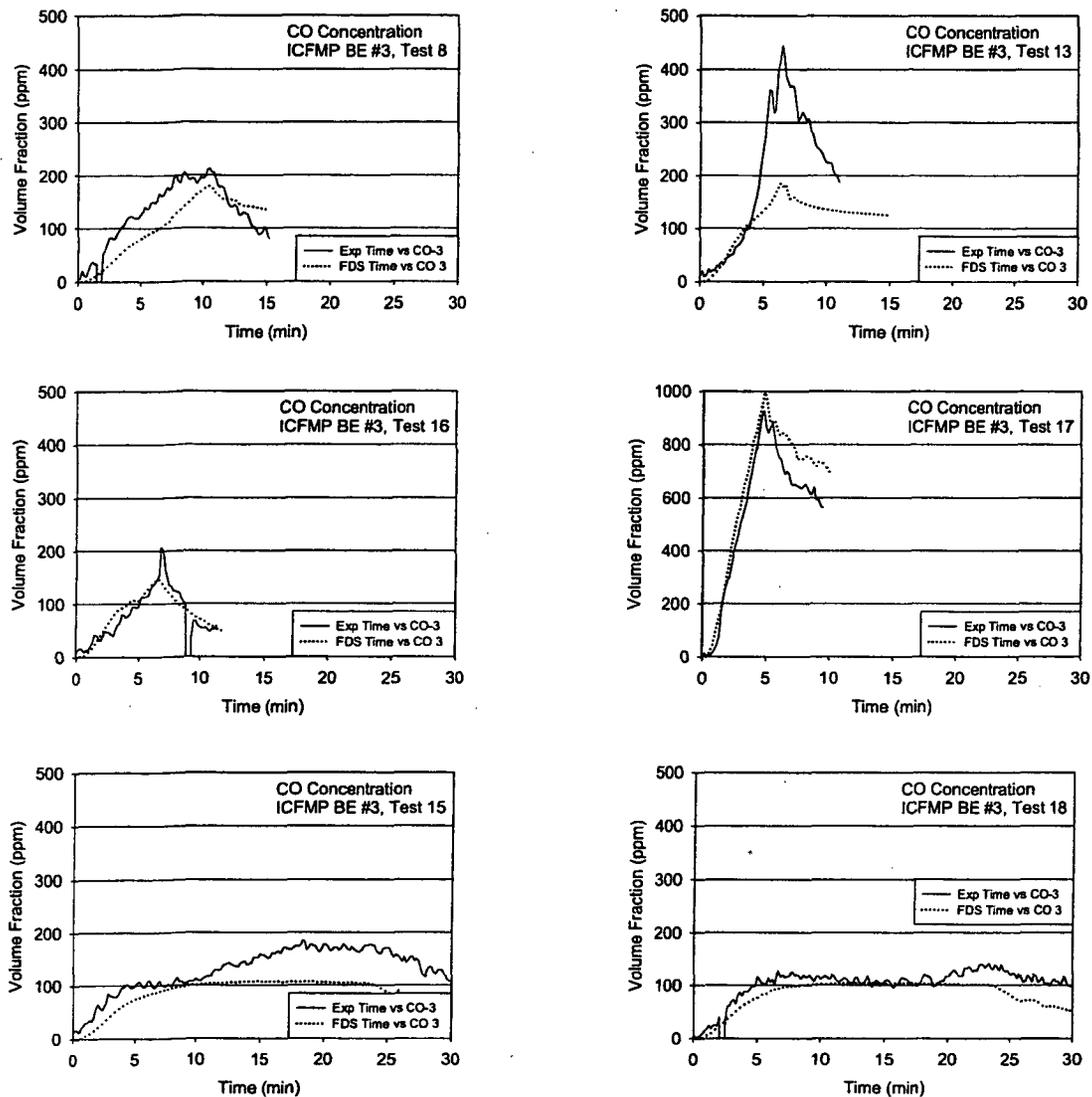
Figure A-30: CO Concentration, ICFMP BE #3, Closed Door (Top Four) and Open Door (Bottom Two) Tests

A.7 Compartment Pressure

Experimental measurements for room pressure are only available from the ICFMP BE #3 test series. The pressure within the compartment is measured at a single point, near the floor. In the simulations of the closed-door tests, the compartment is assumed to leak via a small uniform flow spread over the walls and ceiling. The flow rate is calculated based on the assumption that the leakage rate is proportional to the measured leakage area times the square root of compartment over-pressure:

$$\dot{V} = A_L \sqrt{2(p - p_\infty)/\rho_\infty}$$

Comparisons between measurement and prediction are shown in Figure A-31 and Figure A-32. For those tests in which the door to the compartment is open, the over-pressures are only a few Pascals, whereas when the door is closed, the over-pressures are several hundred Pascals.

Note that in the closed-door tests, there is often a dramatic drop in the predicted compartment pressure. This is the result of the assumption in FDS that the heat release rate was decreased to zero in 1 second at the time in the experiment when the fuel flow was stopped for safety reasons. In reality, the fire did not extinguish immediately because there was an excess of fuel in the pan following the flow stoppage. For the purpose of model comparison, the peak over-pressures are compared in the closed-door tests, and the peak (albeit small) under-pressures are compared in the open-door tests.
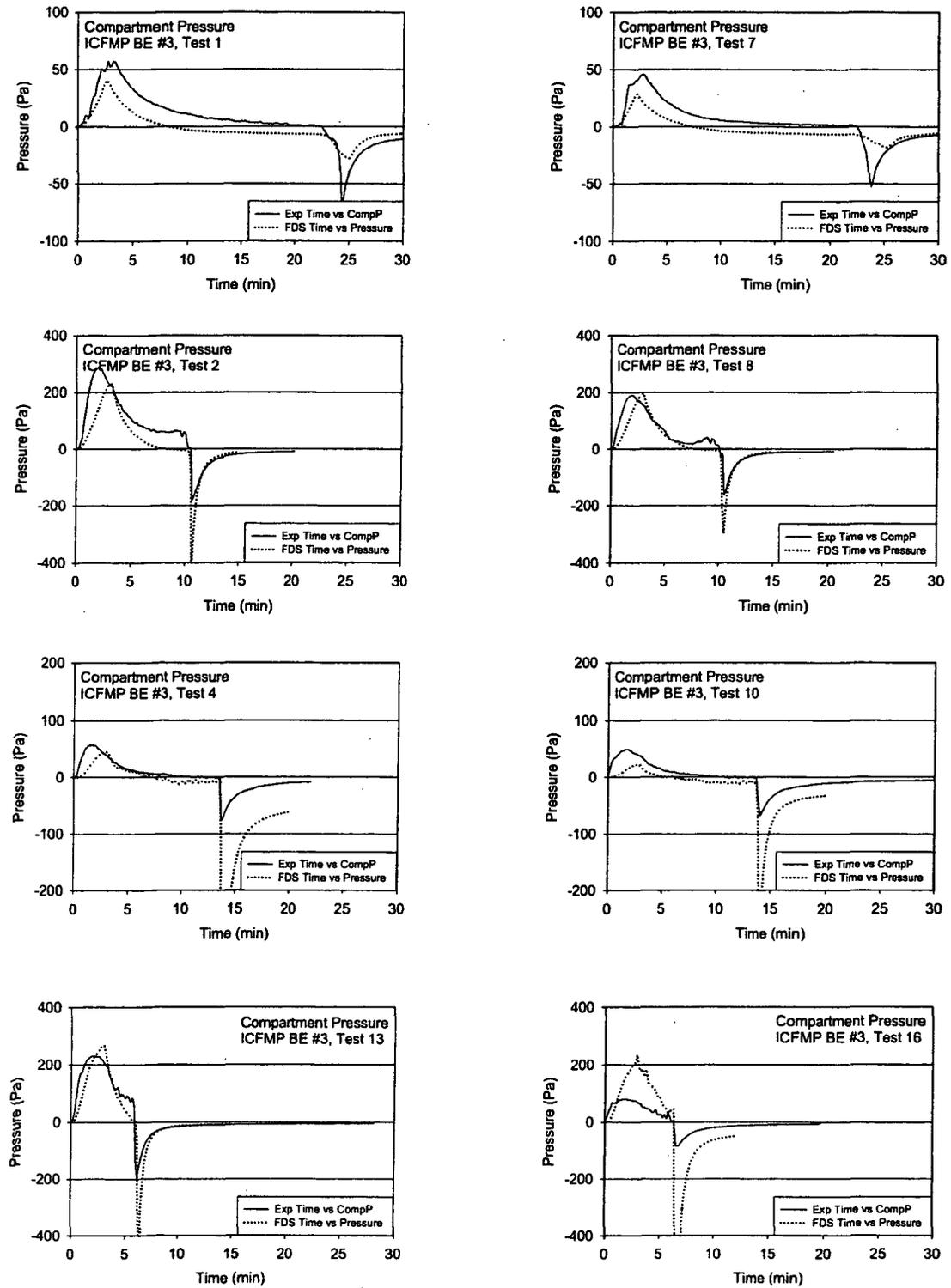
Figure A-31: Compartment Pressure, ICFMP BE #3, Closed-Door Tests
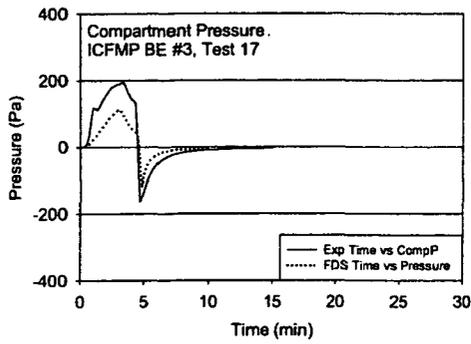
Open Door Tests to Follow
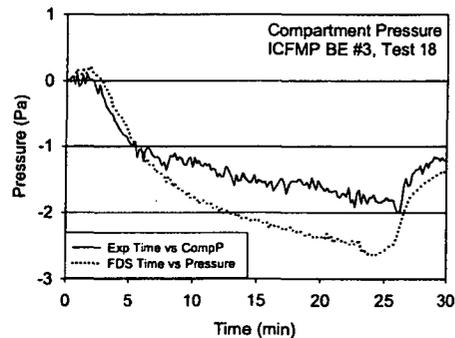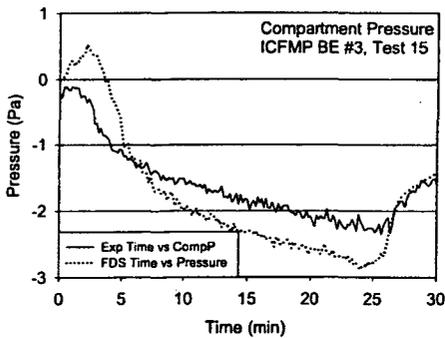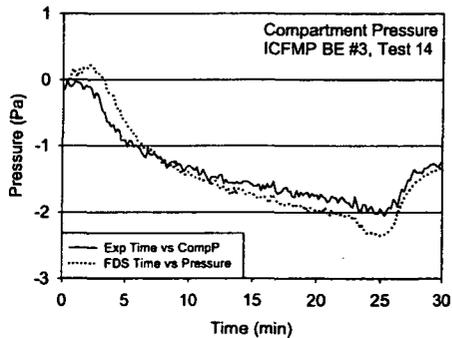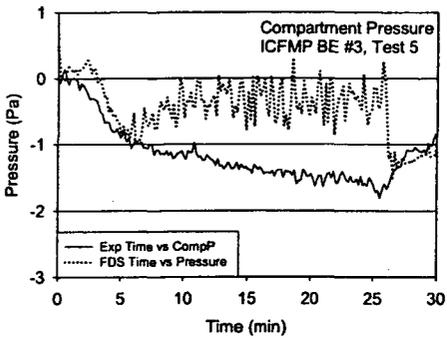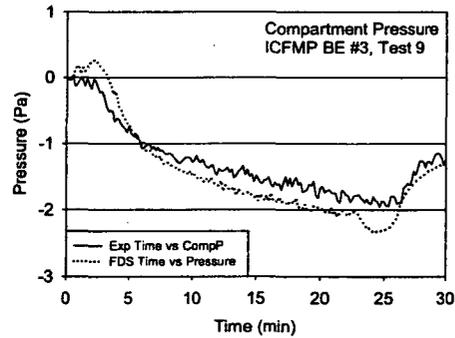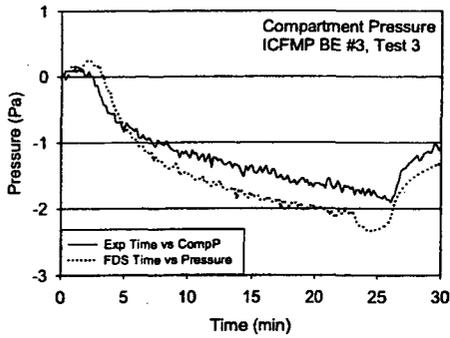
Figure A-32: Compartment Pressure, ICFMP BE #3, Open-Door Tests

Table A-6: Summary of Pressure Comparisons

		Compartment Pressure Rise		
		ΔE (Pa)	ΔM (Pa)	Diff. (%)
ICFMP BE #3	Test 1	58	40	-31
	Test 7	46	28	-38
	Test 2	290	231	-20
	Test 8	189	198	5
	Test 4	57	45	-20
	Test 10	49	22	-56
	Test 13	232	268	16
	Test 16	81	235	191
	Test 17	195	112	-42
	Test 3	-1.9	-2.3	22
	Test 9	-2.0	-2.3	19
	Test 5	-1.8	-1.5	-17
	Test 14	-2.1	-2.4	15
	Test 15	-2.4	-2.9	23
	Test 18	-2.0	-2.7	32

A.8   Target Temperature and Heat Flux

Target temperature and heat flux data are available from ICFMP BE #3, BE #4, and BE #5. In BE #3, the targets were various types of cables in various configurations — horizontal, vertical, in trays, or free-hanging. In BE #4, the targets were three rectangular slabs of different materials instrumented with heat flux gauges and thermocouples. In BE #5, the targets were again cables, in this case, bundled power and control cables in a vertical ladder.

ICFMP BE #3

For each of the four cable targets considered, measurements of the local gas temperature, surface temperature, radiative heat flux, and total heat flux are available. The following pages display comparisons of these quantities for Control Cable B, Horizontal Cable Tray D, Power Cable F, and Vertical Cable Tray G.

FDS does not have a detailed solid phase model that can account for the heat transfer within the bundled, cylindrical, non-homogenous cables. For the bundled cables within horizontal and vertical trays (Targets D and G), FDS assumes them to be rectangular slabs of thickness comparable to the diameter of the individual cables. For the free-hanging Cables B and F, FDS assumes them to be cylinders of uniform composition into which it computes the radial heat transfer as a function of the heat flux to a designated location.

The superposition of gas temperature, heat flux, and surface temperature in the figures on the following pages provides information about how cables heat up in fires. Favorable or unfavorable predictions of cable surface temperatures can often be explained in terms of comparable errors in the prediction of the thermal environment in the vicinity of the cable.
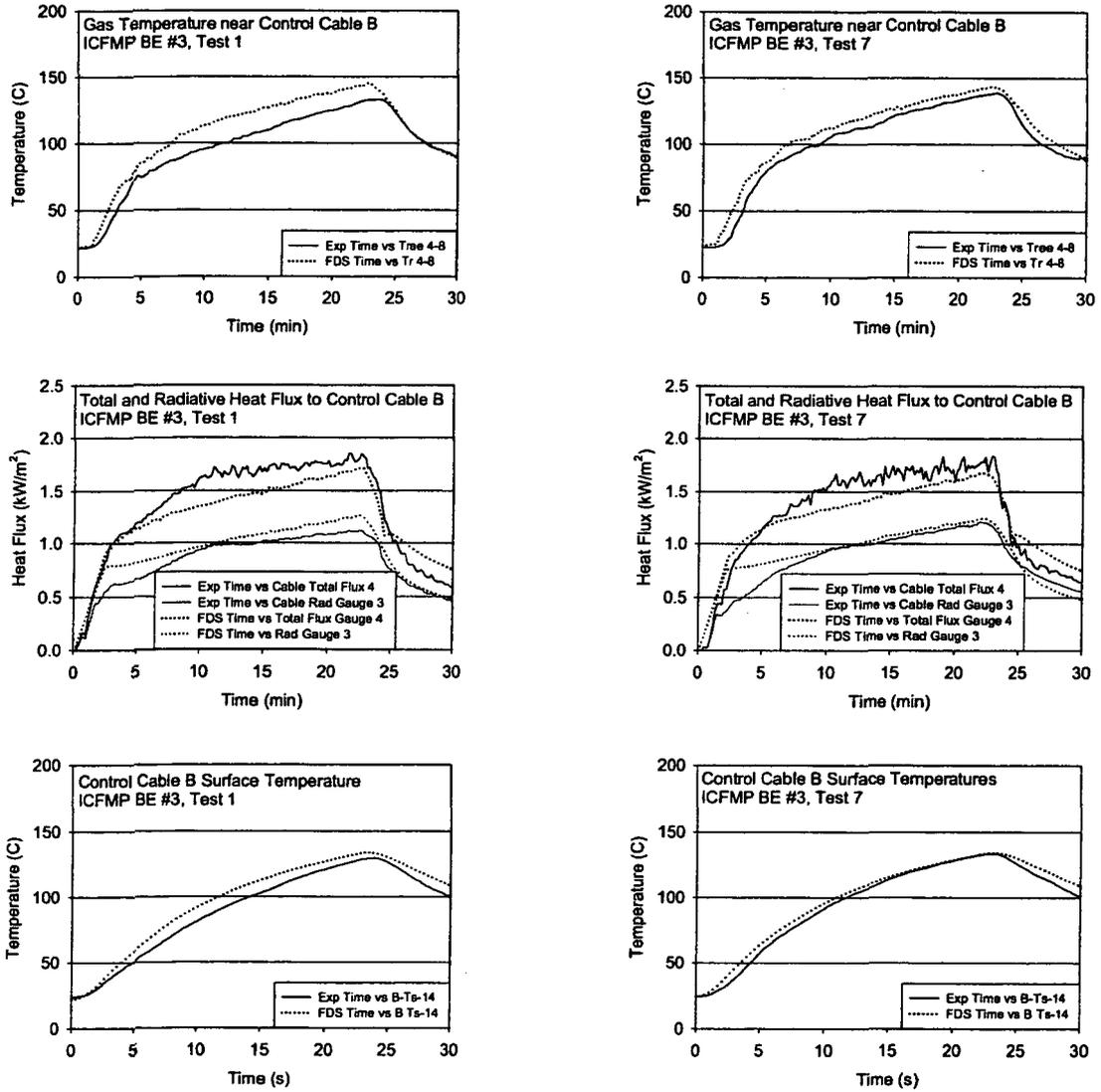
Figure A-33: Thermal Environment near Cable B, ICFMP BE #3, Tests 1 and 7
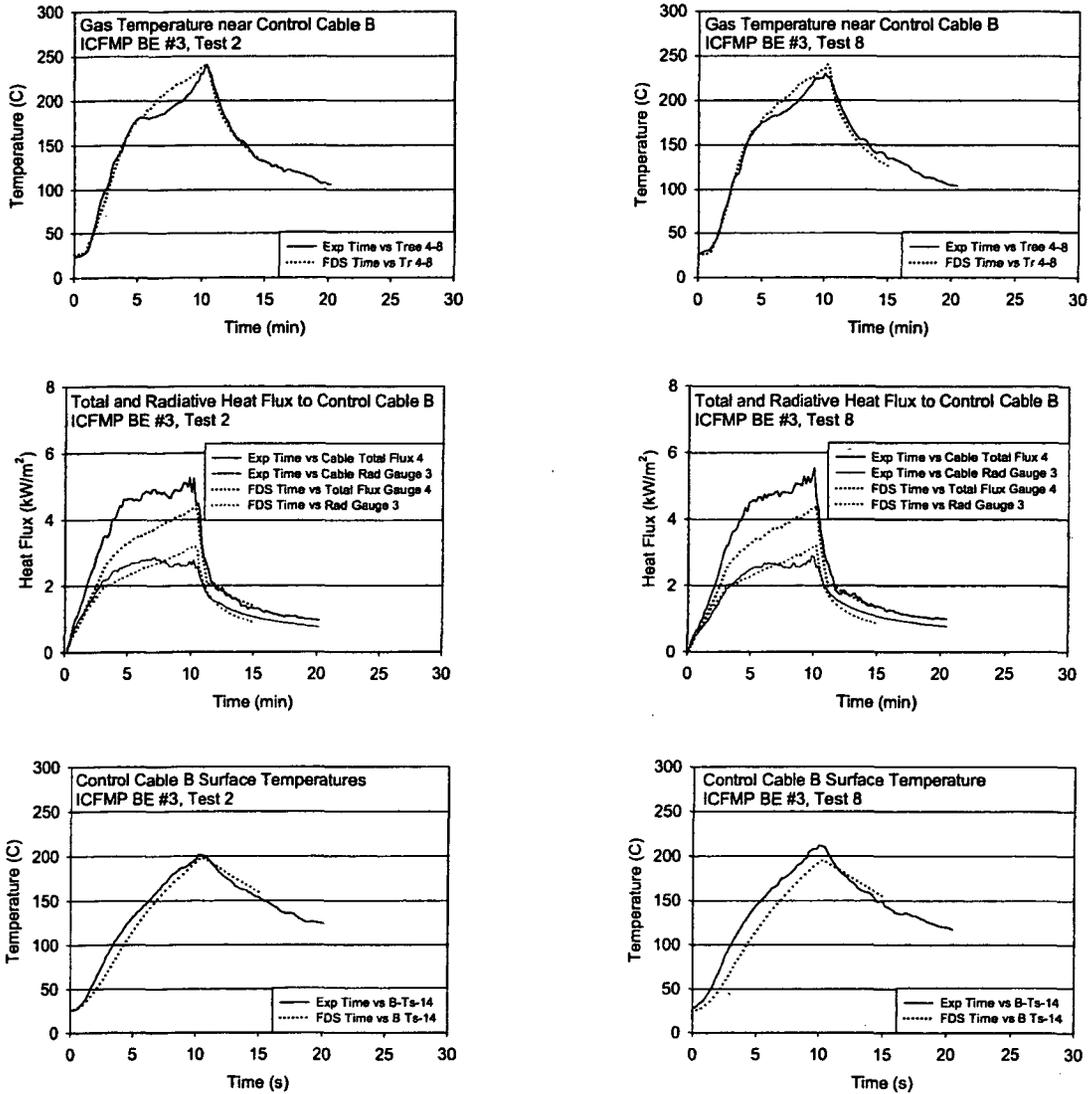
Figure A-34: Thermal Environment near Cable B, ICFMP BE #3, Tests 2 and 8
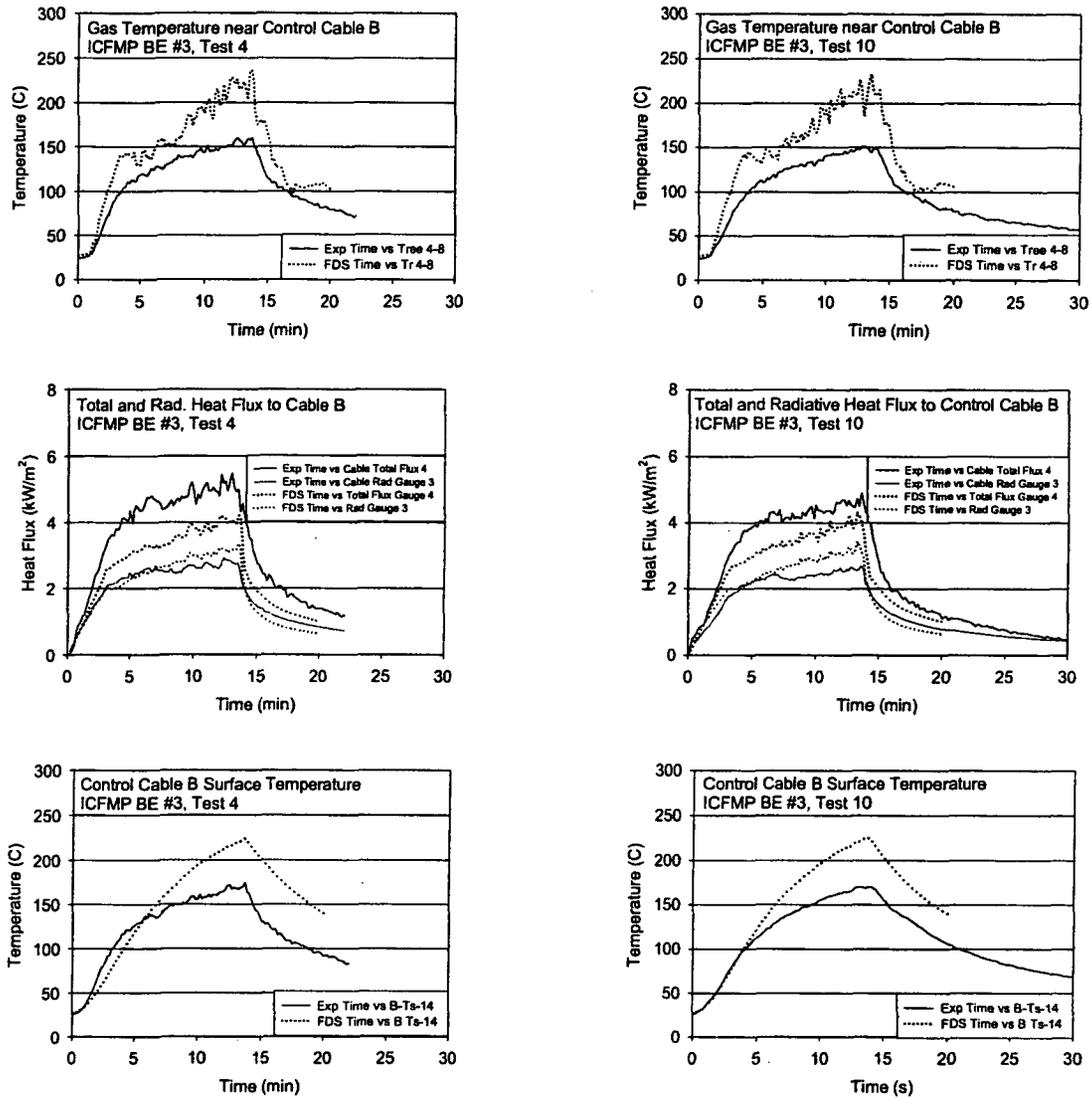
**Figure A-35: Thermal Environment near Cable B, ICFMP BE #3, Tests 4 and 10
(Note the influence of the fan on the gas and surface temperatures.)**
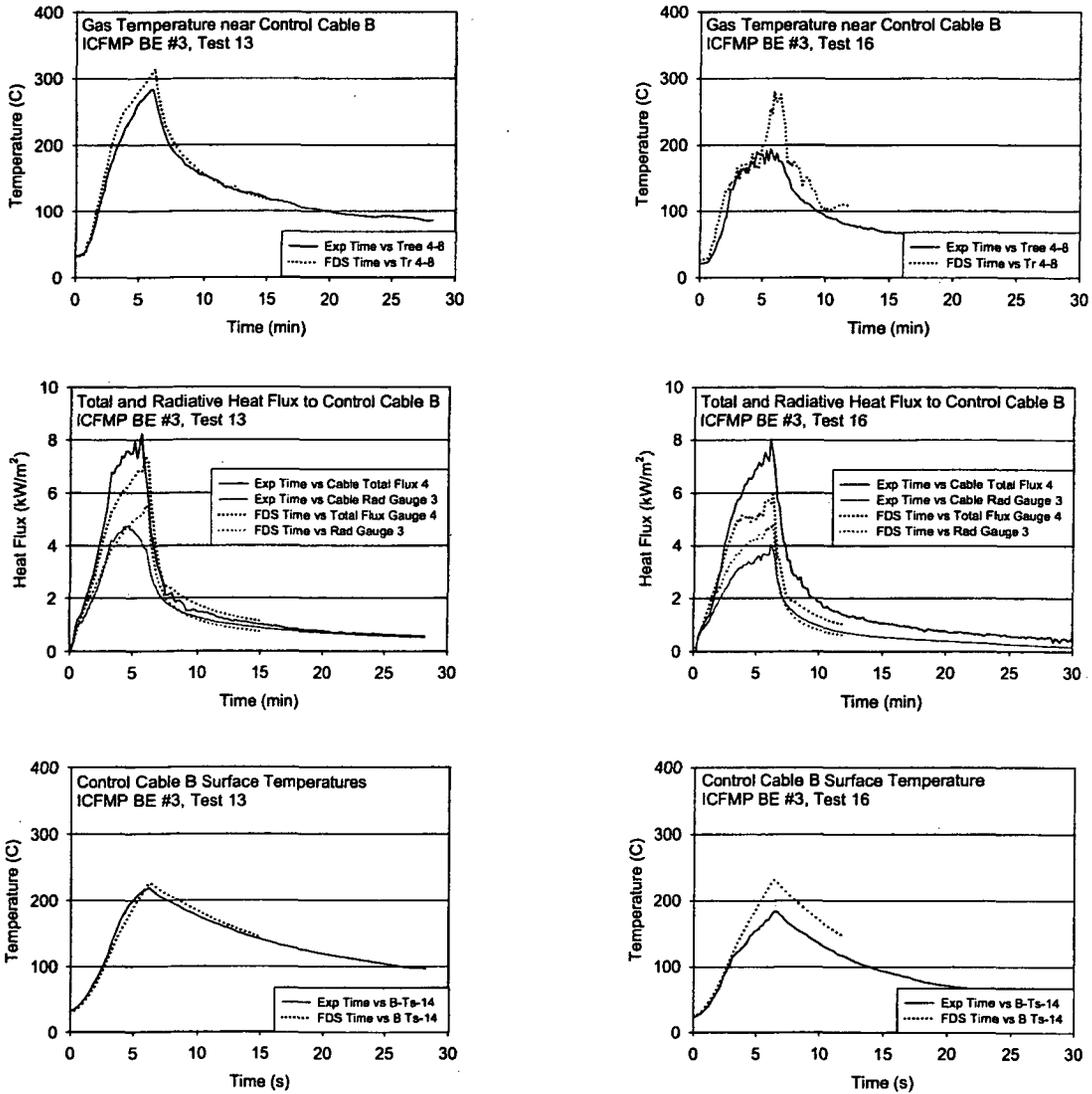
Figure A-36: Thermal Environment near Cable B, ICFMP BE #3, Tests 13 and 16 (Note the influence of the fan in Test 16.)
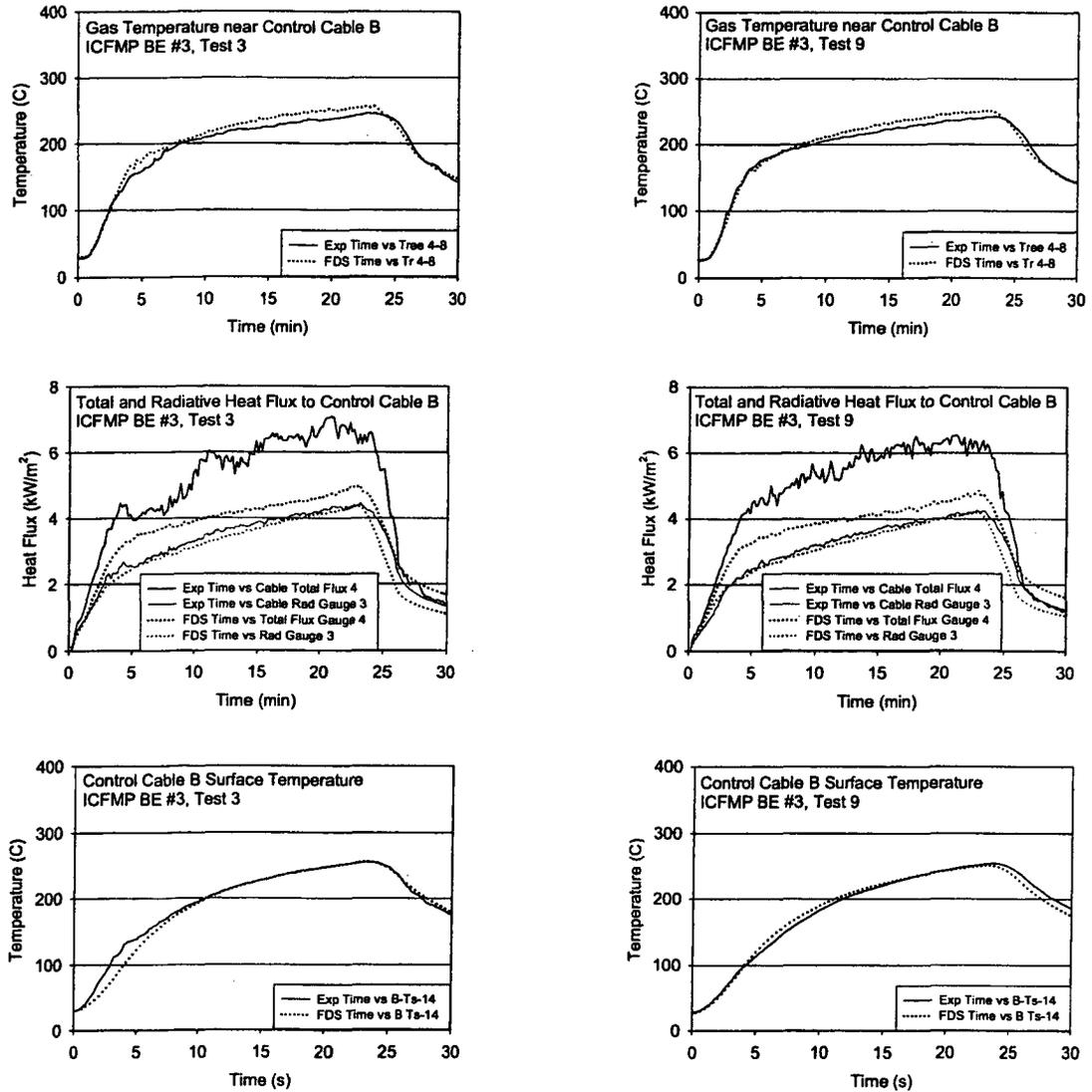
Figure A-37: Thermal Environment near Cable B, ICFMP BE #3, Tests 3 and 9
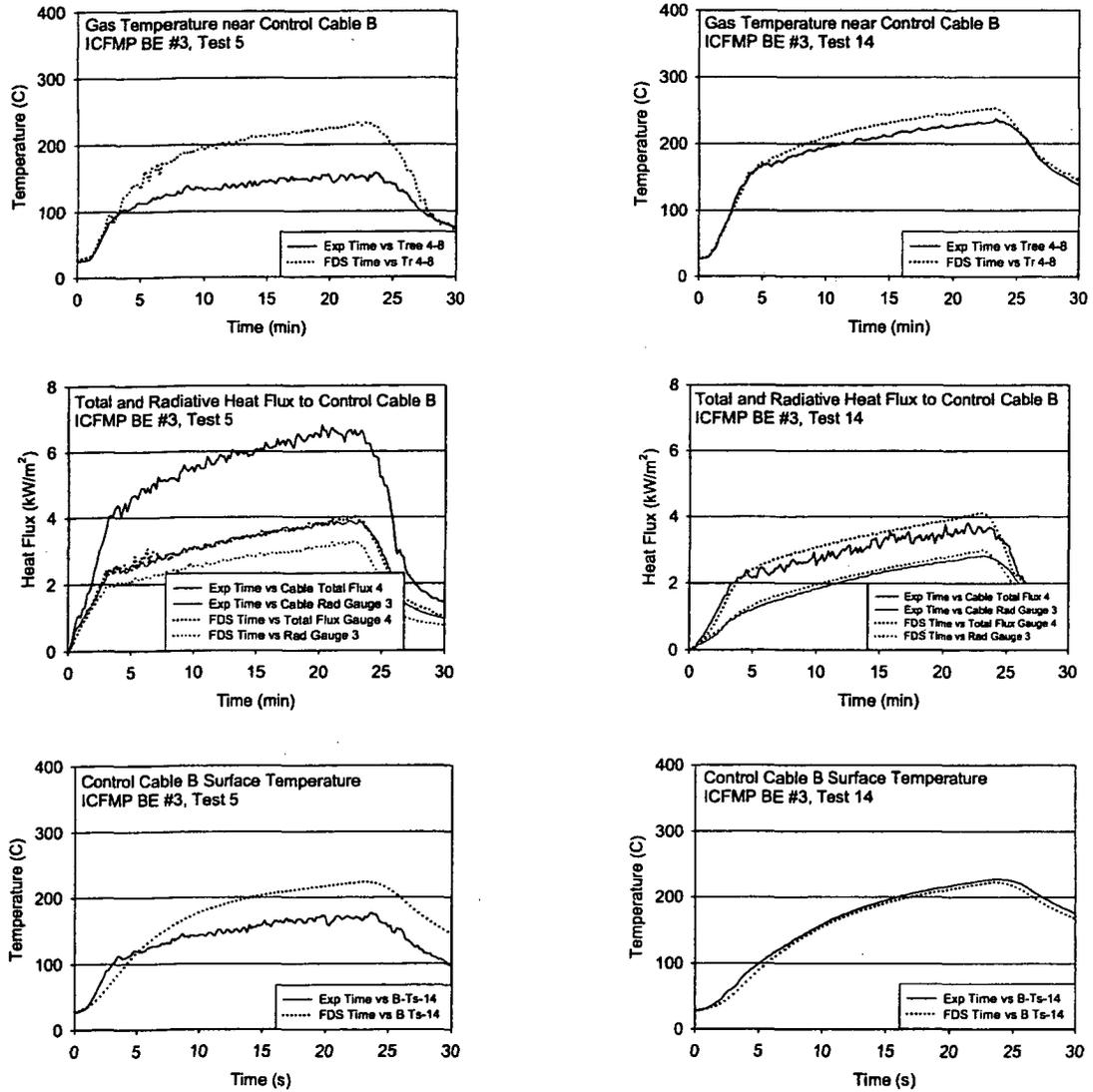
Figure A-38: Thermal Environment near Cable B, ICFMP BE #3, Tests 5 and 14 (Note the influence of the fan in Test 5.)
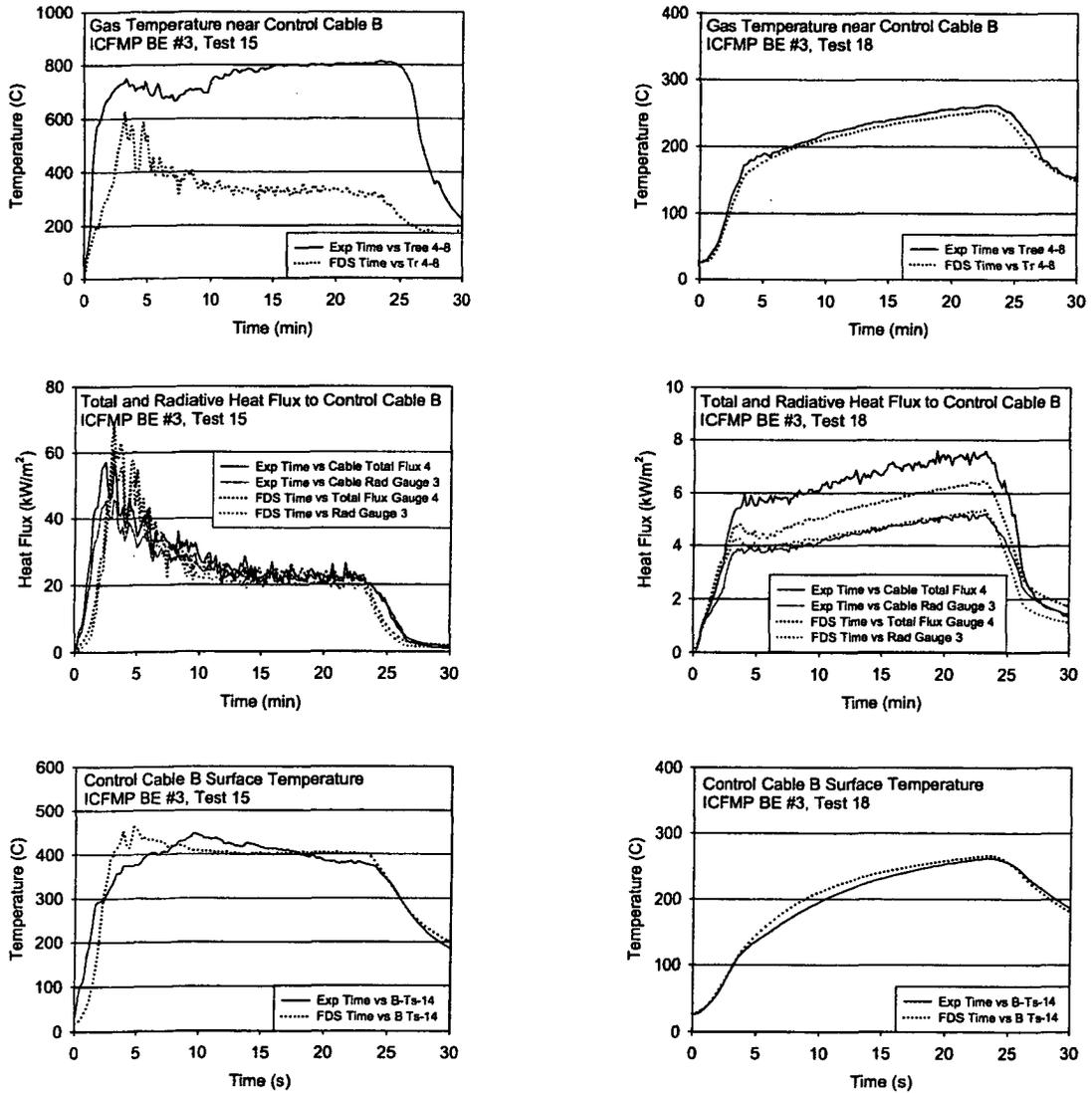
Figure A-39: Thermal Environment near Cable B, ICFMP BE #3, Tests 15 and 18 (Note that the cable was very close to the fire in Test 15.)
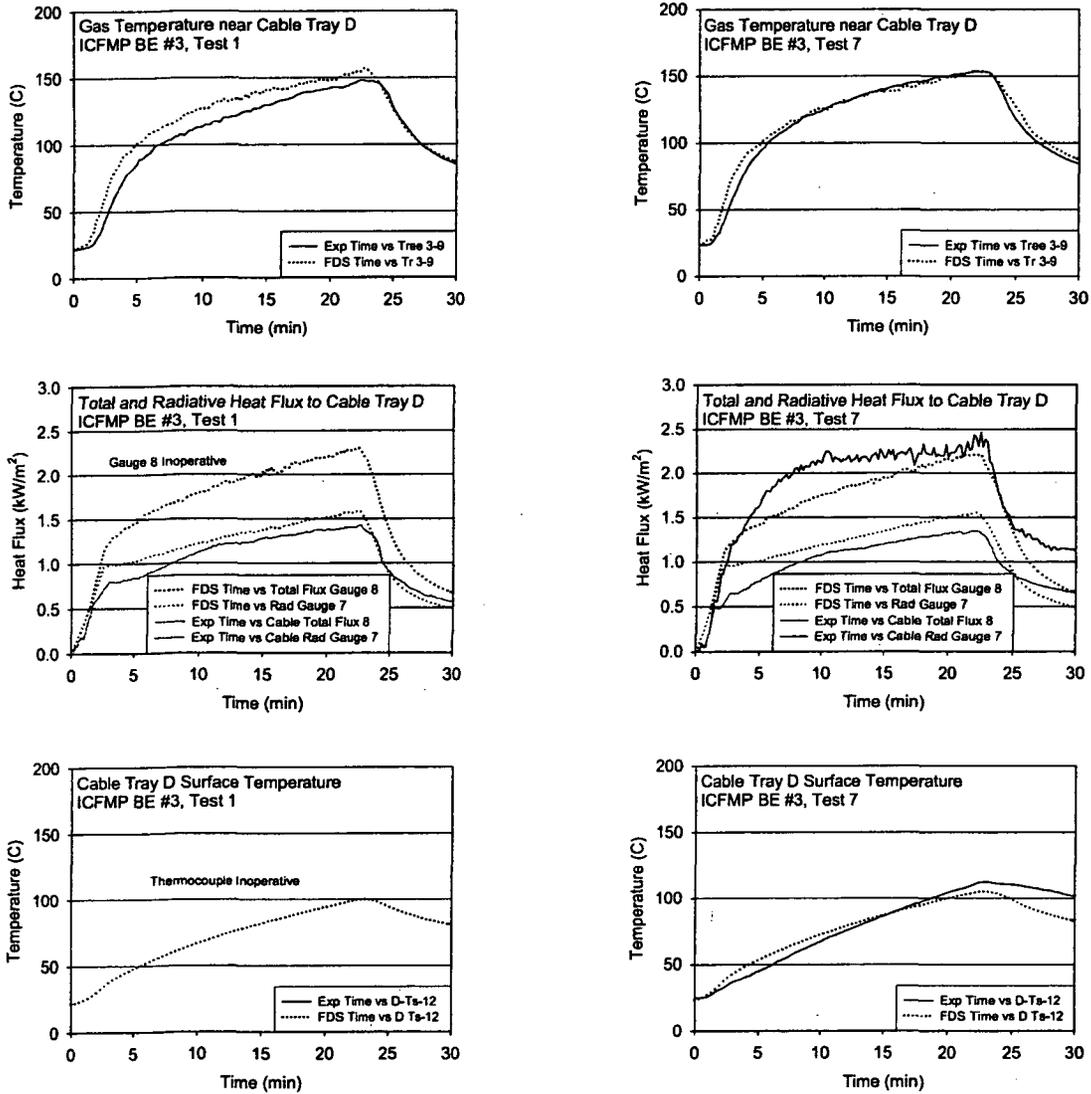
Figure A-40: Thermal Environment near Cable Tray D, ICFMP BE #3, Tests 1 and 7
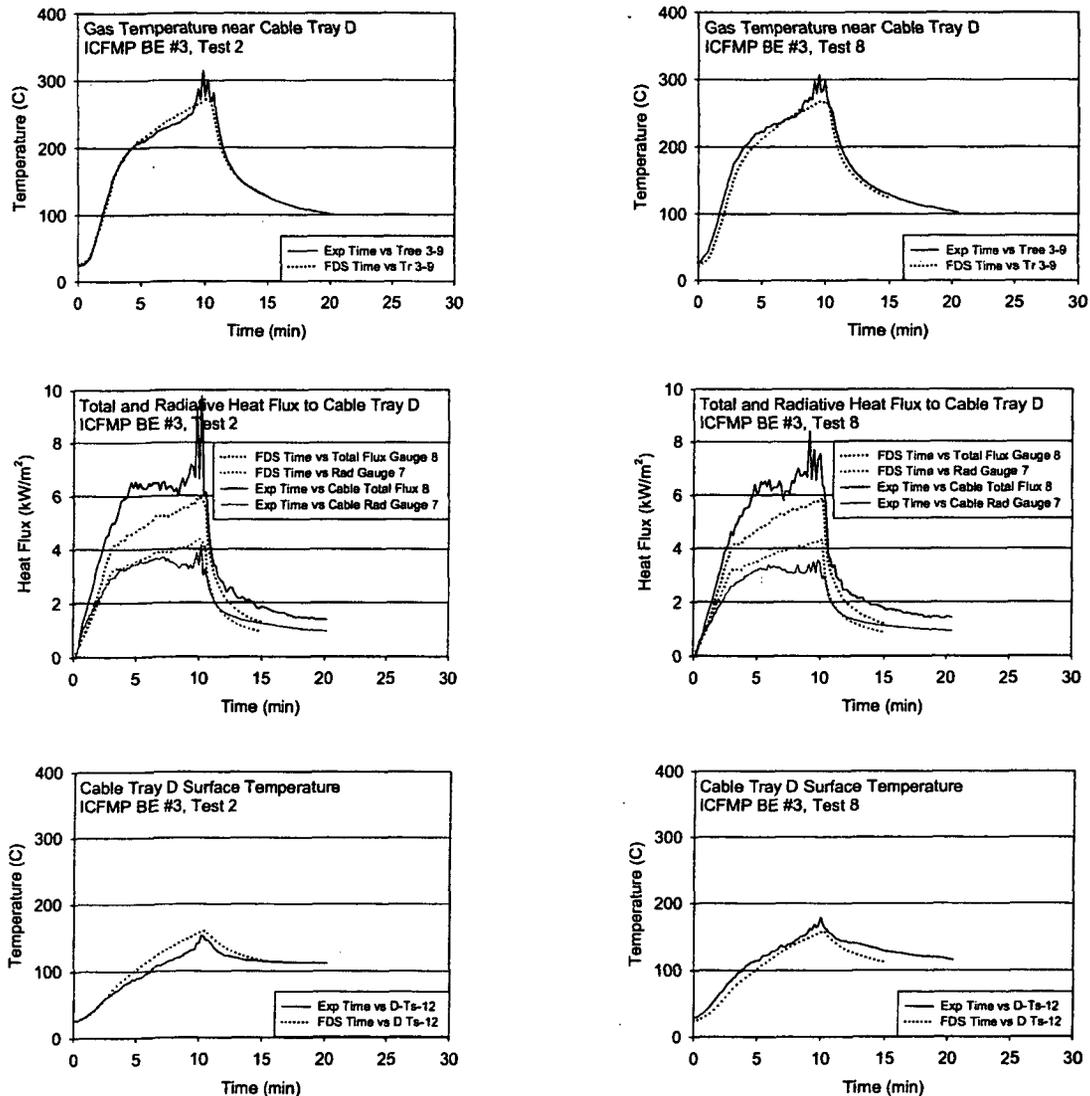
Figure A-41: Thermal Environment near Cable Tray D, ICFMP BE #3, Tests 2 and 8
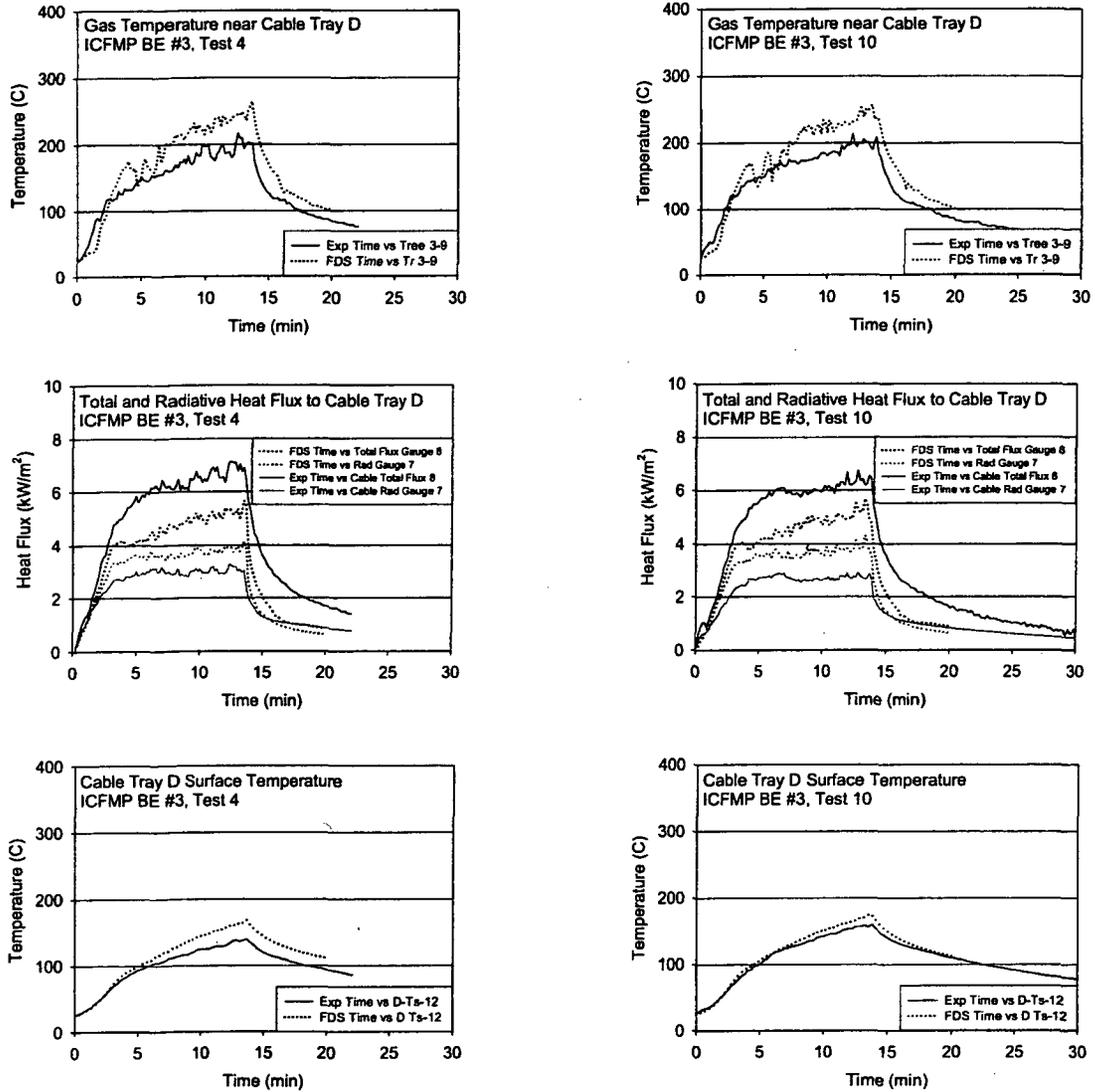
Figure A-42: Thermal Environment near Cable Tray D, ICFMP BE #3, Tests 4 and 10
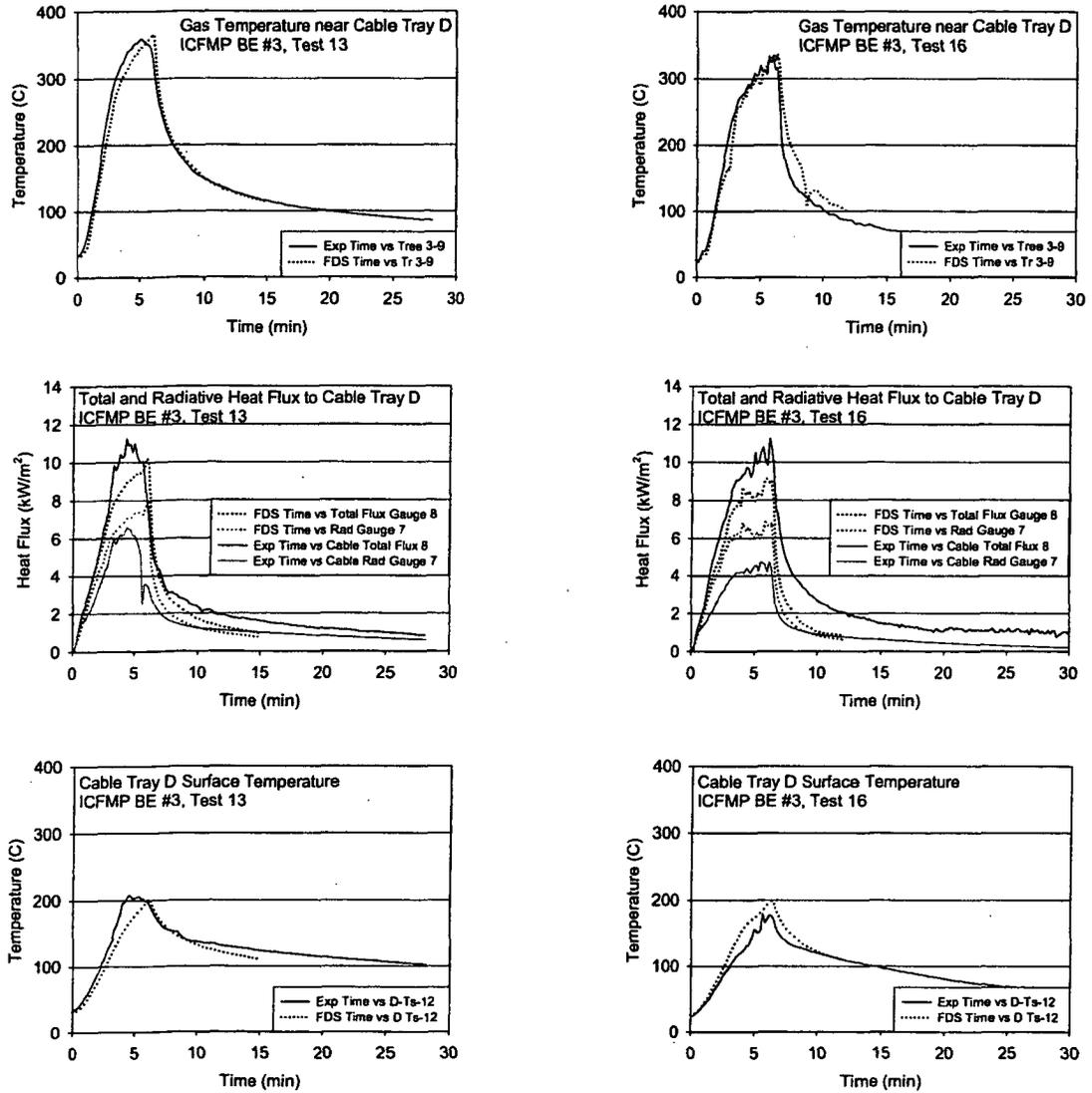
Figure A-43: Thermal Environment near Cable Tray D, ICFMP BE #3, Tests 13 and 16
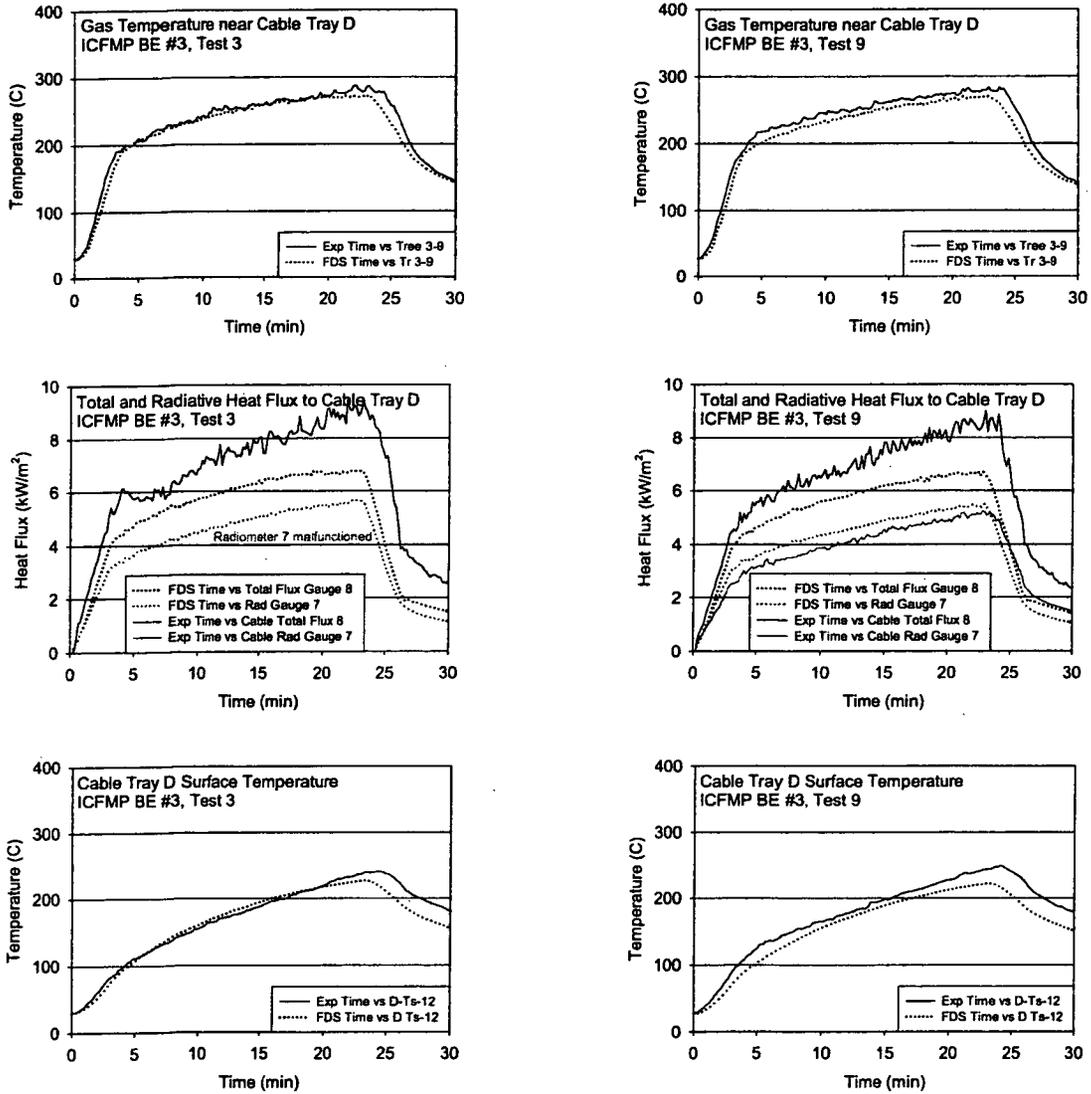
Figure A-44: Thermal Environment near Cable Tray D, ICFMP BE #3, Tests 3 and 9
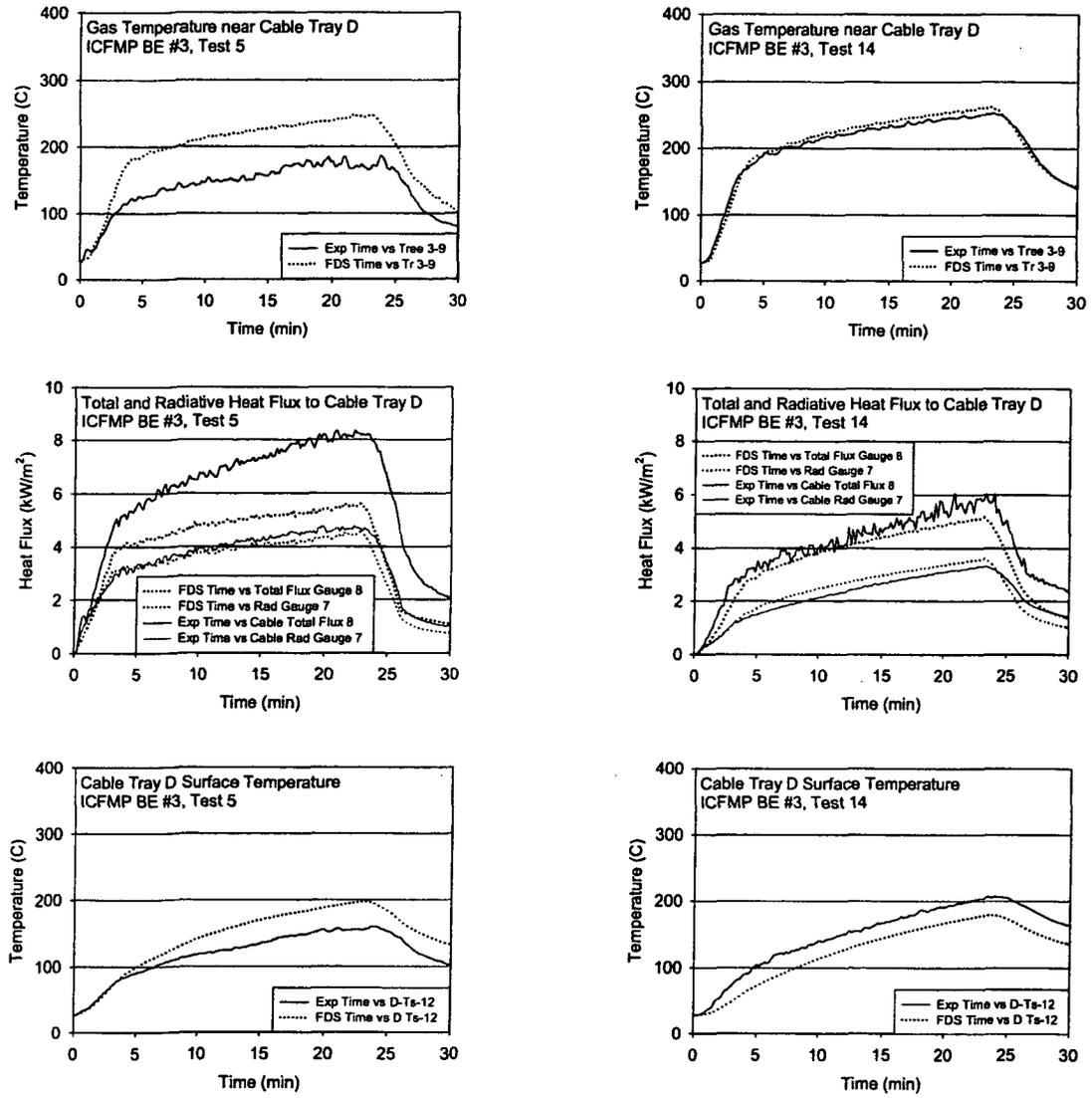
Figure A-45: Thermal Environment near Cable Tray D, ICFMP BE #3, Tests 5 and 14
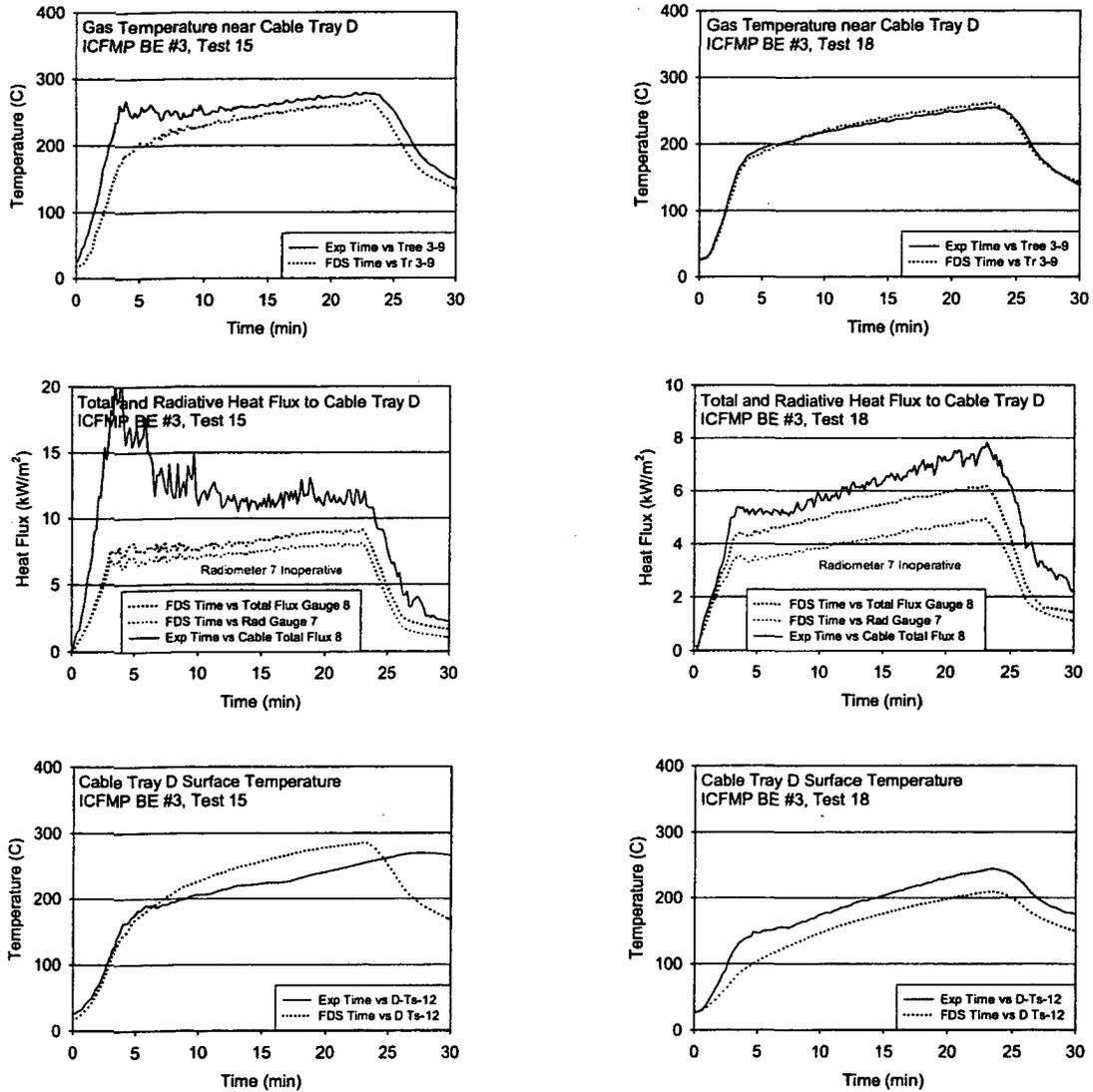
Figure A-46: Thermal Environment near Cable Tray D, ICFMP BE #3, Tests 15 and 18
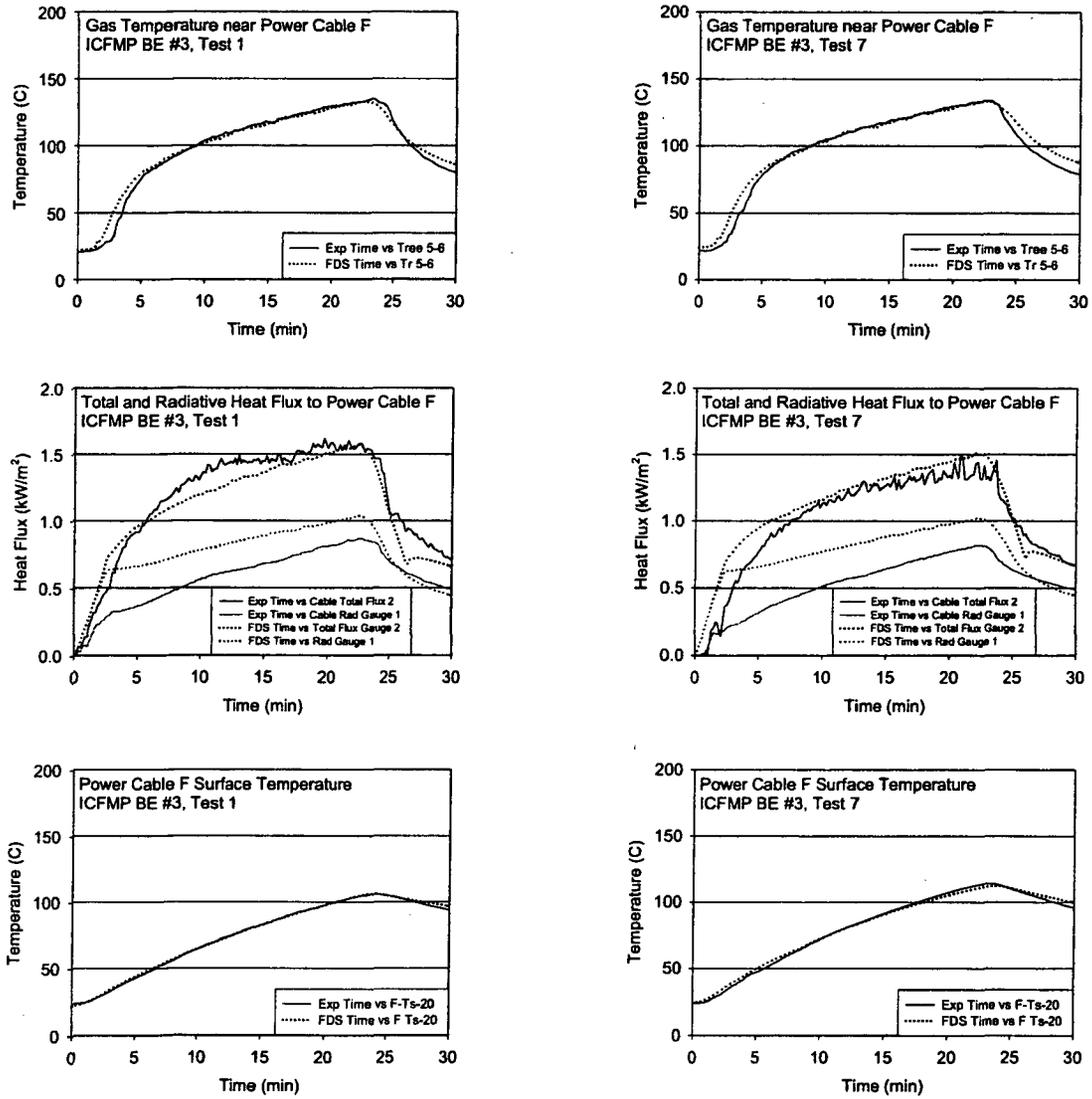
Figure A-47: Thermal Environment near Power Cable F, ICFMP BE #3, Tests 1 and 7
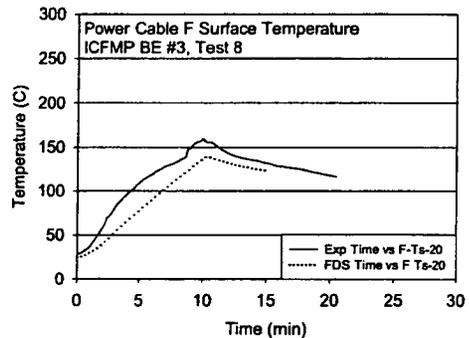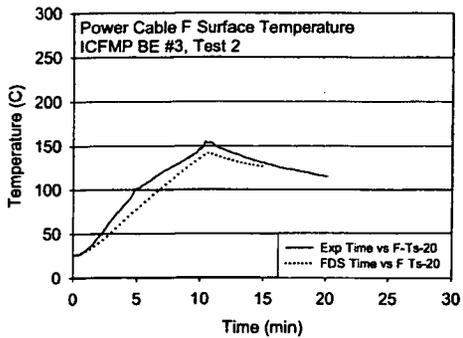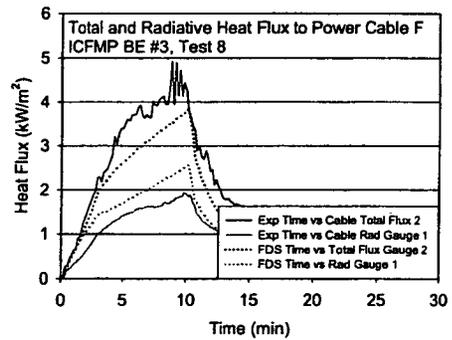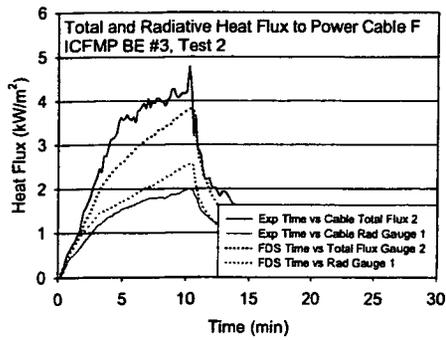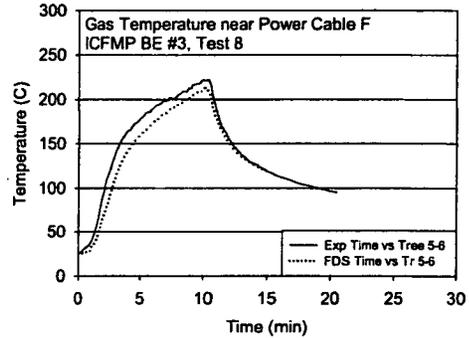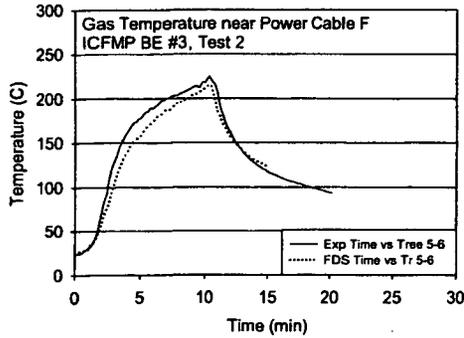
Figure A-48: Thermal Environment near Power Cable F, ICFMP BE #3, Tests 2 and 8
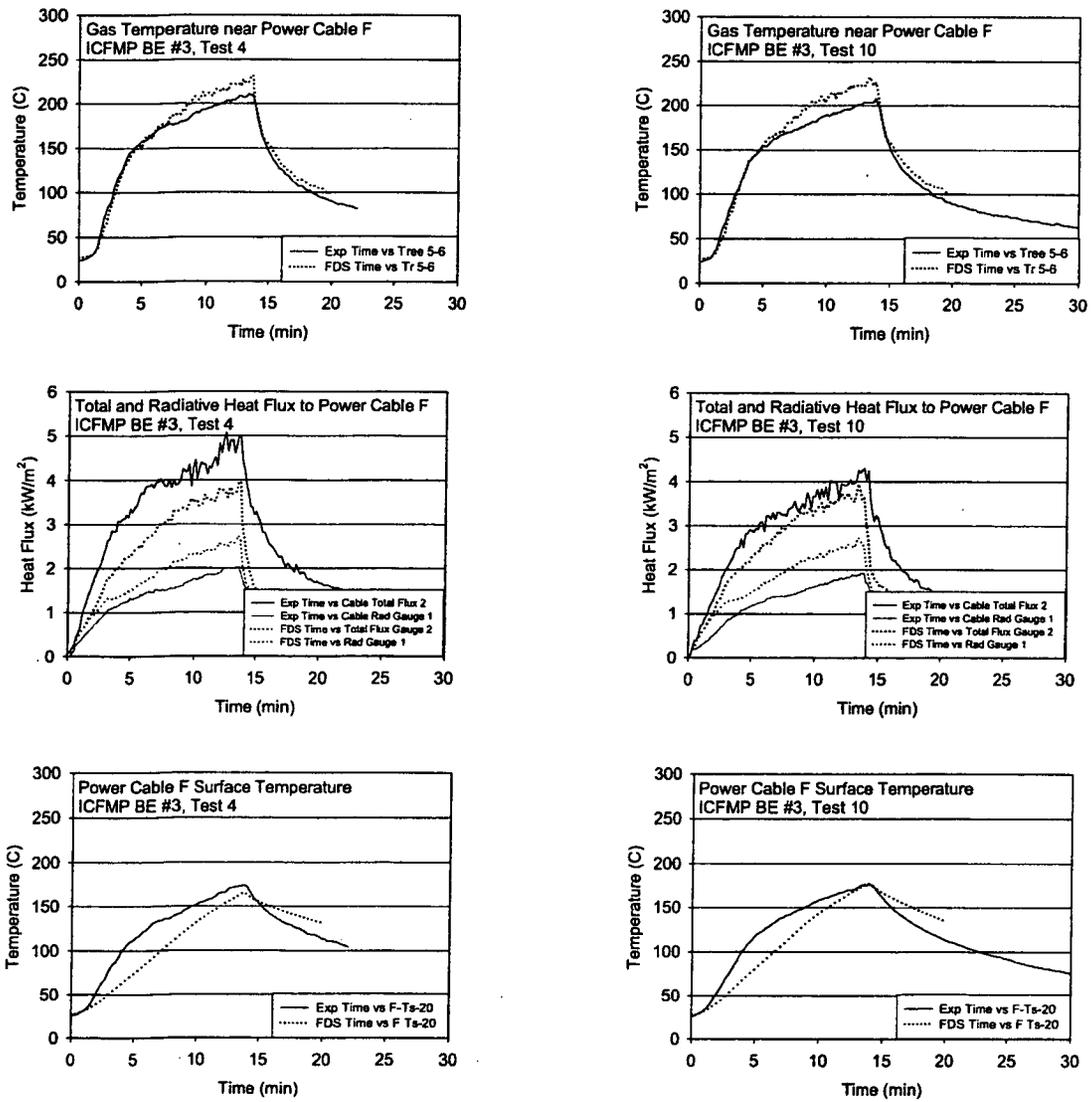
Figure A-49: Thermal Environment near Power Cable F, ICFMP BE #3, Tests 4 and 10
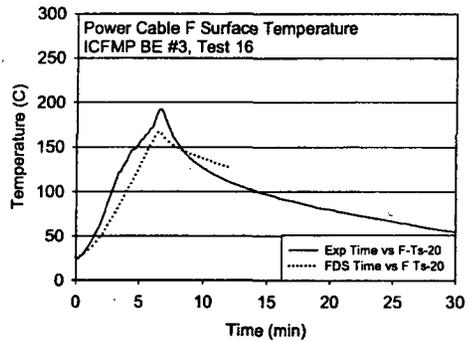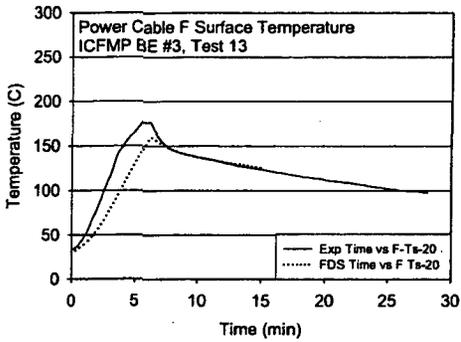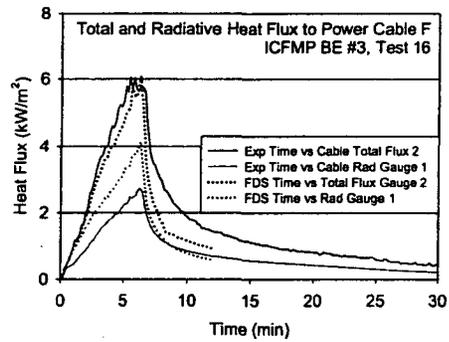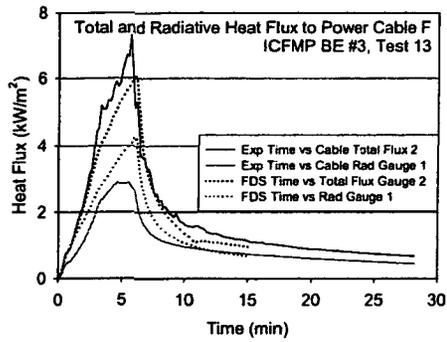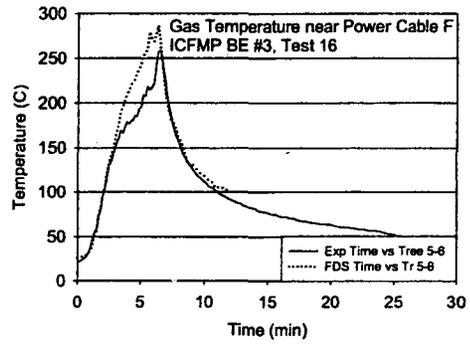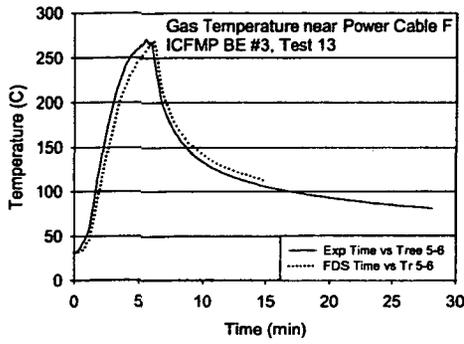
Figure A-50: Thermal Environment near Power Cable F, ICFMP BE #3, Tests 13 and 16
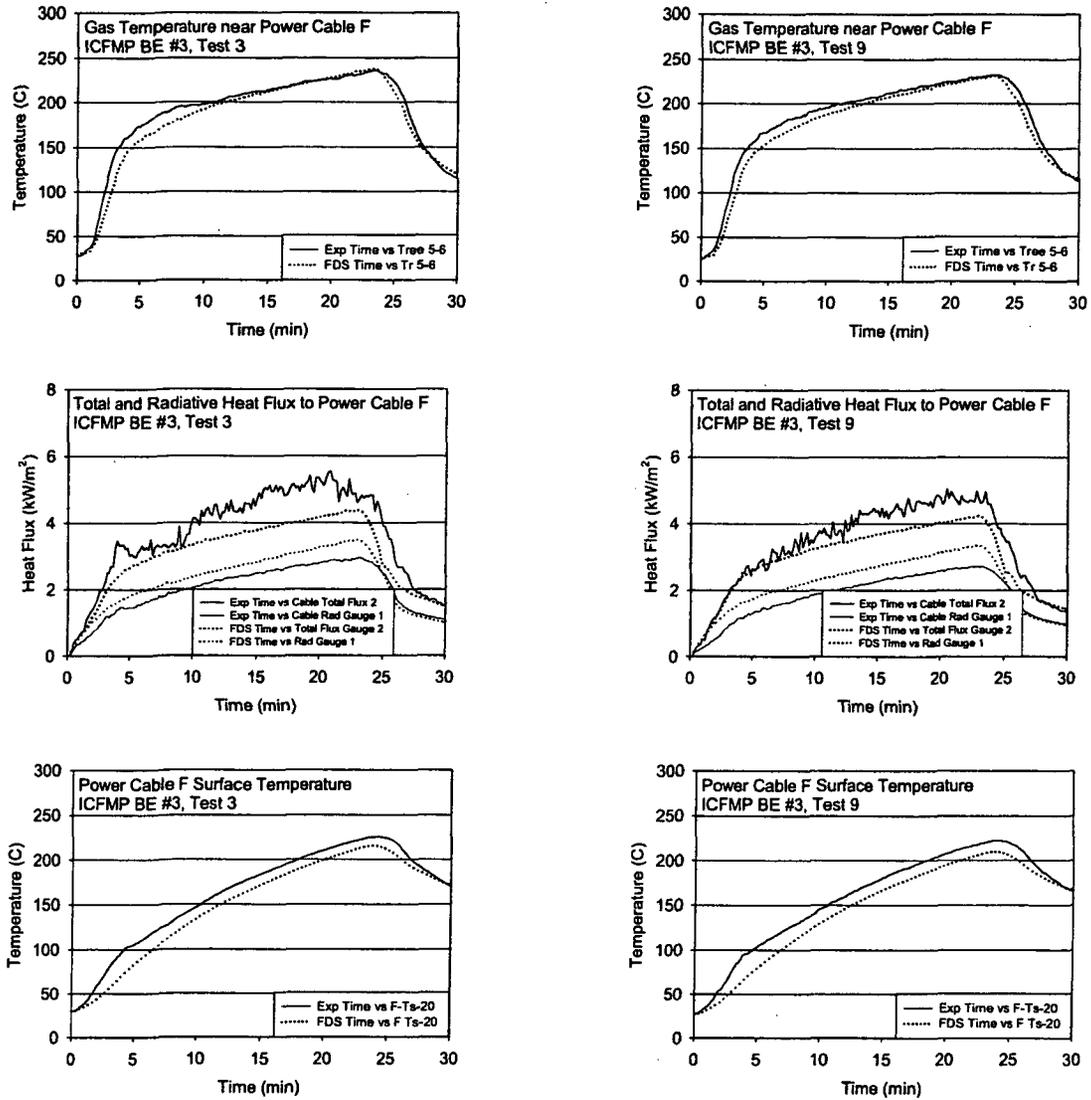
Figure A-51: Thermal Environment near Power Cable F, ICFMP BE #3, Tests 3 and 9
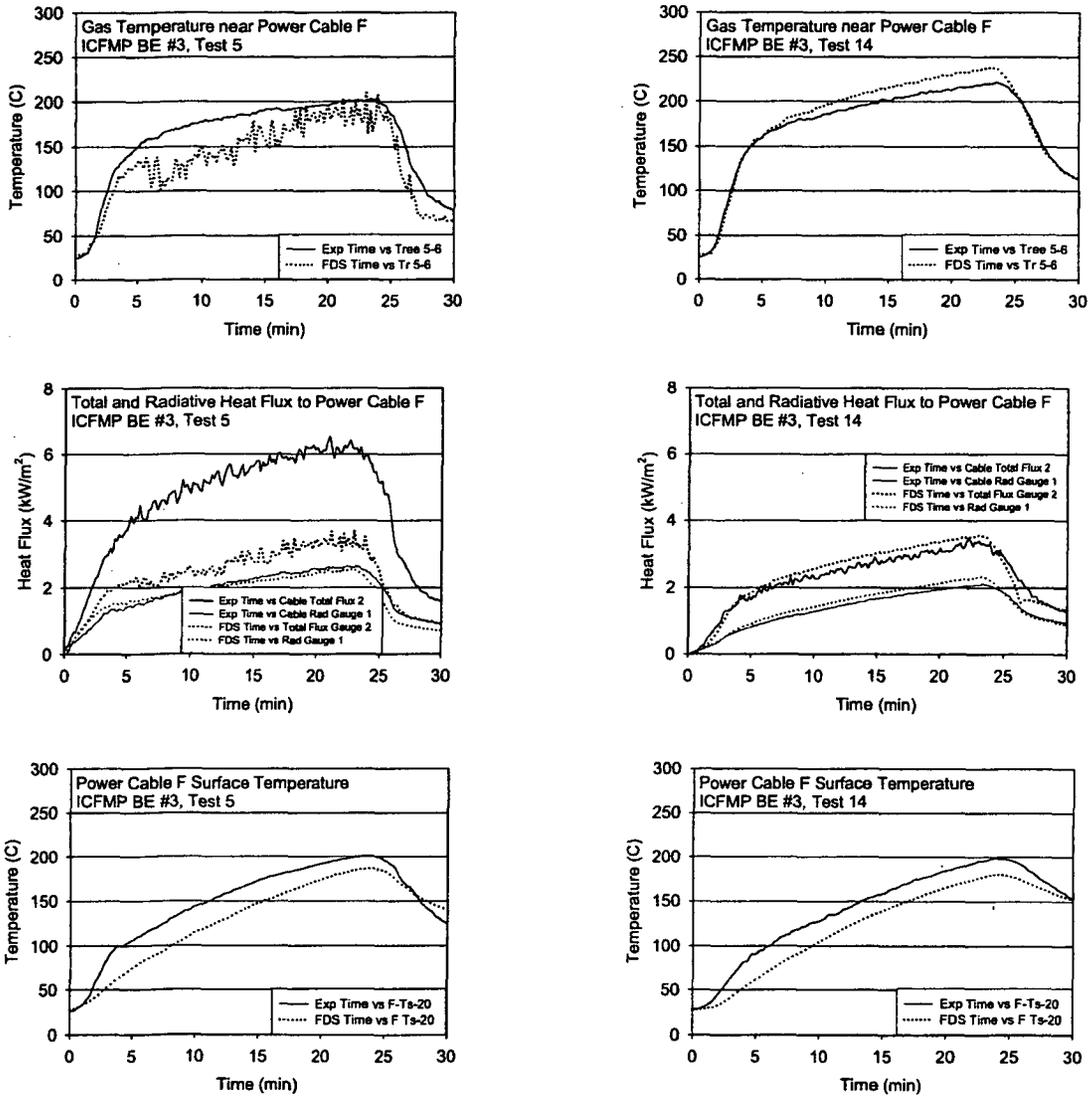
Figure A-52: Thermal Environment near Power Cable F, ICFMP BE #3, Tests 5 and 14
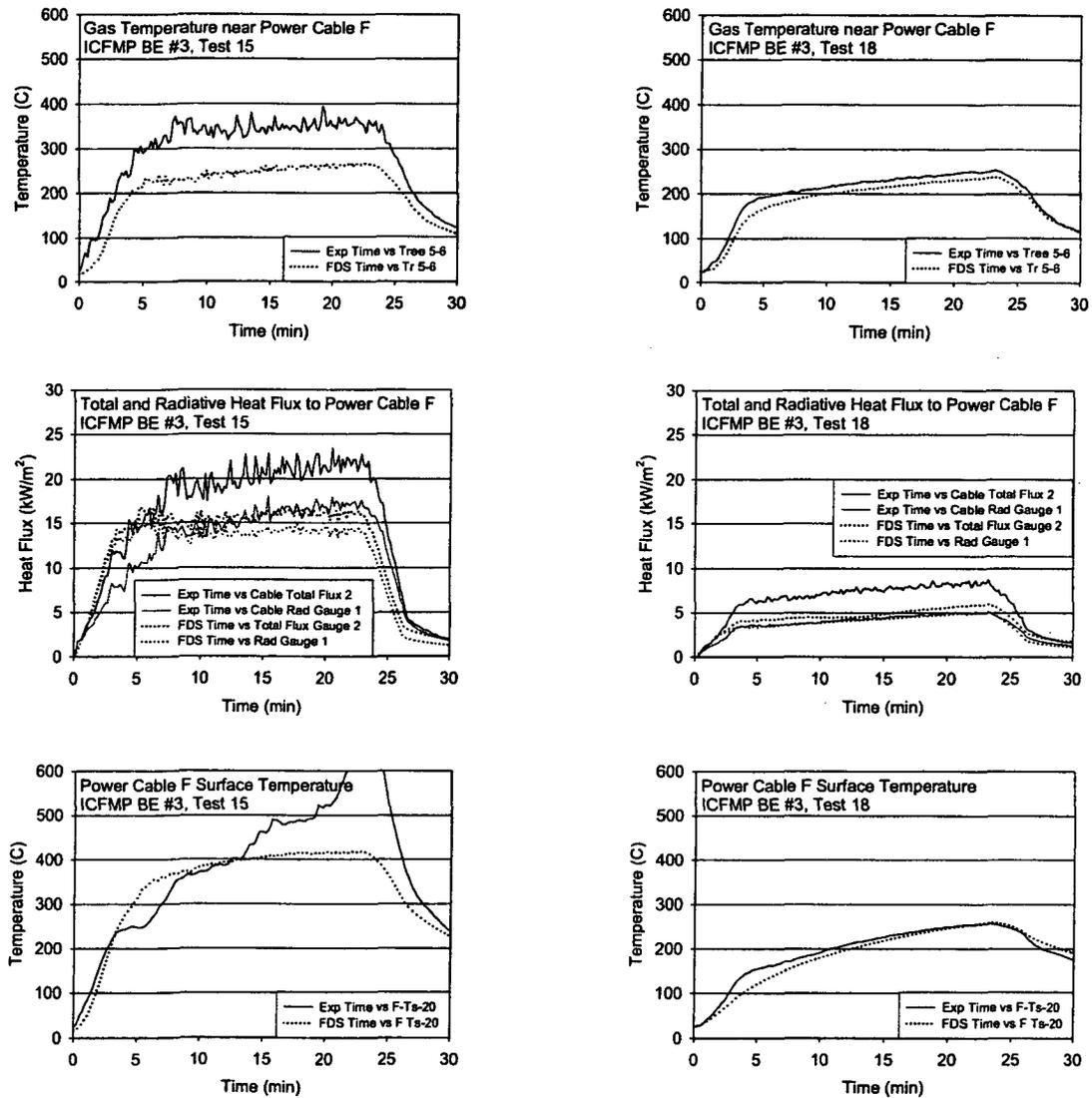
Figure A-53: Thermal Environment near Power Cable F, ICFMP BE #3, Tests 15 and 18
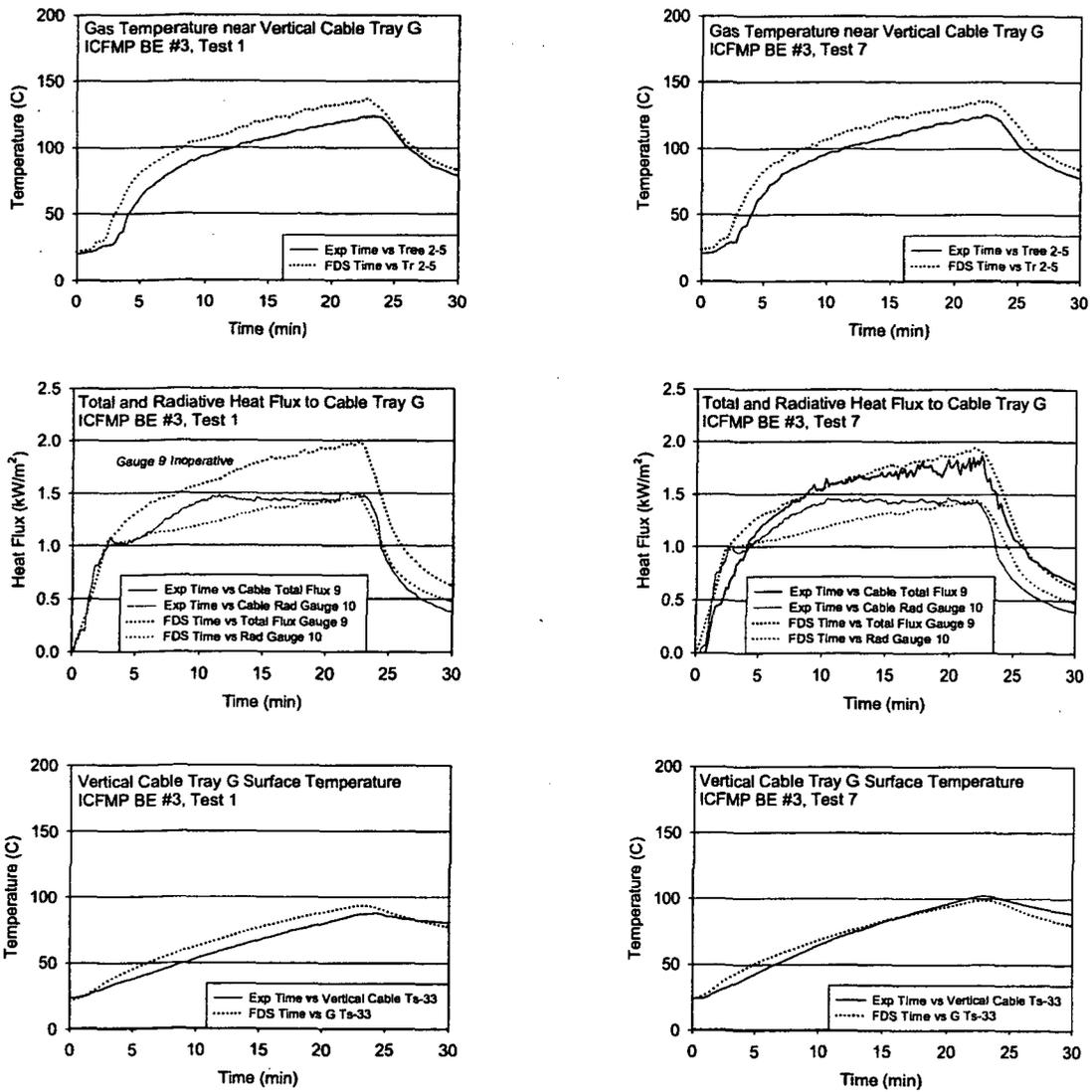
Figure A-54: Thermal Environment near Vertical Cable Tray G, ICFMP BE #3, Tests 1 and 7
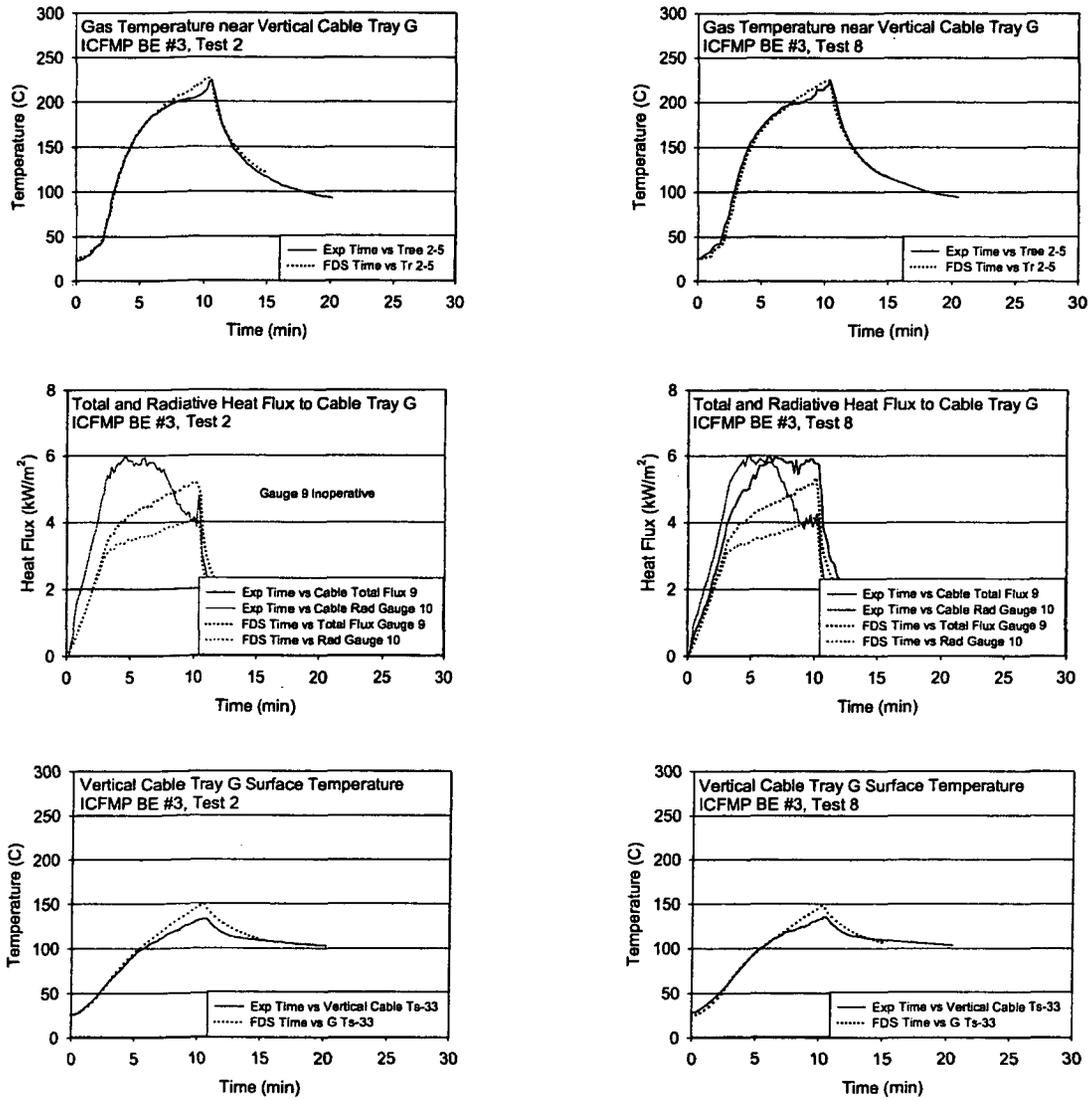
Figure A-55: Thermal Environment near Vertical Cable Tray G, ICFMP BE #3, Tests 2 and 8
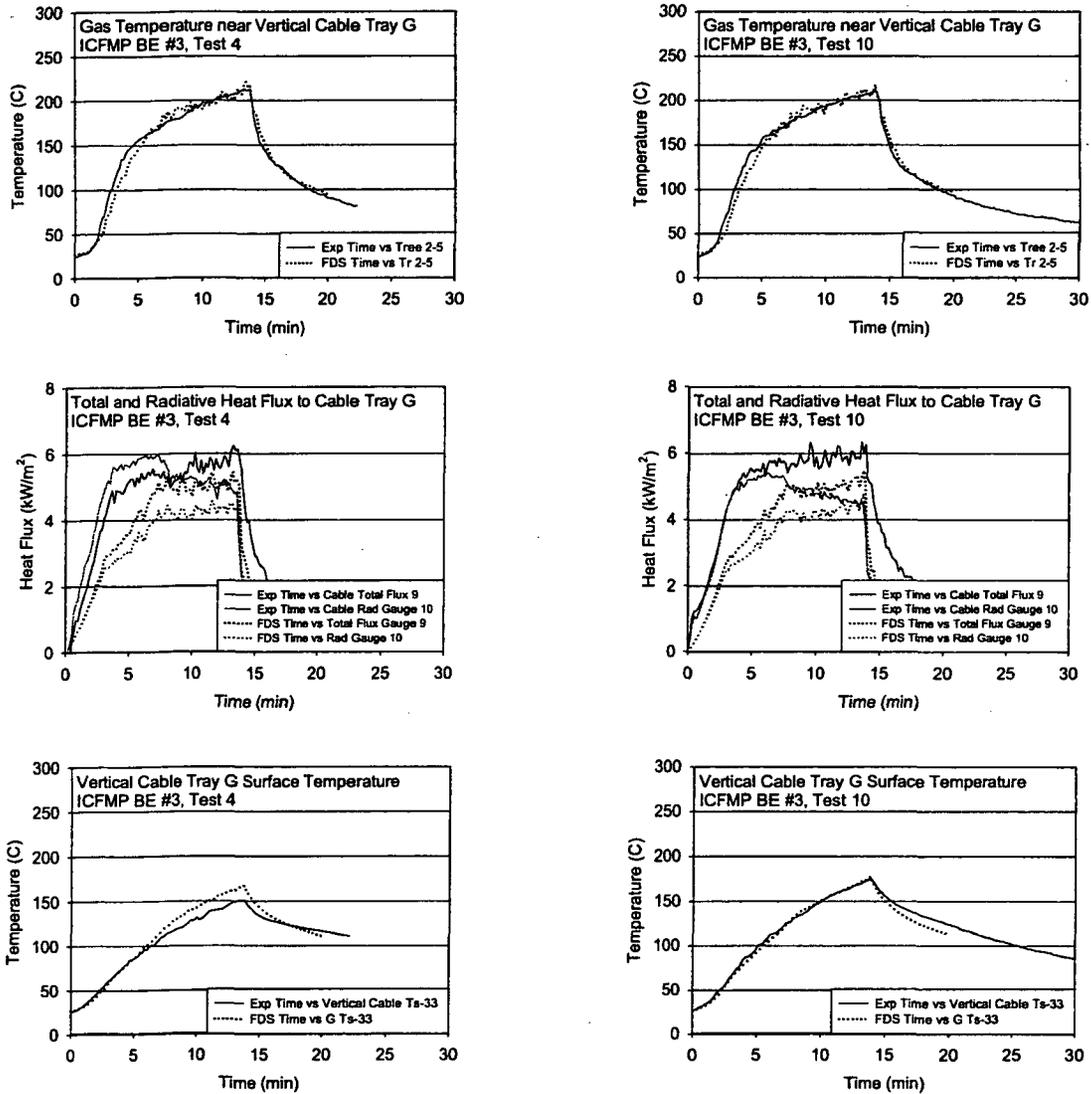
Figure A-56: Thermal Environment near Vertical Cable Tray G, ICFMP BE #3, Tests 4 and 10
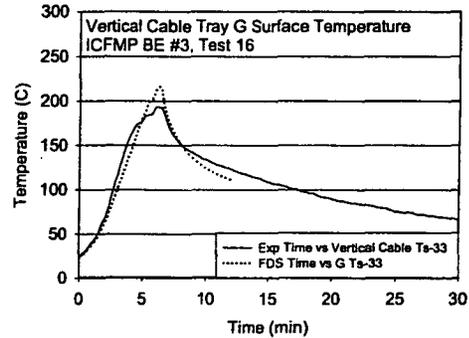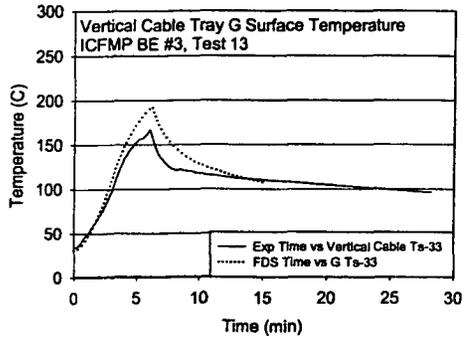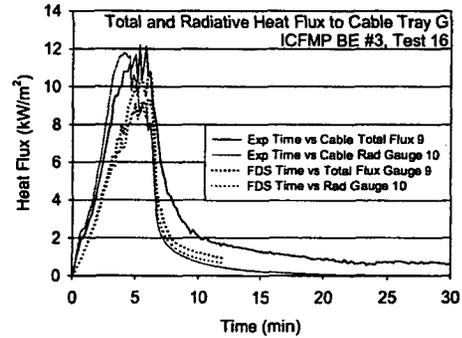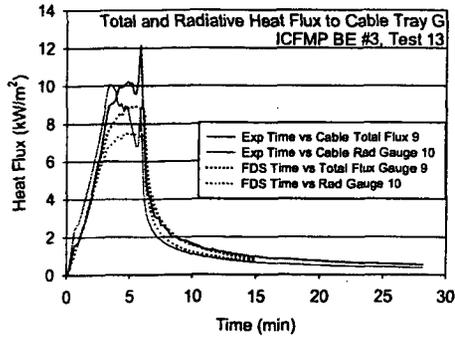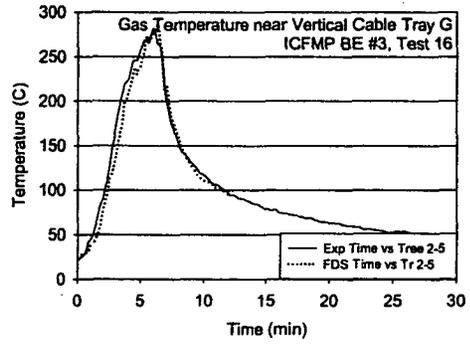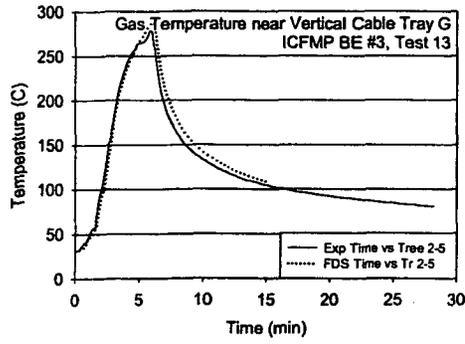
Figure A-57: Thermal Environment near Vertical Cable Tray G, ICFMP BE #3, Tests 4 and 10
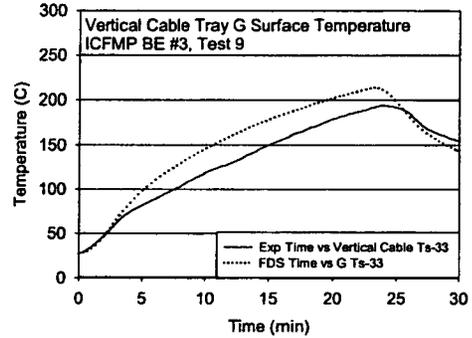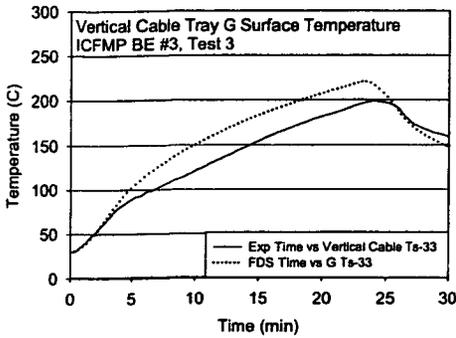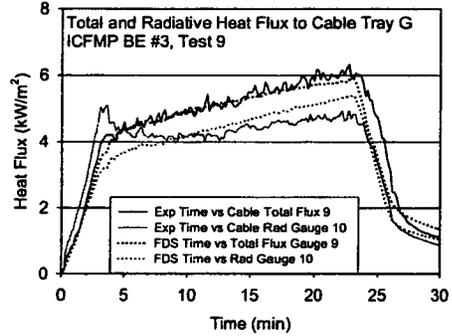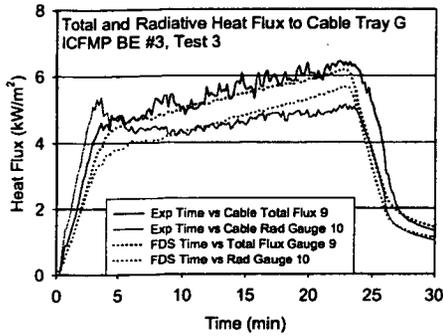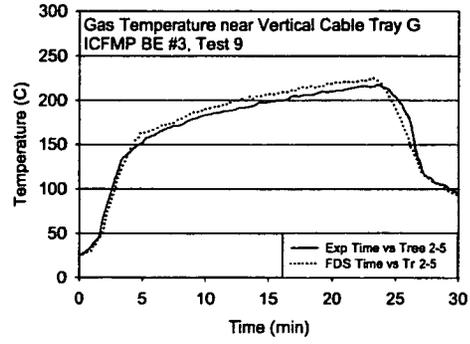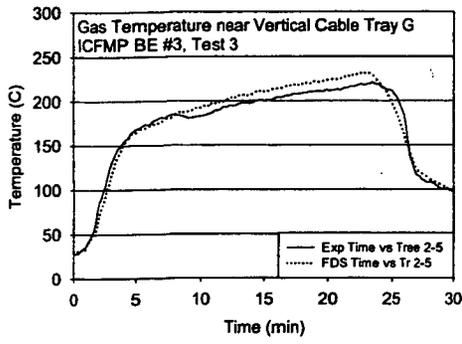
Figure A-58: Thermal Environment near Vertical Cable Tray G, ICFMP BE #3, Tests 3 and 9
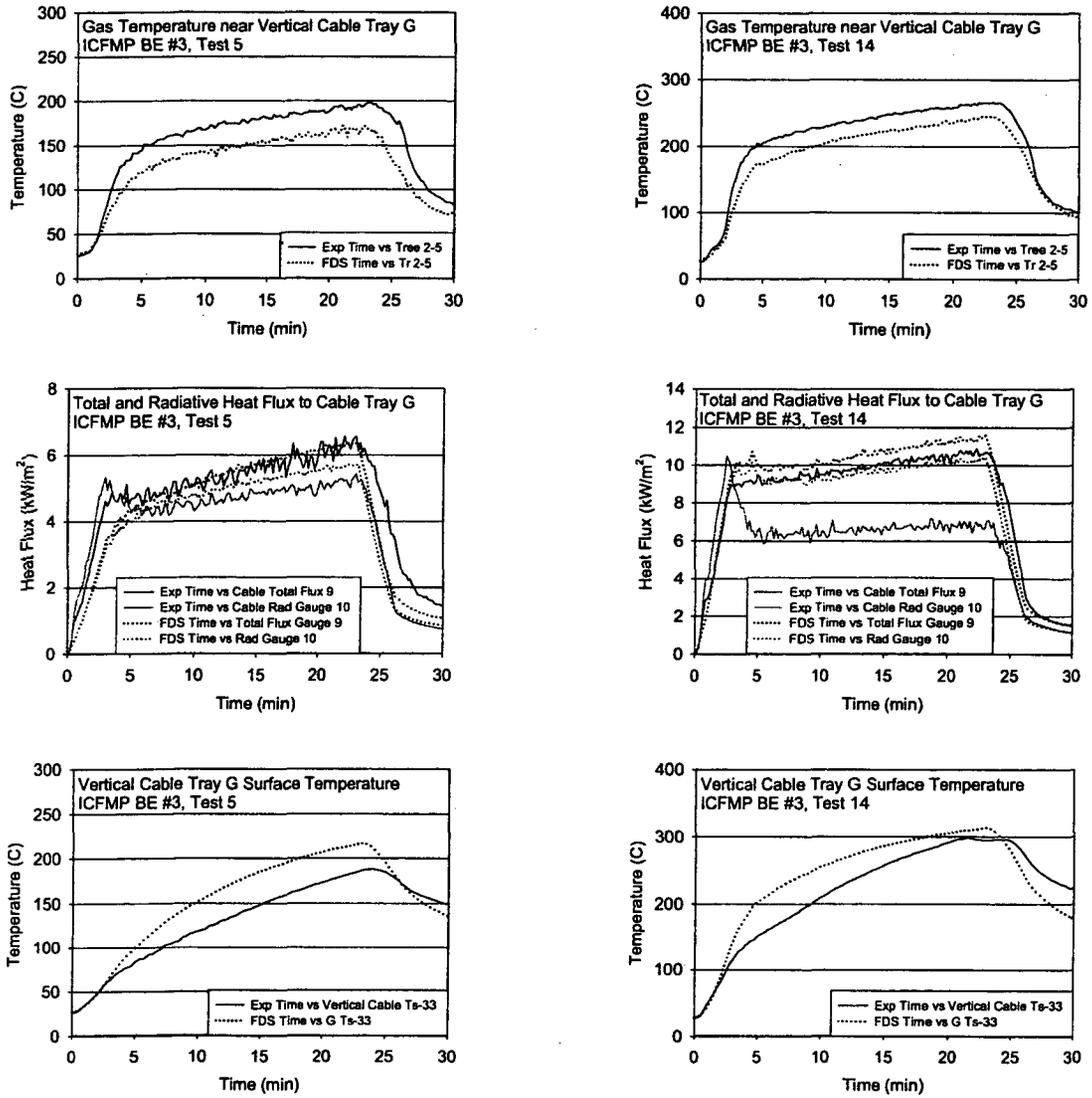
Figure A-59: Thermal Environment near Vertical Cable Tray G, ICFMP BE #3, Tests 5 and 14
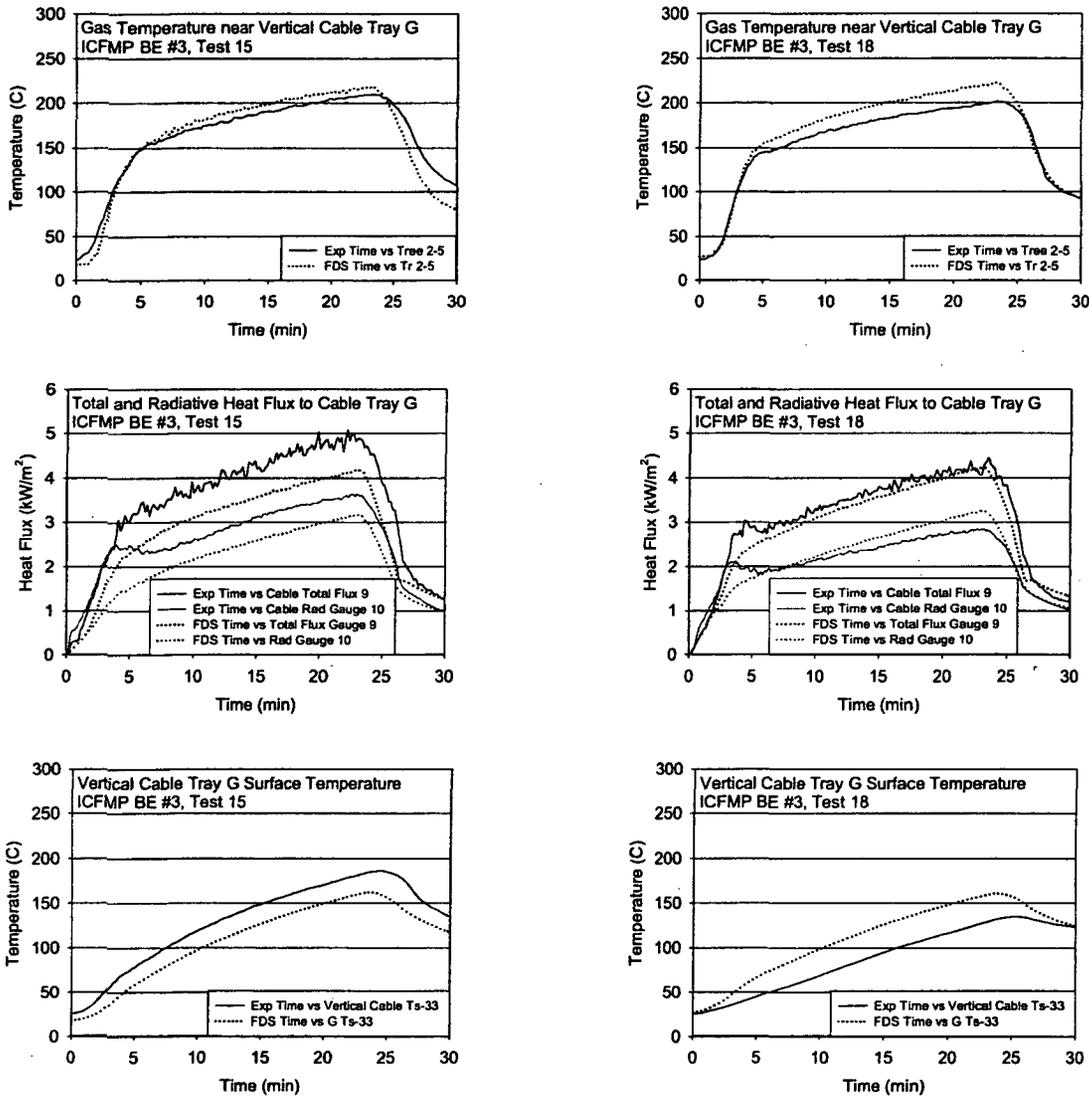
Figure A-60: Thermal Environment near Vertical Cable Tray G, ICFMP BE #3, Tests 15 and 18

ICFMP BE #4

The targets in BE #4, Test 1 are three material probes made of concrete, aerated (light) concrete, and steel. Figure A-61 displays a snapshot from FDS, showing the fire and the locations of the three targets.
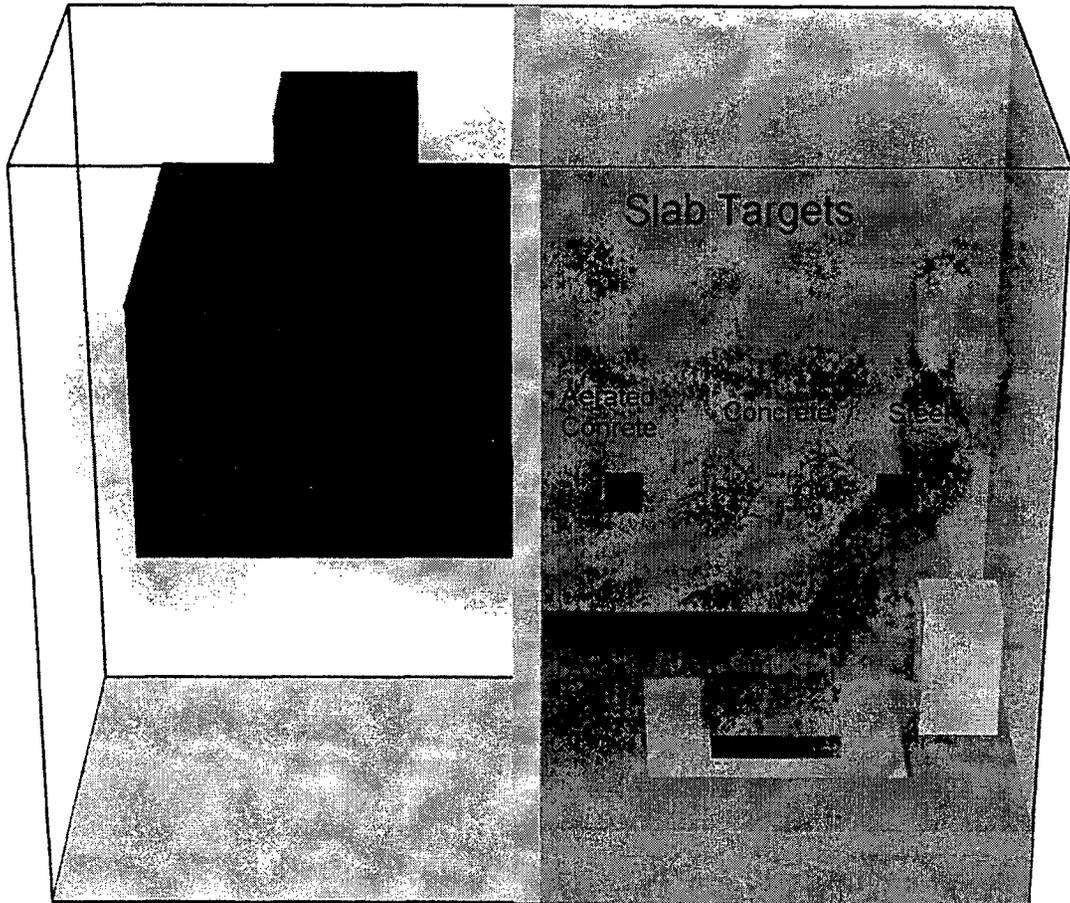
Figure A-61: Location of Three Slab Targets in ICFMP BE #4
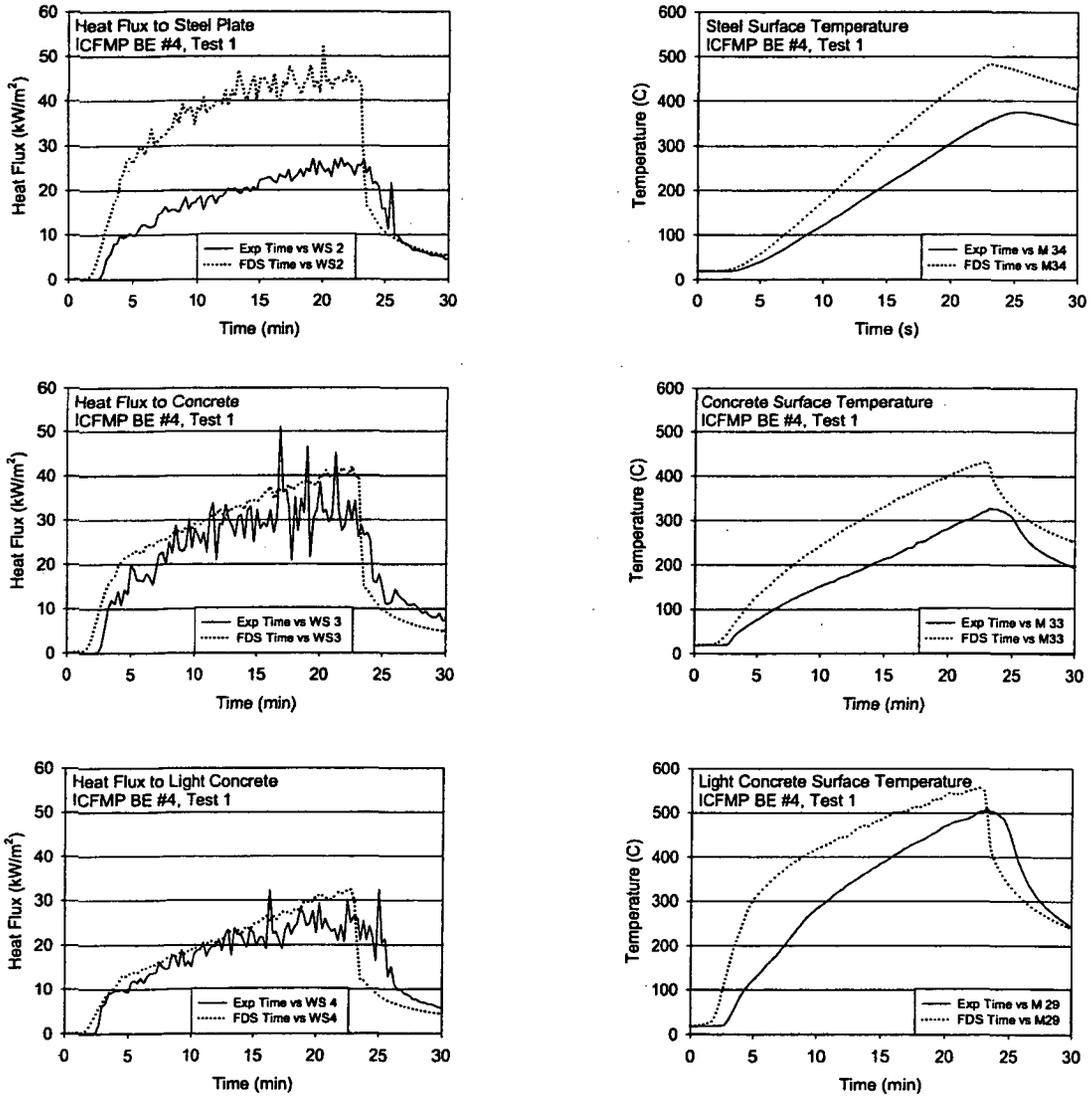
Figure A-62: Heat Flux and Surface Temperatures of Target Slabs, ICFMP BE #4, Test 1

ICFMP BE #5

A vertical cable tray was positioned near a wall opposite the fire. Heat flux gauges were located in between two bundles of cables, one containing power cables, and the other containing control cables. On the following pages are plots of the gas temperature, heat flux, and cable surface temperatures at four vertical locations above the floor:

<u>200 cm</u> (Gas Temperature TR 5-3, Heat Flux WS 2, Cable Temperature TCO 1-3 and TCO 3.3)

<u>280 cm</u> (TR 5-4, WS 3, TCO 1-5 and TCO 3-5)

<u>360 cm</u> (TR 5-5, WS 4, TCO 1-7 and TCO 3-7)

<u>440 cm</u> (TR 5-6, WS 5, TCO 1-9 and TCO 3-9)
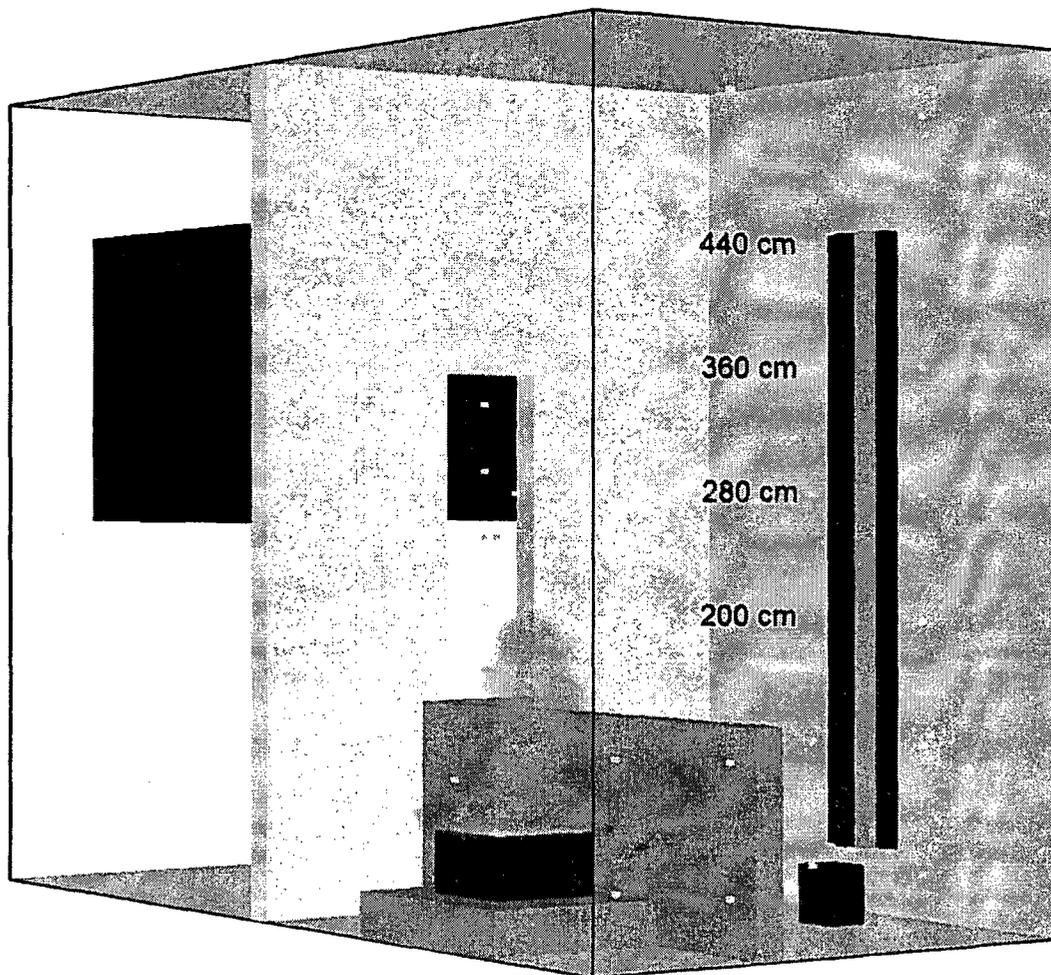
Figure A-63: Location of Targets, ICFMP BE #5, Test 4
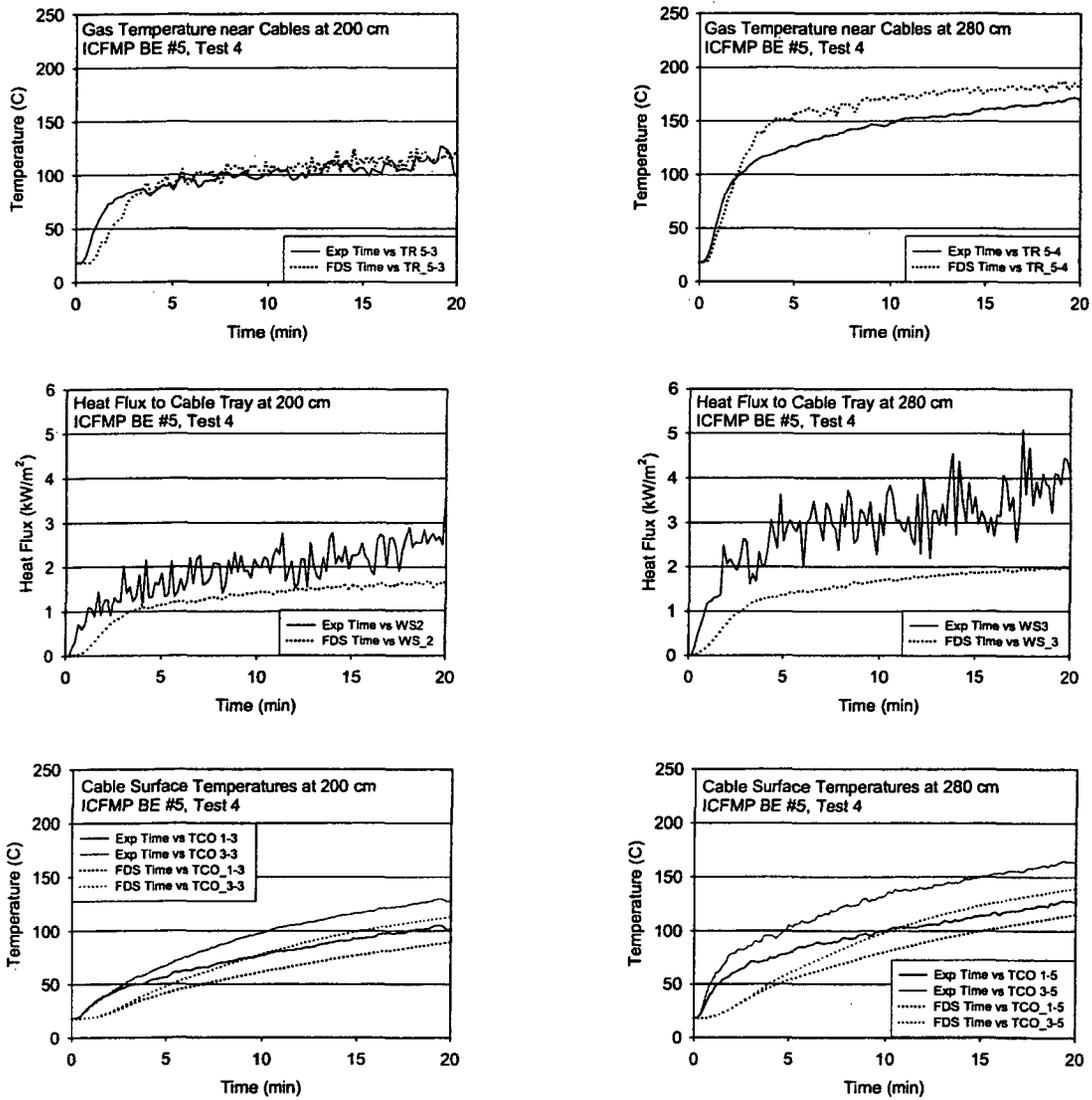
Figure A-64: Thermal Environment near Vertical Cable Tray, ICFMP BE #5, Test 4
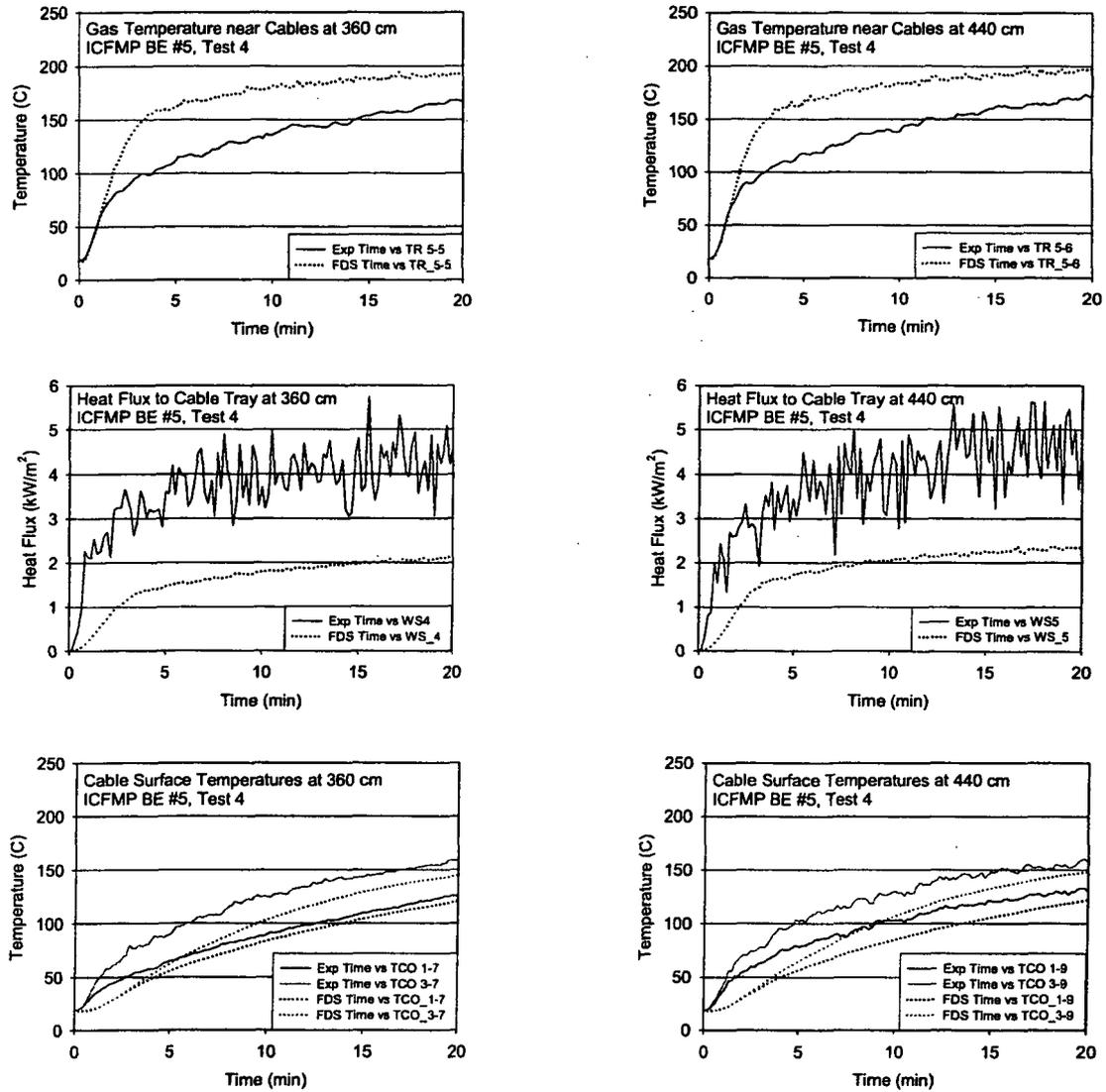
Figure A-65: Thermal Environment near Vertical Cable Tray, ICFMP BE #5, Test 4

Table A-7: Summary of Target Heat Flux and Surface Temperature

			Radiation Heat Flux			Total Heat Flux			Surface Temperature Rise		
			ΔE (kW/m²)	ΔM (kW/m²)	Diff. (%)	ΔE (kW/m²)	ΔM (kW/m²)	Diff. (%)	ΔE (°C)	ΔM (°C)	Diff. (%)
ICFMP BE #3	Test 1	Cable B	1.12	1.26	13	1.85	1.72	-7	106	112	5
		Cable D	1.44	1.59	11	–	2.30	--	--	78	--
		Cable F	0.87	1.04	20	1.60	1.57	-2	83	84	2
		Cable G	1.51	1.47	-3	–	1.99	--	64	71	11
	Test 7	Cable B	1.20	1.24	3	1.84	1.69	-8	109	110	1
		Cable D	1.35	1.55	15	2.52	2.21	-12	87	81	-7
		Cable F	0.82	1.02	24	1.51	1.51	0	90	88	-2
		Cable G	1.47	1.45	-2	1.89	1.94	3	78	75	-4
	Test 2	Cable B	2.88	3.20	11	5.26	4.32	-18	176	172	-2
		Cable D	4.16	4.36	5	9.83	5.90	-40	126	134	6
		Cable F	1.99	2.58	29	4.77	3.82	-20	129	116	-10
		Cable G	5.97	4.05	-32	–	5.16	--	107	123	15
	Test 8	Cable B	2.91	3.22	11	5.58	4.39	-21	183	170	-7
		Cable D	3.55	4.33	22	8.51	5.88	-31	150	133	-11
		Cable F	1.93	2.56	33	4.93	3.82	-22	131	114	-13
		Cable G	6.03	4.22	-30	5.98	5.34	-11	107	123	15
	Test 4	Cable B	2.92	3.37	15	5.52	4.21	-24	149	197	32
		Cable D	3.26	4.14	27	7.23	5.66	-22	113	141	24
		Cable F	2.02	2.74	35	5.02	3.97	-21	149	139	-7
		Cable G	6.00	4.56	-24	6.42	5.45	-15	125	140	12
	Test 10	Cable B	2.69	3.44	28	4.91	4.33	-12	144	198	38
		Cable D	2.91	4.32	48	6.71	5.68	-15	132	147	11
		Cable F	1.93	2.74	42	4.36	3.95	-9	150	150	0
		Cable G	5.42	4.78	-12	6.20	5.49	-12	148	150	1
ICFMP BE 3#	Test 13	Cable B	4.77	5.53	16	8.26	7.31	-12	186	195	5
		Cable D	6.58	7.90	20	11.22	10.22	-9	173	172	-1
		Cable F	2.90	4.26	47	7.28	6.10	-16	143	128	-11
		Cable G	10.06	7.51	-25	12.12	8.95	-27	133	163	22
	Test 16	Cable B	4.12	4.83	17	8.37	6.03	-28	160	206	28
		Cable D	4.83	6.86	42	11.67	9.10	-22	156	172	11
		Cable F	2.76	4.12	50	6.13	6.11	0	168	141	-16
		Cable G	11.96	9.37	-22	12.23	10.73	-12	169	191	13
	Test 17	Cable B	1.30	1.68	29	2.36	2.57	9	--	70	--
		Cable D	1.52	2.35	55	3.29	3.40	4	--	59	--
		Cable F	0.88	1.28	45	1.85	2.05	11	--	46	--
		Cable G	2.42	2.09	-14	3.07	2.66	-13	--	51	--
	Test 3	Cable B	4.45	4.36	-2	7.10	4.97	-30	226	226	0
		Cable D	–	5.63	--	9.45	6.77	-28	210	197	-6
		Cable F	2.95	3.48	18	5.55	4.38	-21	195	185	-5
		Cable G	5.36	5.67	6	6.45	6.18	-4	169	191	13
	Test 9	Cable B	4.29	4.22	-2	6.58	4.85	-26	228	225	-1
		Cable D	5.26	5.49	4	9.06	6.70	-26	220	195	-11
		Cable F	2.73	3.36	23	5.08	4.25	-16	195	183	-6
		Cable G	5.15	5.42	5	6.37	5.92	-7	166	187	12
	Test 5	Cable B	3.88	3.28	-15	6.86	4.03	-41	150	195	30
		Cable D	4.78	4.55	-5	8.52	5.61	-34	132	169	28
		Cable F	2.65	2.56	-3	6.45	3.70	-43	175	159	-9

		Cable G	5.45	5.70	5	6.69	6.37	-5	161	189	17
ICFMP BE #3	Test 14	Cable B	2.84	3.00	6	3.82	4.13	8	199	194	-2
		Cable D	3.32	3.61	9	6.07	5.16	-15	178	151	-15
		Cable F	2.12	2.33	10	3.46	3.57	3	171	152	-11
		Cable G	10.50	10.45	-1	10.90	11.61	6	270	286	6
	Test 15	Cable B	46.49	60.77	31	57.72	68.82	19	416	445	7
		Cable D	--	8.17	--	20.87	9.16	-56	243	267	10
		Cable F	18.29	15.42	-16	23.94	17.03	-29	669	400	-40
		Cable G	3.73	3.17	-15	5.12	4.18	-18	161	144	-11
	Test 18	Cable B	5.23	5.37	3	7.61	6.47	-15	236	239	1
		Cable D	--	4.95	--	7.83	6.20	-21	217	182	-16
		Cable F	5.18	5.04	-3	8.74	5.97	-32	232	233	1
		Cable G	2.85	3.26	15	4.45	4.25	-5	109	133	22

		Total Heat Flux			Surface Temperature Rise			Surface Temperature Rise		
		Exp (kW/m^2)	FDS (kW/m^2)	Diff. (%)	Exp (°C)	FDS (°C)	Diff. (%)	Exp (°C)	FDS (°C)	Diff. (%)
BE #4	Steel	27.2	47.1	73	356	454	28			
	Concrete	33	42.0	27	308	413	34			
	Lt. Concrete	26	32.4	25	489	537	10			
BE #5	200 cm	2.9	1.7	-42	87	71	-19	112	95	-15
	280 cm	4	2.0	-50	110	97	-11	146	121	-17
	360 cm	4.5	2.1	-53	107	102	-5	140	126	-10
	440 cm	4.5	2.4	-47	114	104	-9	142	130	-8

A.9 Heat Flux and Surface Temperature of Compartment Walls

Heat fluxes and surfaces temperatures at compartment walls, floor, and ceiling are available from ICFMP BE #3. Wall temperatures are also available from BE #4 and BE #5. This category is similar to that of the previous section, "Target Heat Flux and Surface Temperature," with the exception that the focus here is on compartment walls, ceiling, and floors, which some models treat differently than "targets." FDS makes no distinction.

ICFMP BE #3

Thirty-six heat flux gauges were positioned at various locations on all four walls of the compartment, as well as the ceiling and floor. Comparisons between measured and predicted heat fluxes and surface temperatures are shown on the following pages for a selected number of locations. Over half of the measurement points are in roughly the same relative location to the fire and, hence, the measurements and predictions are similar. For this reason, data for the east and north walls are shown because the data from the south and west walls are comparable. Data from the south wall is used in cases where the corresponding instrument on the north wall failed, or in cases where the fire was positioned close to the south wall.

For each test, eight locations are used for comparison, two on the long (mainly north) wall, two on the short (east) wall, two on the floor, and two on the ceiling. Of the two locations for each panel, one is considered in the *far-field*, relatively remote from the fire, and one is in the *near-field*, relatively close to the fire. How close or far varies from test to test, depending on the availability of working flux gauges. The two short wall locations are equally remote from the fire; thus, one location is in the lower layer, and one is in the upper layer. Table A-8 lists the locations for each test.

The heat flux gauges used on the compartment walls measured the *net*, not total, heat flux. FDS predicts the *net* heat flux, but this prediction cannot be compared directly with the measured *net* heat flux because the predicted and measured wall temperatures can differ, and this affects the *net* heat flux. In a sense, the *net* heat flux and surface temperature are coupled, and it is difficult to assess the accuracy of the models if the two quantities cannot be decoupled. For the purpose of comparing predictions and measurements, the following correction has been applied to both the measured and predicted *net* heat fluxes:

$$\dot{q}''_{total} = \dot{q}''_{net} + \sigma(T_s^4 - T_\infty^4) + h(T_s - T_\infty)$$

T_s is the temperature of the surface. A constant convective heat transfer coefficient is assumed (5 W/m^2/K) and an emissivity of 1. After applying the correction, it is easier to compare *total* heat fluxes that are independent of the surface temperature.
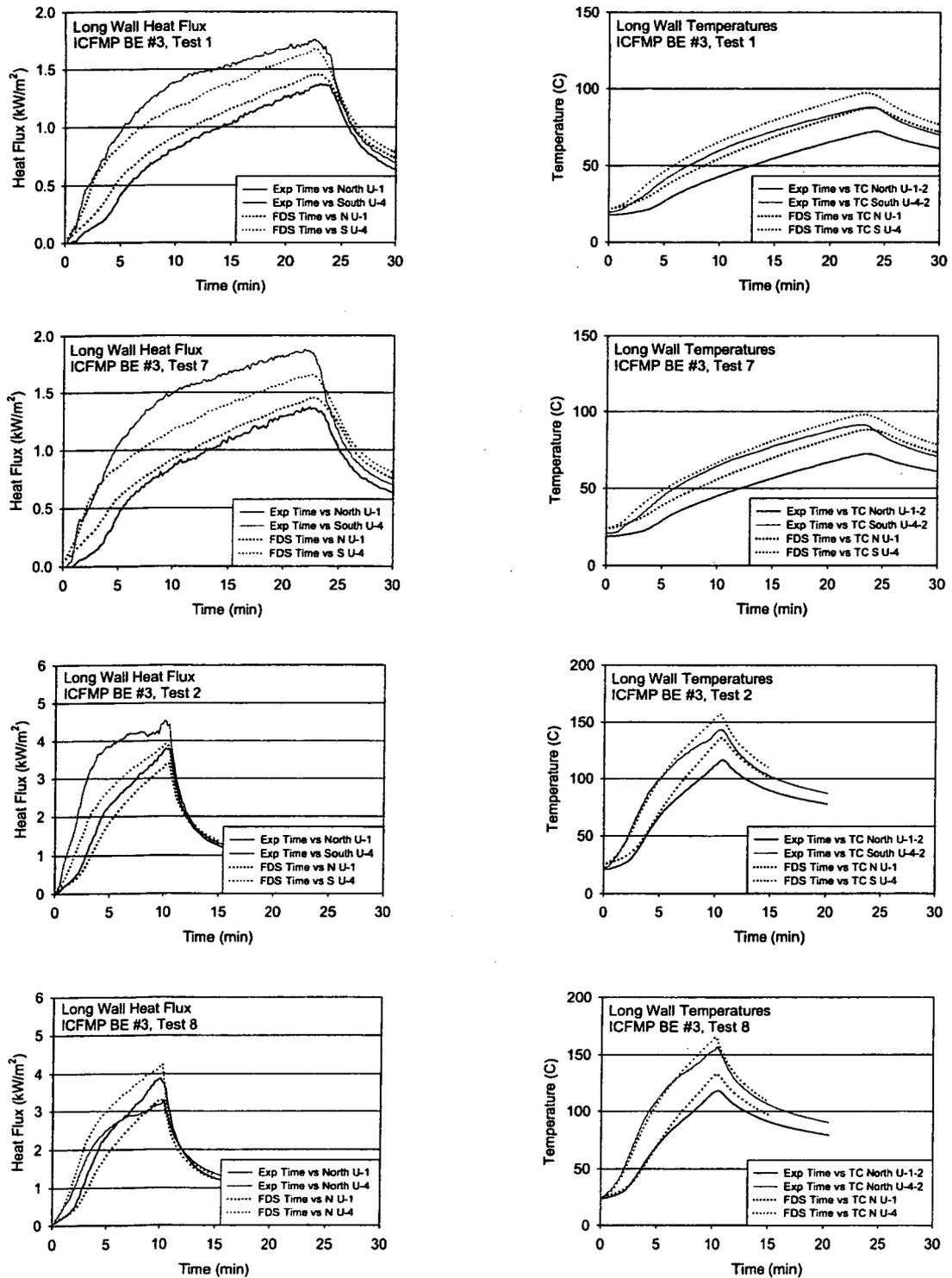
Figure A-66: Long-Wall Heat Flux and Surface Temperature, ICFMP BE #3, Closed-Door Tests
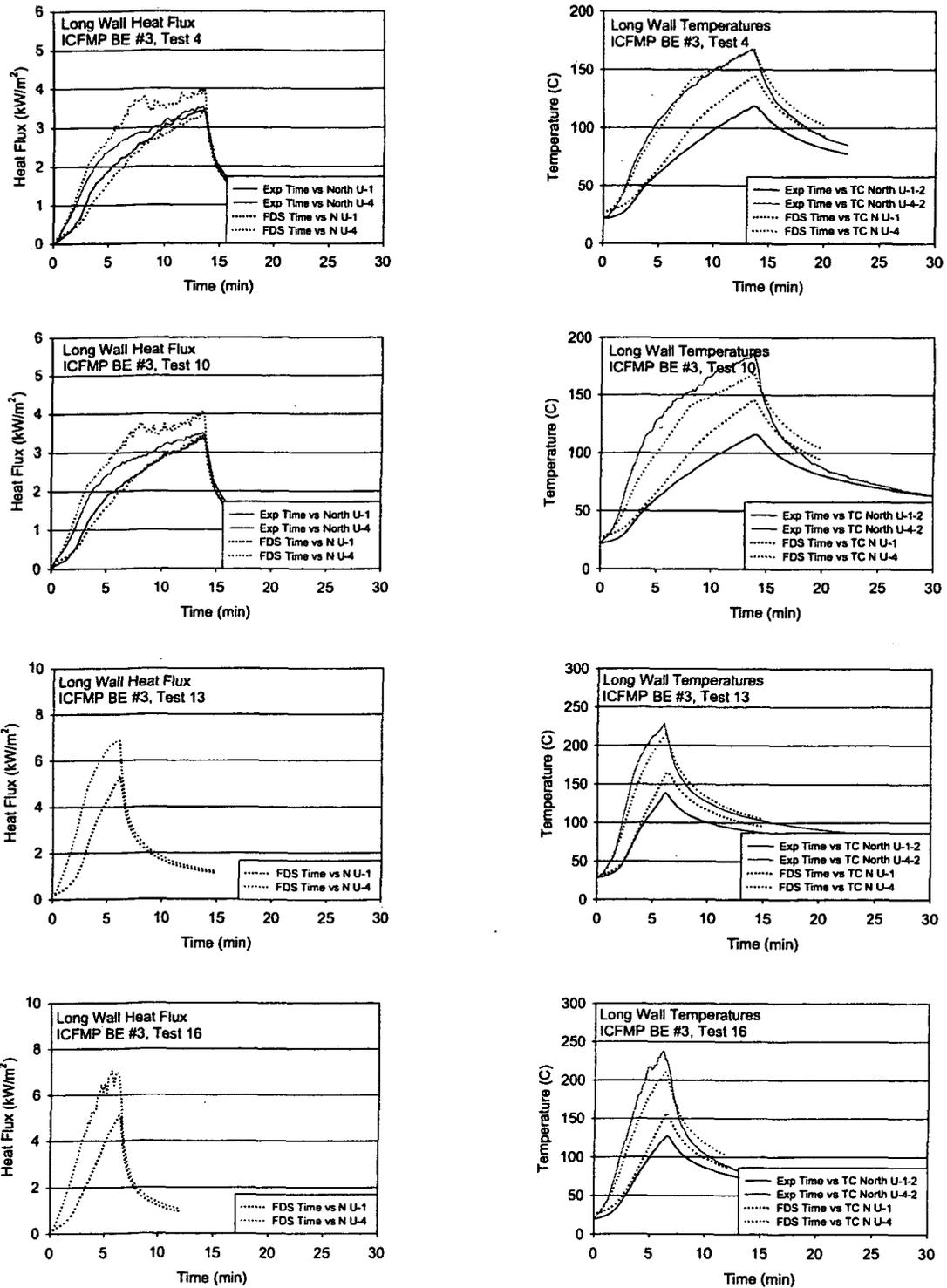
Figure A-67: Long-Wall Heat Flux and Surface Temperature, ICFMP BE #3, Closed-Door Tests
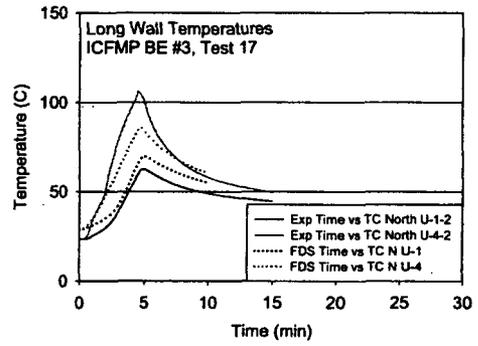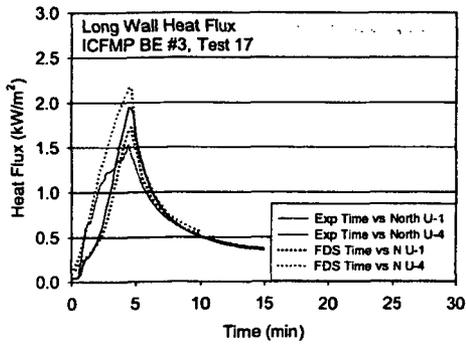
Open Door Tests to Follow
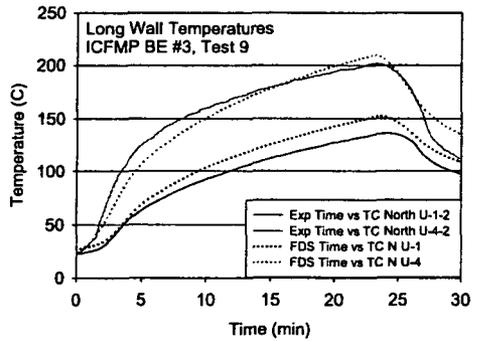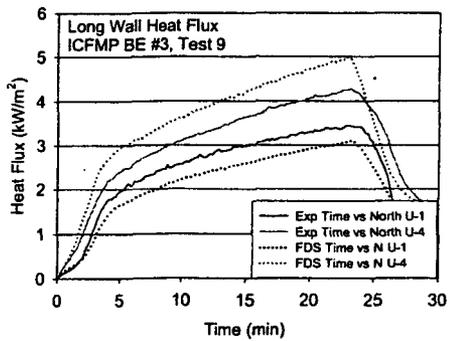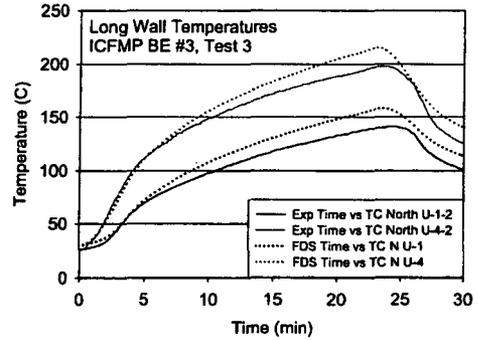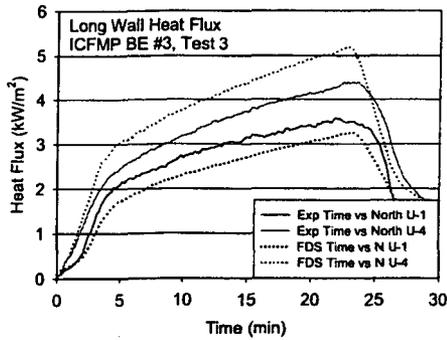
Figure A-68: Long-Wall Heat Flux and Surface Temperature, ICFMP BE #3, Closed-Door Tests
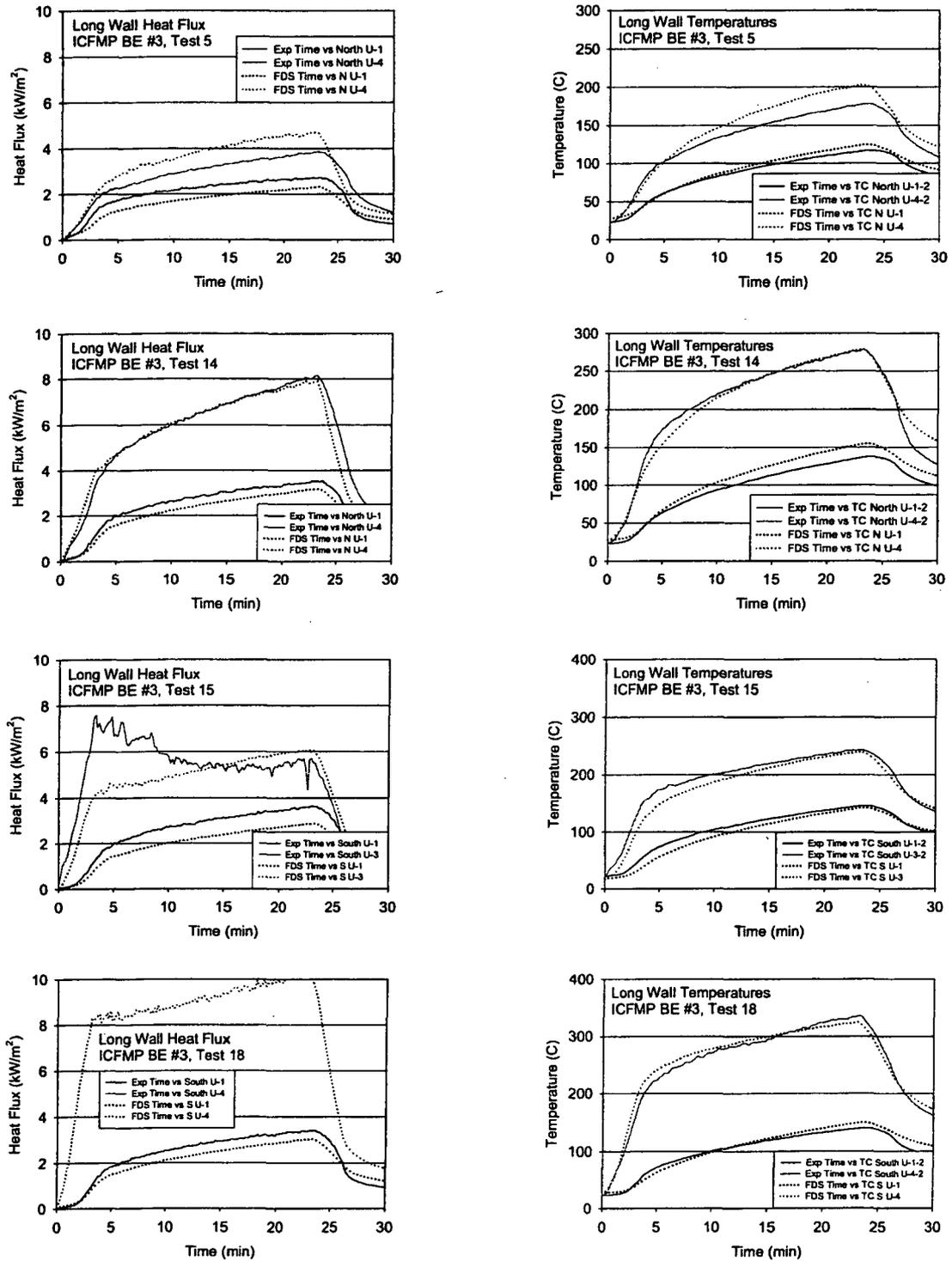
Figure A-69: Long-Wall Heat Flux and Surface Temperature, ICFMP BE #3, Open-Door Tests
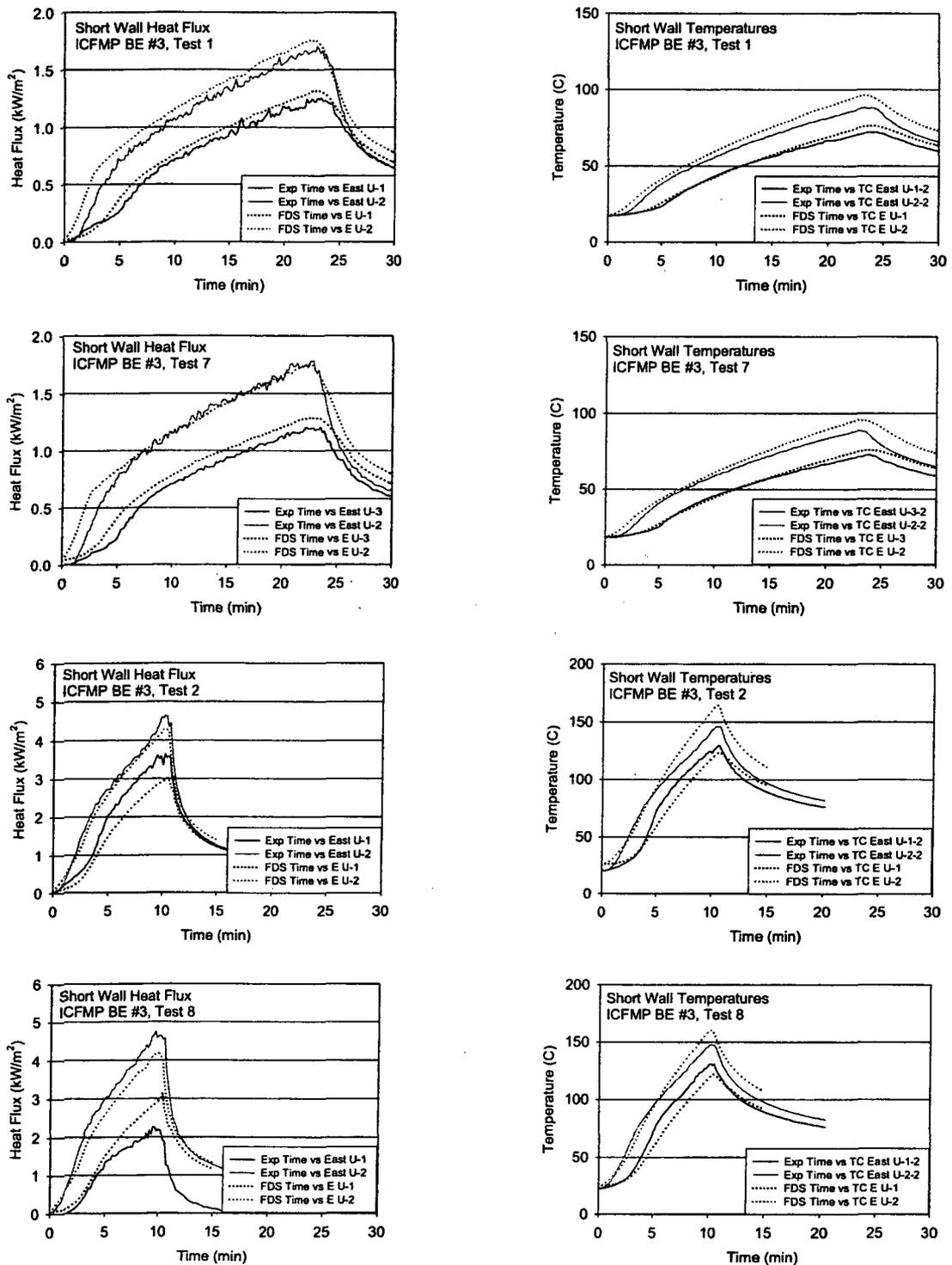
Figure A-70: Short-Wall Heat Flux and Surface Temperature, ICFMP BE #3, Closed-Door Tests
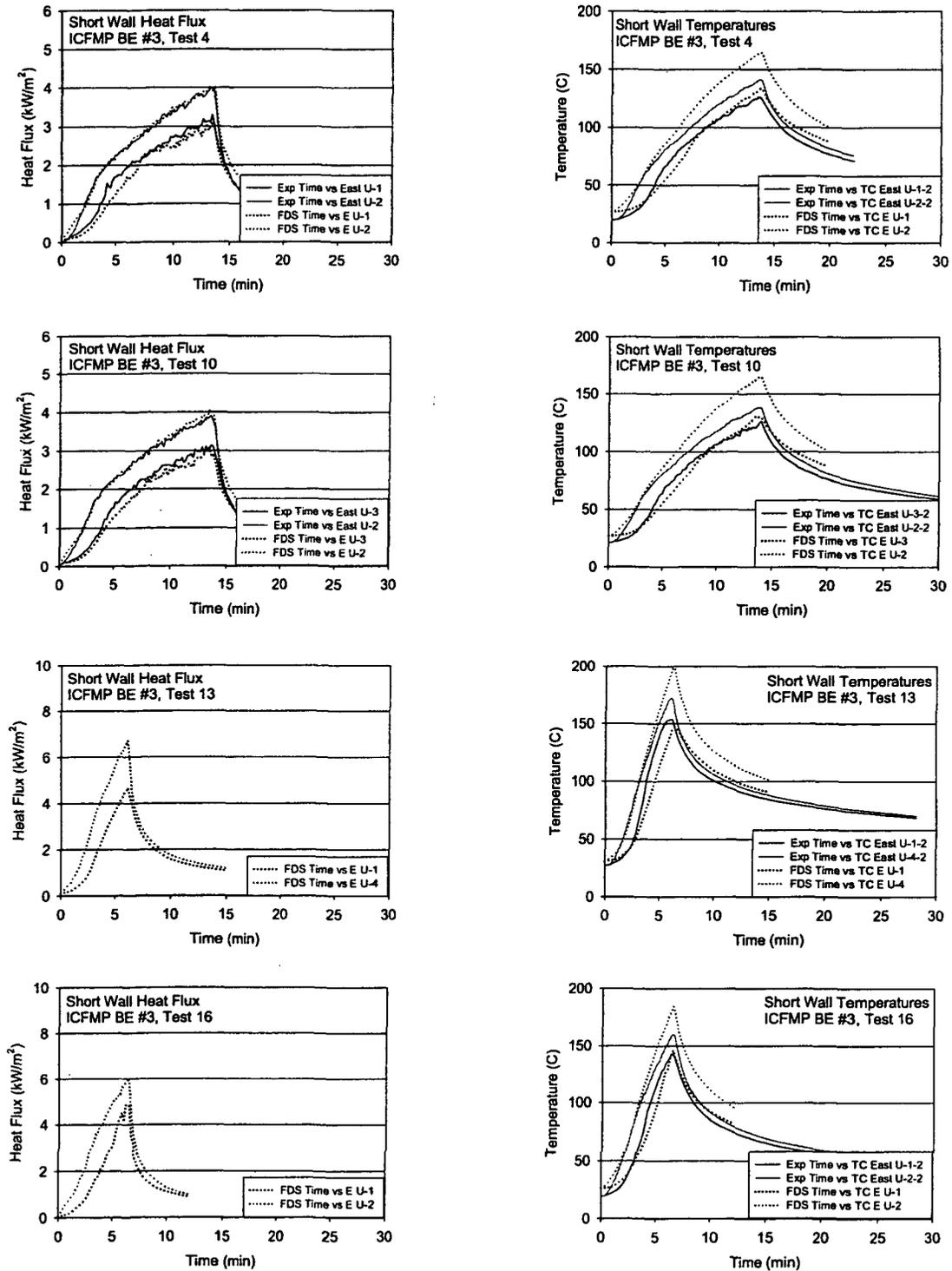
Figure A-71: Short-Wall Heat Flux and Surface Temperature, ICFMP BE #3, Closed-Door Tests
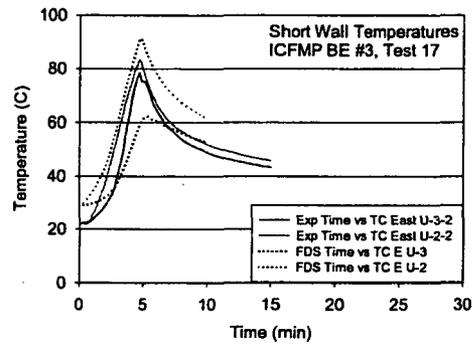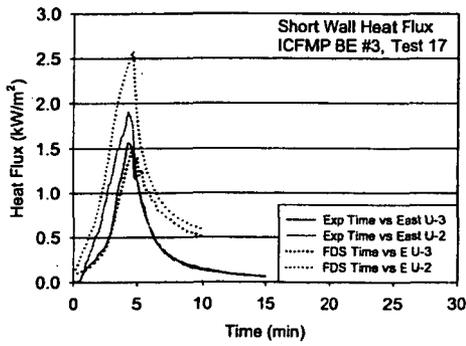
Open Door Tests to Follow
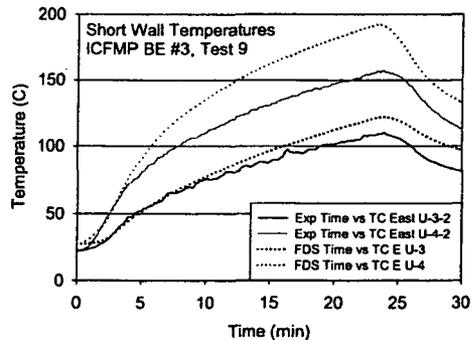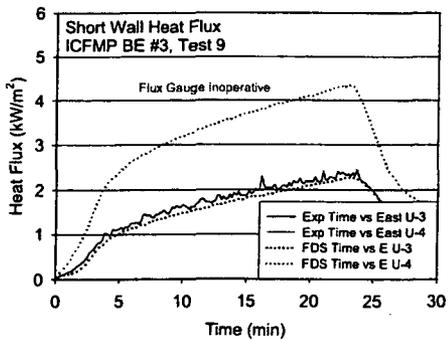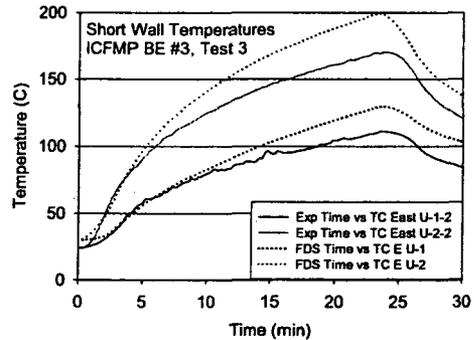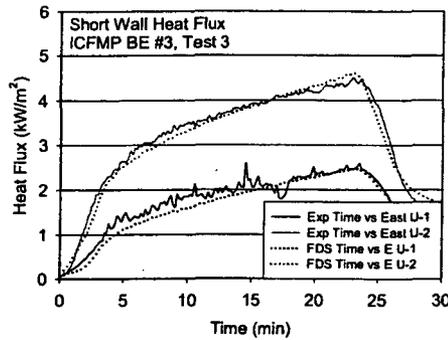
Figure A-72: Short-Wall Heat Flux and Surface Temperature, ICFMP BE #3, Open-Door Tests
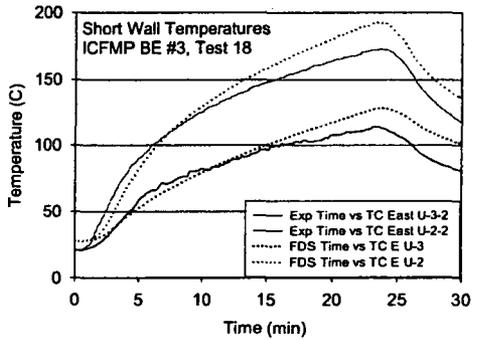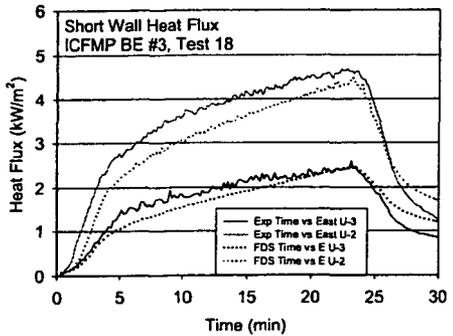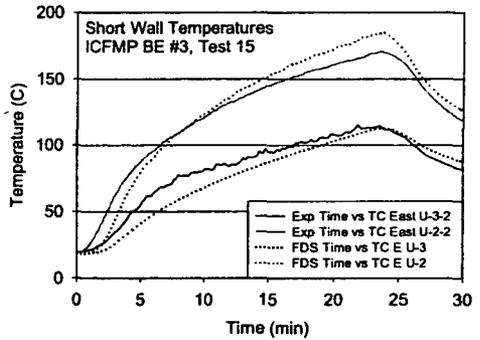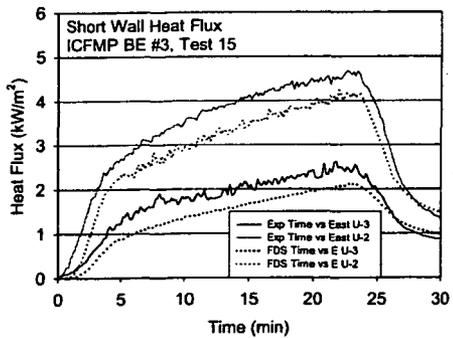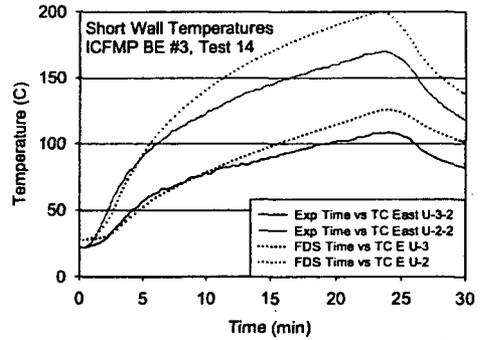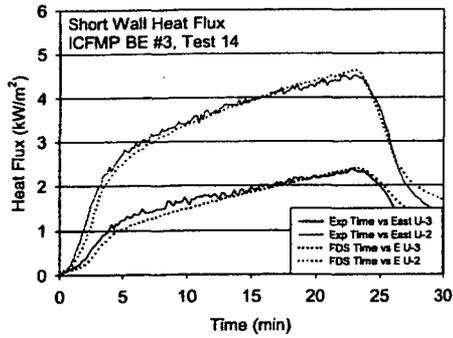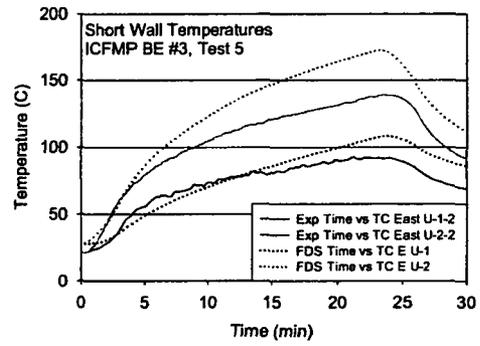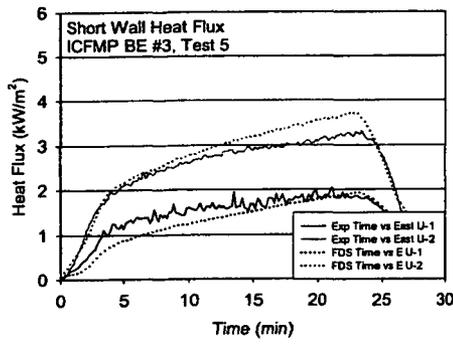
Figure A-73: Short-Wall Heat Flux and Surface Temperature, ICFMP BE #3, Open-Door Tests
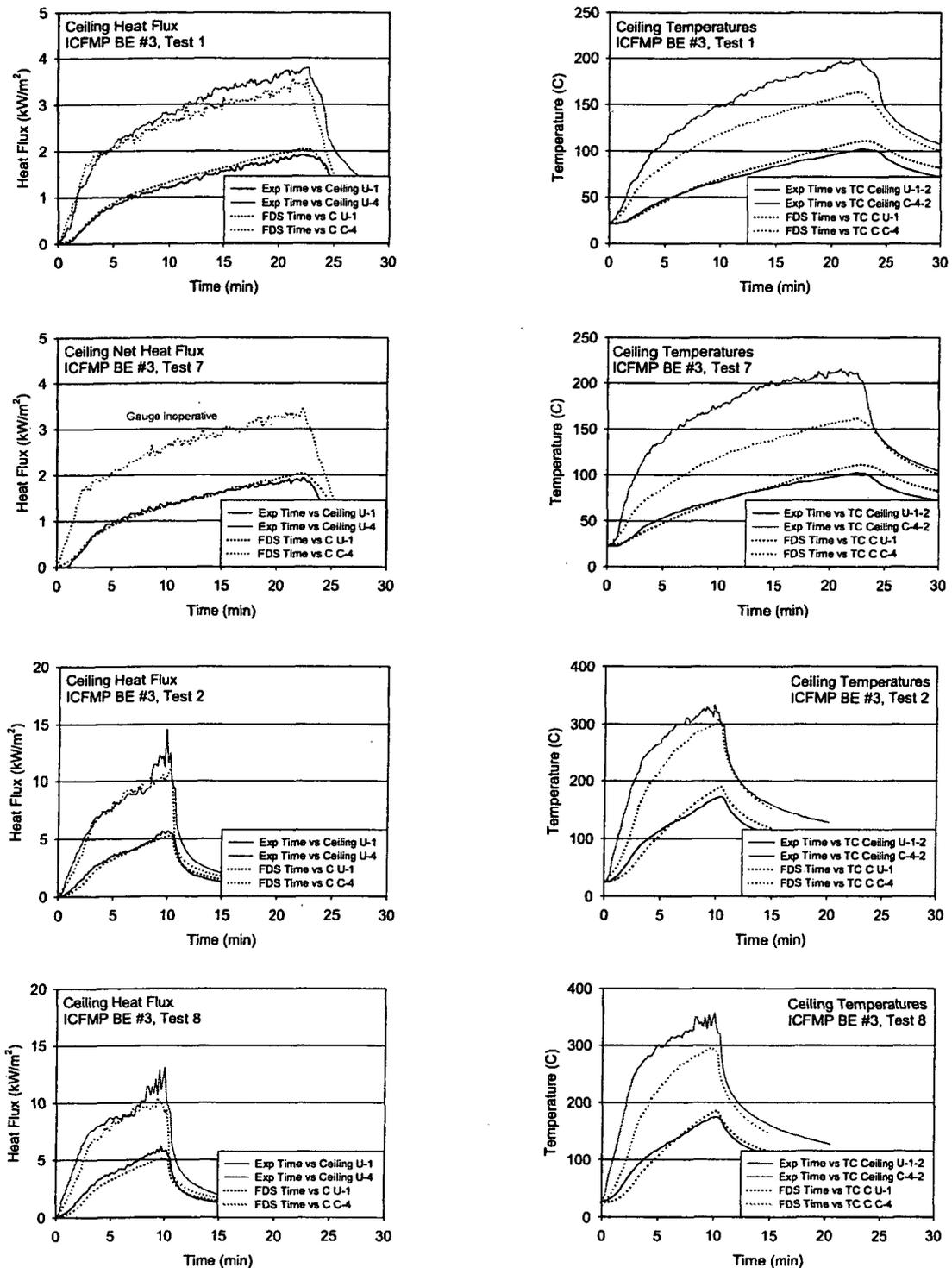
Figure A-74: Ceiling Heat Flux and Surface Temperature, ICFMP BE #3, Closed-Door Tests
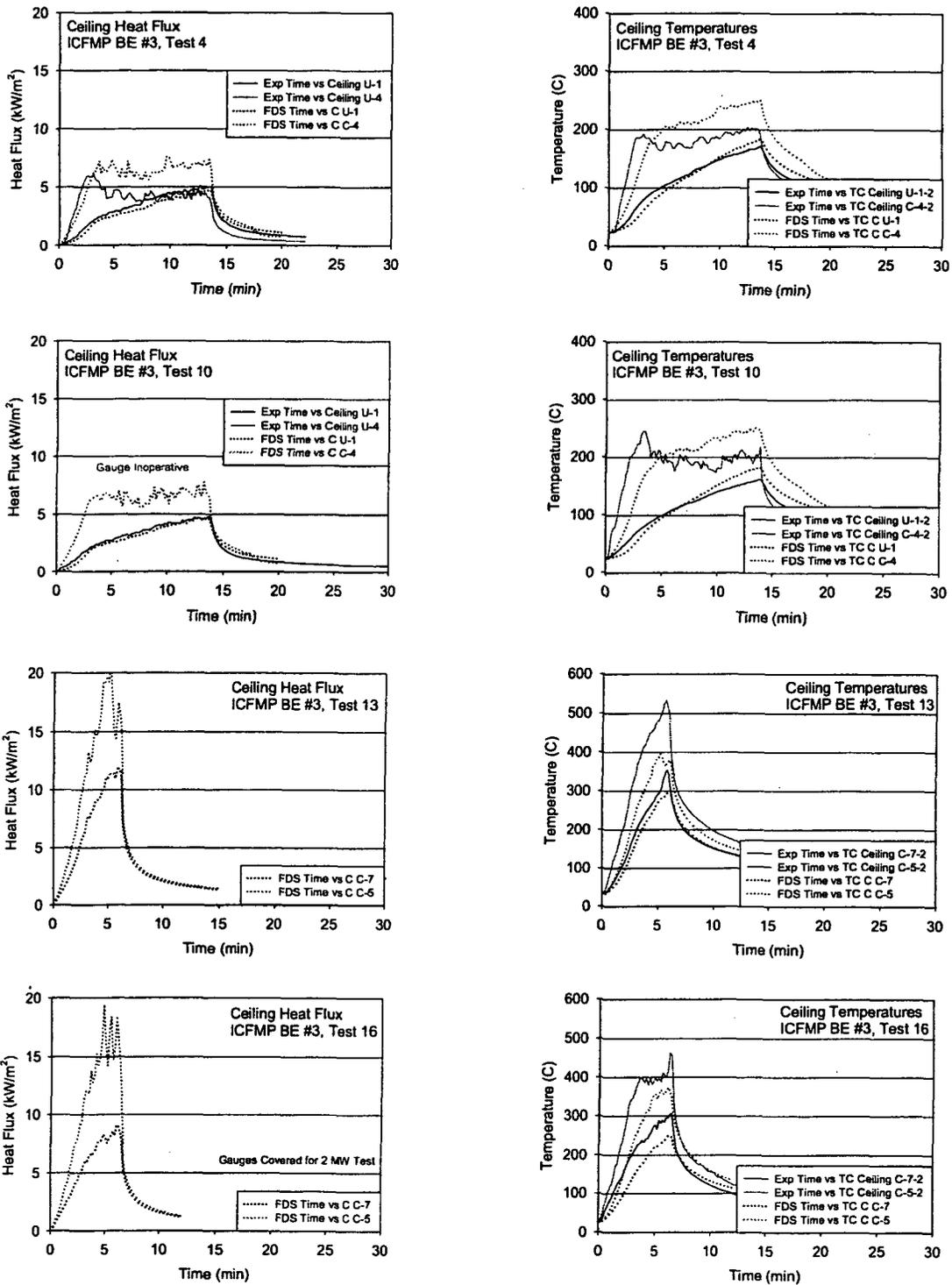
Figure A-75: Ceiling Heat Flux and Surface Temperature, ICFMP BE #3, Closed-Door Tests
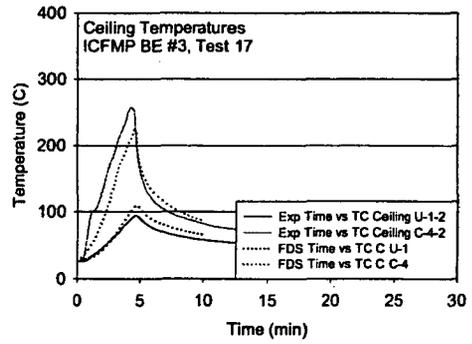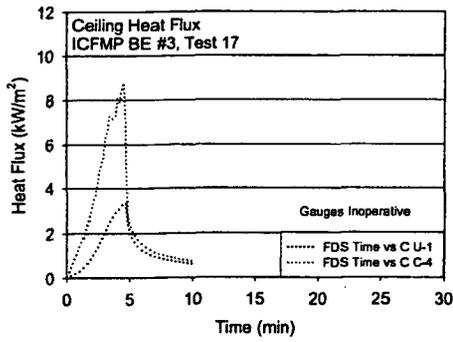
Open Door Tests to Follow
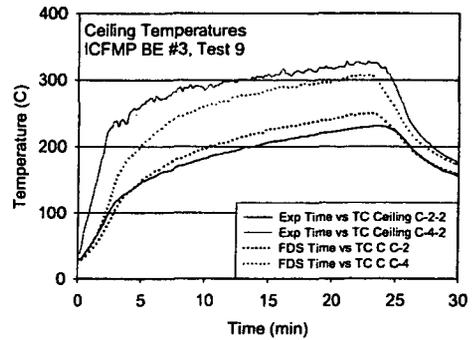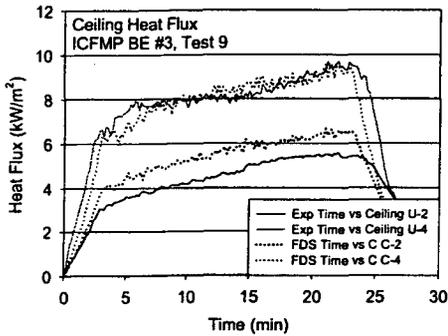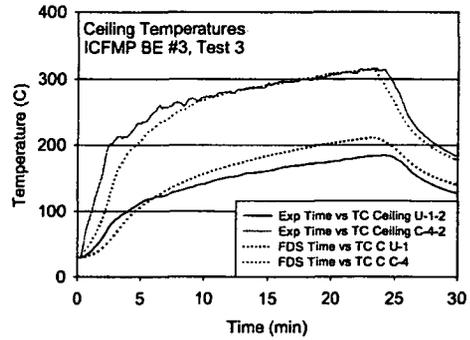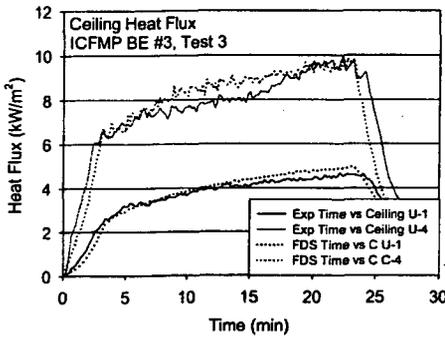
Figure A-76: Ceiling Heat Flux and Surface Temperature, ICFMP BE #3, Open-Door Tests
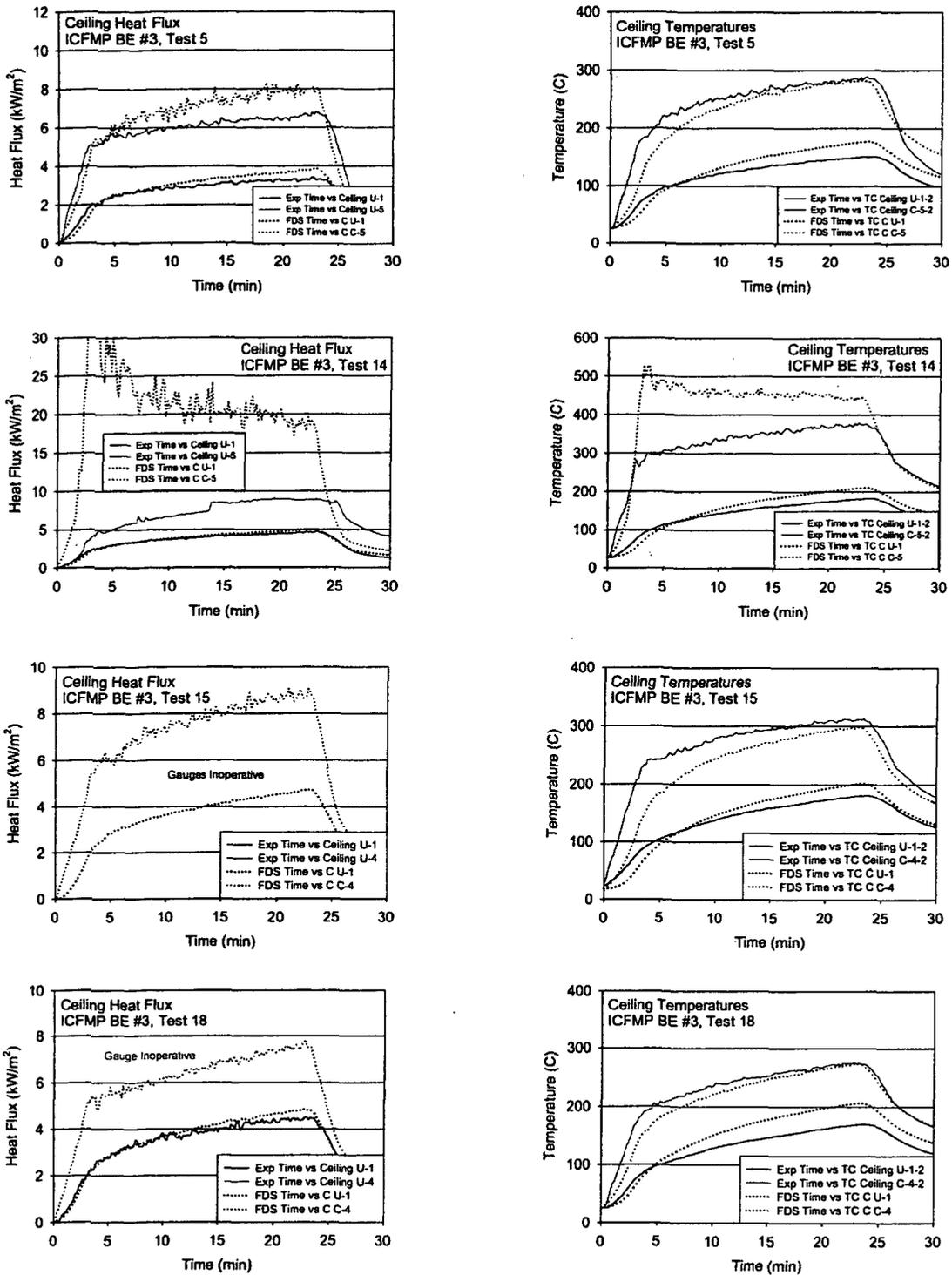
Figure A-77: Ceiling Heat Flux and Surface Temperature, ICFMP BE #3, Open-Door Tests
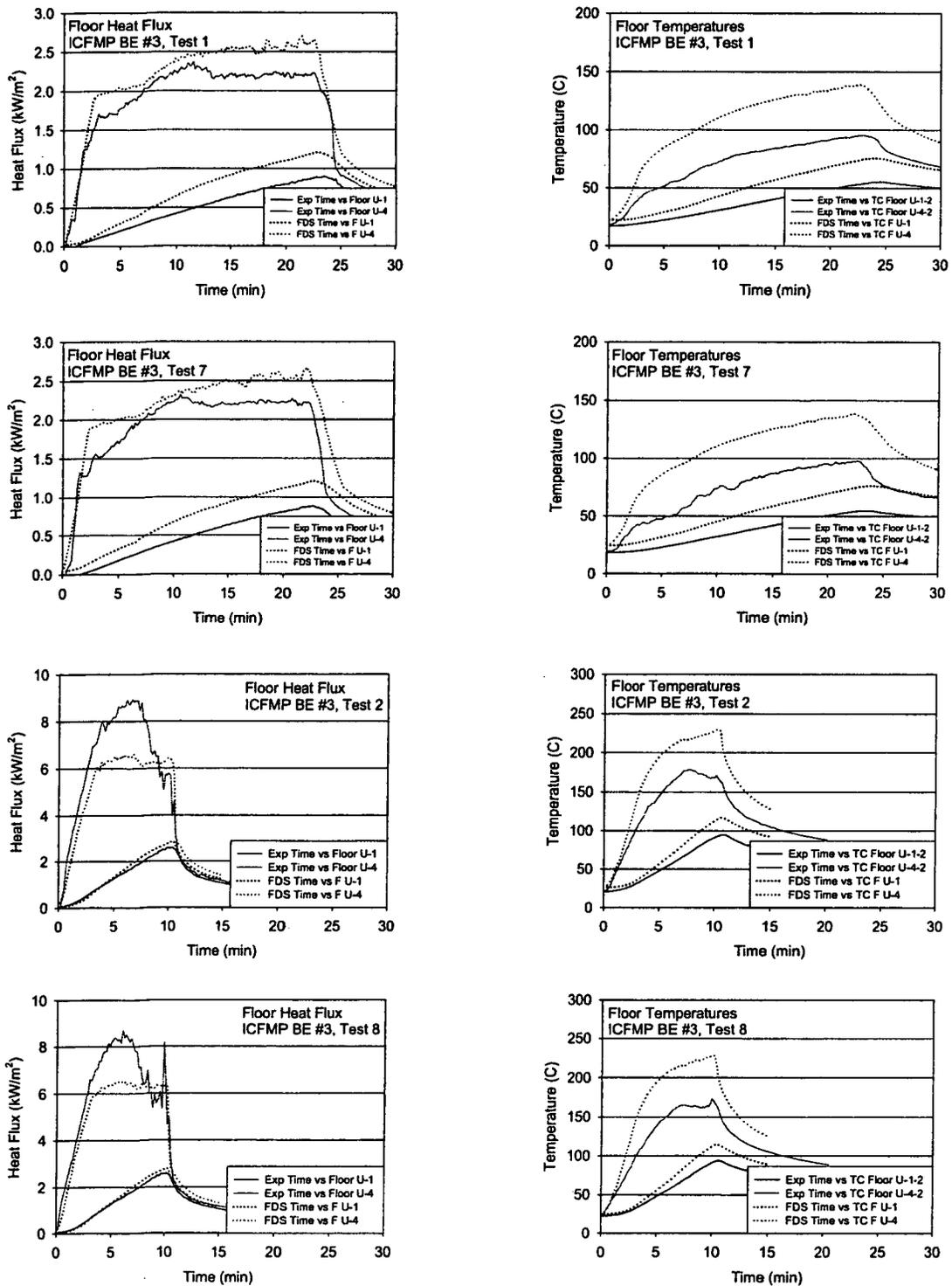
Figure A-78: Floor Heat Flux and Surface Temperature, ICFMP BE #3, Closed-Door Tests
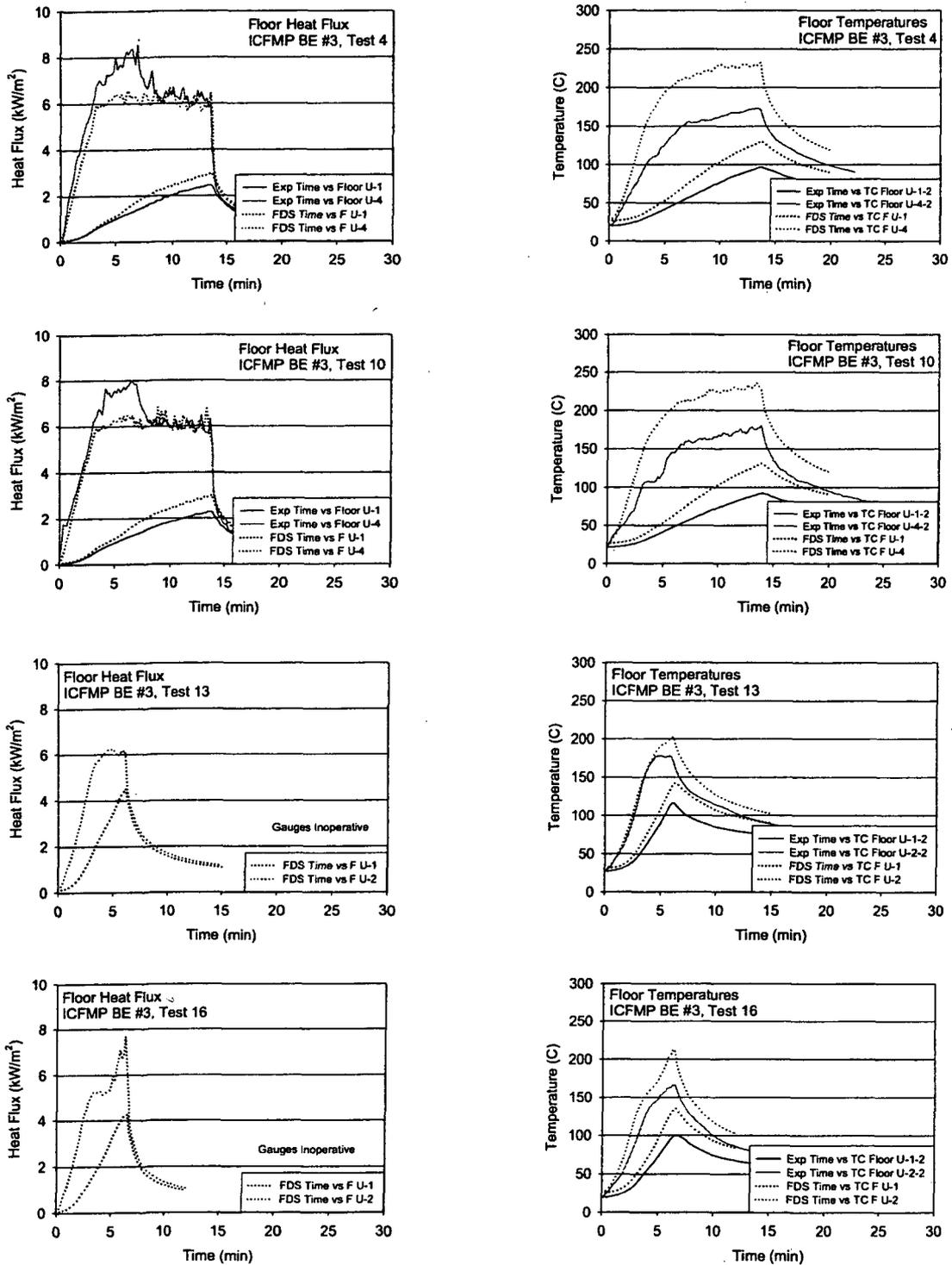
Figure A-79: Floor Heat Flux and Surface Temperature, ICFMP BE #3, Closed-Door Tests
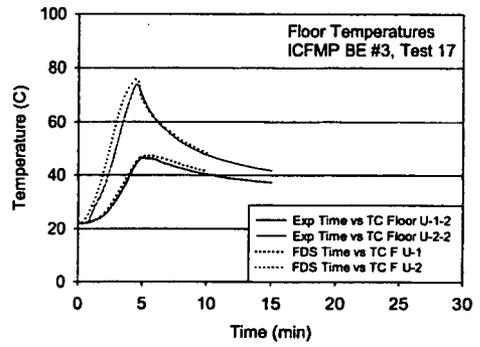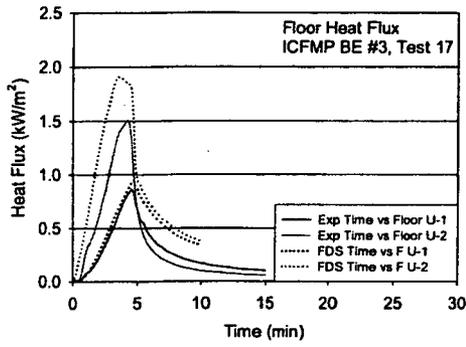
Open Door Tests to Follow
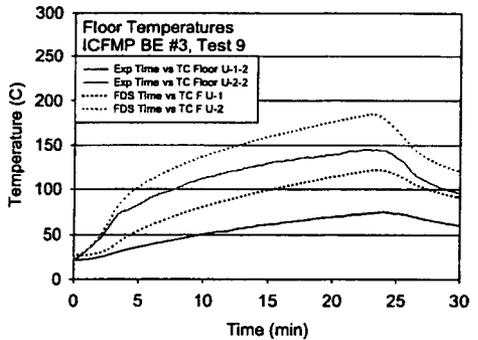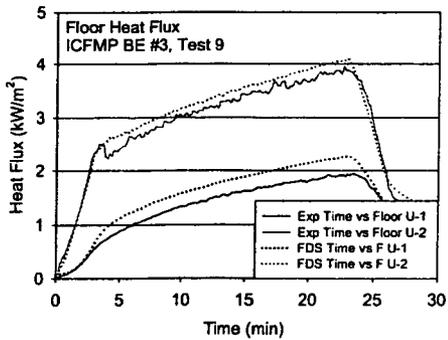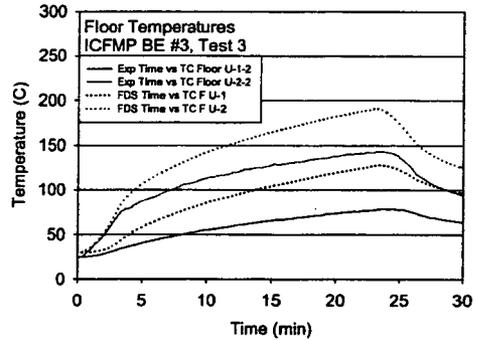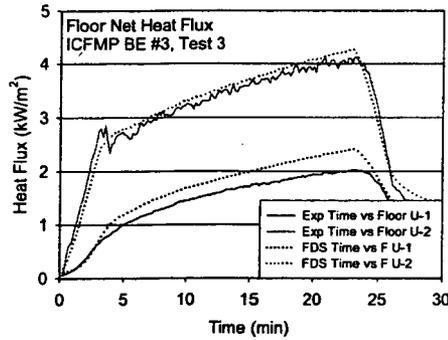
Figure A-80: Floor Heat Flux and Surface Temperature, ICFMP BE #3, Open-Door Tests
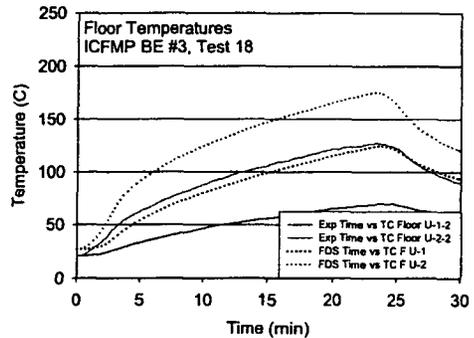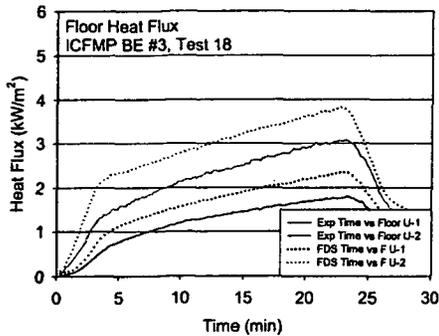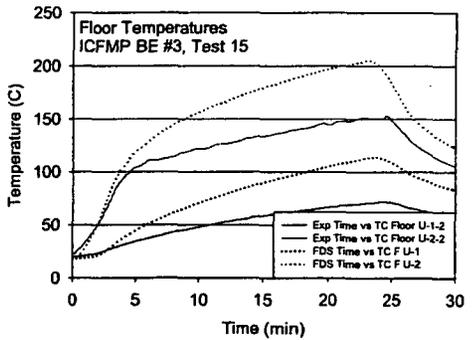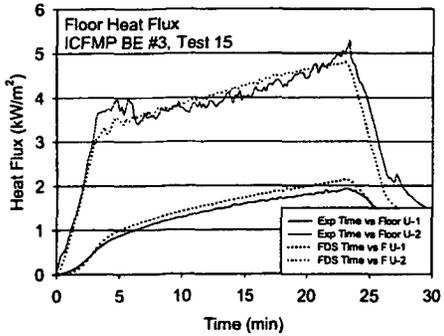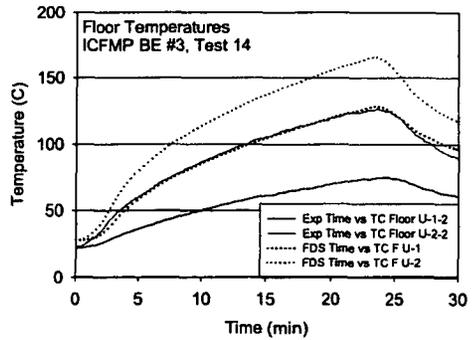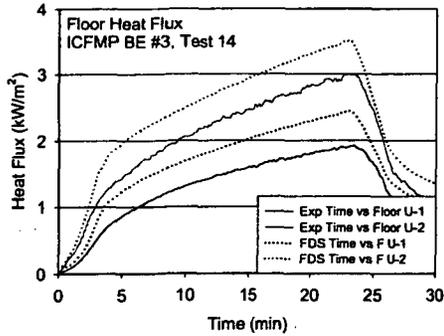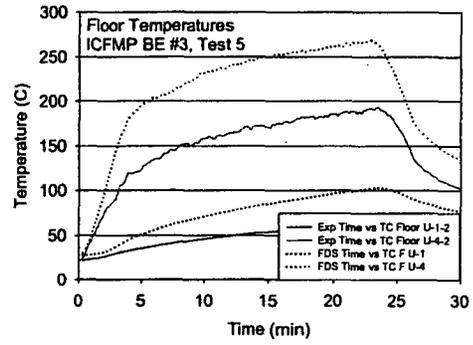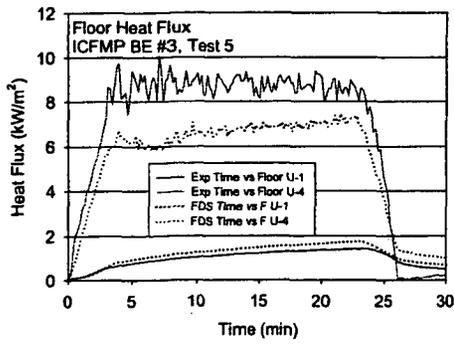
Figure A-81: Floor Heat Flux and Surface Temperature, ICFMP BE #3, Open-Door Tests

ICFMP BE #4

Three thermocouples were positioned on the back wall of the compartment. Because the fire leaned toward the back wall, the temperatures measured by the thermocouples are considerably hotter than most of the other wall surface points considered in this report.
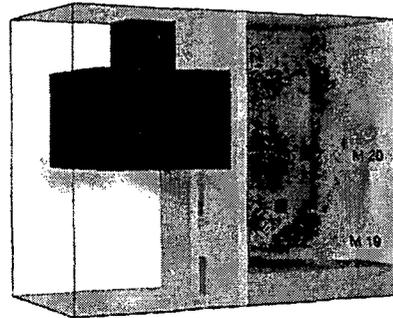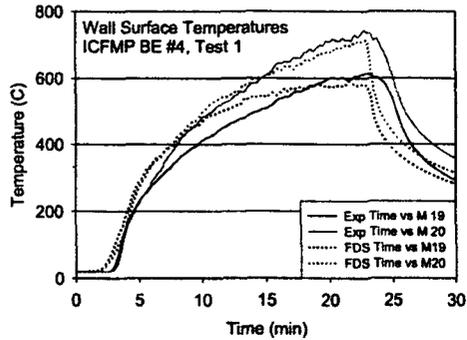
Figure A-82: Back Wall Surface Temperatures, ICFMP BE #4, Test 1
(Note that the smoke has been artificially lightened in the picture on the right.)

ICFMP BE #5

Wall surface temperatures were measured in two locations in the BE #5 test series.
The thermocouples labeled TW 1-x (Wall Chain 1) were against the back wall; those labeled TW 2-x (Wall Chain 2) were behind the vertical cable tray. Seven thermocouples were in each chain, spaced 80 cm (31.5 inches) apart. In Figure A-84, the lowest (1), middle (4), and highest (7) locations are used for comparison. Nearby gas temperature comparisons have been added for reference.
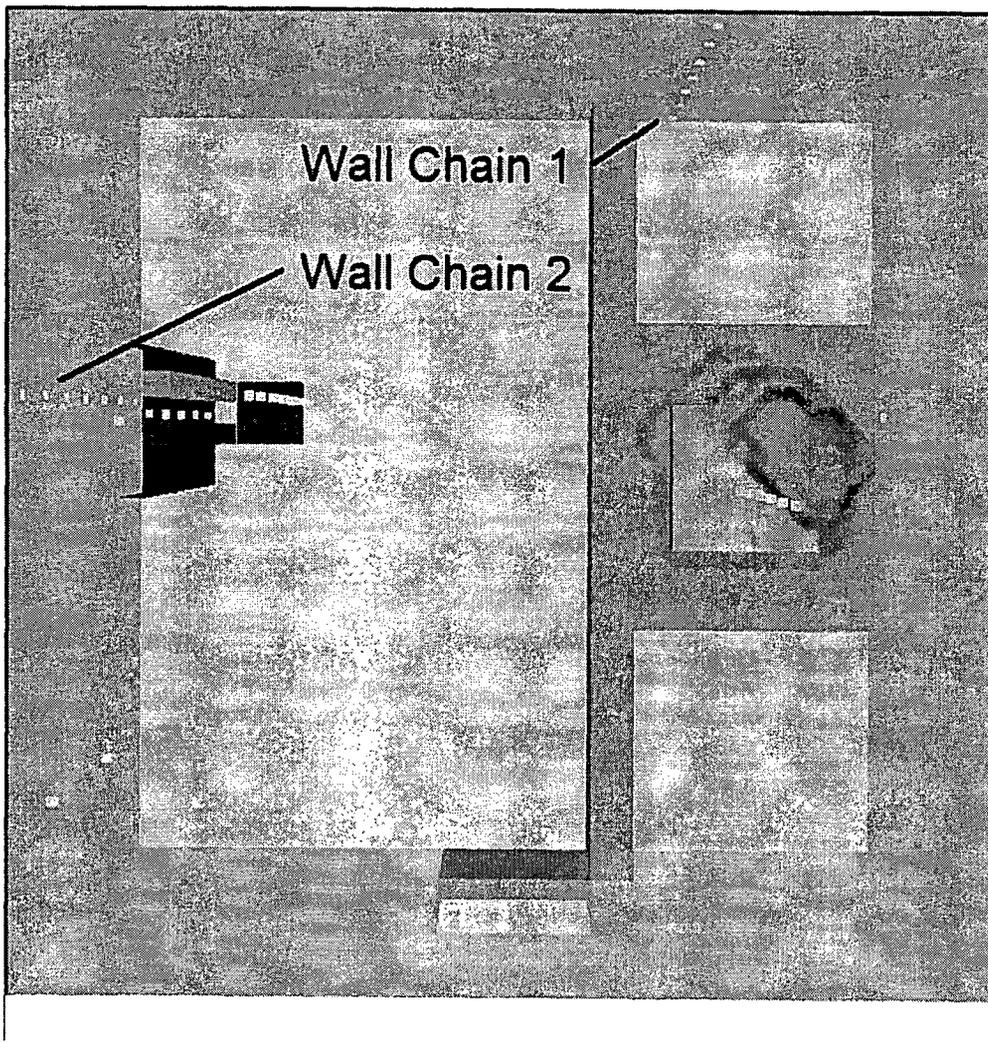
Figure A-83: Top View of Compartment, ICFMP BE #5, Test 4
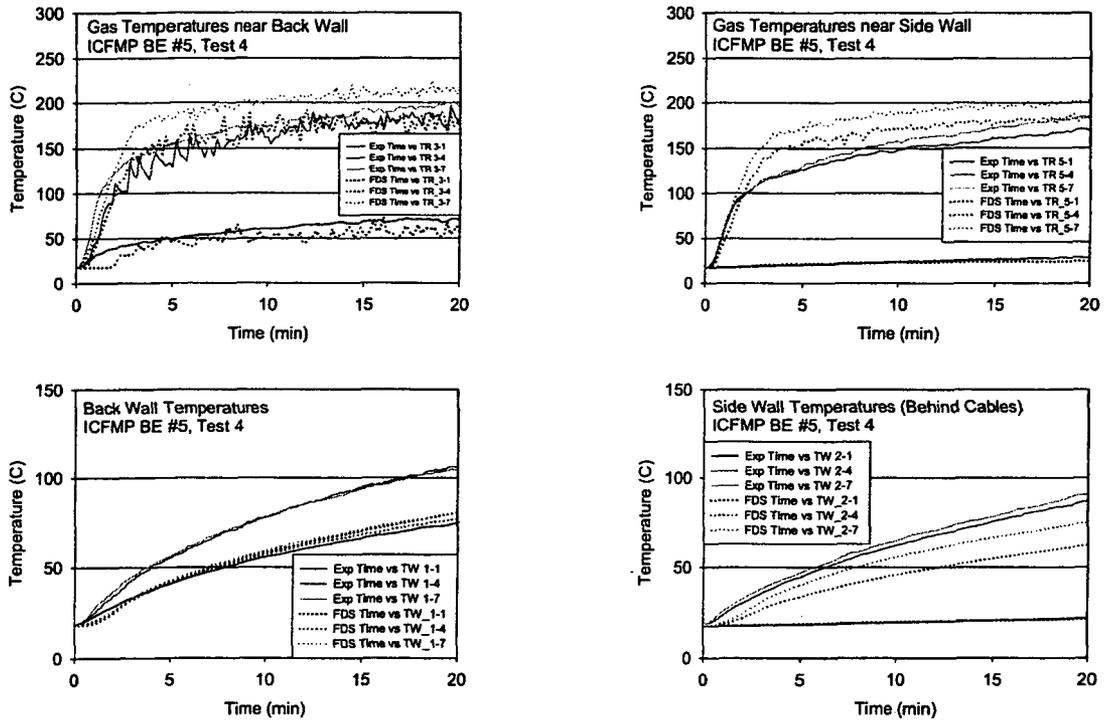
Figure A-84: Back and Side Wall Surface Temperatures, ICFMP BE #5, Test 4

Table A-8: Summary of Wall Heat Flux and Surface Temperature

			Total Heat Flux			Surface Temperature Rise		
			ΔE (kW/m²)	ΔM (kW/m²)	Diff. (%)	ΔE (°C)	ΔM (°C)	Diff. (%)
BE #3	Test 1	Long Wall, Far (N1)	1.38	1.43	3	54	66	21
		Long Wall, Near (S4)	1.77	1.66	-6	68	75	11
		Short Wall, Low (E1)	1.26	1.30	3	55	59	6
		Short Wall, High (E2)	1.72	1.74	1	71	79	11
		Floor, Far (F1)	0.92	1.19	28	38	53	40
		Floor, Near (F4)	2.38	2.68	12	77	117	51
		Ceiling, Far (C1)	1.93	2.04	6	81	89	11
		Ceiling, Near (C4)	3.75	3.53	-6	176	142	-19
	Test 7	Long Wall, Far (N1)	1.38	1.41	2	53	64	20
		Long Wall, Near (S4)	1.88	1.62	-14	70	74	5
		Short Wall, Low (E3)	1.22	1.25	2	55	57	5
		Short Wall, High (E2)	1.79	1.71	-4	70	77	9
		Floor, Far (F1)	0.90	1.17	29	36	52	44
		Floor, Near (F4)	2.32	2.63	13	78	114	46
		Ceiling, Far (C1)	1.94	2.00	3	80	87	9
		Ceiling, Near (C4)	–	3.43	–	191	138	-28
	Test 2	Long Wall, Far (N1)	3.78	3.33	-12	96	110	15
		Long Wall, Near (S4)	4.51	3.85	-15	120	131	9
		Short Wall, Low (E1)	3.62	2.95	-19	110	98	-11
		Short Wall, High (E2)	4.62	4.24	-8	125	138	10
		Floor, Far (F1)	2.59	2.78	7	74	91	23
		Floor, Near (F4)	8.90	6.54	-27	156	203	30
		Ceiling, Far (C1)	5.65	5.18	-8	148	163	11
		Ceiling, Near (C4)	14.51	11.05	-24	308	281	-9
	Test 8	Long Wall, Far (N1)	3.84	3.25	-15	95	108	14
		Long Wall, Near (N4)	3.26	4.20	29	132	140	6
		Short Wall, Low (E1)	2.46	3.07	25	109	97	-11
		Short Wall, High (E2)	4.70	4.12	-12	125	135	8
		Floor, Far (F1)	2.56	2.75	8	71	89	26
		Floor, Near (F4)	8.63	6.49	-25	148	203	37
		Ceiling, Far (C1)	6.14	5.09	-17	148	161	9
		Ceiling, Near (C4)	12.92	10.37	-20	325	270	-17
	Test 4	Long Wall, Far (N1)	3.41	3.36	-1	97	118	22
		Long Wall, Near (N4)	3.51	3.92	12	146	141	-3
		Short Wall, Low (E1)	3.26	2.99	-8	106	106	0
		Short Wall, High (E2)	3.97	3.92	-1	121	137	14
		Floor, Far (F1)	2.47	2.91	18	76	103	35
		Floor, Near (F4)	8.51	6.61	-22	152	205	35
		Ceiling, Far (C1)	5.08	4.63	-9	147	157	6
		Ceiling, Near (C4)	6.02	7.55	25	180	224	24
	Test 10	Long Wall, Far (N1)	3.35	3.35	0	94	119	26
		Long Wall, Near (N4)	3.48	4.01	15	163	142	-13
		Short Wall, Low (E3)	3.12	2.98	-5	106	104	-2
		Short Wall, High (E2)	3.88	3.99	3	117	138	18
		Floor, Far (F1)	2.27	2.94	29	71	104	46
		Floor, Near (F4)	7.89	6.78	-14	158	209	32
		Ceiling, Far (C1)	4.79	4.63	-3	138	156	13

		Total Heat Flux			Surface Temperature Rise		
		ΔE (kW/m²)	ΔM (kW/m²)	Diff. (%)	ΔE (°C)	ΔM (°C)	Diff. (%)
	Ceiling, Near (C4)	--	7.68	--	221	225	2
Test 13	Long Wall, Far (N1)	--	5.22	--	110	134	21
	Long Wall, Near (N4)	--	6.78	--	199	183	-8
	Short Wall, Low (E1)	--	4.56	--	127	116	-8
	Short Wall, High (E4)	--	6.61	--	145	168	16
	Floor, Far (F1)	--	4.41	--	89	112	25
	Floor, Near (F2)	--	6.14	--	149	171	15
	Ceiling, Far (C7)	--	11.83	--	319	269	-16
	Ceiling, Near (C5)	--	20.54	--	498	365	-27
Test 16	Long Wall, Far (N1)	--	5.02	--	107	131	23
	Long Wall, Near (N4)	--	7.00	--	217	185	-15
	Short Wall, Low (E1)	--	4.78	--	123	120	-2
	Short Wall, High (E2)	--	5.96	--	141	158	12
	Floor, Far (F1)	--	4.19	--	80	110	37
	Floor, Near (F2)	--	7.61	--	146	187	28
	Ceiling, Far (C7)	--	9.04	--	284	223	-21
	Ceiling, Near (C5)	--	19.34	--	441	348	-21
Test 17	Long Wall, Far (N1)	1.46	1.63	11	39	40	4
	Long Wall, Near (N4)	0.93	2.08	124	82	57	-31
	Short Wall, Low (E3)	1.56	1.42	-9	56	33	-41
	Short Wall, High (E2)	1.90	2.48	31	61	62	2
	Floor, Far (F1)	0.86	0.95	11	24	25	3
	Floor, Near (F2)	1.50	1.91	28	52	54	5
	Ceiling, Far (C1)	--	3.25	--	69	81	17
	Ceiling, Near (C4)	--	8.68	--	230	195	-15
Test 3	Long Wall, Far (N1)	3.50	3.15	-10	114	128	12
	Long Wall, Near (N4)	4.32	5.09	18	172	186	8
	Short Wall, Low (E1)	2.53	2.36	-7	87	100	14
	Short Wall, High (E2)	4.45	4.50	1	146	169	16
	Floor, Far (F1)	1.97	2.31	17	54	98	83
	Floor, Near (F2)	4.07	4.17	2	119	161	36
	Ceiling, Far (C1)	4.62	4.85	5	155	181	16
	Ceiling, Near (C4)	9.88	9.73	-1	287	285	-1
Test 9	Long Wall, Far (N1)	3.42	3.02	-11	113	125	11
	Long Wall, Near (N4)	4.20	4.90	17	178	183	3
	Short Wall, Low (E3)	2.42	2.21	-9	88	95	8
	Short Wall, High (E4)	--	4.29	--	135	165	23
	Floor, Far (F1)	1.91	2.21	15	53	95	79
	Floor, Near (F2)	3.89	4.03	4	122	158	30
	Ceiling, Far (C2)	5.45	6.57	21	203	223	10
	Ceiling, Near (C4)	9.41	9.48	1	290	282	-3
Test 5	Long Wall, Far (N1)	2.68	2.24	-16	94	97	3
	Long Wall, Near (N4)	3.81	4.66	22	155	175	13
	Short Wall, Low (E1)	2.00	1.84	-8	71	80	12
	Short Wall, High (E2)	3.29	3.62	10	118	145	23
	Floor, Far (F1)	1.40	1.67	19	42	75	79
	Floor, Near (F4)	10.06	7.36	-27	171	241	41
	Ceiling, Far (C1)	3.37	3.77	12	125	150	19
	Ceiling, Near (C5)	6.74	8.25	22	263	256	-3

			Total Heat Flux			Surface Temperature Rise		
			ΔE (kW/m²)	ΔM (kW/m²)	Diff. (%)	ΔE (°C)	ΔM (°C)	Diff. (%)
Test 14		Long Wall, Far (N1)	3.50	3.08	-12	114	127	11
		Long Wall, Near (N4)	8.10	7.82	-3	255	251	-1
		Short Wall, Low (E3)	2.35	2.30	-2	87	98	13
		Short Wall, High (E2)	4.47	4.54	2	148	172	17
		Floor, Far (F1)	1.89	2.37	25	52	101	93
		Floor, Near (F2)	2.97	3.42	15	104	138	33
		Ceiling, Far (C1)	4.69	4.94	5	158	183	16
		Ceiling, Near (C5)	8.99	41.91	366	352	499	42
Test 15		Long Wall, Far (S1)	3.64	2.90	-20	124	124	0
		Long Wall, Near (S3)	7.46	6.13	-18	220	221	1
		Short Wall, Low (E3)	2.61	2.14	-18	96	95	-2
		Short Wall, High (E2)	4.65	4.27	-8	151	167	10
		Floor, Far (F1)	1.95	2.16	11	52	96	83
		Floor, Near (F2)	5.23	4.85	-7	132	187	42
		Ceiling, Far (C1)	--	4.75	--	157	184	18
		Ceiling, Near (C4)	--	9.10	--	287	281	-2
Test 18		Long Wall, Far (S1)	3.40	2.96	-13	118	123	4
		Long Wall, Near (S4)	--	10.19	--	312	298	-5
		Short Wall, Low (E3)	2.58	2.39	-8	94	101	7
		Short Wall, High (E2)	4.67	4.40	-6	153	166	9
		Floor, Far (F1)	1.79	2.27	27	50	97	96
		Floor, Near (F2)	3.06	3.75	23	107	149	39
		Ceiling, Far (C1)	4.48	4.76	6	145	180	24
		Ceiling, Near (C4)	--	7.68	--	250	248	-1

			Wall Temperature Rise			Wall Temperature Rise		
			ΔE (°C)	ΔM (°C)	Diff. (%)	Exp. (°C)	FDS (°C)	Diff. (%)
BE #4 Test 1		M 19; M 20	596	573	-4	722	695	-4
BE #5	Test 4	TW 1-1; TW 2-1	56	62	11	4	4	-18
		TW 1-4; TW 2-4	87	59	-32	68	44	-35
		TW 1-7; TW 2-7	86	63	-27	72	57	-21
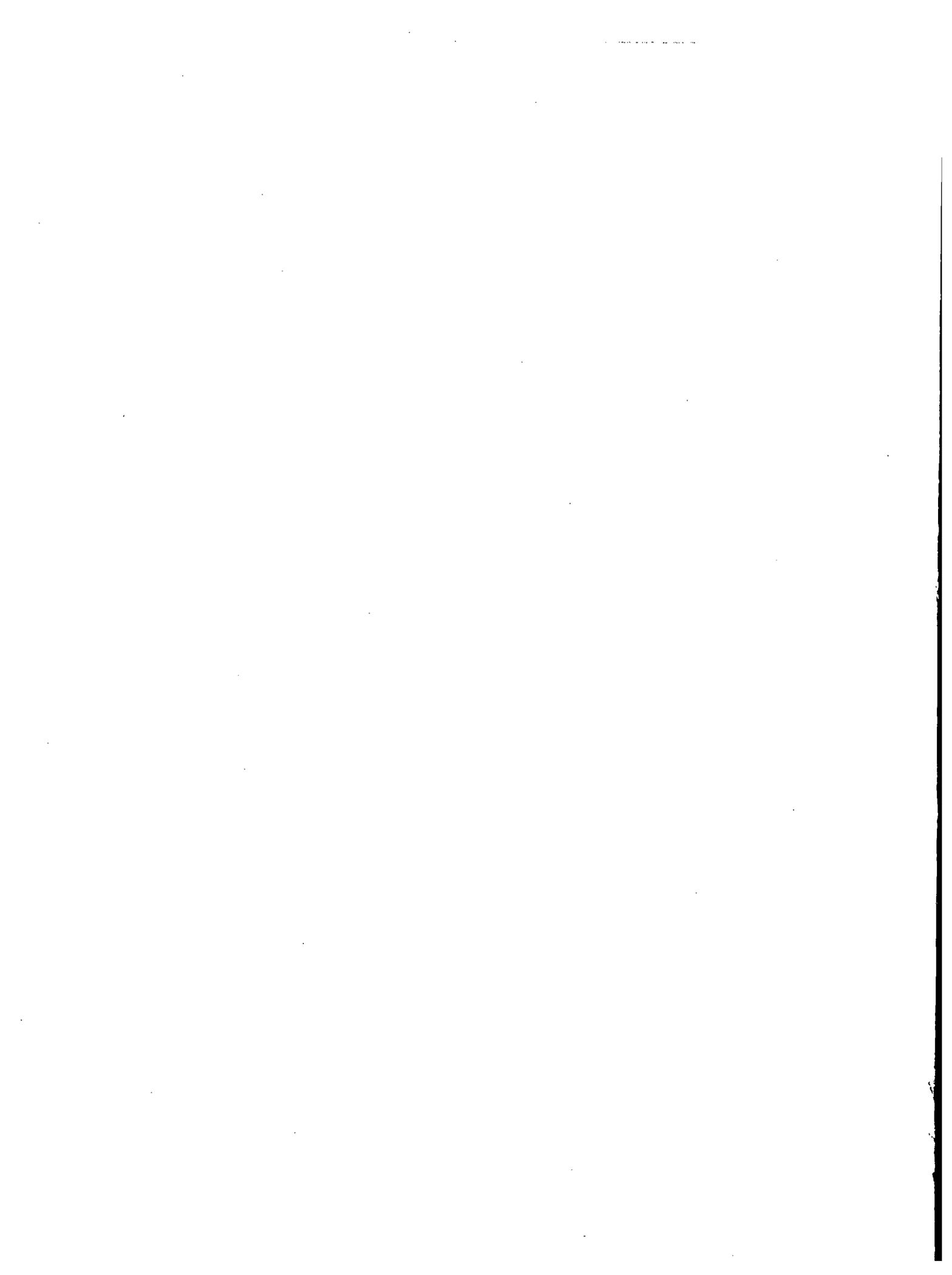
B
FDS INPUT FILES

This appendix lists the FDS input files for all six test series. For those series with multiple tests, a single input file has been compiled that contains all of the input parameters used in the entire series. The data structure used by FDS (FORTRAN NAMELIST) allows one to "comment out" unwanted input parameters by replacing the first character of the input line. For example, the fires for ICFMP BE #2 are specified by the following lines:

```
Fires for Cases 1, 2 and 3
&OBST XB=15.4,16.6,  6.6,  7.8,  0.0,  1.0,SURF_IDS='FIRE1','STEEL','STEEL' /
cOBST XB=15.2,16.8,  6.4,  8.0,  0.0,  1.0,SURF_IDS='FIRE2','STEEL','STEEL' /
cOBST XB=15.2,16.8,  6.4,  8.0,  0.0,  1.0,SURF_IDS='FIRE3','STEEL','STEEL' /
```

The "c" at the start of the last two lines, used for BE #2 Cases 2 and 3, means that these lines are currently inactive. The "&" character indicates that the line is active. Turning on fans, opening doors, selecting fires, etc., are accomplished simply by commenting the appropriate lines in or out.

Note that electronic versions of the input files are available. It is not recommended that the lines of input below be "cut and pasted" into electronic form. FDS text input files are often corrupted by characters introduced by word processing software like Microsoft Word®.

B.1   ICFMP BE #2

```
&HEAD CHID='ICFMP2_composite',TITLE='NRC Benchmark Exercise #2' /

&GRID IBAR=32,JBAR=32,KBAR=144 /
&PDIM XBAR0=14.0,XBAR=18.0,YBAR0= 5.2,YBAR= 9.2,ZBAR0= 0.0,ZBAR=19.0 /
&GRID IBAR=72,JBAR=18,KBAR=60 /
&PDIM XBAR0= 0.0,XBAR=27.0,YBAR0= 0.0,YBAR= 5.2,ZBAR0= 0.0,ZBAR=19.0 /
&GRID IBAR=72,JBAR=15,KBAR=60 /
&PDIM XBAR0= 0.0,XBAR=27.0,YBAR0= 9.2,YBAR=13.8,ZBAR0= 0.0,ZBAR=19.0 /
&GRID IBAR=48,JBAR=15,KBAR=60 /
&PDIM XBAR0= 0.0,XBAR=14.0,YBAR0= 5.2,YBAR= 9.2,ZBAR0= 0.0,ZBAR=19.0 /
&GRID IBAR=30,JBAR=15,KBAR=60 /
&PDIM XBAR0=18.0,XBAR=27.0,YBAR0= 5.2,YBAR= 9.2,ZBAR0= 0.0,ZBAR=19.0 /

&TIME TWFIN=600.,SYNCHRONIZE=.TRUE. /
&MISC REACTION='HEPTANE',SURF_DEFAULT='STEEL' /

&SURF ID='SUCK',VOLUME_FLUX=11.0,RGB=1.0,0.0,0.0 /

&SURF ID         = 'CONCRETE'
      FYI        = 'Specified in ICFMP exercise'
      DELTA      = 0.1
      C_P        = 0.90
      EMISSIVITY = 0.95
      KS         = 2.0
      RGB        = 0.7,0.7,0.7 /

&SURF ID         = 'STEEL'
      FYI        = 'Specified in ICFMP exercise'
      DELTA      = 0.001
      C_P        = 0.425
      EMISSIVITY = 0.95
      KS         = 54.
      RGB        = 0.4,0.4,0.4 /

&SURF ID='FIRE1',HRRPUA=1290.,RAMP_Q='fire1',RGB=1.0,1.0,0.0 /
&RAMP ID='fire1',T=  0.,F=0.0  /
&RAMP ID='fire1',T= 13.,F=0.67 /
&RAMP ID='fire1',T= 90.,F=0.92 /
&RAMP ID='fire1',T=288.,F=1.00 /
&RAMP ID='fire1',T=327.,F=0.96 /
&RAMP ID='fire1',T=409.,F=0.73 /
&RAMP ID='fire1',T=438.,F=0.00 /

&SURF ID='FIRE2',HRRPUA=1273.,RAMP_Q='fire2',RGB=1.0,1.0,0.0 /
&RAMP ID='fire2',T=  0.,F=0.0  /
&RAMP ID='fire2',T= 14.,F=0.66 /
&RAMP ID='fire2',T= 30.,F=0.78 /
&RAMP ID='fire2',T= 91.,F=0.94 /
&RAMP ID='fire2',T=193.,F=1.00 /
&RAMP ID='fire2',T=282.,F=0.96 /
&RAMP ID='fire2',T=340.,F=0.84 /
&RAMP ID='fire2',T=372.,F=0.07 /
&RAMP ID='fire2',T=395.,F=0.00 /

&SURF ID='FIRE3',HRRPUA=1421.,RAMP_Q='fire3',RGB=1.0,1.0,0.0 /
&RAMP ID='fire3',T=  0.,F=0.0  /
&RAMP ID='fire3',T= 13.,F=0.67 /
&RAMP ID='fire3',T= 63.,F=0.88 /
&RAMP ID='fire3',T=166.,F=0.99 /
&RAMP ID='fire3',T=256.,F=1.00 /
&RAMP ID='fire3',T=292.,F=0.95 /
&RAMP ID='fire3',T=330.,F=0.07 /
&RAMP ID='fire3',T=345.,F=0.00 /
```

```
&REAC ID='HEPTANE'
      FYI='Heptane, C_7 H_16'
      DTSAM=10.
      MW_FUEL=100.
      NU_O2=11.
      NU_CO2=7.
      NU_H2O=8.
      SOOT_YIELD=0.015 /

Fires for Cases 1, 2 and 3
&OBST XB=15.4,16.6,  6.6,  7.8, 0.0, 1.0,SURF_IDS='FIRE1','STEEL','STEEL' /
cOBST XB=15.2,16.8,  6.4,  8.0, 0.0, 1.0,SURF_IDS='FIRE2','STEEL','STEEL' /
cOBST XB=15.2,16.8,  6.4,  8.0, 0.0, 1.0,SURF_IDS='FIRE3','STEEL','STEEL' /

&OBST XB= 1.2,  6.2,  9.7,12.5, 0.0, 9.4,BLOCK_COLOR='GREEN' / Obstruction
&OBST XB=18.0,25.0,  9.7,12.5, 0.0, 4.0,BLOCK_COLOR='CYAN' /  Obstruction
&OBST XB=10.0,11.0,  6.4, 7.4,12.0,16.1,SURF_IDS='STEEL','STEEL','STEEL' /
Case 3 Ventilation
cOBST XB=10.0,11.0,  6.4, 7.4,12.0,16.1,SURF_IDS='STEEL','STEEL','SUCK' /
&OBST XB=10.0,27.0,  6.4, 7.4,16.1,17.1 / Horizontal Part of Exhaust Duct


Leakage
&VENT XB= 0.0,  0.0,  6.6,  7.2, 0.2, 1.0,SURF_ID='OPEN',VENT_COLOR='RED'   /
&VENT XB= 0.0,  0.0,  6.6,  7.2,11.8,12.4,SURF_ID='OPEN',VENT_COLOR='RED'   /
&VENT XB=27.0,27.0,  6.6,  7.2, 0.2, 1.0,SURF_ID='OPEN',VENT_COLOR='RED'   /
&VENT XB=27.0,27.0,  6.6,  7.2,11.8,12.4,SURF_ID='OPEN',VENT_COLOR='RED'   /

cVENT XB= 0.0,  0.0,  8.9,  9.7, 0.0, 4.0,SURF_ID='OPEN'    / Open Door, Case 3
cVENT XB=27.0,27.0,  8.9,  9.7, 0.0, 4.0,SURF_ID='OPEN'    / Open Door, Case 3
&VENT PBZ=0.0,SURF_ID='CONCRETE'    / Concrete Floor

&THCP XYZ=1.5,6.9,  2.0,QUANTITY='TEMPERATURE',LABEL='T1.1',DTSAM=10. /
&THCP XYZ=1.5,6.9,  4.0,QUANTITY='TEMPERATURE',LABEL='T1.2' /
&THCP XYZ=1.5,6.9,  6.0,QUANTITY='TEMPERATURE',LABEL='T1.3' /
&THCP XYZ=1.5,6.9,  8.0,QUANTITY='TEMPERATURE',LABEL='T1.4' /
&THCP XYZ=1.5,6.9,10.0,QUANTITY='TEMPERATURE',LABEL='T1.5' /
&THCP XYZ=1.5,6.9,12.0,QUANTITY='TEMPERATURE',LABEL='T1.6' /
&THCP XYZ=1.5,6.9,14.0,QUANTITY='TEMPERATURE',LABEL='T1.7' /
&THCP XYZ=1.5,6.9,16.0,QUANTITY='TEMPERATURE',LABEL='T1.8' /
&THCP XYZ=1.5,6.9,17.0,QUANTITY='TEMPERATURE',LABEL='T1.9' /
&THCP XYZ=1.5,6.9,18.0,QUANTITY='TEMPERATURE',LABEL='T1.10' /

&THCP XYZ=6.5,6.9,  2.0,QUANTITY='TEMPERATURE',LABEL='T2.1' /
&THCP XYZ=6.5,6.9,  4.0,QUANTITY='TEMPERATURE',LABEL='T2.2' /
&THCP XYZ=6.5,6.9,  6.0,QUANTITY='TEMPERATURE',LABEL='T2.3' /
&THCP XYZ=6.5,6.9,  8.0,QUANTITY='TEMPERATURE',LABEL='T2.4' /
&THCP XYZ=6.5,6.9,10.0,QUANTITY='TEMPERATURE',LABEL='T2.5' /
&THCP XYZ=6.5,6.9,12.0,QUANTITY='TEMPERATURE',LABEL='T2.6' /
&THCP XYZ=6.5,6.9,14.0,QUANTITY='TEMPERATURE',LABEL='T2.7' /
&THCP XYZ=6.5,6.9,16.0,QUANTITY='TEMPERATURE',LABEL='T2.8' /
&THCP XYZ=6.5,6.9,17.0,QUANTITY='TEMPERATURE',LABEL='T2.9' /
&THCP XYZ=6.5,6.9,18.0,QUANTITY='TEMPERATURE',LABEL='T2.10' /

&THCP XYZ=20.5,6.9,  2.0,QUANTITY='TEMPERATURE',LABEL='T3.1' /
&THCP XYZ=20.5,6.9,  4.0,QUANTITY='TEMPERATURE',LABEL='T3.2' /
&THCP XYZ=20.5,6.9,  6.0,QUANTITY='TEMPERATURE',LABEL='T3.3' /
&THCP XYZ=20.5,6.9,  8.0,QUANTITY='TEMPERATURE',LABEL='T3.4' /
&THCP XYZ=20.5,6.9,10.0,QUANTITY='TEMPERATURE',LABEL='T3.5' /
&THCP XYZ=20.5,6.9,12.0,QUANTITY='TEMPERATURE',LABEL='T3.6' /
&THCP XYZ=20.5,6.9,14.0,QUANTITY='TEMPERATURE',LABEL='T3.7' /
&THCP XYZ=20.5,6.9,16.0,QUANTITY='TEMPERATURE',LABEL='T3.8' /
&THCP XYZ=20.5,6.9,17.0,QUANTITY='TEMPERATURE',LABEL='T3.9' /
&THCP XYZ=20.5,6.9,18.0,QUANTITY='TEMPERATURE',LABEL='T3.10' /

&THCP XYZ=16.0,7.2,  7.0,QUANTITY='TEMPERATURE',LABEL='TG.1' /
&THCP XYZ=16.0,7.2,13.0,QUANTITY='TEMPERATURE',LABEL='TG.2' /

&THCP XYZ= 1.5,6.9, 2.0,QUANTITY='LAYER HEIGHT',LABEL='HGL Height 1' /
&THCP XYZ= 1.5,6.9, 2.0,QUANTITY='UPPER TEMPERATURE',LABEL='HGL Temp 1' /
&THCP XYZ= 6.5,6.9, 2.0,QUANTITY='LAYER HEIGHT',LABEL='HGL Height 2' /
&THCP XYZ= 6.5,6.9, 2.0,QUANTITY='UPPER TEMPERATURE',LABEL='HGL Temp 2' /
```

```
&THCP XYZ=20.5,6.9, 2.0,QUANTITY='LAYER HEIGHT',LABEL='HGL Height 3' /
&THCP XYZ=20.5,6.9, 2.0,QUANTITY='UPPER TEMPERATURE',LABEL='HGL Temp 3' /

&SLCF PBY=7.2,QUANTITY='TEMPERATURE',VECTOR=.TRUE. /
&SLCF PBY=7.2,QUANTITY='HRRPUV' /
&SLCF PBY=7.2,QUANTITY='MIXTURE_FRACTION' /
&SLCF PBX=16.,QUANTITY='TEMPERATURE',VECTOR=.TRUE. /
&SLCF PBX=16.,QUANTITY='HRRPUV' /
&SLCF PBX=16.,QUANTITY='MIXTURE_FRACTION' /

&BNDF QUANTITY='WALL_TEMPERATURE' /
&BNDF QUANTITY='GAUGE_HEAT_FLUX' /


Roof Approximation

&OBST XB= 0.0,27.0, 0.0, 0.3,12.1,12.4,SURF_ID='STEEL',SAWTOOTH=.FALSE. /
&OBST XB= 0.0,27.0,13.5,13.8,12.1,12.4,SURF_ID='STEEL',SAWTOOTH=.FALSE. /
&OBST XB= 0.0,27.0, 0.0, 0.5,12.4,12.7,SURF_ID='STEEL',SAWTOOTH=.FALSE. /
&OBST XB= 0.0,27.0,13.3,13.8,12.4,12.7,SURF_ID='STEEL',SAWTOOTH=.FALSE. /
&OBST XB= 0.0,27.0, 0.0, 0.8,12.7,12.9,SURF_ID='STEEL',SAWTOOTH=.FALSE. /
&OBST XB= 0.0,27.0,13.0,13.8,12.7,12.9,SURF_ID='STEEL',SAWTOOTH=.FALSE. /
&OBST XB= 0.0,27.0, 0.0, 1.0,12.9,13.2,SURF_ID='STEEL',SAWTOOTH=.FALSE. /
&OBST XB= 0.0,27.0,12.8,13.8,12.9,13.2,SURF_ID='STEEL',SAWTOOTH=.FALSE. /
&OBST XB= 0.0,27.0, 0.0, 1.3,13.2,13.5,SURF_ID='STEEL',SAWTOOTH=.FALSE. /
&OBST XB= 0.0,27.0,12.5,13.8,13.2,13.5,SURF_ID='STEEL',SAWTOOTH=.FALSE. /
&OBST XB= 0.0,27.0, 0.0, 1.5,13.5,13.7,SURF_ID='STEEL',SAWTOOTH=.FALSE. /
&OBST XB= 0.0,27.0,12.3,13.8,13.5,13.7,SURF_ID='STEEL',SAWTOOTH=.FALSE. /
&OBST XB= 0.0,27.0, 0.0, 1.8,13.7,14.0,SURF_ID='STEEL',SAWTOOTH=.FALSE. /
&OBST XB= 0.0,27.0,12.0,13.8,13.7,14.0,SURF_ID='STEEL',SAWTOOTH=.FALSE. /
&OBST XB= 0.0,27.0, 0.0, 2.0,14.0,14.3,SURF_ID='STEEL',SAWTOOTH=.FALSE. /
&OBST XB= 0.0,27.0,11.8,13.8,14.0,14.3,SURF_ID='STEEL',SAWTOOTH=.FALSE. /
&OBST XB= 0.0,27.0, 0.0, 2.3,14.3,14.5,SURF_ID='STEEL',SAWTOOTH=.FALSE. /
&OBST XB= 0.0,27.0,11.5,13.8,14.3,14.5,SURF_ID='STEEL',SAWTOOTH=.FALSE. /
&OBST XB= 0.0,27.0, 0.0, 2.6,14.5,14.8,SURF_ID='STEEL',SAWTOOTH=.FALSE. /
&OBST XB= 0.0,27.0,11.2,13.8,14.5,14.8,SURF_ID='STEEL',SAWTOOTH=.FALSE. /
&OBST XB= 0.0,27.0, 0.0, 2.8,14.8,15.0,SURF_ID='STEEL',SAWTOOTH=.FALSE. /
&OBST XB= 0.0,27.0,11.0,13.8,14.8,15.0,SURF_ID='STEEL',SAWTOOTH=.FALSE. /
&OBST XB= 0.0,27.0, 0.0, 3.1,15.0,15.3,SURF_ID='STEEL',SAWTOOTH=.FALSE. /
&OBST XB= 0.0,27.0,10.7,13.8,15.0,15.3,SURF_ID='STEEL',SAWTOOTH=.FALSE. /
&OBST XB= 0.0,27.0, 0.0, 3.3,15.3,15.6,SURF_ID='STEEL',SAWTOOTH=.FALSE. /
&OBST XB= 0.0,27.0,10.5,13.8,15.3,15.6,SURF_ID='STEEL',SAWTOOTH=.FALSE. /
&OBST XB= 0.0,27.0, 0.0, 3.6,15.6,15.8,SURF_ID='STEEL',SAWTOOTH=.FALSE. /
&OBST XB= 0.0,27.0,10.2,13.8,15.6,15.8,SURF_ID='STEEL',SAWTOOTH=.FALSE. /
&OBST XB= 0.0,27.0, 0.0, 3.8,15.8,16.1,SURF_ID='STEEL',SAWTOOTH=.FALSE. /
&OBST XB= 0.0,27.0,10.0,13.8,15.8,16.1,SURF_ID='STEEL',SAWTOOTH=.FALSE. /
&OBST XB= 0.0,27.0, 0.0, 4.1,16.1,16.4,SURF_ID='STEEL',SAWTOOTH=.FALSE. /
&OBST XB= 0.0,27.0, 9.7,13.8,16.1,16.4,SURF_ID='STEEL',SAWTOOTH=.FALSE. /
&OBST XB= 0.0,27.0, 0.0, 4.3,16.4,16.6,SURF_ID='STEEL',SAWTOOTH=.FALSE. /
&OBST XB= 0.0,27.0, 9.5,13.8,16.4,16.6,SURF_ID='STEEL',SAWTOOTH=.FALSE. /
&OBST XB= 0.0,27.0, 0.0, 4.6,16.6,16.9,SURF_ID='STEEL',SAWTOOTH=.FALSE. /
&OBST XB= 0.0,27.0, 9.2,13.8,16.6,16.9,SURF_ID='STEEL',SAWTOOTH=.FALSE. /
&OBST XB= 0.0,27.0, 0.0, 4.9,16.9,19.0,SURF_ID='STEEL',SAWTOOTH=.FALSE. /
&OBST XB= 0.0,27.0, 8.9,13.8,16.9,19.0,SURF_ID='STEEL',SAWTOOTH=.FALSE. /
```

B.2 ICFMP BE #3

```
&HEAD CHID='ICFMP3_composite',TITLE='NRC ICFMP Benchmark Exercise 3' /

Numerical grid with stretching to put finer grid over fire
&GRID IBAR=100,JBAR=36,KBAR=32 /
&PDIM XBAR=21.7,YBAR=7.04,ZBAR=3.82 /
&TRNX IDERIV=0,CC=10.8,PC=10.8 /
&TRNX IDERIV=1,CC=10.8,PC=0.5 /
&TRNY IDERIV=0,CC= 3.58,PC=3.58 / Comment out for Tests 14, 15 and 18
&TRNY IDERIV=1,CC= 3.58,PC=0.5  / Comment out for Tests 14, 15 and 18

&TIME TWFIN=1800. /

&MISC TMPA=30.,SURF_DEFAULT='MARINITE',NFRAMES=1800,REACTION='HEPTANE' /

&REAC ID='HEPTANE'
      FYI='Heptane, C_7 H_16'
      DTSAM=10.
      MW_FUEL=100.
      NU_O2=11.
      NU_CO2=7.
      NU_H2O=8.
      CO_YIELD=0.006
      SOOT_YIELD=0.015 /

cREAC ID='TOLUENE'
      FYI='Toluene, C_7 H_8, Test 17 only'
      MW_FUEL=92.
      NU_O2=9.
      NU_CO2=7.
      NU_H2O=4.
      SOOT_YIELD=0.195 /

Definitions of fan and extraction duct
&SURF ID='INFLOW' ,VOLUME_FLUX=-0.90,RGB=1,0,0,VEL_T=0.0,4.0,PARTICLES=.TRUE. /
&SURF ID='OUTFLOW',VOLUME_FLUX= 1.70,RGB=1,1,0,RAMP_V='exhaust' /
&RAMP ID='exhaust',T=  0.,F=0.0 /
&RAMP ID='exhaust',T=  1.,F=0.6 /
&RAMP ID='exhaust',T=180.,F=1.0 /
&RAMP ID='exhaust',T=400.,F=0.9 /

Definitions of cables. Note that RADIUS tells FDS to do
a 1-D heat transfer calc into a cylinder instead of a slab.
&SURF ID='PVC TRAY CONTROL',   RAMP_KS='k_pvc',RAMP_C_P='cp_pvc',DENSITY=1380.,
      EMISSIVITY=0.95,RGB=1,0,0,DELTA=0.01 /
&SURF ID='PVC SINGLE CONTROL',RAMP_KS='k_pvc',RAMP_C_P='cp_pvc',DENSITY=1380.,
      EMISSIVITY=0.95,RGB=1,0,0,RADIUS=0.005 /
&SURF ID='PVC SINGLE POWER',   RAMP_KS='k_pvc',RAMP_C_P='cp_pvc',DENSITY=1380.,
      EMISSIVITY=0.95,RGB=1,0,0,RADIUS=0.008 /
&RAMP ID='k_pvc',T= 23.,F=0.192 /
&RAMP ID='k_pvc',T= 50.,F=0.175 /
&RAMP ID='k_pvc',T= 75.,F=0.172 /
&RAMP ID='k_pvc',T=100.,F=0.147 /
&RAMP ID='k_pvc',T=125.,F=0.141 /
&RAMP ID='k_pvc',T=150.,F=0.134 /
&RAMP ID='cp_pvc',T= 23.,F=1.289 /
&RAMP ID='cp_pvc',T= 50.,F=1.353 /
&RAMP ID='cp_pvc',T= 75.,F=1.407 /
&RAMP ID='cp_pvc',T=100.,F=1.469 /
&RAMP ID='cp_pvc',T=125.,F=1.530 /
&RAMP ID='cp_pvc',T=150.,F=1.586 /

&SURF ID='XLP TRAY CONTROL',   RAMP_KS='k_xlp',RAMP_C_P='cp_xlp',DENSITY=1374.,
      EMISSIVITY=0.95,RGB=0,1,0,DELTA=0.01 /
&SURF ID='XLP SINGLE CONTROL',RAMP_KS='k_xlp',RAMP_C_P='cp_xlp',DENSITY=1374.,
```

```
        EMISSIVITY=0.95,RGB=0,1,0,RADIUS=0.005 /
&SURF ID='XLP SINGLE POWER',  RAMP_KS='k_xlp',RAMP_C_P='cp_xlp',DENSITY=1374.,
        EMISSIVITY=0.95,RGB=0,1,0,RADIUS=0.0095 /
&RAMP ID='k_xlp',T= 23.,F=0.235 /
&RAMP ID='k_xlp',T= 50.,F=0.232 /
&RAMP ID='k_xlp',T= 75.,F=0.223 /
&RAMP ID='k_xlp',T=100.,F=0.210 /
&RAMP ID='k_xlp',T=125.,F=0.190 /
&RAMP ID='k_xlp',T=150.,F=0.192 /
&RAMP ID='cp_xlp',T= 23.,F=1.390 /
&RAMP ID='cp_xlp',T= 50.,F=1.476 /
&RAMP ID='cp_xlp',T= 75.,F=1.526 /
&RAMP ID='cp_xlp',T=100.,F=1.560 /
&RAMP ID='cp_xlp',T=125.,F=1.585 /
&RAMP ID='cp_xlp',T=150.,F=1.607 /


&SURF ID                 = 'STEEL SHEET'
      RGB                = 0.20,0.20,0.20
      C_DELTA_RHO        = 28.
      BACKING            = 'EXPOSED'
      DELTA              = 0.00635 /

&SURF ID                 = 'FERALOY'
      RGB                = 0.40,0.40,0.40
      C_DELTA_RHO        = 25.
      BACKING            = 'EXPOSED'
      DELTA              = 0.007 /

&SURF ID='FIRE1',HRRPUA=410.,RGB=1,1,0,RAMP_Q='FIRE1_RAMP' /
&RAMP ID='FIRE1_RAMP',T=    0.,F=0.0 /
&RAMP ID='FIRE1_RAMP',T= 148.,F=1.0 /
&RAMP ID='FIRE1_RAMP',T=1350.,F=1.0 /
&RAMP ID='FIRE1_RAMP',T=1500.,F=0.0 /


&SURF ID='FIRE2',HRRPUA=1190.,RGB=1,1,0,RAMP_Q='FIRE2_RAMP' /
&RAMP ID='FIRE2_RAMP',T=    0.,F=0.0 /
&RAMP ID='FIRE2_RAMP',T= 180.,F=1.0 /
&RAMP ID='FIRE2_RAMP',T= 625.,F=1.0 /
&RAMP ID='FIRE2_RAMP',T= 626.,F=0.0 /


&SURF ID='FIRE3',HRRPUA=1190.,RGB=1,1,0,RAMP_Q='FIRE3_RAMP' /
&RAMP ID='FIRE3_RAMP',T=    0.,F=0.0 /
&RAMP ID='FIRE3_RAMP',T= 180.,F=1.0 /
&RAMP ID='FIRE3_RAMP',T=1380.,F=1.0 /
&RAMP ID='FIRE3_RAMP',T=1560.,F=0.0 /


&SURF ID='FIRE4',HRRPUA=1200.,RGB=1,1,0,RAMP_Q='FIRE4_RAMP' /
&RAMP ID='FIRE4_RAMP',T=    0.,F=0.0 /
&RAMP ID='FIRE4_RAMP',T= 180.,F=1.0 /
&RAMP ID='FIRE4_RAMP',T= 816.,F=1.0 /
&RAMP ID='FIRE4_RAMP',T= 817.,F=0.0 /


&SURF ID='FIRE5',HRRPUA=1190.,RGB=1,1,0,RAMP_Q='FIRE5_RAMP' /
&RAMP ID='FIRE5_RAMP',T=    0.,F=0.0 /
&RAMP ID='FIRE5_RAMP',T= 180.,F=1.0 /
&RAMP ID='FIRE5_RAMP',T=1380.,F=1.0 /
&RAMP ID='FIRE5_RAMP',T=1560.,F=0.0 /


&SURF ID='FIRE7',HRRPUA=400.,RGB=1,1,0,RAMP_Q='FIRE7_RAMP' /
&RAMP ID='FIRE7_RAMP',T=    0.,F=0.0 /
&RAMP ID='FIRE7_RAMP',T= 129.,F=1.0 /
&RAMP ID='FIRE7_RAMP',T=1332.,F=1.0 /
&RAMP ID='FIRE7_RAMP',T=1515.,F=0.0 /


&SURF ID='FIRE8',HRRPUA=1190.,RGB=1,1,0,RAMP_Q='FIRE8_RAMP' /
&RAMP ID='FIRE8_RAMP',T=    0.,F=0.0 /
&RAMP ID='FIRE8_RAMP',T= 176.,F=1.0 /
&RAMP ID='FIRE8_RAMP',T= 610.,F=1.0 /
&RAMP ID='FIRE8_RAMP',T= 611.,F=0.0 /


&SURF ID='FIRE9',HRRPUA=1170.,RGB=1,1,0,RAMP_Q='FIRE9_RAMP' /
```

```
&RAMP ID='FIRE9_RAMP',T=   0.,F=0.0 /
&RAMP ID='FIRE9_RAMP',T= 175.,F=1.0 /
&RAMP ID='FIRE9_RAMP',T=1376.,F=1.0 /
&RAMP ID='FIRE9_RAMP',T=1560.,F=0.0 /

&SURF ID='FIRE10',HRRPUA=1190.,RGB=1,1,0,RAMP_Q='FIRE10_RAMP' /
&RAMP ID='FIRE10_RAMP',T=   0.,F=0.0 /
&RAMP ID='FIRE10_RAMP',T= 176.,F=1.0 /
&RAMP ID='FIRE10_RAMP',T= 826.,F=1.0 /
&RAMP ID='FIRE10_RAMP',T= 827.,F=0.0 /

&SURF ID='FIRE13',HRRPUA=2330.,RGB=1,1,0,RAMP_Q='FIRE13_RAMP' /
&RAMP ID='FIRE13_RAMP',T=   0.,F=0.0 /
&RAMP ID='FIRE13_RAMP',T= 177.,F=1.0 /
&RAMP ID='FIRE13_RAMP',T= 364.,F=1.0 /
&RAMP ID='FIRE13_RAMP',T= 365.,F=0.0 /

&SURF ID='FIRE14',HRRPUA=1180.,RGB=1,1,0,RAMP_Q='FIRE14_RAMP' /
&RAMP ID='FIRE14_RAMP',T=   0.,F=0.0 /
&RAMP ID='FIRE14_RAMP',T= 176.,F=1.0 /
&RAMP ID='FIRE14_RAMP',T=1381.,F=1.0 /
&RAMP ID='FIRE14_RAMP',T=1567.,F=0.0 /

&SURF ID='FIRE15',HRRPUA=1180.,RGB=1,1,0,RAMP_Q='FIRE15_RAMP' /
&RAMP ID='FIRE15_RAMP',T=   0.,F=0.0 /
&RAMP ID='FIRE15_RAMP',T= 180.,F=1.0 /
&RAMP ID='FIRE15_RAMP',T=1380.,F=1.0 /
&RAMP ID='FIRE15_RAMP',T=1567.,F=0.0 /

&SURF ID='FIRE16',HRRPUA=2300.,RGB=1,1,0,RAMP_Q='FIRE16_RAMP' /
&RAMP ID='FIRE16_RAMP',T=   0.,F=0.0 /
&RAMP ID='FIRE16_RAMP',T= 177.,F=1.0 /
&RAMP ID='FIRE16_RAMP',T= 382.,F=1.0 /
&RAMP ID='FIRE16_RAMP',T= 383.,F=0.0 /

&SURF ID='FIRE17',HRRPUA=1160.,RGB=1,1,0,RAMP_Q='FIRE17_RAMP' /
&RAMP ID='FIRE17_RAMP',T=   0.,F=0.0 /
&RAMP ID='FIRE17_RAMP',T= 181.,F=1.0 /
&RAMP ID='FIRE17_RAMP',T= 272.,F=1.0 /
&RAMP ID='FIRE17_RAMP',T= 273.,F=0.0 /

&SURF ID='FIRE18',HRRPUA=1180.,RGB=1,1,0,RAMP_Q='FIRE18_RAMP' /
&RAMP ID='FIRE18_RAMP',T=   0.,F=0.0 /
&RAMP ID='FIRE18_RAMP',T= 178.,F=1.0 /
&RAMP ID='FIRE18_RAMP',T=1380.,F=1.0 /
&RAMP ID='FIRE18_RAMP',T=1567.,F=0.0 /

&SURF ID='MARINITE'
      FYI='BNZ Materials, Marinite I'
      RGB = 0.70,0.70,0.70
      BACKING = 'EXPOSED'
      EMISSIVITY=0.8
      LEAKING=.TRUE.
      DENSITY = 737.
      RAMP_C_P='rampcp'
      RAMP_KS='rampks'
      DELTA=0.0254 /
&RAMP ID='rampks',T= 24.,F=0.13 /
&RAMP ID='rampks',T=149.,F=0.12 /
&RAMP ID='rampks',T=538.,F=0.12 /
&RAMP ID='rampcp',T= 93.,F=1.172 /
&RAMP ID='rampcp',T=205.,F=1.255 /
&RAMP ID='rampcp',T=316.,F=1.339 /
&RAMP ID='rampcp',T=425.,F=1.423 /

&SURF ID      = 'GYPSUM BOARD'
      FYI     = 'NIST SP 1013-1'
      RGB     = 0.80,0.80,0.70
      KS      = 0.16
      C_P     = 0.9
      DENSITY = 790.
```

```
        DELTA    = 0.0254 /

The fire pan, assumed to be 1 m by 1 m
&OBST XB=10.30,11.30,3.08,4.08,0.00,0.20,SURF_IDS='FIRE1' ,'STEEL SHEET','STEEL SHEET' /
cOBST XB=10.30,11.30,3.08,4.08,0.00,0.20,SURF_IDS='FIRE2' ,'STEEL SHEET','STEEL SHEET' /
cOBST XB=10.30,11.30,3.08,4.08,0.00,0.20,SURF_IDS='FIRE3' ,'STEEL SHEET','STEEL SHEET' /
cOBST XB=10.30,11.30,3.08,4.08,0.00,0.20,SURF_IDS='FIRE4' ,'STEEL SHEET','STEEL SHEET' /
cOBST XB=10.30,11.30,3.08,4.08,0.00,0.20,SURF_IDS='FIRE5' ,'STEEL SHEET','STEEL SHEET' /
cOBST XB=10.30,11.30,3.08,4.08,0.00,0.20,SURF_IDS='FIRE7' ,'STEEL SHEET','STEEL SHEET' /
cOBST XB=10.30,11.30,3.08,4.08,0.00,0.20,SURF_IDS='FIRE8' ,'STEEL SHEET','STEEL SHEET' /
cOBST XB=10.30,11.30,3.08,4.08,0.00,0.20,SURF_IDS='FIRE9' ,'STEEL SHEET','STEEL SHEET' /
cOBST XB=10.30,11.30,3.08,4.08,0.00,0.20,SURF_IDS='FIRE10','STEEL SHEET','STEEL SHEET' /
cOBST XB=10.30,11.30,3.08,4.08,0.00,0.20,SURF_IDS='FIRE13','STEEL SHEET','STEEL SHEET' /
cOBST XB=10.30,11.30,4.74,5.74,0.00,0.20,SURF_IDS='FIRE14','STEEL SHEET','STEEL SHEET' /
cOBST XB=10.30,11.30,0.75,1.75,0.00,0.20,SURF_IDS='FIRE15','STEEL SHEET','STEEL SHEET' /
cOBST XB=10.30,11.30,3.08,4.08,0.00,0.20,SURF_IDS='FIRE16','STEEL SHEET','STEEL SHEET' /
cOBST XB=10.30,11.30,3.08,4.08,0.00,0.20,SURF_IDS='FIRE17','STEEL SHEET','STEEL SHEET' /
cOBST XB=11.80,12.80,1.00,2.00,0.00,0.20,SURF_IDS='FIRE18','STEEL SHEET','STEEL SHEET' /

Cables are defined as rectangular objects, but heat transfer controlled by SURF
&OBST XB= 5.85,15.85,1.90,2.10,3.20,3.30,SURF_IDS='XLP TRAY CONTROL','STEEL SHEET','XLP TRAY
CONTROL' /  Cable Tray D
&OBST XB=10.70,11.00,1.10,1.30,2.70,2.90,SURF_ID='PVC SINGLE CONTROL' /  Slab Target E
&OBST XB=10.40,10.70,1.10,1.30,2.70,2.90,SURF_ID='XLP SINGLE CONTROL' /  Control Cable B
&OBST XB= 5.80,15.80,0.40,0.60,2.20,2.30,SURF_ID='XLP SINGLE POWER' / Power Cable F
&OBST XB=10.58,10.88,6.80,7.04,0.00,3.82,SURF_ID='XLP TRAY CONTROL' / Vertical Ladder Tray G
&OBST XB=17.55,17.85,3.37,3.67,3.72,3.82,SURF_ID='FERALOY' / Junction Box

&VENT CB='ZBAR0',SURF_ID='GYPSUM BOARD' / Floor

&VENT XB= 0.00, 0.00,2.51,4.51,0.00,2.00,SURF_ID='OPEN' / Open Door

cVENT XB=10.88,11.58,0.00,0.00,2.05,2.40,SURF_ID='INFLOW'   /   Supply
cVENT XB=10.88,11.58,7.04,7.04,2.05,2.76,SURF_ID='OUTFLOW'  /   Exhaust

&SLCF PBY=3.5,QUANTITY='TEMPERATURE',VECTOR=.TRUE. /
&SLCF PBY=3.5,QUANTITY='HRRPUV' /
&SLCF PBY=3.5,QUANTITY='MIXTURE_FRACTION' /
&SLCF PBX=10.8,QUANTITY='TEMPERATURE',VECTOR=.TRUE. /
&SLCF PBX=10.8,QUANTITY='HRRPUV' /
&SLCF PBX=10.8,QUANTITY='MIXTURE_FRACTION' /

&SLCF XB= 0.00, 0.00,2.60,4.60,0.00,2.00,QUANTITY='TEMPERATURE',VECTOR=.TRUE. /

&BNDF QUANTITY='WALL_TEMPERATURE' /
&BNDF QUANTITY='GAUGE_HEAT_FLUX' /

&PL3D DTSAM=60. /

Gas Phase TC Trees

&THCP XYZ= 5.00, 3.58, 0.35,QUANTITY='THERMOCOUPLE',LABEL='Tr 1-1',DTSAM=10. /
&THCP XYZ= 5.00, 3.58, 0.70,QUANTITY='THERMOCOUPLE',LABEL='Tr 1-2' /
&THCP XYZ= 5.00, 3.58, 1.05,QUANTITY='THERMOCOUPLE',LABEL='Tr 1-3' /
&THCP XYZ= 5.00, 3.58, 1.40,QUANTITY='THERMOCOUPLE',LABEL='Tr 1-4' /
&THCP XYZ= 5.00, 3.58, 1.75,QUANTITY='THERMOCOUPLE',LABEL='Tr 1-5' /
&THCP XYZ= 5.00, 3.58, 2.10,QUANTITY='THERMOCOUPLE',LABEL='Tr 1-6' /
&THCP XYZ= 5.00, 3.58, 2.45,QUANTITY='THERMOCOUPLE',LABEL='Tr 1-7' /
&THCP XYZ= 5.00, 3.58, 2.80,QUANTITY='THERMOCOUPLE',LABEL='Tr 1-8' /
&THCP XYZ= 5.00, 3.58, 3.15,QUANTITY='THERMOCOUPLE',LABEL='Tr 1-9' /
&THCP XYZ= 5.00, 3.58, 3.50,QUANTITY='THERMOCOUPLE',LABEL='Tr 1-10'/

&THCP XYZ=10.85, 6.48, 0.35,QUANTITY='THERMOCOUPLE',LABEL='Tr 2-1' /
&THCP XYZ=10.85, 6.48, 0.70,QUANTITY='THERMOCOUPLE',LABEL='Tr 2-2' /
&THCP XYZ=10.85, 6.48, 1.05,QUANTITY='THERMOCOUPLE',LABEL='Tr 2-3' /
&THCP XYZ=10.85, 6.48, 1.40,QUANTITY='THERMOCOUPLE',LABEL='Tr 2-4' /
&THCP XYZ=10.85, 6.48, 1.75,QUANTITY='THERMOCOUPLE',LABEL='Tr 2-5' /
&THCP XYZ=10.85, 6.48, 2.10,QUANTITY='THERMOCOUPLE',LABEL='Tr 2-6' /
&THCP XYZ=10.85, 6.48, 2.45,QUANTITY='THERMOCOUPLE',LABEL='Tr 2-7' /
&THCP XYZ=10.85, 6.48, 2.80,QUANTITY='THERMOCOUPLE',LABEL='Tr 2-8' /
&THCP XYZ=10.85, 6.48, 3.15,QUANTITY='THERMOCOUPLE',LABEL='Tr 2-9' /
```

B-8

```
&THCP XYZ=10.85, 6.48, 3.50,QUANTITY='THERMOCOUPLE',LABEL='Tr 2-10'/

&THCP XYZ=10.85, 2.20, 0.35,QUANTITY='THERMOCOUPLE',LABEL='Tr 3-1' /
&THCP XYZ=10.85, 2.20, 0.70,QUANTITY='THERMOCOUPLE',LABEL='Tr 3-2' /
&THCP XYZ=10.85, 2.20, 1.05,QUANTITY='THERMOCOUPLE',LABEL='Tr 3-3' /
&THCP XYZ=10.85, 2.20, 1.40,QUANTITY='THERMOCOUPLE',LABEL='Tr 3-4' /
&THCP XYZ=10.85, 2.20, 1.75,QUANTITY='THERMOCOUPLE',LABEL='Tr 3-5' /
&THCP XYZ=10.85, 2.20, 2.10,QUANTITY='THERMOCOUPLE',LABEL='Tr 3-6' /
&THCP XYZ=10.85, 2.20, 2.45,QUANTITY='THERMOCOUPLE',LABEL='Tr 3-7' /
&THCP XYZ=10.85, 2.20, 2.80,QUANTITY='THERMOCOUPLE',LABEL='Tr 3-8' /
&THCP XYZ=10.85, 2.20, 3.15,QUANTITY='THERMOCOUPLE',LABEL='Tr 3-9' /
&THCP XYZ=10.85, 2.20, 3.50,QUANTITY='THERMOCOUPLE',LABEL='Tr 3-10'/

&THCP XYZ=10.85, 1.35, 0.35,QUANTITY='THERMOCOUPLE',LABEL='Tr 4-1' /
&THCP XYZ=10.85, 1.35, 0.70,QUANTITY='THERMOCOUPLE',LABEL='Tr 4-2' /
&THCP XYZ=10.85, 1.35, 1.05,QUANTITY='THERMOCOUPLE',LABEL='Tr 4-3' /
&THCP XYZ=10.85, 1.35, 1.40,QUANTITY='THERMOCOUPLE',LABEL='Tr 4-4' /
&THCP XYZ=10.85, 1.35, 1.75,QUANTITY='THERMOCOUPLE',LABEL='Tr 4-5' /
&THCP XYZ=10.85, 1.35, 2.10,QUANTITY='THERMOCOUPLE',LABEL='Tr 4-6' /
&THCP XYZ=10.85, 1.35, 2.45,QUANTITY='THERMOCOUPLE',LABEL='Tr 4-7' /
&THCP XYZ=10.85, 1.35, 2.80,QUANTITY='THERMOCOUPLE',LABEL='Tr 4-8' /
&THCP XYZ=10.85, 1.35, 3.15,QUANTITY='THERMOCOUPLE',LABEL='Tr 4-9' /
&THCP XYZ=10.85, 1.35, 3.50,QUANTITY='THERMOCOUPLE',LABEL='Tr 4-10'/

&THCP XYZ=10.85, 0.55, 0.35,QUANTITY='THERMOCOUPLE',LABEL='Tr 5-1' /
&THCP XYZ=10.85, 0.55, 0.70,QUANTITY='THERMOCOUPLE',LABEL='Tr 5-2' /
&THCP XYZ=10.85, 0.55, 1.05,QUANTITY='THERMOCOUPLE',LABEL='Tr 5-3' /
&THCP XYZ=10.85, 0.55, 1.40,QUANTITY='THERMOCOUPLE',LABEL='Tr 5-4' /
&THCP XYZ=10.85, 0.55, 1.75,QUANTITY='THERMOCOUPLE',LABEL='Tr 5-5' /
&THCP XYZ=10.85, 0.55, 2.10,QUANTITY='THERMOCOUPLE',LABEL='Tr 5-6' /
&THCP XYZ=10.85, 0.55, 2.45,QUANTITY='THERMOCOUPLE',LABEL='Tr 5-7' /
&THCP XYZ=10.85, 0.55, 2.80,QUANTITY='THERMOCOUPLE',LABEL='Tr 5-8' /
&THCP XYZ=10.85, 0.55, 3.15,QUANTITY='THERMOCOUPLE',LABEL='Tr 5-9' /
&THCP XYZ=10.85, 0.55, 3.50,QUANTITY='THERMOCOUPLE',LABEL='Tr 5-10'/

&THCP XYZ=11.95, 3.58, 0.35,QUANTITY='THERMOCOUPLE',LABEL='Tr 6-1' /
&THCP XYZ=11.95, 3.58, 0.70,QUANTITY='THERMOCOUPLE',LABEL='Tr 6-2' /
&THCP XYZ=11.95, 3.58, 1.05,QUANTITY='THERMOCOUPLE',LABEL='Tr 6-3' /
&THCP XYZ=11.95, 3.58, 1.40,QUANTITY='THERMOCOUPLE',LABEL='Tr 6-4' /
&THCP XYZ=11.95, 3.58, 1.75,QUANTITY='THERMOCOUPLE',LABEL='Tr 6-5' /
&THCP XYZ=11.95, 3.58, 2.10,QUANTITY='THERMOCOUPLE',LABEL='Tr 6-6' /
&THCP XYZ=11.95, 3.58, 2.45,QUANTITY='THERMOCOUPLE',LABEL='Tr 6-7' /
&THCP XYZ=11.95, 3.58, 2.80,QUANTITY='THERMOCOUPLE',LABEL='Tr 6-8' /
&THCP XYZ=11.95, 3.58, 3.15,QUANTITY='THERMOCOUPLE',LABEL='Tr 6-9' /
&THCP XYZ=11.95, 3.58, 3.50,QUANTITY='THERMOCOUPLE',LABEL='Tr 6-10'/

&THCP XYZ=16.70, 3.58, 0.35,QUANTITY='THERMOCOUPLE',LABEL='Tr 7-1' /
&THCP XYZ=16.70, 3.58, 0.70,QUANTITY='THERMOCOUPLE',LABEL='Tr 7-2' /
&THCP XYZ=16.70, 3.58, 1.05,QUANTITY='THERMOCOUPLE',LABEL='Tr 7-3' /
&THCP XYZ=16.70, 3.58, 1.40,QUANTITY='THERMOCOUPLE',LABEL='Tr 7-4' /
&THCP XYZ=16.70, 3.58, 1.75,QUANTITY='THERMOCOUPLE',LABEL='Tr 7-5' /
&THCP XYZ=16.70, 3.58, 2.10,QUANTITY='THERMOCOUPLE',LABEL='Tr 7-6' /
&THCP XYZ=16.70, 3.58, 2.45,QUANTITY='THERMOCOUPLE',LABEL='Tr 7-7' /
&THCP XYZ=16.70, 3.58, 2.80,QUANTITY='THERMOCOUPLE',LABEL='Tr 7-8' /
&THCP XYZ=16.70, 3.58, 3.15,QUANTITY='THERMOCOUPLE',LABEL='Tr 7-9' /
&THCP XYZ=16.70, 3.58, 3.50,QUANTITY='THERMOCOUPLE',LABEL='Tr 7-10'/

Wall TCs

&THCP XYZ= 3.91, 7.04, 1.49,QUANTITY='WALL_TEMPERATURE',IOR=-2,LABEL='TC N U-1'/
&THCP XYZ= 3.91, 7.04, 3.72,QUANTITY='WALL_TEMPERATURE',IOR=-2,LABEL='TC N U-2'/
&THCP XYZ= 9.55, 7.04, 1.87,QUANTITY='WALL_TEMPERATURE',IOR=-2,LABEL='TC N U-3'/
&THCP XYZ=12.15, 7.04, 1.87,QUANTITY='WALL_TEMPERATURE',IOR=-2,LABEL='TC N U-4'/
&THCP XYZ=17.79, 7.04, 1.50,QUANTITY='WALL_TEMPERATURE',IOR=-2,LABEL='TC N U-5'/
&THCP XYZ=17.79, 7.04, 3.73,QUANTITY='WALL_TEMPERATURE',IOR=-2,LABEL='TC N U-6'/

&THCP XYZ= 3.91, 0.00, 1.49,QUANTITY='WALL_TEMPERATURE',IOR= 2,LABEL='TC S U-1'/
&THCP XYZ= 3.91, 0.00, 3.72,QUANTITY='WALL_TEMPERATURE',IOR= 2,LABEL='TC S U-2'/
&THCP XYZ= 9.55, 0.00, 1.87,QUANTITY='WALL_TEMPERATURE',IOR= 2,LABEL='TC S U-3'/
&THCP XYZ=12.15, 0.00, 1.87,QUANTITY='WALL_TEMPERATURE',IOR= 2,LABEL='TC S U-4'/
&THCP XYZ=17.79, 0.00, 1.50,QUANTITY='WALL_TEMPERATURE',IOR= 2,LABEL='TC S U-5'/
```

```
&THCP XYZ=17.79,  0.00,  3.73,QUANTITY='WALL_TEMPERATURE',IOR= 2,LABEL='TC S U-6'/

&THCP XYZ=21.70,  1.59,  1.12,QUANTITY='WALL_TEMPERATURE',IOR=-1,LABEL='TC E U-1'/
&THCP XYZ=21.70,  1.59,  2.43,QUANTITY='WALL_TEMPERATURE',IOR=-1,LABEL='TC E U-2'/
&THCP XYZ=21.70,  5.76,  1.12,QUANTITY='WALL_TEMPERATURE',IOR=-1,LABEL='TC E U-3'/
&THCP XYZ=21.70,  5.76,  2.43,QUANTITY='WALL_TEMPERATURE',IOR=-1,LABEL='TC E U-4'/

&THCP XYZ= 0.00,  1.59,  1.12,QUANTITY='WALL_TEMPERATURE',IOR= 1,LABEL='TC W U-1'/
&THCP XYZ= 0.00,  1.59,  2.43,QUANTITY='WALL_TEMPERATURE',IOR= 1,LABEL='TC W U-2'/
&THCP XYZ= 0.00,  5.76,  1.12,QUANTITY='WALL_TEMPERATURE',IOR= 1,LABEL='TC W U-3'/
&THCP XYZ= 0.00,  5.76,  2.43,QUANTITY='WALL_TEMPERATURE',IOR= 1,LABEL='TC W U-4'/

&THCP XYZ= 3.04,  3.59,  0.00,QUANTITY='WALL_TEMPERATURE',IOR= 3,LABEL='TC F U-1'/
&THCP XYZ= 9.11,  2.00,  0.00,QUANTITY='WALL_TEMPERATURE',IOR= 3,LABEL='TC F U-2'/
&THCP XYZ= 9.11,  5.97,  0.00,QUANTITY='WALL_TEMPERATURE',IOR= 3,LABEL='TC F U-3'/
&THCP XYZ=10.85,  2.39,  0.00,QUANTITY='WALL_TEMPERATURE',IOR= 3,LABEL='TC F U-4'/
&THCP XYZ=10.85,  5.17,  0.00,QUANTITY='WALL_TEMPERATURE',IOR= 3,LABEL='TC F C-5'/
&THCP XYZ=13.02,  2.00,  0.00,QUANTITY='WALL_TEMPERATURE',IOR= 3,LABEL='TC F U-6'/
&THCP XYZ=13.02,  5.97,  0.00,QUANTITY='WALL_TEMPERATURE',IOR= 3,LABEL='TC F U-7'/
&THCP XYZ=18.66,  3.59,  0.00,QUANTITY='WALL_TEMPERATURE',IOR= 3,LABEL='TC F U-8'/

&THCP XYZ= 3.04,  3.59,  3.82,QUANTITY='WALL_TEMPERATURE',IOR=-3,LABEL='TC C U-1'/
&THCP XYZ= 9.11,  2.00,  3.82,QUANTITY='WALL_TEMPERATURE',IOR=-3,LABEL='TC C C-2'/
&THCP XYZ= 9.11,  5.97,  3.82,QUANTITY='WALL_TEMPERATURE',IOR=-3,LABEL='TC C C-3'/
&THCP XYZ=10.85,  2.39,  3.82,QUANTITY='WALL_TEMPERATURE',IOR=-3,LABEL='TC C C-4'/
&THCP XYZ=10.85,  5.17,  3.82,QUANTITY='WALL_TEMPERATURE',IOR=-3,LABEL='TC C C-5'/
&THCP XYZ=13.02,  2.00,  3.82,QUANTITY='WALL_TEMPERATURE',IOR=-3,LABEL='TC C C-6'/
&THCP XYZ=13.02,  5.97,  3.82,QUANTITY='WALL_TEMPERATURE',IOR=-3,LABEL='TC C C-7'/
&THCP XYZ=18.66,  3.59,  3.82,QUANTITY='WALL_TEMPERATURE',IOR=-3,LABEL='TC C U-8'/

Bidirectional Probe TCs

&THCP XYZ= 0.10,  2.81,  0.20,QUANTITY='THERMOCOUPLE',LABEL='TC Door 1'/
&THCP XYZ= 0.10,  2.81,  0.60,QUANTITY='THERMOCOUPLE',LABEL='TC Door 2'/
&THCP XYZ= 0.10,  2.81,  1.00,QUANTITY='THERMOCOUPLE',LABEL='TC Door 3'/
&THCP XYZ= 0.10,  2.81,  1.20,QUANTITY='THERMOCOUPLE',LABEL='TC Door 4'/
&THCP XYZ= 0.10,  2.81,  1.40,QUANTITY='THERMOCOUPLE',LABEL='TC Door 5'/
&THCP XYZ= 0.10,  2.81,  1.60,QUANTITY='THERMOCOUPLE',LABEL='TC Door 6'/
&THCP XYZ= 0.10,  2.81,  1.80,QUANTITY='THERMOCOUPLE',LABEL='TC Door 7'/
&THCP XYZ= 0.10,  2.81,  1.90,QUANTITY='THERMOCOUPLE',LABEL='TC Door 8'/
&THCP XYZ= 0.10,  3.61,  0.20,QUANTITY='THERMOCOUPLE',LABEL='TC Door 9'/
&THCP XYZ= 0.10,  3.61,  0.60,QUANTITY='THERMOCOUPLE',LABEL='TC Door 10'/
&THCP XYZ= 0.10,  3.61,  1.00,QUANTITY='THERMOCOUPLE',LABEL='TC Door 11'/
&THCP XYZ= 0.10,  3.61,  1.20,QUANTITY='THERMOCOUPLE',LABEL='TC Door 12'/
&THCP XYZ= 0.10,  3.61,  1.40,QUANTITY='THERMOCOUPLE',LABEL='TC Door 13'/
&THCP XYZ= 0.10,  3.61,  1.60,QUANTITY='THERMOCOUPLE',LABEL='TC Door 14'/
&THCP XYZ= 0.10,  3.61,  1.80,QUANTITY='THERMOCOUPLE',LABEL='TC Door 15'/
&THCP XYZ= 0.10,  3.61,  1.90,QUANTITY='THERMOCOUPLE',LABEL='TC Door 16'/
&THCP XYZ= 0.10,  4.21,  0.20,QUANTITY='THERMOCOUPLE',LABEL='TC Door 17'/
&THCP XYZ= 0.10,  4.21,  0.60,QUANTITY='THERMOCOUPLE',LABEL='TC Door 18'/
&THCP XYZ= 0.10,  4.21,  1.00,QUANTITY='THERMOCOUPLE',LABEL='TC Door 19'/
&THCP XYZ= 0.10,  4.21,  1.20,QUANTITY='THERMOCOUPLE',LABEL='TC Door 20'/
&THCP XYZ= 0.10,  4.21,  1.40,QUANTITY='THERMOCOUPLE',LABEL='TC Door 21'/
&THCP XYZ= 0.10,  4.21,  1.60,QUANTITY='THERMOCOUPLE',LABEL='TC Door 22'/
&THCP XYZ= 0.10,  4.21,  1.80,QUANTITY='THERMOCOUPLE',LABEL='TC Door 23'/
&THCP XYZ= 0.10,  4.21,  1.90,QUANTITY='THERMOCOUPLE',LABEL='TC Door 24'/
&THCP XYZ=11.35,  0.00,  2.40,QUANTITY='THERMOCOUPLE',LABEL='TC Supply 25'/
&THCP XYZ=11.35,  7.04,  2.40,QUANTITY='THERMOCOUPLE',LABEL='TC Exhaust 26'/
&THCP XYZ= 0.00,  0.30,  0.08,QUANTITY='THERMOCOUPLE',LABEL='TC Leak 27'/

Cable TCs

&THCP XYZ=10.55,  1.30,  2.80,QUANTITY='WALL_TEMPERATURE',IOR=-3,LABEL='B Ts-14'/
&THCP XYZ=10.55,  1.30,  2.80,QUANTITY='INSIDE_WALL_TEMPERATURE',IOR=-3,LABEL='B Tc-
15',DEPTH=0.0012 /
&THCP XYZ=10.85,  2.00,  3.20,QUANTITY='WALL_TEMPERATURE',IOR=-3,LABEL='D Ts-12'/
&THCP XYZ=10.85,  1.25,  2.70,QUANTITY='WALL_TEMPERATURE',IOR=-3,LABEL='E Ts-16'/
&THCP XYZ=10.85,  1.25,  2.85,QUANTITY='WALL_TEMPERATURE',IOR= 3,LABEL='E Ts-16p'/
&THCP XYZ=10.85,  1.25,  2.70,QUANTITY='INSIDE_WALL_TEMPERATURE',IOR=-3,LABEL='E Tc-
17',DEPTH=0.0025 /
&THCP XYZ=10.85,  0.50,  2.20,QUANTITY='WALL_TEMPERATURE',IOR=-3,LABEL='F Ts-20'/
```

B-10

```
&THCP XYZ=14.85, 2.00, 3.20,QUANTITY='WALL_TEMPERATURE',IOR=-3,LABEL='D Ts-26'/
&THCP XYZ=14.85, 0.50, 2.20,QUANTITY='WALL_TEMPERATURE',IOR=-3,LABEL='F Ts-30'/
&THCP XYZ=10.80, 6.80, 0.35,QUANTITY='WALL_TEMPERATURE',IOR=-2,LABEL='G Ts-31'/
&THCP XYZ=10.80, 6.80, 0.70,QUANTITY='WALL_TEMPERATURE',IOR=-2,LABEL='G Ts-32'/
&THCP XYZ=10.80, 6.80, 1.75,QUANTITY='WALL_TEMPERATURE',IOR=-2,LABEL='G Ts-33'/
&THCP XYZ=10.80, 6.80, 2.45,QUANTITY='WALL_TEMPERATURE',IOR=-2,LABEL='G Ts-35'/
&THCP XYZ=10.80, 6.80, 3.15,QUANTITY='WALL_TEMPERATURE',IOR=-2,LABEL='G Ts-36'/
&THCP XYZ=17.70, 3.58, 3.72,QUANTITY='BACK_WALL_TEMPERATURE',IOR=-3,LABEL='Junction Box TC-37'/
&THCP XYZ=17.70, 3.58, 3.72,QUANTITY='WALL_TEMPERATURE',IOR=-3,LABEL='Junction Box Ts-38'/
&THCP XYZ=17.55, 3.52, 3.77,QUANTITY='WALL_TEMPERATURE',IOR=-1,LABEL='Junction Box Ts-39'/
```

Aspirated TCs

```
&THCP XYZ= 0.10, 3.61, 0.20,QUANTITY='TEMPERATURE',LABEL='ATC Door 1'/
&THCP XYZ= 0.10, 3.61, 1.00,QUANTITY='TEMPERATURE',LABEL='ATC Door 2'/
&THCP XYZ= 0.10, 3.61, 1.80,QUANTITY='TEMPERATURE',LABEL='ATC Door 3'/
&THCP XYZ=11.35, 7.04, 2.40,QUANTITY='TEMPERATURE',LABEL='ATC Exhaust 4'/
&THCP XYZ=10.85, 0.55, 1.05,QUANTITY='TEMPERATURE',LABEL='ATC 5'/
&THCP XYZ=10.85, 0.55, 2.80,QUANTITY='TEMPERATURE',LABEL='ATC 6'/
```

Wall Flux Gauges

```
&THCP XYZ= 3.91, 7.04, 1.49,QUANTITY='HEAT_FLUX',IOR=-2,LABEL='N U-1'/
&THCP XYZ= 3.91, 7.04, 3.72,QUANTITY='HEAT_FLUX',IOR=-2,LABEL='N U-2'/
&THCP XYZ= 9.55, 7.04, 1.87,QUANTITY='HEAT_FLUX',IOR=-2,LABEL='N U-3'/
&THCP XYZ=12.15, 7.04, 1.87,QUANTITY='HEAT_FLUX',IOR=-2,LABEL='N U-4'/
&THCP XYZ=17.79, 7.04, 1.50,QUANTITY='HEAT_FLUX',IOR=-2,LABEL='N U-5'/
&THCP XYZ=17.79, 7.04, 3.73,QUANTITY='HEAT_FLUX',IOR=-2,LABEL='N U-6'/

&THCP XYZ= 3.91, 0.00, 1.49,QUANTITY='HEAT_FLUX',IOR= 2,LABEL='S U-1'/
&THCP XYZ= 3.91, 0.00, 3.72,QUANTITY='HEAT_FLUX',IOR= 2,LABEL='S U-2'/
&THCP XYZ= 9.55, 0.00, 1.87,QUANTITY='HEAT_FLUX',IOR= 2,LABEL='S U-3'/
&THCP XYZ=12.15, 0.00, 1.87,QUANTITY='HEAT_FLUX',IOR= 2,LABEL='S U-4'/
&THCP XYZ=17.79, 0.00, 1.50,QUANTITY='HEAT_FLUX',IOR= 2,LABEL='S U-5'/
&THCP XYZ=17.79, 0.00, 3.73,QUANTITY='HEAT_FLUX',IOR= 2,LABEL='S U-6'/

&THCP XYZ=21.70, 1.59, 1.12,QUANTITY='HEAT_FLUX',IOR=-1,LABEL='E U-1'/
&THCP XYZ=21.70, 1.59, 2.43,QUANTITY='HEAT_FLUX',IOR=-1,LABEL='E U-2'/
&THCP XYZ=21.70, 5.76, 1.12,QUANTITY='HEAT_FLUX',IOR=-1,LABEL='E U-3'/
&THCP XYZ=21.70, 5.76, 2.43,QUANTITY='HEAT_FLUX',IOR=-1,LABEL='E U-4'/

&THCP XYZ= 0.00, 1.59, 1.12,QUANTITY='HEAT_FLUX',IOR= 1,LABEL='W U-1'/
&THCP XYZ= 0.00, 1.59, 2.43,QUANTITY='HEAT_FLUX',IOR= 1,LABEL='W U-2'/
&THCP XYZ= 0.00, 5.76, 1.12,QUANTITY='HEAT_FLUX',IOR= 1,LABEL='W U-3'/
&THCP XYZ= 0.00, 5.76, 2.43,QUANTITY='HEAT_FLUX',IOR= 1,LABEL='W U-4'/

&THCP XYZ= 3.04, 3.59, 0.00,QUANTITY='HEAT_FLUX',IOR= 3,LABEL='F U-1'/
&THCP XYZ= 9.11, 2.00, 0.00,QUANTITY='HEAT_FLUX',IOR= 3,LABEL='F U-2'/
&THCP XYZ= 9.11, 5.97, 0.00,QUANTITY='HEAT_FLUX',IOR= 3,LABEL='F U-3'/
&THCP XYZ=10.85, 2.39, 0.00,QUANTITY='HEAT_FLUX',IOR= 3,LABEL='F U-4'/
&THCP XYZ=10.85, 5.17, 0.00,QUANTITY='HEAT_FLUX',IOR= 3,LABEL='F C-5'/
&THCP XYZ=13.02, 2.00, 0.00,QUANTITY='HEAT_FLUX',IOR= 3,LABEL='F U-6'/
&THCP XYZ=13.02, 5.97, 0.00,QUANTITY='HEAT_FLUX',IOR= 3,LABEL='F U-7'/
&THCP XYZ=18.66, 3.59, 0.00,QUANTITY='HEAT_FLUX',IOR= 3,LABEL='F U-8'/

&THCP XYZ= 3.04, 3.59, 3.82,QUANTITY='HEAT_FLUX',IOR=-3,LABEL='C U-1'/
&THCP XYZ= 9.11, 2.00, 3.82,QUANTITY='HEAT_FLUX',IOR=-3,LABEL='C C-2'/
&THCP XYZ= 9.11, 5.97, 3.82,QUANTITY='HEAT_FLUX',IOR=-3,LABEL='C C-3'/
&THCP XYZ=10.85, 2.39, 3.82,QUANTITY='HEAT_FLUX',IOR=-3,LABEL='C C-4'/
&THCP XYZ=10.85, 5.17, 3.82,QUANTITY='HEAT_FLUX',IOR=-3,LABEL='C C-5'/
&THCP XYZ=13.02, 2.00, 3.82,QUANTITY='HEAT_FLUX',IOR=-3,LABEL='C C-6'/
&THCP XYZ=13.02, 5.97, 3.82,QUANTITY='HEAT_FLUX',IOR=-3,LABEL='C C-7'/
&THCP XYZ=18.66, 3.59, 3.82,QUANTITY='HEAT_FLUX',IOR=-3,LABEL='C U-8'/
```

Rad and Total Flux Gauges

```
&THCP XYZ=10.87, 0.50, 2.20,QUANTITY='GAUGE_HEAT_FLUX',IOR=-3,LABEL='Total Flux Gauge 2'/
&THCP XYZ=10.87, 1.25, 2.70,QUANTITY='GAUGE_HEAT_FLUX',IOR=-3,LABEL='Total Flux Gauge 4'/
&THCP XYZ=10.87, 1.30, 2.80,QUANTITY='GAUGE_HEAT_FLUX',IOR=-2,LABEL='Total Flux Gauge 6'/
&THCP XYZ=10.87, 2.00, 3.20,QUANTITY='GAUGE_HEAT_FLUX',IOR=-3,LABEL='Total Flux Gauge 8'/
&THCP XYZ=10.81, 6.80, 1.75,QUANTITY='GAUGE_HEAT_FLUX',IOR=-2,LABEL='Total Flux Gauge 9'/
```

```
&THCP XYZ=10.87, 0.50, 2.20,QUANTITY='RADIOMETER',IOR=-3,LABEL='Rad Gauge 1'/
&THCP XYZ=10.87, 1.25, 2.70,QUANTITY='RADIOMETER',IOR=-3,LABEL='Rad Gauge 3'/
&THCP XYZ=10.87, 1.30, 2.80,QUANTITY='RADIOMETER',IOR= 2,LABEL='Rad Gauge 5'/
&THCP XYZ=10.87, 2.00, 3.20,QUANTITY='RADIOMETER',IOR=-3,LABEL='Rad Gauge 7'/
&THCP XYZ=10.81, 6.80, 1.75,QUANTITY='RADIOMETER',IOR=-2,LABEL='Rad Gauge 10'/
```

Gaseous Sampling

```
&THCP XYZ= 6.85, 3.48, 3.22,QUANTITY='oxygen',          LABEL='O2 1'/
&THCP XYZ= 6.85, 3.48, 0.50,QUANTITY='oxygen',          LABEL='O2 2'/
&THCP XYZ= 6.85, 3.48, 3.22,QUANTITY='carbon monoxide',LABEL='CO 3'/
&THCP XYZ= 6.85, 3.48, 3.22,QUANTITY='carbon dioxide' ,LABEL='CO2 4'/
```

Bidirectional Probes

```
&THCP XYZ= 0.10, 2.71, 0.20,QUANTITY='VELOCITY',    LABEL='BP Door 1'/
&THCP XYZ= 0.10, 2.71, 0.60,QUANTITY='VELOCITY',    LABEL='BP Door 2'/
&THCP XYZ= 0.10, 2.71, 1.00,QUANTITY='VELOCITY',    LABEL='BP Door 3'/
&THCP XYZ= 0.10, 2.71, 1.40,QUANTITY='VELOCITY',    LABEL='BP Door 4'/
&THCP XYZ= 0.10, 2.71, 1.80,QUANTITY='VELOCITY',    LABEL='BP Door 5'/
&THCP XYZ= 0.10, 3.51, 0.20,QUANTITY='VELOCITY',    LABEL='BP Door 6'/
&THCP XYZ= 0.10, 3.51, 0.60,QUANTITY='VELOCITY',    LABEL='BP Door 7'/
&THCP XYZ= 0.10, 3.51, 1.00,QUANTITY='VELOCITY',    LABEL='BP Door 8'/
&THCP XYZ= 0.10, 3.51, 1.40,QUANTITY='VELOCITY',    LABEL='BP Door 9'/
&THCP XYZ= 0.10, 3.51, 1.80,QUANTITY='VELOCITY',    LABEL='BP Door 10'/
&THCP XYZ= 0.10, 4.31, 0.20,QUANTITY='VELOCITY',    LABEL='BP Door 11'/
&THCP XYZ= 0.10, 4.31, 0.60,QUANTITY='VELOCITY',    LABEL='BP Door 12'/
&THCP XYZ= 0.10, 4.31, 1.00,QUANTITY='VELOCITY',    LABEL='BP Door 13'/
&THCP XYZ= 0.10, 4.31, 1.40,QUANTITY='VELOCITY',    LABEL='BP Door 14'/
&THCP XYZ= 0.10, 4.31, 1.80,QUANTITY='VELOCITY',    LABEL='BP Door 15'/
&THCP XYZ=11.35, 0.00, 2.40,QUANTITY='VELOCITY',    LABEL='BP Supply 16'/
&THCP XYZ=11.35, 7.04, 2.40,QUANTITY='VELOCITY',    LABEL='BP Exhaust 17'/
&THCP XYZ= 0.00, 0.30, 0.08,QUANTITY='VELOCITY',    LABEL='BP Leak 18'/
```

Smoke Obscuration/Concentration

```
&THCP XYZ=21.10, 0.50, 3.60,QUANTITY='soot density',   LABEL='Smoke Concentration'/
```

Compartment Pressure

```
&THCP XYZ=10.85, 0.10, 0.10,QUANTITY='PRESSURE',   LABEL='Pressure'/
```

Integrated Quantities

```
&THCP XB= 0.00, 0.00,2.51,4.51,0.00,2.00,QUANTITY='MASS FLOW',LABEL='Door Mass FLOW' /
&THCP XB= 0.00, 0.00,2.51,4.51,0.00,2.00,QUANTITY='HEAT FLOW',LABEL='E-FLOW' /

&THCP XYZ=16.70, 3.58, 3.00,QUANTITY='LAYER HEIGHT',LABEL='Layer Height' /
&THCP XYZ=16.70, 3.58, 3.00,QUANTITY='UPPER TEMPERATURE',LABEL='HGL Temp' /
&THCP XYZ=16.70, 3.58, 3.00,QUANTITY='LOWER TEMPERATURE',LABEL='LGL Temp' /
```

B.3 ICFMP BE #4

```
&HEAD CHID='ICFMP4_01',TITLE='NRC ICFMP Benchmark Exercise 4, Test 1' /
&GRID IBAR=36,JBAR=72,KBAR=56 /
&PDIM XBAR0=0.0,XBAR=3.6,YBAR0=-3.6,YBAR=3.6,ZBAR=5.7 /

&TIME TWFIN=1800. /

&MISC TMPA=19.,SURF_DEFAULT='LIGHT CONCRETE',NFRAMES=1800,REACTION='DODECANE' /

&REAC ID='DODECANE'
      FYI='C_11.64 H_25.29'
      MW_FUEL=165.0
      NU_O2=17.96
      NU_CO2=11.64
      NU_H2O=12.65
      EPUMO2=12736.
      DTSAM=15.
      CO_YIELD=0.012
      SOOT_YIELD=0.042 /

&SURF ID='BURNER',HRRPUA=1000.,RAMP_Q='el',RGB = 0.40,0.40,0.40,TMPWAL=216. /
&RAMP ID='el',T=    0.0, F=0.0      /
&RAMP ID='el',T=   92.0, F=0.11984 /
&RAMP ID='el',T=  180.0, F=1.5836  /
&RAMP ID='el',T=  260.0, F=2.62364 /
&RAMP ID='el',T=  600.0, F=3.19716 /
&RAMP ID='el',T=  822.0, F=3.35124 /
&RAMP ID='el',T=  870.0, F=3.3812  /
&RAMP ID='el',T=1368.0, F=3.51816 /
&RAMP ID='el',T=1395.0, F=0.0      /

&SURF ID    = 'CONCRETE'
      RGB   = 0.66,0.66,0.66
      C_P   = 0.88
      DENSITY = 2400.
      KS    = 2.1
      DELTA = 0.25
      BACKING='INSULATED' /

&SURF ID    = 'CONCRETE TARGET'
      RGB   = 0.76,0.76,0.76
      C_P   = 0.88
      DENSITY = 2400.
      KS    = 2.1
      DELTA = 0.10
      BACKING='INSULATED' /

&SURF ID    = 'AERATED CONCRETE'
      RGB   = 0.46,0.46,0.46
      C_P   = 1.35
      DENSITY = 420.
      KS    = 0.11
      DELTA = 0.10
      BACKING='INSULATED' /

&SURF ID    = 'LIGHT CONCRETE'
      RGB   = 0.76,0.76,0.76
      C_P   = 0.84
      DENSITY = 1500.
      KS    = 0.75
      DELTA = 0.25
      BACKING='INSULATED' /

&SURF ID              = 'STEEL SHEET'
      RGB             = 0.20,0.20,0.20
```

```
        C_DELTA_RHO          = 28.
        BACKING              = 'EXPOSED'
        DELTA                = 0.00635 /

&SURF ID                     = 'STEEL PLATE'
      RGB                    = 0.20,0.20,0.20
      C_P                    = 0.48
      DENSITY                = 7743.
      KS                     = 44.5
      BACKING                = 'INSULATED'
      DELTA                  = 0.02 /

&SURF ID='HOOD',VOLUME_FLUX=1.0,RGB=0,0,1,RAMP_V='HOOD1' /

&RAMP ID='HOOD1',T=   0.,F=2.12 /
&RAMP ID='HOOD1',T=  15.,F=2.24 /
&RAMP ID='HOOD1',T=  30.,F=2.41 /
&RAMP ID='HOOD1',T=  45.,F=2.26 /
&RAMP ID='HOOD1',T= 195.,F=2.55 /
&RAMP ID='HOOD1',T= 210.,F=3.20 /
&RAMP ID='HOOD1',T= 225.,F=3.08 /
&RAMP ID='HOOD1',T= 240.,F=3.20 /
&RAMP ID='HOOD1',T= 255.,F=3.26 /
&RAMP ID='HOOD1',T= 405.,F=3.30 /
&RAMP ID='HOOD1',T= 886.,F=3.51 /
&RAMP ID='HOOD1',T=1449.,F=3.66 /
&RAMP ID='HOOD1',T=1711.,F=2.65 /
&RAMP ID='HOOD1',T=1755.,F=3.03 /
&RAMP ID='HOOD1',T=1770.,F=2.68 /
&RAMP ID='HOOD1',T=1785.,F=2.86 /
&RAMP ID='HOOD1',T=1800.,F=2.82 /


&SURF ID='FUCHS',VOLUME_FLUX=0.5,RGB=0,1,1,RAMP_V='FUCHS1' /

&RAMP ID='FUCHS1',T=   0.,F=0.00 /
&RAMP ID='FUCHS1',T= 150.,F=0.00 /
&RAMP ID='FUCHS1',T= 165.,F=0.08 /
&RAMP ID='FUCHS1',T= 180.,F=0.44 /
&RAMP ID='FUCHS1',T= 195.,F=0.83 /
&RAMP ID='FUCHS1',T= 210.,F=1.32 /
&RAMP ID='FUCHS1',T= 225.,F=1.41 /
&RAMP ID='FUCHS1',T= 551.,F=2.18 /
&RAMP ID='FUCHS1',T= 615.,F=2.17 /
&RAMP ID='FUCHS1',T= 666.,F=2.13 /
&RAMP ID='FUCHS1',T= 720.,F=2.25 /
&RAMP ID='FUCHS1',T= 859.,F=1.92 /
&RAMP ID='FUCHS1',T=1011.,F=1.57 /
&RAMP ID='FUCHS1',T=1245.,F=1.09 /
&RAMP ID='FUCHS1',T=1405.,F=0.43 /
&RAMP ID='FUCHS1',T=1650.,F=0.14 /
&RAMP ID='FUCHS1',T=1800.,F=0.06 /


&OBST XB= 1.30, 1.30, 1.30, 2.30, 0.60, 0.70,SURF_ID='STEEL SHEET' /
&OBST XB= 2.30, 2.30, 1.30, 2.30, 0.60, 0.70,SURF_ID='STEEL SHEET' /
&OBST XB= 1.30, 2.30, 1.30, 1.30, 0.60, 0.70,SURF_ID='STEEL SHEET' /
&OBST XB= 1.30, 2.30, 2.30, 2.30, 0.60, 0.70,SURF_ID='STEEL SHEET' /
&OBST XB= 1.30, 2.30, 1.30, 2.30, 0.50, 0.60,SURF_IDS='BURNER','STEEL SHEET','STEEL SHEET' /

&OBST XB= 0.00, 3.60, 0.00, 0.80, 0.00, 0.60,SURF_ID='AERATED CONCRETE' / Floor
&OBST XB= 0.00, 3.60, 2.80, 3.60, 0.00, 0.60,SURF_ID='AERATED CONCRETE' /
&OBST XB= 0.00, 0.80, 0.80, 2.80, 0.00, 0.60,SURF_ID='AERATED CONCRETE' /
&OBST XB= 2.80, 3.60, 0.80, 2.80, 0.00, 0.60,SURF_ID='AERATED CONCRETE' /
&OBST XB= 0.80, 2.80, 0.80, 2.80, 0.00, 0.40,SURF_ID='CONCRETE' /

&OBST XB= 0.00, 1.45, -.25, 0.00, 0.00, 5.70,SURF_ID='CONCRETE' /  Wall with door
&OBST XB= 2.15, 3.60, -.25, 0.00, 0.00, 5.70,SURF_ID='CONCRETE' /
&OBST XB= 1.45, 2.15, -.25, 0.00, 3.60, 5.70,SURF_ID='CONCRETE' /

&OBST XB= 1.50, 2.10, 2.90, 3.50, 0.60, 1.60,SURF_ID='CONCRETE TARGET' /  Barrel
&HOLE XB= 1.60, 2.00, 3.00, 3.40, 0.60, 1.50 /  Hollow interior of Barrel
```

```
&OBST XB= 0.35, 0.35,-2.90,-0.25, 2.60, 4.60,SURF_ID='STEEL SHEET' /  Hood
&OBST XB= 3.25, 3.25,-2.90,-0.25, 2.60, 4.60,SURF_ID='STEEL SHEET' /  Hood
&OBST XB= 0.35, 3.25,-2.90,-2.90, 2.60, 4.60,SURF_ID='STEEL SHEET' /  Hood
&OBST XB= 0.35, 1.30,-2.90,-0.25, 4.60, 4.60,SURF_ID='STEEL SHEET' /  Hood
&OBST XB= 2.30, 3.25,-2.90,-0.25, 4.60, 4.60,SURF_ID='STEEL SHEET' /  Hood
&OBST XB= 1.30, 2.30,-2.90,-1.95, 4.60, 4.60,SURF_ID='STEEL SHEET' /  Hood
&OBST XB= 1.30, 2.30,-0.95,-0.25, 4.60, 4.60,SURF_ID='STEEL SHEET' /  Hood
&OBST XB= 1.30, 2.30,-1.95,-0.95, 4.60, 5.60,SURF_IDS='STEEL SHEET','STEEL SHEET','HOOD' /
Exhaust

&OBST XB= 0.00, 0.10, 0.50, 0.80, 1.55, 1.85,SURF_ID='AERATED CONCRETE' /  Aerated concrete
target
&OBST XB= 0.00, 0.10, 1.75, 2.05, 1.55, 1.85,SURF_ID='CONCRETE TARGET' /   Concrete target
&VENT XB= 0.00, 0.00, 2.65, 2.95, 1.55, 1.85,SURF_ID='STEEL PLATE' /   Steel target

&VENT XB= 0.00, 3.60, 0.00, 3.60, 5.70, 5.70,SURF_ID='CONCRETE' / Ceiling
&VENT XB= 0.00, 0.42, 0.13, 3.60, 5.70, 5.70,SURF_ID='FUCHS' /   FUCHS fan1
&VENT XB= 3.18, 3.60, 0.13, 3.60, 5.70, 5.70,SURF_ID='FUCHS' /   FUCHS fan2

&VENT XB= 0.00, 0.00,-3.60,-0.25, 0.00, 5.70,SURF_ID='OPEN' /
&VENT XB= 3.60, 3.60,-3.60,-0.25, 0.00, 5.70,SURF_ID='OPEN' /
&VENT CB='YBAR0',SURF_ID='OPEN' /

&SLCF PBX=1.8,QUANTITY='TEMPERATURE',VECTOR=.TRUE. /
&SLCF PBX=1.8,QUANTITY='HRRPUV' /
&SLCF PBX=1.8,QUANTITY='MIXTURE_FRACTION' /

&BNDF QUANTITY='WALL_TEMPERATURE' /
&BNDF QUANTITY='GAUGE_HEAT_FLUX' /
&BNDF QUANTITY='INCIDENT_HEAT_FLUX' /
&BNDF QUANTITY='HEAT_FLUX' /
&BNDF QUANTITY='CONVECTIVE_FLUX' /
&BNDF QUANTITY='RADIATIVE_FLUX' /
&BNDF QUANTITY='BURNING_RATE' /

&PL3D DTSAM=300. /


TC Trees

&THCP XYZ= 1.75, 1.95, 1.00, QUANTITY='TEMPERATURE',LABEL='M1', DTSAM=15. /
&THCP XYZ= 1.75, 1.95, 1.50, QUANTITY='TEMPERATURE',LABEL='M2' /
&THCP XYZ= 1.75, 1.95, 2.40, QUANTITY='TEMPERATURE',LABEL='M3' /
&THCP XYZ= 1.75, 1.95, 3.35, QUANTITY='TEMPERATURE',LABEL='M4' /
&THCP XYZ= 1.75, 1.95, 4.30, QUANTITY='TEMPERATURE',LABEL='M5' /
&THCP XYZ= 1.75, 1.95, 5.20, QUANTITY='TEMPERATURE',LABEL='M6' /

&THCP XYZ= 2.75, 0.85, 1.50, QUANTITY='TEMPERATURE',LABEL='M7' /
&THCP XYZ= 2.45, 3.45, 1.50, QUANTITY='TEMPERATURE',LABEL='M8' /
&THCP XYZ= 0.95, 0.60, 1.50, QUANTITY='TEMPERATURE',LABEL='M9' /
&THCP XYZ= 0.90, 2.80, 1.50, QUANTITY='TEMPERATURE',LABEL='M10' /

&THCP XYZ= 2.75, 0.85, 3.35, QUANTITY='TEMPERATURE',LABEL='M11' /
&THCP XYZ= 2.45, 3.45, 3.35, QUANTITY='TEMPERATURE',LABEL='M12' /
&THCP XYZ= 0.95, 0.60, 3.35, QUANTITY='TEMPERATURE',LABEL='M13' /
&THCP XYZ= 0.90, 2.80, 3.35, QUANTITY='TEMPERATURE',LABEL='M14' /

&THCP XYZ= 2.75, 0.85, 5.20, QUANTITY='TEMPERATURE',LABEL='M15' /
&THCP XYZ= 2.45, 3.45, 5.20, QUANTITY='TEMPERATURE',LABEL='M16' /
&THCP XYZ= 0.95, 0.60, 5.20, QUANTITY='TEMPERATURE',LABEL='M17' /
&THCP XYZ= 0.90, 2.80, 5.20, QUANTITY='TEMPERATURE',LABEL='M18' /

&THCP XYZ= 1.80, 1.80, 4.00, QUANTITY='UPPER TEMPERATURE',LABEL='Tup' /
&THCP XYZ= 1.80, 1.80, 4.00, QUANTITY='LOWER TEMPERATURE',LABEL='Tlow' /
&THCP XYZ= 1.80, 1.80, 4.00, QUANTITY='LAYER HEIGHT',LABEL='Layer height' /

&THCP XYZ= 2.45, 3.60, 1.50, QUANTITY='WALL_TEMPERATURE',LABEL='M19',IOR=-2 /
&THCP XYZ= 2.45, 3.60, 3.35, QUANTITY='WALL_TEMPERATURE',LABEL='M20',IOR=-2 /
&THCP XYZ= 0.00, 1.90, 1.70, QUANTITY='WALL_TEMPERATURE',LABEL='M21',IOR= 1 /

&THCP XYZ= 2.45, 3.60, 1.50, QUANTITY='WALL_TEMPERATURE',LABEL='M22',IOR=-2 /
```

```
&THCP XYZ= 2.45, 3.60, 3.35, QUANTITY='WALL_TEMPERATURE',LABEL='M23',IOR=-2 /
&THCP XYZ= 0.00, 1.90, 1.70, QUANTITY='WALL_TEMPERATURE',LABEL='M24',IOR= 1 /

&THCP XYZ= 1.80, 1.80, 0.60, QUANTITY='WALL_TEMPERATURE',LABEL='M25',IOR= 3 /

&THCP XYZ= 0.10, 0.65, 1.70, QUANTITY='INSIDE_WALL_TEMPERATURE',LABEL='M26',IOR= 1,DEPTH=0.02 /
&THCP XYZ= 0.10, 0.65, 1.70, QUANTITY='INSIDE_WALL_TEMPERATURE',LABEL='M27',IOR= 1,DEPTH=0.05 /
&THCP XYZ= 0.10, 0.65, 1.70, QUANTITY='INSIDE_WALL_TEMPERATURE',LABEL='M28',IOR= 1,DEPTH=0.08 /
&THCP XYZ= 0.10, 0.65, 1.70, QUANTITY='INSIDE_WALL_TEMPERATURE',LABEL='M29',IOR= 1,DEPTH=0.00 /

&THCP XYZ= 0.10, 1.90, 1.70, QUANTITY='INSIDE_WALL_TEMPERATURE',LABEL='M30',IOR= 1,DEPTH=0.02 /
&THCP XYZ= 0.10, 1.90, 1.70, QUANTITY='INSIDE_WALL_TEMPERATURE',LABEL='M31',IOR= 1,DEPTH=0.05 /
&THCP XYZ= 0.10, 1.90, 1.70, QUANTITY='INSIDE_WALL_TEMPERATURE',LABEL='M32',IOR= 1,DEPTH=0.08 /
&THCP XYZ= 0.10, 1.90, 1.70, QUANTITY='INSIDE_WALL_TEMPERATURE',LABEL='M33',IOR= 1,DEPTH=0.00 /

&THCP XYZ= 0.00, 2.80, 1.70, QUANTITY='INSIDE_WALL_TEMPERATURE',LABEL='M34',IOR= 1,DEPTH=0.00 /
&THCP XYZ= 0.00, 2.80, 1.70, QUANTITY='INSIDE_WALL_TEMPERATURE',LABEL='M35',IOR= 1,DEPTH=0.02 /

&THCP XYZ= 1.80, 0.00, 0.80, QUANTITY='TEMPERATURE',LABEL='M54' /
&THCP XYZ= 1.80, 0.00, 1.40, QUANTITY='TEMPERATURE',LABEL='M55' /
&THCP XYZ= 1.80, 0.00, 1.80, QUANTITY='TEMPERATURE',LABEL='M56' /
&THCP XYZ= 1.80, 0.00, 2.40, QUANTITY='TEMPERATURE',LABEL='M57' /
&THCP XYZ= 1.80, 0.00, 2.80, QUANTITY='TEMPERATURE',LABEL='M58' /
&THCP XYZ= 1.80, 0.00, 3.40, QUANTITY='TEMPERATURE',LABEL='M59' /

&THCP XYZ= 3.60, 1.50, 1.80, QUANTITY='GAUGE_HEAT_FLUX',LABEL='WS1',IOR=-1 /
&THCP XYZ= 0.00, 2.80, 1.70, QUANTITY='GAUGE_HEAT_FLUX',LABEL='WS2',IOR= 1 /
&THCP XYZ= 0.00, 1.90, 1.70, QUANTITY='GAUGE_HEAT_FLUX',LABEL='WS3',IOR= 1 /
&THCP XYZ= 0.00, 0.70, 1.70, QUANTITY='GAUGE_HEAT_FLUX',LABEL='WS4',IOR= 1 /

&THCP XYZ= 1.80, 1.80, 0.60, QUANTITY='MASS_LOSS',LABEL='GV1',IOR= 3 /

&THCP XYZ= 1.75, 1.95, 1.50, QUANTITY='VELOCITY',LABEL='V1' /
&THCP XYZ= 1.75, 1.95, 3.35, QUANTITY='VELOCITY',LABEL='V2' /

&THCP XYZ= 1.80, 0.00, 0.80, QUANTITY='VELOCITY',LABEL='V3' /
&THCP XYZ= 1.80, 0.00, 1.40, QUANTITY='VELOCITY',LABEL='V4' /
&THCP XYZ= 1.80, 0.00, 1.80, QUANTITY='VELOCITY',LABEL='V5' /
&THCP XYZ= 1.80, 0.00, 2.40, QUANTITY='VELOCITY',LABEL='V6' /
&THCP XYZ= 1.80, 0.00, 2.80, QUANTITY='VELOCITY',LABEL='V7' /
&THCP XYZ= 1.80, 0.00, 3.40, QUANTITY='VELOCITY',LABEL='V8' /

&THCP XYZ= 0.10, 1.90, 3.80, QUANTITY='oxygen',          LABEL='GA1-O2' /
&THCP XYZ= 0.10, 1.90, 3.80, QUANTITY='carbon monoxide',LABEL='GA1-CO' /
&THCP XYZ= 0.10, 1.90, 3.80, QUANTITY='carbon dioxide', LABEL='GA1-CO2' /

&THCP XYZ= 1.80,-1.45, 4.50, QUANTITY='oxygen',          LABEL='GA2-O2' /
&THCP XYZ= 1.80,-1.45, 4.50, QUANTITY='carbon monoxide',LABEL='GA2-CO' /
&THCP XYZ= 1.80,-1.45, 4.50, QUANTITY='carbon dioxide', LABEL='GA2-CO2' /

&THCP XYZ= 1.10, 2.40, 5.40, QUANTITY='PRESSURE',LABEL='P1' /
&THCP XYZ= 0.30, 2.00, 2.80, QUANTITY='PRESSURE',LABEL='P2' /

&THCP XB= 1.45, 2.15, 0.00, 0.00, 0.60, 3.60,QUANTITY='MASS FLOW',LABEL='Gin+Gout(Door)' /
&THCP XB= 0.00, 3.60, 0.00, 3.60, 5.70, 5.70,QUANTITY='MASS FLOW',LABEL='Gout(FUCHS)' /
&THCP XB= 1.45, 2.15, 0.00, 0.00, 0.60, 3.60,QUANTITY='HEAT FLOW',LABEL='HeatFlow(Door)' /
&THCP XB= 0.00, 3.60, 0.00, 3.60, 5.70, 5.70,QUANTITY='HEAT FLOW',LABEL='HeatFlow(FUCHS)' /
```

B-16

B.4 ICFMP BE #5

```
&HEAD CHID='ICFMP5_04',TITLE='NRC Benchmark Exercise 5, Test 4' /

&GRID IBAR=36,JBAR=72,KBAR=56 /
&PDIM XBAR0=0.0,XBAR=3.6,YBAR0=-3.6,YBAR=3.6,ZBAR=5.6 /

&TIME TWFIN=1800. /

&MISC TMPA=18.,SURF_DEFAULT='LIGHT CONCRETE',NFRAMES=1800,REACTION='ETHANOL' /

&REAC ID='ETHANOL'
      FYI='Ethanol, C_2 H_6 O'
      EPUMO2=12842.
      DTSAM=10.
      SOOT_YIELD=0.
      CO_YIELD=0.
      MW_FUEL=46.
      NU_O2=3.
      NU_H2O=3.
      NU_CO2=2.
      RADIATIVE_FRACTION=0.20 /

&SURF ID='FIRE',HRRPUA=2041.,RAMP_Q='ramp_e',RGB=1,1,0,TMPWAL=78. /

&RAMP ID='ramp_e',T=    0.,F=0.0  /
&RAMP ID='ramp_e',T=   60.,F=0.12 /
&RAMP ID='ramp_e',T=  120.,F=0.22 /
&RAMP ID='ramp_e',T=  180.,F=0.28 /
&RAMP ID='ramp_e',T=  240.,F=0.29 /
&RAMP ID='ramp_e',T=  300.,F=0.30 /
&RAMP ID='ramp_e',T=  480.,F=0.32 /
&RAMP ID='ramp_e',T=  600.,F=0.33 /
&RAMP ID='ramp_e',T=  900.,F=0.34 /
&RAMP ID='ramp_e',T= 1800.,F=0.36 /

&SURF ID='BURNER',HRRPUA=1111.1,RGB=1,0,0,RAMP_Q='ramp4' /

&RAMP ID='ramp4',T=    0.,F=0.0 /
&RAMP ID='ramp4',T=1200.,F=0.0 /
&RAMP ID='ramp4',T=1201.,F=0.5 /
&RAMP ID='ramp4',T=2100.,F=0.5 /
&RAMP ID='ramp4',T=2120.,F=1.0 /
&RAMP ID='ramp4',T=2280.,F=1.0 /
&RAMP ID='ramp4',T=2300.,F=0.0 /

&SURF ID     = 'CONCRETE'
      RGB    = 0.66,0.66,0.66
      C_P    = 0.88
      DENSITY = 2400.
      KS     = 2.1
      EMISSIVITY=0.75
      DELTA = 0.25 /

&SURF ID     = 'LIGHT CONCRETE'
      RGB    = 0.76,0.76,0.76
      C_P    = 0.84
      DENSITY = 1500.
      KS     = 0.75
      EMISSIVITY=0.75
      DELTA = 0.25 /

&SURF ID     = 'AERATED CONCRETE'
      RGB    = 0.46,0.46,0.46
      C_P    = 1.35
      DENSITY = 420.
```

```
        KS      = 0.11
        EMISSIVITY=0.75
        DELTA = 0.20   /

&SURF ID      = 'PVC IC'
        RGB     = 1,0,0
        TMPIGN= 314.
        HEAT_OF_COMBUSTION=11200.
        HEAT_OF_VAPORIZATION=3910.
        RADIUS=0.007
        EMISSIVITY=0.8
        RAMP_KS='k_pvc'
        RAMP_C_P='cp_pvc'
        DENSITY=1380.  /

&SURF ID      = 'PVC POWER'
        RGB     = 0,1,0
        TMPIGN= 313.
        HEAT_OF_COMBUSTION=18100.
        HEAT_OF_VAPORIZATION=4930.
        RADIUS=0.015
        EMISSIVITY=0.8
        RAMP_KS='k_pvc'
        RAMP_C_P='cp_pvc'
        EMISSIVITY=0.8
        DENSITY=1380.  /


&RAMP ID='k_pvc',T= 23.,F=0.192 /
&RAMP ID='k_pvc',T= 50.,F=0.175 /
&RAMP ID='k_pvc',T= 75.,F=0.172 /
&RAMP ID='k_pvc',T=100.,F=0.147 /
&RAMP ID='k_pvc',T=125.,F=0.141 /
&RAMP ID='k_pvc',T=150.,F=0.134 /
&RAMP ID='cp_pvc',T= 23.,F=1.289 /
&RAMP ID='cp_pvc',T= 50.,F=1.353 /
&RAMP ID='cp_pvc',T= 75.,F=1.407 /
&RAMP ID='cp_pvc',T=100.,F=1.469 /
&RAMP ID='cp_pvc',T=125.,F=1.530 /
&RAMP ID='cp_pvc',T=150.,F=1.586 /


&SURF ID                 = 'STEEL SHEET'
        RGB              = 0.20,0.20,0.20
        C_DELTA_RHO      = 28.
        BACKING          = 'EXPOSED'
        DELTA            = 0.00635 /

&SURF ID='HOOD',VOLUME_FLUX=2.76,RGB=0,0,1 /

&OBST XB= 2.60, 3.30, 1.50, 2.20, 0.30, 0.70,SURF_IDS='FIRE','STEEL SHEET','STEEL SHEET' /

&OBST XB= 2.35, 3.60, 1.10, 2.60, 0.00, 0.30,SURF_ID='AERATED CONCRETE' / Base for fire pan
&OBST XB= 2.15, 2.35, 0.00, 3.60, 0.00, 1.40,SURF_ID='AERATED CONCRETE' / 1.4 m high Divider

&OBST XB= 0.35, 0.35, 1.80, 2.40, 0.50, 4.50,SURF_ID='STEEL SHEET' / Cable Tray
&OBST XB= 0.30, 0.40, 1.80, 1.80, 0.50, 4.50,SURF_ID='STEEL SHEET' /
&OBST XB= 0.30, 0.40, 2.40, 2.40, 0.50, 4.50,SURF_ID='STEEL SHEET' /

&OBST XB= 0.35, 0.45, 1.95, 2.05, 0.50, 4.50,SURF_ID='PVC IC' /      Cables
&OBST XB= 0.35, 0.45, 2.15, 2.25, 0.50, 4.50,SURF_ID='PVC POWER' /

Burner
&OBST XB= 0.45, 0.75, 1.95, 2.25, 0.00, 0.40,SURF_IDS='BURNER','STEEL SHEET','STEEL SHEET' /

&OBST XB= 0.00, 1.45, -.25, 0.00, 0.00, 5.60,SURF_ID='LIGHT CONCRETE' /  Walls surrounding door
&OBST XB= 2.15, 3.60, -.25, 0.00, 0.00, 5.60,SURF_ID='LIGHT CONCRETE' /
&OBST XB= 1.45, 2.15, -.25, 0.00, 3.60, 5.60,SURF_ID='LIGHT CONCRETE' /
&OBST XB= 1.45, 2.15, -.10, 0.00, 0.00, 1.40,SURF_ID='AERATED CONCRETE' /  Door Blocker

&OBST XB= 0.35, 0.35,-2.90,-0.25, 2.60, 4.60,SURF_ID='STEEL SHEET' /  Hood
&OBST XB= 3.25, 3.25,-2.90,-0.25, 2.60, 4.60,SURF_ID='STEEL SHEET' /  Hood
&OBST XB= 0.35, 3.25,-2.90,-2.90, 2.60, 4.60,SURF_ID='STEEL SHEET' /  Hood
```

B-18

```
&OBST XB= 0.35,  1.30,-2.90,-0.25,  4.60,  4.60,SURF_ID='STEEL SHEET' /   Hood
&OBST XB= 2.30,  3.25,-2.90,-0.25,  4.60,  4.60,SURF_ID='STEEL SHEET' /   Hood
&OBST XB= 1.30,  2.30,-2.90,-1.95,  4.60,  4.60,SURF_ID='STEEL SHEET' /   Hood
&OBST XB= 1.30,  2.30,-0.95,-0.25,  4.60,  4.60,SURF_ID='STEEL SHEET' /   Hood
&OBST XB= 1.30,  2.30,-1.95,-0.95,  4.60,  5.60,SURF_IDS='STEEL SHEET','STEEL SHEET','HOOD' /
Exhaust

&VENT XB= 0.00,  0.00,-3.60,-0.25,  0.00,  5.60,SURF_ID='OPEN' /
&VENT XB= 3.60,  3.60,-3.60,-0.25,  0.00,  5.60,SURF_ID='OPEN' /
&VENT CB='YBAR0',SURF_ID='OPEN' /
&VENT CB='ZBAR0',SURF_ID='CONCRETE' /  Floor

&SLCF PBX=1.8,QUANTITY='TEMPERATURE',VECTOR=.TRUE. /
&SLCF PBX=1.8,QUANTITY='HRRPUV' /
&SLCF PBX=1.8,QUANTITY='MIXTURE_FRACTION' /

&SLCF PBY=2.1,QUANTITY='TEMPERATURE',VECTOR=.TRUE. /
&SLCF PBY=2.1,QUANTITY='HRRPUV' /
&SLCF PBY=2.1,QUANTITY='MIXTURE_FRACTION' /

&BNDF QUANTITY='WALL_TEMPERATURE' /
&BNDF QUANTITY='GAUGE_HEAT_FLUX' /
&BNDF QUANTITY='INCIDENT_HEAT_FLUX' /
&BNDF QUANTITY='HEAT_FLUX' /
&BNDF QUANTITY='CONVECTIVE_FLUX' /
&BNDF QUANTITY='RADIATIVE_FLUX' /
&BNDF QUANTITY='BURNING_RATE' /

&PL3D DTSAM=60. /

TC Trees

&THCP XYZ= 2.90, 1.80, 0.40, QUANTITY='TEMPERATURE',LABEL='TP_1', DTSAM=10. /
&THCP XYZ= 2.90, 1.80, 1.20, QUANTITY='TEMPERATURE',LABEL='TP_2' /
&THCP XYZ= 2.90, 1.80, 2.00, QUANTITY='TEMPERATURE',LABEL='TP_3' /
&THCP XYZ= 2.90, 1.80, 2.80, QUANTITY='TEMPERATURE',LABEL='TP_4' /
&THCP XYZ= 2.90, 1.80, 3.60, QUANTITY='TEMPERATURE',LABEL='TP_5' /
&THCP XYZ= 2.90, 1.80, 4.40, QUANTITY='TEMPERATURE',LABEL='TP_6' /
&THCP XYZ= 2.90, 1.80, 5.20, QUANTITY='TEMPERATURE',LABEL='TP_7' /

&THCP XYZ= 0.60, 0.60, 0.40, QUANTITY='TEMPERATURE',LABEL='TR_1-1' /
&THCP XYZ= 0.60, 0.60, 1.20, QUANTITY='TEMPERATURE',LABEL='TR_1-2' /
&THCP XYZ= 0.60, 0.60, 2.00, QUANTITY='TEMPERATURE',LABEL='TR_1-3' /
&THCP XYZ= 0.60, 0.60, 2.80, QUANTITY='TEMPERATURE',LABEL='TR_1-4' /
&THCP XYZ= 0.60, 0.60, 3.60, QUANTITY='TEMPERATURE',LABEL='TR_1-5' /
&THCP XYZ= 0.60, 0.60, 4.40, QUANTITY='TEMPERATURE',LABEL='TR_1-6' /
&THCP XYZ= 0.60, 0.60, 5.20, QUANTITY='TEMPERATURE',LABEL='TR_1-7' /

&THCP XYZ= 3.00, 0.60, 0.40, QUANTITY='TEMPERATURE',LABEL='TR_2-1' /
&THCP XYZ= 3.00, 0.60, 1.20, QUANTITY='TEMPERATURE',LABEL='TR_2-2' /
&THCP XYZ= 3.00, 0.60, 2.00, QUANTITY='TEMPERATURE',LABEL='TR_2-3' /
&THCP XYZ= 3.00, 0.60, 2.80, QUANTITY='TEMPERATURE',LABEL='TR_2-4' /
&THCP XYZ= 3.00, 0.60, 3.60, QUANTITY='TEMPERATURE',LABEL='TR_2-5' /
&THCP XYZ= 3.00, 0.60, 4.40, QUANTITY='TEMPERATURE',LABEL='TR_2-6' /
&THCP XYZ= 3.00, 0.60, 5.20, QUANTITY='TEMPERATURE',LABEL='TR_2-7' /

&THCP XYZ= 3.00, 3.00, 0.40, QUANTITY='TEMPERATURE',LABEL='TR_3-1' /
&THCP XYZ= 3.00, 3.00, 1.20, QUANTITY='TEMPERATURE',LABEL='TR_3-2' /
&THCP XYZ= 3.00, 3.00, 2.00, QUANTITY='TEMPERATURE',LABEL='TR_3-3' /
&THCP XYZ= 3.00, 3.00, 2.80, QUANTITY='TEMPERATURE',LABEL='TR_3-4' /
&THCP XYZ= 3.00, 3.00, 3.60, QUANTITY='TEMPERATURE',LABEL='TR_3-5' /
&THCP XYZ= 3.00, 3.00, 4.40, QUANTITY='TEMPERATURE',LABEL='TR_3-6' /
&THCP XYZ= 3.00, 3.00, 5.20, QUANTITY='TEMPERATURE',LABEL='TR_3-7' /

&THCP XYZ= 0.60, 3.00, 0.40, QUANTITY='TEMPERATURE',LABEL='TR_4-1' /
&THCP XYZ= 0.60, 3.00, 1.20, QUANTITY='TEMPERATURE',LABEL='TR_4-2' /
&THCP XYZ= 0.60, 3.00, 2.00, QUANTITY='TEMPERATURE',LABEL='TR_4-3' /
&THCP XYZ= 0.60, 3.00, 2.80, QUANTITY='TEMPERATURE',LABEL='TR_4-4' /
&THCP XYZ= 0.60, 3.00, 3.60, QUANTITY='TEMPERATURE',LABEL='TR_4-5' /
&THCP XYZ= 0.60, 3.00, 4.40, QUANTITY='TEMPERATURE',LABEL='TR_4-6' /
&THCP XYZ= 0.60, 3.00, 5.20, QUANTITY='TEMPERATURE',LABEL='TR_4-7' /
```

```
&THCP XYZ= 0.85, 2.20, 0.40, QUANTITY='TEMPERATURE',LABEL='TR_5-1' /
&THCP XYZ= 0.85, 2.20, 1.20, QUANTITY='TEMPERATURE',LABEL='TR_5-2' /
&THCP XYZ= 0.85, 2.20, 2.00, QUANTITY='TEMPERATURE',LABEL='TR_5-3' /
&THCP XYZ= 0.85, 2.20, 2.80, QUANTITY='TEMPERATURE',LABEL='TR_5-4' /
&THCP XYZ= 0.85, 2.20, 3.60, QUANTITY='TEMPERATURE',LABEL='TR_5-5' /
&THCP XYZ= 0.85, 2.20, 4.40, QUANTITY='TEMPERATURE',LABEL='TR_5-6' /
&THCP XYZ= 0.85, 2.20, 5.20, QUANTITY='TEMPERATURE',LABEL='TR_5-7' /

&THCP XYZ= 2.60, 3.60, 0.40, QUANTITY='WALL_TEMPERATURE',LABEL='TW_1-1',IOR=-2 /
&THCP XYZ= 2.60, 3.60, 1.20, QUANTITY='WALL_TEMPERATURE',LABEL='TW_1-2',IOR=-2 /
&THCP XYZ= 2.60, 3.60, 2.00, QUANTITY='WALL_TEMPERATURE',LABEL='TW_1-3',IOR=-2 /
&THCP XYZ= 2.60, 3.60, 2.80, QUANTITY='WALL_TEMPERATURE',LABEL='TW_1-4',IOR=-2 /
&THCP XYZ= 2.60, 3.60, 3.60, QUANTITY='WALL_TEMPERATURE',LABEL='TW_1-5',IOR=-2 /
&THCP XYZ= 2.60, 3.60, 4.40, QUANTITY='WALL_TEMPERATURE',LABEL='TW_1-6',IOR=-2 /
&THCP XYZ= 2.60, 3.60, 5.20, QUANTITY='WALL_TEMPERATURE',LABEL='TW_1-7',IOR=-2 /

&THCP XYZ= 0.00, 2.20, 0.40, QUANTITY='WALL_TEMPERATURE',LABEL='TW_2-1',IOR=1 /
&THCP XYZ= 0.00, 2.20, 1.20, QUANTITY='WALL_TEMPERATURE',LABEL='TW_2-2',IOR=1 /
&THCP XYZ= 0.00, 2.20, 2.00, QUANTITY='WALL_TEMPERATURE',LABEL='TW_2-3',IOR=1 /
&THCP XYZ= 0.00, 2.20, 2.80, QUANTITY='WALL_TEMPERATURE',LABEL='TW_2-4',IOR=1 /
&THCP XYZ= 0.00, 2.20, 3.60, QUANTITY='WALL_TEMPERATURE',LABEL='TW_2-5',IOR=1 /
&THCP XYZ= 0.00, 2.20, 4.40, QUANTITY='WALL_TEMPERATURE',LABEL='TW_2-6',IOR=1 /
&THCP XYZ= 0.00, 2.20, 5.20, QUANTITY='WALL_TEMPERATURE',LABEL='TW_2-7',IOR=1 /

&THCP XYZ= 3.10, 1.60, 0.70, QUANTITY='WALL_TEMPERATURE',LABEL='T E',IOR=3 /

&THCP XYZ= 1.80,-0.15, 1.60, QUANTITY='TEMPERATURE',LABEL='TB_2-1' /
&THCP XYZ= 1.80,-0.15, 2.05, QUANTITY='TEMPERATURE',LABEL='TB_2-2' /
&THCP XYZ= 1.80,-0.15, 2.50, QUANTITY='TEMPERATURE',LABEL='TB_2-3' /
&THCP XYZ= 1.80,-0.15, 2.95, QUANTITY='TEMPERATURE',LABEL='TB_2-4' /
&THCP XYZ= 1.80,-0.15, 3.40, QUANTITY='TEMPERATURE',LABEL='TB_2-5' /

&THCP XYZ= 3.59, 2.15, 1.05, QUANTITY='TEMPERATURE',LABEL='TB_3' /

&THCP XYZ= 1.80,-1.80, 4.50, QUANTITY='TEMPERATURE',LABEL='TB_4' /

&THCP XYZ= 2.60, 3.60, 1.20, QUANTITY='BACK_WALL_TEMPERATURE',LABEL='TWO_1',IOR=-2 /
&THCP XYZ= 0.00, 2.20, 1.20, QUANTITY='BACK_WALL_TEMPERATURE',LABEL='TWO_2',IOR= 1 /

&THCP XYZ= 0.44, 2.24, 1.20, QUANTITY='WALL_TEMPERATURE',LABEL='TCO_1-1',IOR=1 /
&THCP XYZ= 0.44, 2.24, 1.60, QUANTITY='WALL_TEMPERATURE',LABEL='TCO_1-2',IOR=1 /
&THCP XYZ= 0.44, 2.24, 2.00, QUANTITY='WALL_TEMPERATURE',LABEL='TCO_1-3',IOR=1 /
&THCP XYZ= 0.44, 2.24, 2.40, QUANTITY='WALL_TEMPERATURE',LABEL='TCO_1-4',IOR=1 /
&THCP XYZ= 0.44, 2.24, 2.80, QUANTITY='WALL_TEMPERATURE',LABEL='TCO_1-5',IOR=1 /
&THCP XYZ= 0.44, 2.24, 3.20, QUANTITY='WALL_TEMPERATURE',LABEL='TCO_1-6',IOR=1 /
&THCP XYZ= 0.44, 2.24, 3.60, QUANTITY='WALL_TEMPERATURE',LABEL='TCO_1-7',IOR=1 /
&THCP XYZ= 0.44, 2.24, 4.00, QUANTITY='WALL_TEMPERATURE',LABEL='TCO_1-8',IOR=1 /
&THCP XYZ= 0.44, 2.24, 4.40, QUANTITY='WALL_TEMPERATURE',LABEL='TCO_1-9',IOR=1 /

&THCP XYZ= 0.44, 2.05, 1.20, QUANTITY='WALL_TEMPERATURE',LABEL='TCO_3-1',IOR=1 /
&THCP XYZ= 0.44, 2.05, 1.60, QUANTITY='WALL_TEMPERATURE',LABEL='TCO_3-2',IOR=1 /
&THCP XYZ= 0.44, 2.05, 2.00, QUANTITY='WALL_TEMPERATURE',LABEL='TCO_3-3',IOR=1 /
&THCP XYZ= 0.44, 2.05, 2.40, QUANTITY='WALL_TEMPERATURE',LABEL='TCO_3-4',IOR=1 /
&THCP XYZ= 0.44, 2.05, 2.80, QUANTITY='WALL_TEMPERATURE',LABEL='TCO_3-5',IOR=1 /
&THCP XYZ= 0.44, 2.05, 3.20, QUANTITY='WALL_TEMPERATURE',LABEL='TCO_3-6',IOR=1 /
&THCP XYZ= 0.44, 2.05, 3.60, QUANTITY='WALL_TEMPERATURE',LABEL='TCO_3-7',IOR=1 /
&THCP XYZ= 0.44, 2.05, 4.00, QUANTITY='WALL_TEMPERATURE',LABEL='TCO_3-8',IOR=1 /
&THCP XYZ= 0.44, 2.05, 4.40, QUANTITY='WALL_TEMPERATURE',LABEL='TCO_3-9',IOR=1 /

&THCP XYZ= 0.41, 2.13, 1.20, QUANTITY='GAUGE_HEAT_FLUX',LABEL='WS_1',IOR=1 /
&THCP XYZ= 0.41, 2.13, 2.00, QUANTITY='GAUGE_HEAT_FLUX',LABEL='WS_2',IOR=1 /
&THCP XYZ= 0.41, 2.13, 2.80, QUANTITY='GAUGE_HEAT_FLUX',LABEL='WS_3',IOR=1 /
&THCP XYZ= 0.41, 2.13, 3.60, QUANTITY='GAUGE_HEAT_FLUX',LABEL='WS_4',IOR=1 /
&THCP XYZ= 0.41, 2.13, 4.40, QUANTITY='GAUGE_HEAT_FLUX',LABEL='WS_5',IOR=1 /

&THCP XYZ= 2.90, 1.80, 1.20, QUANTITY='PRESSURE',LABEL='DP_1-1' /
&THCP XYZ= 2.90, 1.80, 2.80, QUANTITY='PRESSURE',LABEL='DP_1-2' /
&THCP XYZ= 2.90, 1.80, 4.40, QUANTITY='PRESSURE',LABEL='DP_1-3' /

&THCP XYZ= 1.80,-0.15, 1.60, QUANTITY='PRESSURE',LABEL='DP_2-1' /
```

```
&THCP XYZ= 1.80,-0.15, 2.05, QUANTITY='PRESSURE',LABEL='DP_2-2' /
&THCP XYZ= 1.80,-0.15, 2.50, QUANTITY='PRESSURE',LABEL='DP_2-3' /
&THCP XYZ= 1.80,-0.15, 2.95, QUANTITY='PRESSURE',LABEL='DP_2-4' /
&THCP XYZ= 1.80,-0.15, 3.40, QUANTITY='PRESSURE',LABEL='DP_2-5' /

&THCP XYZ= 3.59, 2.15, 1.05, QUANTITY='PRESSURE',LABEL='DP_3' /

&THCP XYZ= 1.80,-1.80, 4.50, QUANTITY='PRESSURE',LABEL='DP_4' /

&THCP XYZ= 0.10, 0.65, 0.55, QUANTITY='PRESSURE',LABEL='DP_5-1' /
&THCP XYZ= 0.10, 0.65, 2.75, QUANTITY='PRESSURE',LABEL='DP_5-2' /
&THCP XYZ= 0.10, 0.65, 4.95, QUANTITY='PRESSURE',LABEL='DP_5-3' /

&THCP XYZ= 0.30, 2.10, 2.00, QUANTITY='oxygen',          LABEL='GA1-O2' /
&THCP XYZ= 0.30, 2.10, 2.00, QUANTITY='carbon monoxide',LABEL='GA1-CO' /
&THCP XYZ= 0.30, 2.10, 2.00, QUANTITY='carbon dioxide', LABEL='GA1-CO2' /

&THCP XYZ= 0.30, 2.10, 4.40, QUANTITY='oxygen',          LABEL='GA2-O2' /
&THCP XYZ= 0.30, 2.10, 4.40, QUANTITY='carbon monoxide',LABEL='GA2-CO' /
&THCP XYZ= 0.30, 2.10, 4.40, QUANTITY='carbon dioxide', LABEL='GA2-CO2' /

&THCP XB= 1.45, 2.15, 0.00, 0.00, 1.40, 3.60,QUANTITY='MASS FLOW',LABEL='Gin + Gout(Door)' /
&THCP XB= 1.45, 2.15, 0.00, 0.00, 1.40, 3.60,QUANTITY='HEAT FLOW',LABEL='Heat Flow(Door)' /
```

B.5 FM/SNL Test Series

```
&HEAD CHID='FM_SNL_composite',TITLE='FM-SNL Test Series' /

&GRID IBAR=48,JBAR=48,KBAR=120 /
&PDIM XBAR0=11.0,XBAR=13.4,YBAR0=4.9,YBAR=7.3,ZBAR=6.1 /
&GRID IBAR=64,JBAR=24,KBAR=32 /
&PDIM XBAR0= 0.0,XBAR=13.4,YBAR0=0.0,YBAR=4.9,ZBAR=6.1 /
&GRID IBAR=54,JBAR=12,KBAR=32 /
&PDIM XBAR0= 0.0,XBAR=11.0,YBAR0=4.9,YBAR= 7.3,ZBAR=6.1 /
&GRID IBAR=64,JBAR=24,KBAR=32 /
&PDIM XBAR0= 0.0,XBAR=13.4,YBAR0=7.3,YBAR=12.2,ZBAR=6.1 /
&GRID IBAR=24,JBAR=64,KBAR=32 /
&PDIM XBAR0=13.4,XBAR=18.3,YBAR0=0.0,YBAR=12.2,ZBAR=6.1 /

&TIME TWFIN=900.,SYNCHRONIZE=.TRUE. /   1800 s for Test 21

&MISC TMPA=21.,SURF_DEFAULT='MARINITE',REACTION='PROPENE' /

&REAC ID='PROPENE'
      FYI='Propylene, C_3 H_6'
      MW_FUEL=42
      NU_O2=4.5
      NU_CO2=3.
      NU_H2O=3.
      DTSAM=5.
      SOOT_YIELD=0.02 /

&SURF ID='MARINITE',DENSITY=1000.,C_P=1.16,KS=0.23,DELTA=0.025,RGB=.7,.7,.7 /

&SURF ID='burner4',HRRPUA=806.,RAMP_Q='fire',RGB=1,0,0 /
&SURF ID='burner5',HRRPUA=806.,RAMP_Q='fire',RGB=1,0,0 /
&RAMP ID='fire',T=  0.0,F=0.0 /
&RAMP ID='fire',T= 60.0,F=0.0625 /
&RAMP ID='fire',T=120.0,F=0.25   /
&RAMP ID='fire',T=180.0,F=0.5625 /
&RAMP ID='fire',T=240.0,F=1.0    /
&RAMP ID='fire',T=600.0,F=1.0    /
&RAMP ID='fire',T=601.0,F=0.0    /

&SURF ID='burner21',HRRPUA=734.,RAMP_Q='fire21',RGB=1,0,0 /
&RAMP ID='fire21',T=   0.0,F=0.0 /
&RAMP ID='fire21',T=  60.0,F=0.0625 /
&RAMP ID='fire21',T= 120.0,F=0.25   /
&RAMP ID='fire21',T= 180.0,F=0.5625 /
&RAMP ID='fire21',T= 240.0,F=1.0    /
&RAMP ID='fire21',T=1140.0,F=1.0    /
&RAMP ID='fire21',T=1141.0,F=0.0    /

&SURF ID='duct4',VOLUME_FLUX=-0.11,RGB=0,0,1 /
&SURF ID='duct5',VOLUME_FLUX=-0.76,RGB=0,0,1,RAMP_V='ductramp5' /
&RAMP ID='ductramp5',T=  0.,F=0. /
&RAMP ID='ductramp5',T=  1.,F=1. /
&RAMP ID='ductramp5',T=540.,F=1. /
&RAMP ID='ductramp5',T=541.,F=0. /

&OBST XB=11.8,12.6, 5.7,6.5,0.0,0.2,SURF_IDS='burner4', 'MARINITE','MARINITE' /sand burner
cOBST XB=11.8,12.6, 5.7,6.5,0.0,0.2,SURF_IDS='burner5','MARINITE','MARINITE' /sand burner
cOBST XB= 8.7, 9.5, 7.4,8.2,0.0,0.2,SURF_IDS='burner21','MARINITE','MARINITE' /sand burner

cOBST XB= 8.5, 9.7, 8.8,8.8,0.0,2.4,SURF_ID='STEEL' / cabinet back panel
cOBST XB= 8.5, 8.5, 6.8,8.8,0.0,2.4,SURF_ID='STEEL' / cabinet side panel
cOBST XB= 9.7, 9.7, 6.8,8.8,0.0,2.4,SURF_ID='STEEL' / cabinet side panel
cOBST XB= 8.5, 9.7, 6.8,8.8,2.4,2.4,SURF_ID='STEEL' / cabinet top  panel

&OBST XB= 2.8, 3.4, 2.8, 3.4, 4.9, 6.1, SURF_IDS='MARINITE','MARINITE','duct' /#1 injection duct
```

```
&OBST XB= 2.8, 3.4, 2.8, 3.4, 4.6, 4.6 / deflector plate

&OBST XB= 8.9, 9.5, 2.8, 3.4, 4.9, 6.1, SURF_IDS='MARINITE','MARINITE','duct' /#2 injection duct
&OBST XB= 8.9, 9.5, 2.8, 3.4, 4.6, 4.6 / deflector plate

&OBST XB=15.0,15.6, 2.8, 3.4, 4.9, 6.1, SURF_IDS='MARINITE','MARINITE','duct' /#3 injection duct
&OBST XB=15.0,15.6, 2.8, 3.4, 4.6, 4.6 / deflector plate

&OBST XB= 2.8, 3.4, 8.9, 9.5, 4.9, 6.1, SURF_IDS='MARINITE','MARINITE','duct' /#4 injection duct
&OBST XB= 2.8, 3.4, 8.9, 9.5, 4.6, 4.6 / deflector plate

&OBST XB= 8.9, 9.5, 8.9, 9.5, 4.9, 6.1, SURF_IDS='MARINITE','MARINITE','duct' /#5 injection duct
&OBST XB= 8.9, 9.5, 8.9, 9.5, 4.6, 4.6 / deflector plate

&OBST XB=15.0,15.6, 8.9, 9.5, 4.9, 6.1, SURF_IDS='MARINITE','MARINITE','duct' /#6 injection duct
&OBST XB=15.0,15.6, 8.9, 9.5, 4.6, 4.6 / deflector plate

&VENT XB= 0.0, 0.6, 5.2, 7.0, 6.1, 6.1, SURF_ID='OPEN' / exhaust vent

&SLCF PBY=6.1,QUANTITY='TEMPERATURE',VECTOR=.TRUE. /

&THCP XYZ= 3.05, 6.10,5.98,QUANTITY='TEMPERATURE',LABEL='Sector3 Ch11',DTSAM=5 /
&THCP XYZ= 3.05, 6.10,5.49,QUANTITY='TEMPERATURE',LABEL='Sector3 Ch12' /
&THCP XYZ= 3.05, 6.10,4.27,QUANTITY='TEMPERATURE',LABEL='Sector3 Ch13' /
&THCP XYZ= 3.05, 6.10,3.05,QUANTITY='TEMPERATURE',LABEL='Sector3 Ch14' /
&THCP XYZ= 3.05, 6.10,1.83,QUANTITY='TEMPERATURE',LABEL='Sector3 Ch15' /
&THCP XYZ= 9.15, 6.10,5.98,QUANTITY='TEMPERATURE',LABEL='Sector2 Ch6' /
&THCP XYZ= 9.15, 6.10,5.49,QUANTITY='TEMPERATURE',LABEL='Sector2 Ch7' /
&THCP XYZ= 9.15, 6.10,4.27,QUANTITY='TEMPERATURE',LABEL='Sector2 Ch8' /
&THCP XYZ= 9.15, 6.10,3.05,QUANTITY='TEMPERATURE',LABEL='Sector2 Ch9' /
&THCP XYZ= 9.15, 6.10,1.83,QUANTITY='TEMPERATURE',LABEL='Sector2 Ch10' /
&THCP XYZ=15.25, 6.10,5.98,QUANTITY='TEMPERATURE',LABEL='Sector1 Ch1' /
&THCP XYZ=15.25, 6.10,5.49,QUANTITY='TEMPERATURE',LABEL='Sector1 Ch2' /
&THCP XYZ=15.25, 6.10,4.27,QUANTITY='TEMPERATURE',LABEL='Sector1 Ch3' /
&THCP XYZ=15.25, 6.10,3.05,QUANTITY='TEMPERATURE',LABEL='Sector1 Ch4' /
&THCP XYZ=15.25, 6.10,1.83,QUANTITY='TEMPERATURE',LABEL='Sector1 Ch5' /
&THCP XYZ=15.25, 1.52,5.98,QUANTITY='TEMPERATURE',LABEL='Station1 Ch16' /
&THCP XYZ=15.25, 1.52,5.49,QUANTITY='TEMPERATURE',LABEL='Station1 Ch41' /
&THCP XYZ=15.25, 1.52,4.27,QUANTITY='TEMPERATURE',LABEL='Station1 Ch42' /
&THCP XYZ=15.25, 1.52,3.05,QUANTITY='TEMPERATURE',LABEL='Station1 Ch43' /
&THCP XYZ=15.25, 1.52,1.83,QUANTITY='TEMPERATURE',LABEL='Station1 Ch44' /
&THCP XYZ= 9.14, 1.52,5.98,QUANTITY='TEMPERATURE',LABEL='Station2 Ch17' /
&THCP XYZ= 9.14, 1.52,5.49,QUANTITY='TEMPERATURE',LABEL='Station2 Ch45' /
&THCP XYZ= 9.14, 1.52,4.27,QUANTITY='TEMPERATURE',LABEL='Station2 Ch46' /
&THCP XYZ= 9.14, 1.52,3.05,QUANTITY='TEMPERATURE',LABEL='Station2 Ch47' /
&THCP XYZ= 9.14, 1.52,1.83,QUANTITY='TEMPERATURE',LABEL='Station2 Ch48' /
&THCP XYZ= 3.05, 1.52,5.98,QUANTITY='TEMPERATURE',LABEL='Station3 Ch18' /
&THCP XYZ=.3.05, 1.52,5.49,QUANTITY='TEMPERATURE',LABEL='Station3 Ch49' /
&THCP XYZ= 3.05, 1.52,4.27,QUANTITY='TEMPERATURE',LABEL='Station3 Ch50' /
&THCP XYZ= 3.05, 1.52,3.05,QUANTITY='TEMPERATURE',LABEL='Station3 Ch51' /
&THCP XYZ= 3.05, 1.52,1.83,QUANTITY='TEMPERATURE',LABEL='Station3 Ch52' /
&THCP XYZ=12.19, 3.05,5.98,QUANTITY='TEMPERATURE',LABEL='Station4 Ch19' /
&THCP XYZ=12.19, 3.05,5.49,QUANTITY='TEMPERATURE',LABEL='Station4 Ch53' /
&THCP XYZ=12.19, 3.05,4.27,QUANTITY='TEMPERATURE',LABEL='Station4 Ch54' /
&THCP XYZ=12.19, 3.05,3.05,QUANTITY='TEMPERATURE',LABEL='Station4 Ch55' /
&THCP XYZ=12.19, 3.05,1.83,QUANTITY='TEMPERATURE',LABEL='Station4 Ch56' /
&THCP XYZ= 6.10, 3.05,5.98,QUANTITY='TEMPERATURE',LABEL='Station5 Ch20' /
&THCP XYZ= 6.10, 3.05,5.49,QUANTITY='TEMPERATURE',LABEL='Station5 Ch57' /
&THCP XYZ= 6.10, 3.05,4.27,QUANTITY='TEMPERATURE',LABEL='Station5 Ch58' /
&THCP XYZ= 6.10, 3.05,3.05,QUANTITY='TEMPERATURE',LABEL='Station5 Ch59' /
&THCP XYZ= 6.10, 3.05,1.83,QUANTITY='TEMPERATURE',LABEL='Station5 Ch60' /
&THCP XYZ=12.19, 9.14,5.98,QUANTITY='TEMPERATURE',LABEL='Station6 Ch21' /
&THCP XYZ=12.19, 9.14,5.49,QUANTITY='TEMPERATURE',LABEL='Station6 Ch61' /
&THCP XYZ=12.19, 9.14,4.27,QUANTITY='TEMPERATURE',LABEL='Station6 Ch62' /
&THCP XYZ=12.19, 9.14,3.05,QUANTITY='TEMPERATURE',LABEL='Station6 Ch63' /
&THCP XYZ=12.19, 9.14,1.83,QUANTITY='TEMPERATURE',LABEL='Station6 Ch64' /
&THCP XYZ= 6.10, 9.14,5.98,QUANTITY='TEMPERATURE',LABEL='Station7 Ch22' /
&THCP XYZ= 6.10, 9.14,5.49,QUANTITY='TEMPERATURE',LABEL='Station7 Ch65' /
&THCP XYZ= 6.10, 9.14,4.27,QUANTITY='TEMPERATURE',LABEL='Station7 Ch66' /
&THCP XYZ= 6.10, 9.14,3.05,QUANTITY='TEMPERATURE',LABEL='Station7 Ch67' /
&THCP XYZ= 6.10, 9.14,1.83,QUANTITY='TEMPERATURE',LABEL='Station7 Ch68' /
```

```
&THCP XYZ=15.24,10.67,5.98,QUANTITY='TEMPERATURE',LABEL='Station8 Ch23' /
&THCP XYZ=15.24,10.67,5.49,QUANTITY='TEMPERATURE',LABEL='Station8 Ch69' /
&THCP XYZ=15.24,10.67,4.27,QUANTITY='TEMPERATURE',LABEL='Station8 Ch70' /
&THCP XYZ=15.24,10.67,3.05,QUANTITY='TEMPERATURE',LABEL='Station8 Ch71' /
&THCP XYZ=15.24,10.67,1.83,QUANTITY='TEMPERATURE',LABEL='Station8 Ch72' /
&THCP XYZ= 9.14,10.67,5.98,QUANTITY='TEMPERATURE',LABEL='Station9 Ch24' /
&THCP XYZ= 9.14,10.67,5.49,QUANTITY='TEMPERATURE',LABEL='Station9 Ch73' /
&THCP XYZ= 9.14,10.67,4.27,QUANTITY='TEMPERATURE',LABEL='Station9 Ch74' /
&THCP XYZ= 9.14,10.67,3.05,QUANTITY='TEMPERATURE',LABEL='Station9 Ch75' /
&THCP XYZ= 9.14,10.67,1.83,QUANTITY='TEMPERATURE',LABEL='Station9 Ch76' /
&THCP XYZ= 3.05,10.67,5.98,QUANTITY='TEMPERATURE',LABEL='Station10 Ch25' /
&THCP XYZ= 3.05,10.67,5.49,QUANTITY='TEMPERATURE',LABEL='Station10 Ch77' /
&THCP XYZ= 3.05,10.67,4.27,QUANTITY='TEMPERATURE',LABEL='Station10 Ch78' /
&THCP XYZ= 3.05,10.67,3.05,QUANTITY='TEMPERATURE',LABEL='Station10 Ch79' /
&THCP XYZ= 3.05,10.67,1.83,QUANTITY='TEMPERATURE',LABEL='Station10 Ch80' /
&THCP XYZ=16.76, 4.57,5.98,QUANTITY='TEMPERATURE',LABEL='Station11 Ch26' /
&THCP XYZ= 1.52, 4.57,5.98,QUANTITY='TEMPERATURE',LABEL='Station12 Ch27' /
&THCP XYZ=12.19, 6.10,5.98,QUANTITY='TEMPERATURE',LABEL='Station13 Ch28' / (Centerline Plume)
&THCP XYZ= 6.10, 6.10,5.98,QUANTITY='TEMPERATURE',LABEL='Station14 Ch29' /
&THCP XYZ=16.76, 7.62,5.98,QUANTITY='TEMPERATURE',LABEL='Station15 Ch30' /
&THCP XYZ= 1.52, 7.62,5.98,QUANTITY='TEMPERATURE',LABEL='Station16 Ch31' /
```

B-24

B.6 NBS Multi-Room Test Series

```
&HEAD CHID='NBS_composite',TITLE='NBS Multiroom Tests' /

&GRID IBAR=24,JBAR=34,KBAR=22 /
&PDIM XBAR0= 9.8,XBAR=12.2,YBAR0=0.0,YBAR=3.4,ZBAR=2.2 /

&GRID IBAR=122,JBAR=24,KBAR=24 /
&PDIM XBAR0= 0.0,XBAR=12.2,YBAR0=3.4,YBAR=5.8,ZBAR=2.4 /

cGRID IBAR=122,JBAR=24,KBAR=24 /
cPDIM XBAR0= 2.4,XBAR= 4.6,YBAR0=0.0,YBAR=3.4,ZBAR=2.4 /

&TIME TWFIN=1200. /
&MISC TMPA=23.,NFRAMES=2400,SURF_DEFAULT='GYPSUM BOARD',REACTION='METHANE' /

&SURF ID='burner',HRRPUA=1222.,RGB=1,0,0,RAMP_Q='burner_ramp' /
&RAMP ID='burner_ramp',T=   0.,F=0. /
&RAMP ID='burner_ramp',T=   1.,F=1. /
&RAMP ID='burner_ramp',T=900.,F=1. /
&RAMP ID='burner_ramp',T=901.,F=0. /

&SURF ID     = 'GYPSUM BOARD'
      FYI    = 'NBSIR 88-3752'
      RGB    = 0.80,0.80,0.70
      KS     = 0.17
      C_P    = 1.09
      DENSITY=  930.
      DELTA  = 0.013 /

&SURF ID     = 'CALCIUM SILICATE'
      FYI    = 'NBSIR 88-3752'
      RGB    = 0.70,0.70,0.70
      KS     = 0.12
      C_P    = 1.25
      DENSITY=  720.
      EMISSIVITY = 0.83
      DELTA  = 0.013 /

&SURF ID     = 'CERAMIC FIBER'
      FYI    = 'NBSIR 88-3752'
      RGB    = 0.40,0.40,0.40
      KS     = 0.09
      C_P    = 1.04
      DENSITY=  128.
      EMISSIVITY = 0.97
      DELTA  = 0.050 /

&SURF ID     = 'FIRE BRICK'
      FYI    = 'NBSIR 88-3752'
      RGB    = 0.90,0.60,0.60
      KS     = 0.36
      C_P    = 1.04
      DENSITY=  750.
      EMISSIVITY = 0.80
      DELTA  = 0.113 /

&SURF ID     = 'CONCRETE'
      FYI    = 'NBSIR 88-3752'
      RGB    = 0.60,0.60,0.60
      KS     = 1.8
      C_P    = 1.04
      DENSITY= 2280.
      DELTA  = 0.102 /

&SURF ID                   = 'STEEL'
```

```
        RGB                = 0.20,0.20,0.20
        C_DELTA_RHO        = 20.
        DELTA              = 0.005 /

&REAC ID='METHANE'
      FYI='Methane, C H_4'
      MW_FUEL=16
      NU_O2=2.
      NU_CO2=1.
      NU_H2O=2.
      DTSAM = 10.
      RADIATIVE_FRACTION=0.20
      SOOT_YIELD=0.005 /

&OBST XB=10.9,11.2, 0.0, 0.3, 0.4, 0.5,SURF_IDS='burner','STEEL','STEEL' /  Burner
&OBST XB= 9.8,11.1, 2.3, 3.4, 0.0, 2.2,SURF_ID6='CERAMIC FIBER','CERAMIC FIBER','CERAMIC FIBER',
      'GYPSUM BOARD','CERAMIC FIBER','CERAMIC FIBER' /  Room 1 cut-out
&OBST XB=11.1,11.2, 3.3, 3.4, 0.0, 2.2 /  Door jamb (Room 1)
&OBST XB=12.0,12.2, 3.3, 3.4, 0.0, 2.2 /  Door jamb (Room 1)
&OBST XB=11.2,12.0, 3.3, 3.4, 1.6, 2.2 /  Door Sill (Room 1)
&OBST XB= 3.2, 4.6, 2.2, 3.4, 0.0, 2.4 /  Room 3 cut-out
&OBST XB= 2.4, 3.2, 3.3, 3.4, 2.0, 2.4 /  Door Sill (Room 3)

&VENT XB= 0.0, 0.0, 4.2, 5.0, 0.0, 2.0,SURF_ID='OPEN' /  Open Door at end of hallway
&VENT XB= 9.8,12.2, 0.0, 3.4, 0.0, 0.0,SURF_ID='FIRE BRICK' /  Floor of Room 1
&VENT XB= 9.8,12.2, 0.0, 3.4, 2.2, 2.2,SURF_ID='CERAMIC FIBER' /  Ceiling of Room 1
&VENT XB= 9.8, 9.8, 0.0, 3.4, 0.0, 2.2,SURF_ID='CERAMIC FIBER' /  Wall of Room 1
&VENT XB=12.2,12.2, 0.0, 3.4, 0.0, 2.2,SURF_ID='CERAMIC FIBER' /  Wall of Room 1
&VENT XB= 9.8,12.2, 0.0, 0.0, 0.0, 2.2,SURF_ID='CERAMIC FIBER' /  Wall of Room 1
&VENT XB= 2.4, 4.6, 0.0, 3.4, 0.0, 0.0,SURF_ID='CONCRETE' /  Floor of Room 3

&BNDF QUANTITY='GAUGE_HEAT_FLUX' /
&BNDF QUANTITY='WALL_TEMPERATURE' /

&SLCF PBY= 4.6,QUANTITY='TEMPERATURE',VECTOR=.TRUE. /  Hallway (Room 2)
&SLCF PBZ= 2.0,QUANTITY='TEMPERATURE',VECTOR=.TRUE. /  Ceiling
&SLCF PBX=11.7,QUANTITY='TEMPERATURE',VECTOR=.TRUE. /  Room 1
&SLCF PBX= 2.8,QUANTITY='TEMPERATURE',VECTOR=.TRUE. /  Room 3

&THCP XYZ=10.0, 2.0, 0.15,QUANTITY='THERMOCOUPLE',LABEL='TC 1-1',DTSAM=10. /
&THCP XYZ=10.0, 2.0, 0.36,QUANTITY='THERMOCOUPLE',LABEL='TC 1-2' /
&THCP XYZ=10.0, 2.0, 0.66,QUANTITY='THERMOCOUPLE',LABEL='TC 1-3' /
&THCP XYZ=10.0, 2.0, 0.97,QUANTITY='THERMOCOUPLE',LABEL='TC 1-4' /
&THCP XYZ=10.0, 2.0, 1.27,QUANTITY='THERMOCOUPLE',LABEL='TC 1-5' /
&THCP XYZ=10.0, 2.0, 1.57,QUANTITY='THERMOCOUPLE',LABEL='TC 1-6' /
&THCP XYZ=10.0, 2.0, 1.88,QUANTITY='THERMOCOUPLE',LABEL='TC 1-7' /
&THCP XYZ=10.0, 2.0, 2.03,QUANTITY='THERMOCOUPLE',LABEL='TC 1-8' /
&THCP XYZ=10.0, 2.0, 2.15,QUANTITY='THERMOCOUPLE',LABEL='TC 1-9' /

&THCP XYZ=11.7, 2.3, 0.15,QUANTITY='THERMOCOUPLE',LABEL='TC 2-1' /
&THCP XYZ=11.7, 2.3, 0.30,QUANTITY='THERMOCOUPLE',LABEL='TC 2-2' /
&THCP XYZ=11.7, 2.3, 0.61,QUANTITY='THERMOCOUPLE',LABEL='TC 2-3' /
&THCP XYZ=11.7, 2.3, 0.91,QUANTITY='THERMOCOUPLE',LABEL='TC 2-4' /
&THCP XYZ=11.7, 2.3, 1.22,QUANTITY='THERMOCOUPLE',LABEL='TC 2-5' /
&THCP XYZ=11.7, 2.3, 1.52,QUANTITY='THERMOCOUPLE',LABEL='TC 2-6' /

&THCP XYZ=10.8, 4.6, 0.15,QUANTITY='THERMOCOUPLE',LABEL='TC 3-1' /
&THCP XYZ=10.8, 4.6, 0.30,QUANTITY='THERMOCOUPLE',LABEL='TC 3-2' /
&THCP XYZ=10.8, 4.6, 0.61,QUANTITY='THERMOCOUPLE',LABEL='TC 3-3' /
&THCP XYZ=10.8, 4.6, 0.91,QUANTITY='THERMOCOUPLE',LABEL='TC 3-4' /
&THCP XYZ=10.8, 4.6, 1.22,QUANTITY='THERMOCOUPLE',LABEL='TC 3-5' /
&THCP XYZ=10.8, 4.6, 1.52,QUANTITY='THERMOCOUPLE',LABEL='TC 3-6' /
&THCP XYZ=10.8, 4.6, 1.83,QUANTITY='THERMOCOUPLE',LABEL='TC 3-7' /
&THCP XYZ=10.8, 4.6, 2.13,QUANTITY='THERMOCOUPLE',LABEL='TC 3-8' /
&THCP XYZ=10.8, 4.6, 2.29,QUANTITY='THERMOCOUPLE',LABEL='TC 3-9' /
&THCP XYZ=10.8, 4.6, 2.40,QUANTITY='WALL_TEMPERATURE',LABEL='TC 3-10',IOR=-3 /

&THCP XYZ= 6.7, 4.6, 0.15,QUANTITY='THERMOCOUPLE',LABEL='TC 4-1' /
&THCP XYZ= 6.7, 4.6, 0.30,QUANTITY='THERMOCOUPLE',LABEL='TC 4-2' /
&THCP XYZ= 6.7, 4.6, 0.61,QUANTITY='THERMOCOUPLE',LABEL='TC 4-3' /
&THCP XYZ= 6.7, 4.6, 0.91,QUANTITY='THERMOCOUPLE',LABEL='TC 4-4' /
```

```
&THCP XYZ= 6.7,  4.6,  1.22,QUANTITY='THERMOCOUPLE',LABEL='TC 4-5' /
&THCP XYZ= 6.7,  4.6,  1.52,QUANTITY='THERMOCOUPLE',LABEL='TC 4-6' /
&THCP XYZ= 6.7,  4.6,  1.83,QUANTITY='THERMOCOUPLE',LABEL='TC 4-7' /
&THCP XYZ= 6.7,  4.6,  2.13,QUANTITY='THERMOCOUPLE',LABEL='TC 4-8' /
&THCP XYZ= 6.7,  4.6,  2.29,QUANTITY='THERMOCOUPLE',LABEL='TC 4-9' /
&THCP XYZ= 6.7,  4.6,  2.40,QUANTITY='WALL_TEMPERATURE',LABEL='TC 4-10',IOR=-3 /

&THCP XYZ= 0.5,  5.5,  0.15,QUANTITY='THERMOCOUPLE',LABEL='TC 5-1' /
&THCP XYZ= 0.5,  5.5,  0.30,QUANTITY='THERMOCOUPLE',LABEL='TC 5-2' /
&THCP XYZ= 0.5,  5.5,  0.61,QUANTITY='THERMOCOUPLE',LABEL='TC 5-3' /
&THCP XYZ= 0.5,  5.5,  0.91,QUANTITY='THERMOCOUPLE',LABEL='TC 5-4' /
&THCP XYZ= 0.5,  5.5,  1.22,QUANTITY='THERMOCOUPLE',LABEL='TC 5-5' /
&THCP XYZ= 0.5,  5.5,  1.52,QUANTITY='THERMOCOUPLE',LABEL='TC 5-6' /
&THCP XYZ= 0.5,  5.5,  1.83,QUANTITY='THERMOCOUPLE',LABEL='TC 5-7' /
&THCP XYZ= 0.5,  5.5,  2.13,QUANTITY='THERMOCOUPLE',LABEL='TC 5-8' /
&THCP XYZ= 0.5,  5.5,  2.29,QUANTITY='THERMOCOUPLE',LABEL='TC 5-9' /
&THCP XYZ= 0.5,  5.5,  2.40,QUANTITY='WALL_TEMPERATURE',LABEL='TC 5-10',IOR=-3 /

&THCP XYZ= 0.1,  4.6,  0.15,QUANTITY='THERMOCOUPLE',LABEL='TC 6-1' /
&THCP XYZ= 0.1,  4.6,  0.30,QUANTITY='THERMOCOUPLE',LABEL='TC 6-2' /
&THCP XYZ= 0.1,  4.6,  0.61,QUANTITY='THERMOCOUPLE',LABEL='TC 6-3' /
&THCP XYZ= 0.1,  4.6,  0.91,QUANTITY='THERMOCOUPLE',LABEL='TC 6-4' /
&THCP XYZ= 0.1,  4.6,  1.22,QUANTITY='THERMOCOUPLE',LABEL='TC 6-5' /
&THCP XYZ= 0.1,  4.6,  1.52,QUANTITY='THERMOCOUPLE',LABEL='TC 6-6' /
&THCP XYZ= 0.1,  4.6,  1.83,QUANTITY='THERMOCOUPLE',LABEL='TC 6-7' /
&THCP XYZ= 0.1,  4.6,  2.13,QUANTITY='THERMOCOUPLE',LABEL='TC 6-8' /

&THCP XYZ= 2.8,  2.8,  0.15,QUANTITY='THERMOCOUPLE',LABEL='TC 7-1' /
&THCP XYZ= 2.8,  2.8,  0.61,QUANTITY='THERMOCOUPLE',LABEL='TC 7-2' /
&THCP XYZ= 2.8,  2.8,  0.91,QUANTITY='THERMOCOUPLE',LABEL='TC 7-3' /
&THCP XYZ= 2.8,  2.8,  1.07,QUANTITY='THERMOCOUPLE',LABEL='TC 7-4' /
&THCP XYZ= 2.8,  2.8,  1.22,QUANTITY='THERMOCOUPLE',LABEL='TC 7-5' /
&THCP XYZ= 2.8,  2.8,  1.52,QUANTITY='THERMOCOUPLE',LABEL='TC 7-6' /
&THCP XYZ= 2.8,  2.8,  1.83,QUANTITY='THERMOCOUPLE',LABEL='TC 7-7' /
&THCP XYZ= 2.8,  2.8,  1.93,QUANTITY='THERMOCOUPLE',LABEL='TC 7-8' /

&THCP XYZ= 4.4,  2.0,  0.15,QUANTITY='THERMOCOUPLE',LABEL='TC 8-1' /
&THCP XYZ= 4.4,  2.0,  0.61,QUANTITY='THERMOCOUPLE',LABEL='TC 8-2' /
&THCP XYZ= 4.4,  2.0,  0.91,QUANTITY='THERMOCOUPLE',LABEL='TC 8-3' /
&THCP XYZ= 4.4,  2.0,  1.07,QUANTITY='THERMOCOUPLE',LABEL='TC 8-4' /
&THCP XYZ= 4.4,  2.0,  1.22,QUANTITY='THERMOCOUPLE',LABEL='TC 8-5' /
&THCP XYZ= 4.4,  2.0,  1.52,QUANTITY='THERMOCOUPLE',LABEL='TC 8-6' /
&THCP XYZ= 4.4,  2.0,  1.83,QUANTITY='THERMOCOUPLE',LABEL='TC 8-7' /
&THCP XYZ= 4.4,  2.0,  2.13,QUANTITY='THERMOCOUPLE',LABEL='TC 8-8' /
&THCP XYZ= 4.4,  2.0,  2.29,QUANTITY='THERMOCOUPLE',LABEL='TC 8-9' /
&THCP XYZ= 4.4,  2.0,  2.40,QUANTITY='WALL_TEMPERATURE',LABEL='TC 8-10',IOR=-3 /

&THCP XYZ=10.0,  2.0,  0.15,QUANTITY='LAYER HEIGHT',LABEL='Layer Height 1' /
&THCP XYZ=10.0,  2.0,  0.15,QUANTITY='UPPER TEMPERATURE',LABEL='Layer Temp 1' /
&THCP XYZ=11.7,  2.3,  0.15,QUANTITY='LAYER HEIGHT',LABEL='Layer Height 2' /
&THCP XYZ=11.7,  2.3,  0.15,QUANTITY='UPPER TEMPERATURE',LABEL='Layer Temp 2' /
&THCP XYZ=10.8,  4.6,  0.15,QUANTITY='LAYER HEIGHT',LABEL='Layer Height 3' /
&THCP XYZ=10.8,  4.6,  0.15,QUANTITY='UPPER TEMPERATURE',LABEL='Layer Temp 3' /
&THCP XYZ= 6.7,  4.6,  0.15,QUANTITY='LAYER HEIGHT',LABEL='Layer Height 4' /
&THCP XYZ= 6.7,  4.6,  0.15,QUANTITY='UPPER TEMPERATURE',LABEL='Layer Temp 4' /
&THCP XYZ= 0.5,  5.5,  0.15,QUANTITY='LAYER HEIGHT',LABEL='Layer Height 5' /
&THCP XYZ= 0.5,  5.5,  0.15,QUANTITY='UPPER TEMPERATURE',LABEL='Layer Temp 5' /
&THCP XYZ= 0.1,  4.6,  0.15,QUANTITY='LAYER HEIGHT',LABEL='Layer Height 6' /
&THCP XYZ= 0.1,  4.6,  0.15,QUANTITY='UPPER TEMPERATURE',LABEL='Layer Temp 6' /
&THCP XYZ= 2.8,  2.8,  0.15,QUANTITY='LAYER HEIGHT',LABEL='Layer Height 7' /
&THCP XYZ= 2.8,  2.8,  0.15,QUANTITY='UPPER TEMPERATURE',LABEL='Layer Temp 7' /
&THCP XYZ= 4.4,  2.0,  0.15,QUANTITY='LAYER HEIGHT',LABEL='Layer Height 8' /
&THCP XYZ= 4.4,  2.0,  0.15,QUANTITY='UPPER TEMPERATURE',LABEL='Layer Temp 8' /
```

U.S. NUCLEAR REGULATORY COMMISSION

BIBLIOGRAPHIC DATA SHEET

(See instructions on the reverse)

1. REPORT NUMBER
(Assigned by NRC, Add Vol., Supp., Rev., and Addendum Numbers, if any.)
NUREG-1824

2. TITLE AND SUBTITLE

Verification and Validation of Selected Fire Models for Nuclear Power Plant Applications
Volume 7: FDS

3. DATE REPORT PUBLISHED

MONTH	YEAR
May	2007

4. FIN OR GRANT NUMBER

5. AUTHOR(S)

K. McGrattan (NIST)

6. TYPE OF REPORT

Technical

7. PERIOD COVERED *(Inclusive Dates)*

8. PERFORMING ORGANIZATION - NAME AND ADDRESS *(If NRC, provide Division, Office or Region, U.S. Nuclear Regulatory Commission, and mailing address; if contractor, provide name and mailing address.)*

U.S. Nuclear Regulatory Commission, Office of Regulatory Research (RES), Washington, DC 20555-0001
Electric Power Research Institute (EPRI), 3412 Hillview Avenue, Palo Alto, CA 94303
Science Applications International Corp. (SAIC), 4920 El Camino Real, Los Altos, CA 94022
National Institute of Standards and Technology (NIST/BFRL), 100 Bureau Drive, Stop 8600, Gaithersburg, MD 20899-8600

9. SPONSORING ORGANIZATION - NAME AND ADDRESS *(If NRC, type "Same as above"; if contractor, provide NRC Division, Office or Region, U.S. Nuclear Regulatory Commission, and mailing address.)*

U.S. Nuclear Regulatory Commission, Office of Regulatory Research (RES), Washington, DC 20555-0001
Electric Power Research Institute (EPRI), 3412 Hillview Avenue, Palo Alto, CA 94303

10. SUPPLEMENTARY NOTES

11. ABSTRACT *(200 words or less)*

There is a movement to introduce risk-informed and performance-base analyses into fire protection engineering practice, both domestically and worldwide. The move towards risk-informed decision-making in nuclear power regulation was directed by the U.S. Nuclear Regulatory Commission.
One key tool needed to support risk-informed, performance-based fire protection is the availability of verified and validated fire models that can accurately predict the consequences of fires. Section 2.4.1.2. of NFPA 805, Performance-Base Standard for Fire Protection for Light-Water Reactor Electric Generating Plants, 2001 Edition requires that only fire models acceptable to the Authority Having Jurisdiction (AHJ) shall be used in fire modeling calculations. Futhermore, Sections 2.4.1.2.2. and 2.4.1.2.3. of NFPA 805 state that fire models shall be applied within the limitations of the given model, and shall be verified and validated. This report is the first effort to document the verification and validation (V&V) of five models that are commomly used in nuclear power plant applications. The project was performed in accordance with the guidelines that the American Society for Testing and Materials (ASTM) set forth in ASTM E 1355, Standard Guide for Evaluating the Predictive capability of Deterministic Fire Models. The results of this V&V are reported in the form of color codes describing the accuracies for the model predictions.

12. KEY WORDS/DESCRIPTORS *(List words or phrases that will assist researchers in locating the report.)*

fire, fire modeling, verification, validation, performance-based, risk-informed, firehazards analyses, V&V, FHA, CFAST, FDS, MAGIC, FIVE, FDTs

13. AVAILABILITY STATEMENT

unlimited

14. SECURITY CLASSIFICATION

(This Page)

unclassified

(This Report)

unclassified

15. NUMBER OF PAGES

16. PRICE

Printed
on recycled
paper

Federal Recycling Program